



Working Report 2009-17

Review of Bothnian Sea Shore-Level Displacement Data and Use of a GIS Tool to Estimate Isostatic Uplift

Arto Vuorela
Teea Penttinen
Anne-Maj Lahdenperä

February 2009

Working Report 2009-17

Review of Bothnian Sea Shore-Level Displacement Data and Use of a GIS Tool to Estimate Isostatic Uplift

Arto Vuorela

Teea Penttinen

Anne-Maj Lahdenperä

Pöyry Environment Oy

February 2009

Base maps: ©National Land Survey, permission 41/MML/09

Working Reports contain information on work in progress
or pending completion.

The conclusions and viewpoints presented in the report
are those of author(s) and do not necessarily
coincide with those of Posiva.

Review of Bothnian Sea Shore-Level Displacement Data And Use of a GIS Tool to Estimate Isostatic Uplift

ABSTRACT

The aim and approach of the study were to produce source data estimates necessary for modelling the future biosphere. The study updated the list of ^{14}C datings of sea-level index points, which show when lakes and mires were isolated from the Baltic Sea due to isostatic uplift. The study concentrated on the Bothnian Sea, especially the Olkiluoto area. The older Finnish datings (a list of 260 sea-level index points determined in 1995) were checked and revised as needed. New data was available for 56 Finnish and 41 Swedish index points. State-of-the-art ^{14}C calibration methods were applied.

Various available data were used to estimate the parameters of the glacio-isostatic uplift model's slow component. The component describes the uplift in relation to time using parameters B_s , which is related to the uplift's total duration, and A_s , which is half of the total uplift possible in the period lasting from the Last Glacial Maximum to the distant future. The B_s values were estimated by means of 1) crustal thickness and 2) shoreline displacement curves. In applying method 1, this study revised the function describing the relationship between crustal thickness and B_s and created a new derivative-based method that also estimates the parameter A_s without radiocarbon datings and using only crustal thickness and current uplift maps. In method 2, sea-level index point subsets along the Finnish and Swedish coasts of the Bothnian Sea were selected from the revised database, and their datings and elevations were used to determine the corresponding land uplift parameters. The parameter value distributions were used to produce maps.

The values of the inertia factor B_s are on average 6% higher than those calculated in 2001 but they are 10% lower in the Olkiluoto region. According to the interpolations of the new and old data, the estimated uplift at Olkiluoto for AD 12000 is 2.8 m (7%) less than calculated previously. The derivative-based method predicts an uplift for AD 12000 at Olkiluoto that is only 0.5 m more than that predicted previously. Both the shore-level displacement method and the derivative-based method propose that there is a local maximum of A_s northeast of the Gulf of Bothnia. The northern part of the A_s distribution's maximum is farther east than in the previous results, and the B_s distribution is wider. The remaining slow uplift at Olkiluoto is 91.5–95.5 m according to the derivative method and 83.8 m according to the shore-level displacement method.

The modelling uncertainties include those due to crustal properties and the eustasy model. The fast uplift parameters were only partly revised by means of re-calibration and correction of the Ancylus Lake's level. It would be useful to recalculate the parameters also at other old sites in Fennoscandia using the IntCal04 method and revised versions of the models presented in 2005. Especially the time of the fast component's maximum rate (T_f) could be determined more precisely. The fast uplift is closely related to the period when crustal movements were probable. This period and the solidity of the bedrock were not investigated. It is probable that the blocks bounded by the tectonic lines are moving in different ways. The movements could not be determined in this regional analysis but they seem to be similar on average.

Keywords: glacio-isostatic uplift, isostatic uplift, glacial isostatic adjustment, post-glacial rebound, shoreline displacement, shore-level displacement, isolation, sea-level index point, ^{14}C , Bothnian Sea, eustasy GIS, palaeogeography

Selkämeren alueen rannansiirtymätietojen tarkistus ja GIS-sovellus isostaattisen maankohoamisen arviointiin

TIIVISTELMÄ

Työn näkökulma oli tulevaisuuden biosfäärimallinnuksen tarvitsemissa lähtötiedoissa. ^{14}C -ajoitusten lista, joka koskee järvien ja soiden isolaatiota Selkämerestä maankohoamisen takia, päivitettiin. Työ kohdistui Selkämeren ja erityisesti Olkiluodon alueelle. Aiemmat suomalaiset ajoitukset (vuonna 1995 koottu 260 rannankorkeuden indeksipisteen lista) läpikäytiin. Uutta tietoa oli 56 pisteestä Suomesta ja 41:stä Ruotsista. ^{14}C -kalibroinnin nyky menetelmiä sovellettiin.

Eri aineistoilla arvioitiin edelleen jatkuvan hitaan maannousukomponentin parametrien arvoja glasio-isostaattisessa mallissa, joka kuvaa maankohoamista ajan suhteen parametreilla B_s (joka viittaa maannousun kokonaiskestoon) ja A_s (puolet maksimaalisen jäätikön jälkeen tapahtuvan maannousun kokonaismäärästä). B_s :ää arvioitiin 1) maankuoren paksuuden ja 2) rannansiirtymäkäyrien avulla. Menetelmässä 1 tarkennettiin maankuoren paksuuden ja B_s :n välistä funktiota kuvaavaa yhtälöä sekä kehitettiin uusi derivaattapohjainen menetelmä, jossa myös A_s arvioidaan ilman radiohiiliajoituksia pelkistä maankuoren paksuuden ja nykyisen maankohoamisen kartoista. Menetelmässä 2 valittiin tarkennetusta pisteistöstä Suomen ja Ruotsin Selkämeren rannikoilta osajoukkoja, joiden kunkin ajoituksista ja korkeusasemista ratkaistiin maankohoamisen parametreja. Parametrien arvojen jakaumista tehtiin karttoja.

Hitauskertoimen B_s arvot ovat keskim. 6 % suurempia kuin v. 2001 arvioidut, mutta Olkiluodolle 10 % pienempiä. Aiemmin ratkaistujen alueiden kanssa interpoloiden saatiin Olkiluodolle maankohoamista vuonna 12000 jKr. 2,8 m (7 %) vähemmän kuin aiemman mallin tulosten perusteella. Derivaattamenetelmän perusteella Olkiluodon maannousu vuonna 12000 jKr. on vain 0,5 m suurempi kuin aiempien tulosten perusteella. Sekä rannansiirtymiskäyrä- että derivaattamenetelmän mukaan A_s :llä on paikallinen maksimi Pohjanlahdelta koilliseen. A_s -jakauman maksimin pohjoisosa siirtyi edellisiin tuloksiin verrattuna idemmäksi, samoin B_s :n jakauman maksimi leveni. Olkiluodolle on hidasta maankohoamista jäljellä derivaattamenetelmien mukaan 91,5–95,5 m tai rannansiirtymiskäyrämenetelmän perusteella 83,8 m.

Mallinnuksen epävarmuuksiin kuuluvat muun muassa maankuoren ominaisuudet ja merenpinnan nousumalli. Maankohoamisen nopean komponentin tarkentamista sivuttiin uudelleenkalibroinnin ja Ancyclus-järven tasokorjauksen kautta. Olisi hyödyllistä mm. ratkaista parametreja Fennoskandian muissakin kohteissa IntCal04-menetelmällä ja Pässe & Anderssonin vuonna 2005 esittämällä mutta tarkistetuilla malleilla. Tarkennusta saataisiin etenkin nopean komponentin maksimin ajankohtaan (T_7). Nopea komponentti liittyy erityisesti aikaan jolloin maankuoren liikkeet olivat todennäköisiä. Tätä tai kallioperän eheyttä ei tutkittu. Tektonisten linjojen rajaamat lohkot todennäköisesti liikkuvat eri tavalla. Tässä alueellisen tason tarkastelussa liikkeitä ei määriteltä, mutta ne vaikuttavat pitkällä aikavälillä samanlaisilta.

Avainsanat: glasiaali-isostasia, maankohoaminen, maannouseminen, postglasiaalinen muodonpalautusilmiö, rannansiirtyminen, kuroutuminen, rannankorkeuden indeksipiste, ^{14}C , Selkämeri, eustasia, eustaattinen nousu, GIS, paleomaantiede

ACKNOWLEDGMENTS

This study has been carried out by Pöyry Environment Oy according to a Posiva Oy research contract. On behalf of Posiva, the study was patiently and encouragingly supervised by Ari T. K. Ikonen. The authors would like to thank him and all the experts involved, of whom many are mentioned in the text.

The study is largely based on the extensive work of Associate Professor Tore Pässe and late Leif Andersson, Ph.Lic., who together developed the models. Dr. Arto Miettinen from the Norwegian Polar Institute has reviewed the report and provided useful comments. Dr. Irmeli Vuorela provided comments on the usefulness of the samples. Dr. Högne Jungner and many others helped to interpret if the $\delta^{13}\text{C}$ corrections had been carried out or not. Dr. Markku Oinonen from the Dating Laboratory of the University of Helsinki kindly offered to conduct the $\delta^{13}\text{C}$ corrections of the old Hel-samples and to calculate the 1σ and 2σ lower and upper limits of the datings' calibrations. Prof. Markku Poutanen, Dr. Jaakko Mäkinen and senior researcher Pekka Lehmuskoski, M.Sc., from the Finnish Geodetic Institute helped by providing the latest information on the current apparent land uplift and isostatic uplift and on the elevation systems. Prof. Veli-Pekka Salonen, Helsinki University, and geophysicist Eero Heikkinen, Pöyry Environment Oy, also made useful comments.

TABLE OF CONTENTS

ABSTRACT

TIIVISTELMÄ

ACKNOWLEDGMENTS

ABBREVIATIONS AND SYMBOLS

1	INTRODUCTION.....	7
	1.1 Background	7
	1.2 Objectives.....	10
	1.3 Organisation of the report	11
2	EXISTING DATA.....	13
	2.1 Shoreline displacement.....	13
	2.2 The analysed sites available	15
	2.3 Current land uplift	17
3	METHODOLOGY.....	21
	3.1 Shoreline displacement.....	21
	3.2 On the regional parameter estimation	22
	3.3 Corrections and co-ordinate transformations	25
	3.4 ¹⁴ C dating calibration alternatives and methods	30
	3.4.1 $\delta^{13}\text{C}$ correction	31
	3.4.2 ¹⁴ C Calibration.....	32
4	FORMULAE	35
	4.1 Eustatic rise	35
	4.2 Slow component of isostatic uplift.....	39
	4.3 Fast isostatic uplift component and total uplift.....	43
5	CRUSTAL AND LITHOSPHERE THICKNESSES	47
	5.1 Crust and definitions	47
	5.2 B_s modelling based on lithosphere thickness	52
6	REGIONAL ESTIMATION OF ISOSTATIC LAND UPLIFT PARAMETERS.....	55
	6.1 The derivative-based simple processes	55
	6.2 Estimation based on shore-level curves.....	61
7	RESULTS	65
	7.1 B_s estimates based on crustal thickness maps	65
	7.2 A_s estimates based on B_s maps	70
	7.3 Estimates based on shore-level displacement curves	75
	7.3.1 The shore-level displacement curve plots.....	75

7.3.2	Combination of the old and new shore-level displacement analyses.....	99
7.4	Parameter surface interpolation.....	99
7.4.1	By kriging.....	99
7.4.2	By other means.....	105
7.5	Interpretation of the results.....	105
7.5.1	Derivative-based results.....	105
7.5.2	Shore-level-based results.....	107
8	UNCERTAINTIES AT DIFFERENT STAGES AND THEIR IMPACT.....	113
9	SUMMARY OF THE FORMULAE AND RASTERS USED.....	119
10	CONCLUSIONS.....	121
	REFERENCES.....	125
	APPENDICES.....	139
	APPENDIX 1. SAMPLES BY ERONEN ET AL. (1995).....	141
	Literature references by Eronen et al. (1995).....	161
	APPENDIX 2. CODES USED.....	169
	APPENDIX 3. AGE CALIBRATION PRACTICES FOR LAKES AND PEATS.....	171
	APPENDIX 4. THE NEW SAMPLES (FINLAND AND SWEDEN).....	175
	References of the new samples (Finland and Sweden).....	185
	APPENDIX 5. THE ANALYSIS SITE TABLE.....	187

ABBREVIATIONS AND SYMBOLS

^{14}C	Radiocarbon or carbon-14 isotope, and dating based on it
A_E	Half of the total eustatic rise (a eustasy parameter), (m)
A_f	The <u>fast</u> isostatic uplift magnitude parameter (used in two different ways)
A_s	Download factor, or half of the total uplift (<u>slow</u> isostatic uplift)
AD	Anno Domini (number of years after the traditional date of Christ's birth)
AMS	Accelerator mass spectrometry (radiocarbon dating)
AP	After the present, i.e. date in years after AD 1950
arctan	Arctangent, or inverse tangent function
asl	Above (the current) sea level
B_E	A eustasy parameter, controlling the duration of the eustatic rise
B_f	The <u>fast</u> isostatic uplift parameter for the duration of the fast uplift, used in two different ways
B_s	Inertia factor (year^{-1})
BC	Before Christ
BP	Before the present, i.e. date in years before AD 1950, but in conventional, uncalibrated analysis years
$C_{age_{yr}}$	^{14}C age (BP)
$C_{baseline}$	A correction of the shoreline graphs by Eronen et al. (1995)
C_{old}	A possible combined altitude correction to be applied to old observations
cal BP	Calibrated years BP, i.e. before AD 1950
CSV	Comma separated values (text file format)
ct	Crustal thickness (km)
dd	digital degrees
$\delta^{13}\text{C}$	Carbon 13 isotope content (^{13}C)
$\Delta diff$	Local differential correction (not used here but by Berglund 2005)
ΔE	Transformation from an old to a new (the current) elevation system

<i>E</i>	Eustasy, the model of global changes in sea level (m)
<i>E'</i>	Derivative of eustasy (m/year), please note according to which time axis
<i>E₀₁</i>	Eustasy, the eustatic sea level rise model (m), according to Pässe (2001)
<i>E_{01A}</i>	Eustasy according to Pässe (2001), including Ancylus correction
<i>E₀₅</i> or <i>E_{05t}</i>	Eustasy, the eustatic sea level rise models (m), Pässe & Andersson (2005)
<i>Epoch_{future}</i>	Some future epoch, e.g. AD 2010 or AD 2100
<i>Epoch_E</i>	The latest elevation system's epoch, e.g. AD 2000 for N2000
ETRS 89	European Terrestrial Reference System 1989
EuCRUST-07	A reference model for the European crust
EVRF2007	European Vertical Reference Frame 2007
FGI	the Finnish Geodetic Institute
GEON	GEON Center: All-Russia Research Institute of Geophysical Exploration, or Center for Regional Geophysical and Geoecological Studies
GIA	Glacial isostatic adjustment
GIS	Geographic information system
GPS	Global Positioning System
IntCal04	New Consensus Radiocarbon Calibration Dataset from 0–26 ka BP
JUHTA	(Finnish) Advisory Committee on Information Management in Public Administration
<i>L</i>	Lithospheric thickness (km)
LL	Lower limit
LSQ	Least squares
LU	Land uplift
Moho	Mohorovičić discontinuity, or crustal depth (km)
MS	Microsoft
MSL	mean sea level
MT	magnetotelluric

N2000	New Finnish elevation system
N60	Old Finnish elevation system
NKG2005L U	Nordic uplift model (RH 2000 LU)
PDB	Pee Dee Belemnite carbonate isotope (standard)
RH70	Old Swedish elevation system, 1970
RH2000	New Swedish elevation system
RT 90	Rikets Triangelnät (Swedish Grid)
S	Shore level displacement (m)
S'	Derivative of the shore level displacement (m), please note according to which time axis
S'_{map}	Apparent land uplift value (m) on the apparent land uplift maps
σ or σ_{sample}	Error or standard deviation of a ^{14}C sample (BP)
σ_{yr}	Error or standard deviation of a calibration curve
SKB	Swedish Nuclear Fuel and Waste Management Co
STUK	Radiation and Nuclear Safety Authority, Finland
SWEREF 99	Swedish Reference Frame 1999
t	Time (in cal BP years)
t_{AD}	Time in AD years, therefore calibrated
T_s	Time (cal BP) of the slow uplift's maximum rate (a <u>slow</u> isostatic uplift parameter), i.e. the symmetry point of the arctan function
T_f	Time (cal BP) of the fast uplift's maximum rate (a <u>fast</u> isostatic uplift parameter), used in two different ways, but both as the symmetry point of the normal distribution function or arctan function used
T_E	Time (cal BP) of the eustatic rise's maximum rate (a eustasy parameter), i.e. the symmetry point of the arctan function
U	Isostatic uplift (m), here = the crustal change
U'	Derivative of U (m/year), please note according to which time axis
U_s	Slow component of the isostatic uplift (m)

U_f	Fast component of the isostatic uplift (m)
UL	Upper limit
uncal	Uncalibrated
USGS	United States Geological Survey
UTM33N	Universal Transverse Mercator, Zone 33 North
VPDB	Vienna-PDB
VSEGEI	A.P. Karpinsky Russian Geological Research Institute
WGS 84	World Geodetic System 1984
YVL	(Finnish) Regulatory Guides on Nuclear Safety (Ydinvoimalaitosohjeet)

1 INTRODUCTION

1.1 Background

Olkiluoto Island has been selected as the site of the final repository for spent nuclear fuel in Finland. It is located on the shore of the Gulf of Bothnia in the municipality of Eurajoki in southwestern Finland. The Finnish Parliament ratified the site selection decision in 2001. Safe disposal requires a thorough safety analysis that addresses both the expected future developments and unlikely events that could impair the long-term safety of the repository.

Posiva will compile a portfolio of reports that will be employed in reporting the repository's safety case (Posiva 2008). A safety case is a synthesis of evidence, analyses and arguments that quantify and substantiate the safety, and the level of expert confidence in the safety, of a geological disposal facility for radioactive waste (IAEA 2006, NEA 2004a). The safety case broadens the scope of the safety assessment to include the compilation of a wide range of evidence and arguments that complement and support the reliability of the results of the quantitative analyses. The safety case is a key input to decision-making at several steps in the repository planning and implementation process. It becomes more comprehensive and rigorous as the programme progresses (Posiva 2008).

Posiva's safety case portfolio contains a number of main reports, which will be periodically updated. The results of the biosphere assessment will be included in the main reports of the portfolio. In addition, there will be a number of reports supporting these main reports. Biosphere assessment is an essential part of the safety assessment and it describes the past, present and future conditions of the surface system, tracks the fate of hypothetical releases of radionuclides from the repository reaching the biosphere, and assesses possible radiological consequences for humans and other biota (Vieno & Ikonen 2005, Posiva 2008).

According to STUK's regulatory guide YVL 8.4, the timeframe of the local future development to be assessed consists of several thousands of years, and the main processes to be evaluated are land uplift and the emerging new land areas. The description of the future development of the site must be as realistic as possible and must be based on physical and geoscientific facts as well as good process understanding (STUK 2001).

Land uplift in the Baltic Basin

During the Late Weichselian glacial maximum ca. 18 000 ¹⁴C BP (Landvik et al. 1998, Svendsen et al. 1999), Fennoscandia was covered by a continental ice sheet with a maximum thickness of ca. 2.5 – 3 km (Fjedskaar 1994, Peltier 1994), the weight of which made the Earth's crust move downwards several hundred metres. Land uplift is caused by the Earth's crust aiming to achieve an isostatic balance after the retreat of the ice sheet. The depression created by the Scandinavian Ice Sheet during the Weichselian glaciation is gradually disappearing due to the uplift or rebound of the crust, and part of the mass of the top of the mantle is shifting from outside the area of uplift to its centre (Miettinen 2004).

Glacio-isostatic uplift was extremely rapid at the end of, and immediately after deglaciation. Major late- or postglacial faults in northern Fennoscandia date back to this time (Kujansuu 1964, Lundqvist & Lagerbäck 1976, Lagerbäck 1990, Kuivamäki & Vuorela 1994). The rate of land uplift decreased significantly ca. 8 500 – 8 000 BP (9 500 – 8 800 cal BP) (Eronen et al. 1995, Ristaniemi et al. 1997). Judging from data collected in different parts of Fennoscandia, it seems that land uplift has taken place during the last 10 000 years dominantly and without major irregularities. Regionally observed, land uplift seems to take place plastically; but locally, the uplift consists of movements of bedrock blocks (Kuivamäki & Vuorela 1994).

Since the opening of the ocean connection via the Danish Straits between 8 500 and 8 000 radiocarbon years ago, the shore displacement in the Baltic Sea Basin during the post-glacial times (e.g. Björck 1995, Eronen et al. 1995) has been governed by two factors: the glacio-isostatic uplift and the eustatic sea level changes, of which the former is dependent on climatic variations (Westman et al. 1999, Chivas et al. 2001) and changes of the geoid over long periods of time (Mörner 1977, 1999; Ekman 1996). The eustatic sea level variations only affected the shore displacement when the Baltic Basin was in contact with the ocean, i.e. during the Yoldia Sea and Litorina Sea stages. During the other major Baltic Sea stages (Baltic Ice Lake or Baltic Ice Sea and Ancylus Lake), local water level variations interacted with the isostatic uplift in creating a shoreline pattern that is independent of the oceans. The isostatic uplift is dependent on glacial history and neotectonic movements (Hedenström et al. 2003).

The current apparent isostatic uplift rate at Olkiluoto is 6 mm/y (Eronen et al. 1995), or 6.8 mm/y as the isostatic component (Kahma et al. 2001, Löfman 1999). The land uplift rates are highest in the Gulf of Bothnia region; in the centre of the uplift area, the uplift is about 9 mm/y (Kakkuri 1987, Ekman, 1987, 1989, Ekman & Mäkinen 1996). In southern and southwestern Finland, the uplift is about 3 – 6 mm/y, and it has stopped in the Gulf of Finland. The Fennoscandian lithosphere is still undergoing postglacial rebound (Pässe 1996), and the rebound is estimated to continue for about 20 000 years. Uplift can be considered constant on the timescale of a few centuries (Ekman 1996).

Shore-level displacement investigations

Shoreline or shore-level displacement can be investigated with different methods. One consists of describing the relevant geophysical processes as accurately as possible. Precision levelling may also reveal fairly local land uplift phenomena (Lehmuskoski 2008). Using precision levelling and Global Positioning System (GPS) campaigns, it has been possible to determine the current rate of uplift of inland areas without use of historical shoreline information.

The isolation of lakes and mires from the sea can be analysed with lithostratigraphic interpretation, diatom analysis, and radiocarbon dating. When a basin becomes an independent lake isolated from the sea because of land uplift, or when a basin is connected to the sea because of transgression, the accumulating sediment shows a distinct change. Especially in the early Holocene, clay was deposited in coastal waters, but as lake basins became isolated, gyttja was deposited in the basins. Diatom analyses are used to show how large-lake (i.e. Ancylus Lake) or brackish seawater diatoms are

replaced by fresh-lake diatoms in connection with the isolation. Different diatom species are very sensitive to water salinity changes (Miettinen 2004).

Radiocarbon (^{14}C) dating is a method of obtaining age estimates for organic materials, and it has provided age determinations in archaeology, geology, geophysics, and other branches of science. Radiocarbon determinations can be obtained for wood, charcoal, marine and fresh-water shells, bone, peat, organic-bearing sediments, carbonate deposits, and dissolved carbon dioxide and carbonates in ocean, lake, and groundwater sources. Lake muds and peats are composed of the remains of plants and organics that utilised atmospheric carbon and were deposited after their death in lake or swamp deposits.

Eronen et al. (1995) studied past shoreline changes in south-western Finland, collecting sediment samples originating from the last 8 000 years from 14 lakes at different altitudes in the area between Olkiluoto and Lake Pyhäjärvi, which is 40 km away. The time when the present-day lakes were isolated from the Baltic Sea was determined using diatom analyses and radiocarbon dating, and then used to draw the shoreline displacement curve. Löfman (1999) adapted the mathematical approximation function to the glacio-isostatic uplift in the Olkiluoto area from 20 000 cal BP to 10 000 AP.

Pässe (1990a, 1996, 1998) investigated glacio-isostatic uplift based on the lake-tilting method. By magnifying the function that describes lake-tilting, it was possible to start an iteration process that has produced mathematical expressions for factors that affect both the isostatic movements and the eustatic rise. Later, the main input data, besides the lake tilting information, were 72 shore-level curves from the area covered by Scandinavian ice during the Late Weichselian. In Pässe (1996, 1997, 2001) and Pässe & Andersson (2005), the shore-level curves were compared to the iteratively calculated curves derived from the mathematical expressions. In these reports, the authors presented two components of glacio-isostatic uplift. The main uplift, still in process, acts slowly and is called the slow component. The other component gave rise to fast crustal changes of short duration during the end of deglaciation and is called the fast component (Pässe 2001).

Implications of land uplift

Due to postglacial uplift in the coastal areas of the Bothnian Sea, sea bottom sediments are continuously emerging from the sea and starting a rapid primary succession along the shores. Furthermore, along shallow shores such as in Olkiluoto, especially in geolittoral regions, the amounts of common reed are increasing due to the human-induced eutrophication of coastal waters and due to a great decrease in grazing of animals, resulting in paludification of coves and accumulation of organic matter in shallow and nearly stagnant water. This results in a faster apparent shoreline displacement than mere land uplift or changes in sea level would yield (Miettinen & Haapanen 2002). Land uplift is further accelerated by the transport of materials by seawater, ice, and rivers.

The land uplift has a significant influence on both the abiotic and biotic biosphere. The topography changes, and different types of new soils and landforms continue to emerge from the sea bottom sediments. This leads to the isolation of new islands and the segregation of new lakes (e.g. Haapanen et al. 2007). The land uplift is uneven in

Finland (higher in the northwest than in the southwest). As a consequence, the directions of river flows may change. In rivers now running to the Bothnian Sea in southwestern Finland, the flows may slow down in the future, and more floods are probable in low-lying river valleys. Not only in the coastal area but also inland, especially in the shallow lakes and rivers caused by land uplift and tilting, the characteristics could change due to land uplift and tilting. Most of the peat lands in western Finland have been caused by land uplift (Aario 1932, Brandt 1948, Huikari 1956). In addition, land uplift leads to primary succession, in which a sequence of species colonises and disappears from an exposed landform uninfluenced by a previous community (Begon et al. 2006, Haapanen 2007). This study also provides data for land-uplift-related biosphere issues that will be modelled and reported in more detail in other Posiva reports.

1.2 Objectives

The initiative for this study came from the needs of biosphere modelling. Some issues that are more relevant to the development of bedrock conditions (especially fast uplift) are mentioned but left for further study. A basic element of the biosphere assessment carried out to understand the past, present, and especially future ecosystems and processes is land uplift modelling. This required reviewing the earlier studies of ^{14}C datings related to the isolation of lakes and mires from the Baltic Sea stages due to glacio-isostatic adjustment.

One objective of the study was to reconstruct and evaluate the isostatic uplift and shore level displacement models (especially Pässe 2001), i.e. the models of the past changes in local sea level relative to land. The aim was to be able to model the future Bothnian Sea uplift behaviour. The aim was also to evaluate the modelling method and the input data used to estimate the shoreline level primarily for the future. More raster surfaces were created and the sensitivity of some parameters were evaluated. Another major goal was to produce ArcGIS-compatible raster surfaces and equations for land uplift modelling to be used with a high-resolution statistical terrain model of the Olkiluoto site (Pohjola 2008).

A useful data set for further analysis was put together from the old and newer literature. The older Finnish data set of 260 sea-level index points (Eronen et al. 1995) was rebuilt and corrected. New data available since 1994 was available for 52 lakes and 4 mires in Finland and 41 lakes or mires in Sweden. A total of 357 sea-level index points or basins were used in the study.

However, during the last 10 - 15 years, there has not been very much new research on lake and mire isolation with ^{14}C datings of the threshold altitudes. In addition, many new dating studies have concentrated on the south coast of Finland, mainly on the area southeast of the Salpausselkä formations, the area with the lowest isostatic uplift, which is thus not relevant to the Olkiluoto area and the Bothnian Sea region.

The latest crustal thickness models were taken into account, and the function relating crustal thickness to the inertia factor was revised using new data. A straightforward derivative-based method was created, using the current uplift maps and the estimated inertia factor maps, to create regional estimates of half of the total uplift (A_s).

1.3 Organisation of the report

Chapter 2 first refers to the existing data on shore-level displacement and dating in Fennoscandia. References are given for both old studies (listed in Eronen et al. 1995, APPENDIX 1) and the more recent data, which was collected through literature research for this study (APPENDIX 4). Secondly, the current but somewhat varying estimates of current relative or isostatic uplift are presented.

Chapter 3 first describes the basic formulae for modelling the isostatic uplift (U) using the empirical shoreline information (S , determined in regional field work) and a eustatic sea level rise model (E) for the past. Secondly, the two approaches of the study to determine regional values of isostatic uplift parameters are explained. The first approach only uses the maps or models of current uplift and information on the crustal or lithospheric thickness. Thirdly, Chapter 3 describes the geometry issues, especially the elevation data corrections, and the age calibration issues.

Chapter 4 describes the parameters and formulae for the following model components: the eustatic rise (E) and the isostatic uplift (U), which is a sum of the slow component (U_s) and the fast component (U_f , not currently taking place). Graphs are also shown for various isostatic uplift versions that were previously estimated for Olkiluoto.

Chapter 5 describes the possibilities of using crustal thickness or the even deeper lithospheric thickness to produce regional estimates on how slowly the crust is deforming. The crustal rebound is naturally somewhat slower (and the inertia factor B_s higher) where the uppermost or the most solid layers of the Earth are thicker.

Chapter 6 first presents the formulae that show how the model components' derivatives (U' and E') can be used, together with the inertia B_s estimates e.g. from crustal or lithospheric thickness, to produce regional estimates of A_s (i.e. half of the total uplift in metres that is possible in the period lasting from the Last Glacial Maximum to the distant future). Secondly, the chapter describes the method for estimating the local isostatic uplift parameters A_s and B_s using the eustasy model E and the data of nearby sea-level index points, which include their threshold elevations from the current sea level and their isolation datings.

Chapter 7 shows the results of the two approaches to produce regional estimates of the isostatic uplift parameters. The raster surfaces based on derivatives and isoline maps are also shown. Secondly, the local uplift parameter sites are presented, both the ones defined in other studies and those defined in this one, as well as the new shore-level displacement curves. The site data is used to generalise the surfaces, which are compared with the other results.

Chapter 8 describes the models' uncertainties and their impact on the results.

Chapter 9 gives a summary of the formulae used and the raster surfaces related to the models.

Chapter 10 presents the conclusions and discusses some possible improvements.

2 EXISTING DATA

2.1 Shoreline displacement

Studies on shoreline displacement and the stages of the Baltic Sea have mainly been carried out in the 1970s and 1980s. Eronen has performed the main studies in the field of shoreline displacement, including the following:

- The history of the Litorina Sea and Ancylus transgression (Eronen 1974, 1976)
- Stages of the Baltic Sea and shoreline displacement (Donner & Eronen 1981)
- Lake Pyhäjärvi (Eronen et al. 1982), Shoreline displacement near Helsinki (Eronen & Haila 1982)
- Late Weichselian and Holocene shore displacement in Finland (Eronen 1983, 1990)
- Radiocarbon-dated shoreline data collection in Finland and shore-level displacement of the Baltic in South-western Finland since the Litorina stage (Eronen et al. 1993) and
- Land uplift in the Olkiluoto-Pyhäjärvi area (Eronen et al. 1995).

Glückert has studied the shoreline displacement in the Lohja area (1970), in southwestern Finland (1976), on the Åland Islands (1978a and 1989), and in western Uusimaa (1979). Glückert & Ristaniemi have studied the Ancylus transgression in the Karjalohja area (1980) and west of Helsinki (1982). Ristaniemi has studied shoreline displacement in the Karjalohja-Kisko area (1984) and the Ancylus limit of the ancient Lake Päijänne (1987), Ancylus transgression in the Espoo area (Ristaniemi & Glückert 1987), and Ancylus and Litorina transgression in Finland (Ristaniemi & Glückert 1988). Glückert et al. studied Lake Littoinen (1992) and shoreline displacement in Ostrobothnia (1993). Hyvärinen has also carried out shoreline studies: at Pielis Karelia (1966), near Helsinki (1979, 1980, 1982, 1999) and about the Mastogloia stage (1984).

The post-glacial radiocarbon-dated Finnish shoreline data of the Baltic Sea was summarised by Eronen et al. 1993 and completed in Eronen et al. 1995. Recent radiocarbon-dated shoreline data, published after Eronen et al. 1995, that was used in this study includes the following:

- Land uplift and shoreline displacement in central Ostrobothnia (Glückert et al. 1998)
- Rates of Holocene isostatic uplift and relative sea-level lowering of the Baltic in SW Finland (Eronen et al. 2001)
- Land uplift and relative sea-level changes in the Loviisa area (Miettinen et al. 1999)
- Studies in the eastern part of the Gulf of Finland (Miettinen 2002, 2004)

- Late Holocene sea-level changes along the southern coast of Finland (Miettinen et al. 2007)
- Shore displacement studies in the Helsinki area and near Helsinki (Seppä & Tikkanen 1998, Seppä et al. 2000)

In addition, some recent Swedish shoreline displacement studies were used in this study, e.g. Risberg (1999), Hedenström & Risberg (1999, 2003), Hedenström (2001), and Berglund (2005).

The older Finnish data for 260 sea-level index points (Eronen et al. 1995) was rebuilt and corrected and entered into an MS Excel table, see APPENDIX 1. The newer research reports published since 1994 that were found are presented in APPENDIX 4, after the corresponding new data set table, which was used in this study and which consists of data for 52 lakes and 4 mires from Finland and 41 lakes or mires from Sweden. A total of 357 sea-level index points were used (see Figure 1).

For every sea-level index point, the coordinates, threshold altitude (m above current sea level), original ^{14}C age BP (before present), possible calibrated age (cal BP) of isolation, and radiocarbon laboratory number are listed first. When the original (or corrected) threshold altitude of a sea-level index point (instead of its present threshold altitude) is given, this value was used in calculating the shoreline displacement. When the same article gives multiple datings for a location, the dating was selected that according to the publication is the most probable time of isolation. The datings just before or after the most probable time of isolation were not taken into account.

Many of the existing datings are not suitable for shoreline studies. For example, the bottom peat points that Mäkilä & Grundström (2008) determined in 16 mires in southwestern Finland do not necessarily represent isolation but events that occurred perhaps hundreds of years later. A curve following the uppermost points of their figure 6 would be a close representation of the relationship of isolation to the elevation of the bottom peat. The amount of the delay should however be determined.

Finnish lakes and their effluent streams are so small that typically the threshold altitude is in effect the same as the basin's (water) level in topographic maps. Sometimes the threshold altitude has been measured, especially if the threshold has been artificially changed or if it has been noticed that natural erosion has lowered it. It should be remembered, too, that the threshold altitude of each basin rises due to land uplift (compare old and new topographic maps). The term *original threshold* is used when the threshold has been artificially lowered, e.g. to get more agricultural land, or when the effluent stream has lowered the threshold. Depending on the soil type, erosion can be fast. On sandy soils, the threshold can become lower relatively quickly, but the original threshold altitude can usually be estimated based on the structure of the outlet channel. In Finland, the threshold is typically rock or till, which also tolerates erosion well in the case of small effluents. The original threshold is naturally essential in shoreline displacement studies, and it should be used whenever it is possible to be determined by levelling or other means. If the original threshold is not known, the basin elevation given by the topographic maps needs to be used (Miettinen 2008).

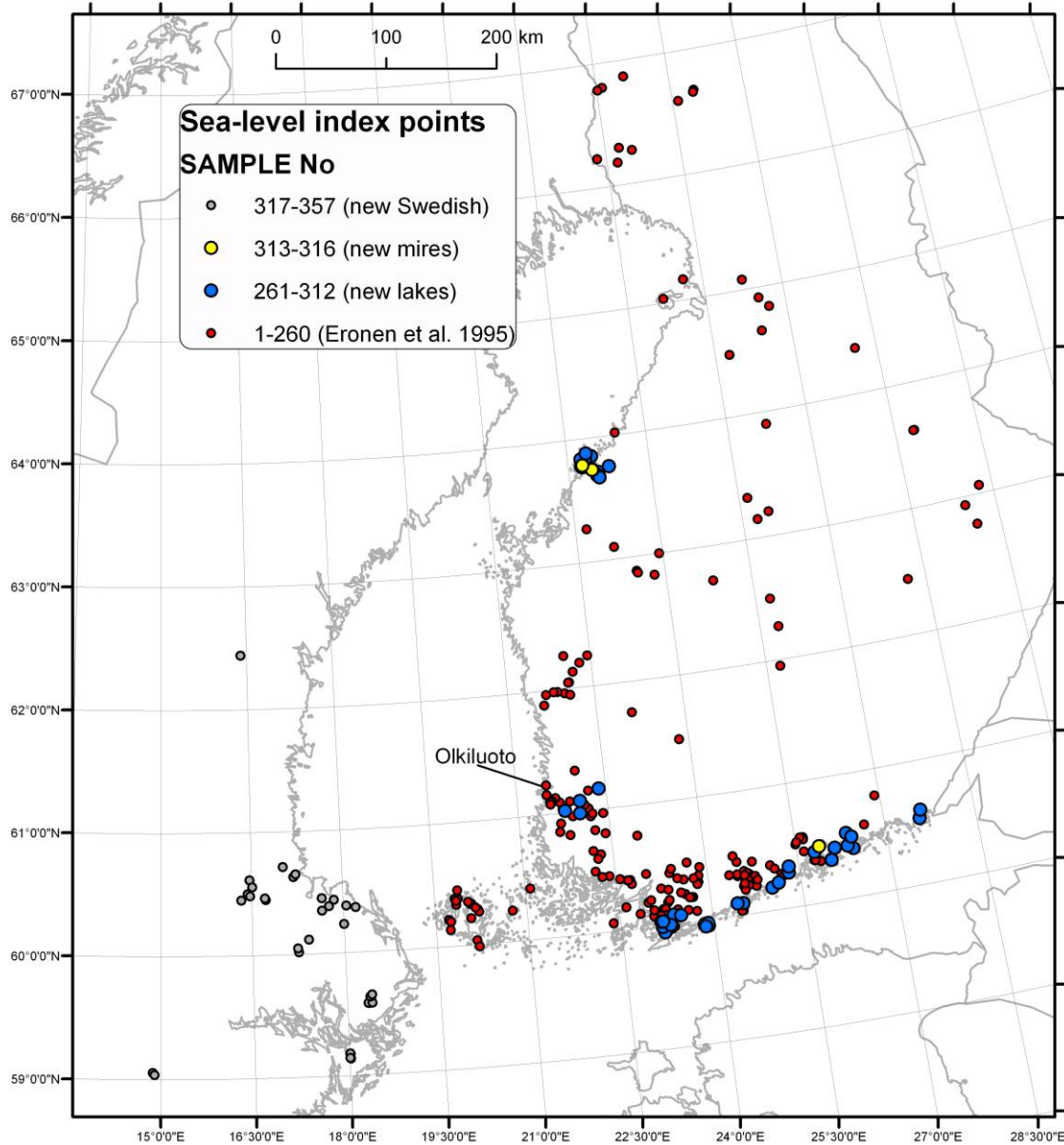


Figure 1. Locations of the sea-level index points used to determine the crustal uplift parameters.

2.2 The analysed sites available

The parameters of the sites analysed by Pässe (1997, 2001) and Pässe & Andersson (2005) were collected into one table that also includes the slow isostatic uplift parameter values (APPENDIX 5). The site numberings had previously varied between the reports and thus didn't serve as IDs. In this study, the 2005 numberings were used, because that report included more points, the identification of which could be kept. See Figure 2 for the sites analysed previously.

Some confusion may occur due to naming. The name Vendsyssel has been changed to Jylland, and the sites Östfold and Östfold N have been excluded from the 2005 report.

The Satakunta site (82) no longer appears after Pässe's 1997 report. Many Finnish names were previously misspelled: Karjalohka is now Karjalohja, Sippo Sipoo, Espoo Espoo, and Lauhanwuori Lauhanvuori.

The existing sea-level index points and the analysed sites of Pässe (2001), Pässe & Andersson (2005) or Nils-Olof Svensson (Lund University) were not available for this study in digital format. Therefore it was necessary to determine or digitise the coordinates of the analysed sites, and thus they were originally not accurate. The site locations were digitised according to Pässe (2001) because it was considered more accurate, but the location of the S Lithuania site was digitised 100 km farther north according to Pässe & Andersson (2005).

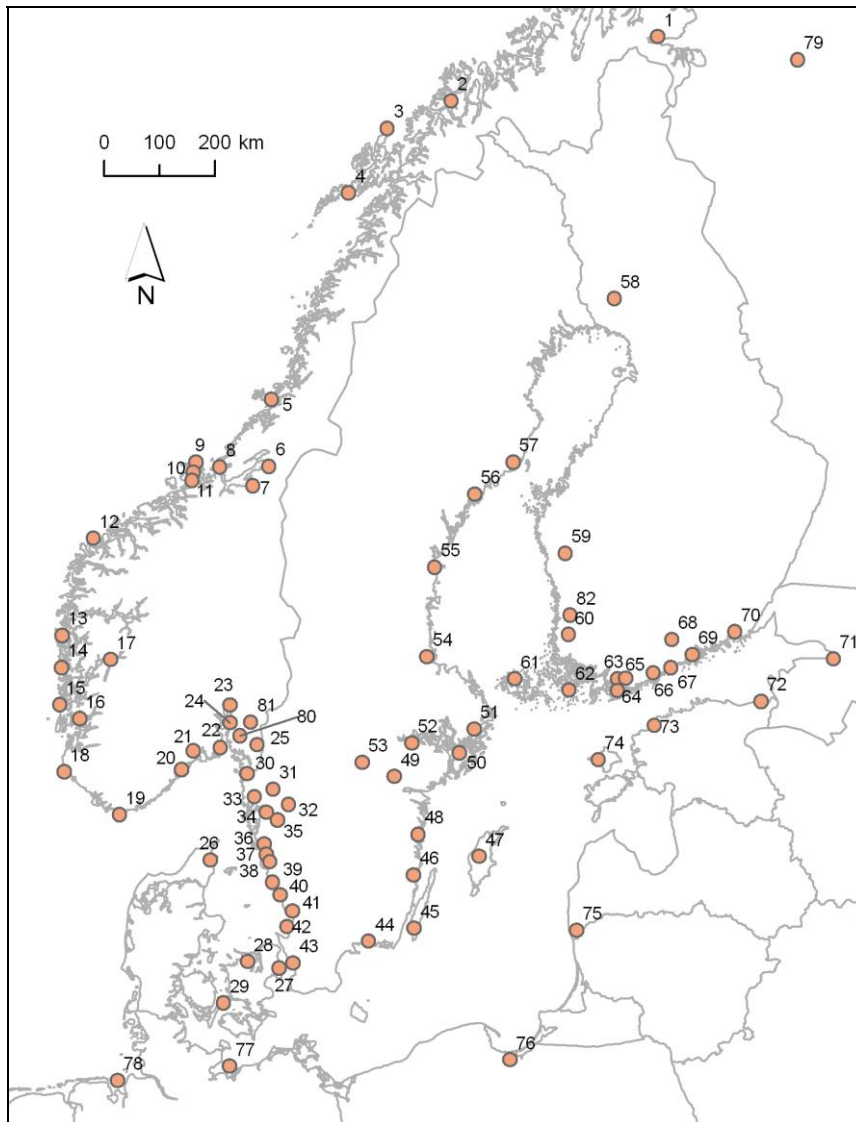


Figure 2. Map of the old sites whose isostatic uplift parameters had already been estimated. Numbering is according to Pässe & Andersson (2005), except for the following sites not included in that report: Östfold, Östfold N, and Satakunta (80, 81, and 82).

2.3 Current land uplift

Below are shown different maps of estimates of the current uplift, to give an idea of their development and the current state of knowledge. It would not be useful to show only the latest map because it will still take decades to confirm certain features in the uplift distribution. A starting point was the version by Ekman (1989), see Figure 3.

The apparent land uplift map describes the relative land uplift, i.e. relative to the sea level of the time, while absolute land uplift (crustal uplift) is measured from the centre of the Earth. Secondly, this report deals especially with glacio-isostatic uplift, which is an effect of post-glacial rebounding in Fennoscandia.

Påsse (2001) shows three more recent relative uplift map versions. The version based on his own modelling (Påsse 2001, Fig. 3-13) was partly a circular argument because the uplift variables A_s and B_s that were used for the map were calculated from the recent relative uplift itself.

In the map presented by Hokkanen (2008), shown in Figure 4, negative values outside the zero line of S' are not shown, and the reliability is weaker outside the outer contour. The map is a digitised version of the one in Koivisto (2004 p. 169), and on p. 198 is told that the map is based mostly on 1st and 2nd precision levelling. The Kajaani or Oulunjärvi anomaly is old information from 1966, which was inaccurate already back then. The Lake Ladoga anomaly, on the other hand, was originally based on Russian measurements and has not been verified. The interval between the two measurements was relatively short (20 years or so), so even small levelling errors may create anomalies. According to Koivisto (2004), the measurements in any case fit together on the Finnish side. The map ought to be updated with the 3rd levelling results (Hokkanen 2008b). The Lake Ladoga anomaly was also shown on the map by Kakkuri & Poutanen (1997). Later data does not confirm this anomaly yet, so more measurements are needed to make conclusions about its existence.

The most recent map of current absolute land uplift was provided by the Finnish Geodetic Institute (FGI). First, Poutanen (2008) sent a version used in Figure 5. It is based on a map by Ågren & Svensson (2007), which in turn is an improved version of a map based on levellings by Vestøl (2006). The data used for producing this and other current uplift maps was not checked. The JUHTA report (2007) also shows the Baltic levelling network and the Nordic uplift model NKG2005LU. Since then, Poutanen had taken Lidberg's latest Nordic Countries' GPS network results, published in his thesis (2007), and simply added about 1.5 mm/year to the values in the original land uplift map, so that the resulting uplift corresponds to the results obtained using the permanent GPS stations in measuring the distance to the centre of the Earth. The Figure 5 map version has not been previously published, but it is based on Lidberg (2007). Lidberg (2008) mentions that the absolute sea level rise (for this area of the globe) is 1.32 mm/year. Such sea level rise estimates are not constant, which is why it is best to publish absolute isostatic uplift maps.



Figure 3. The present apparent land uplift map from Eronen et al. (1995, redrawn from Ekman 1989), mm/year. Projection unknown.

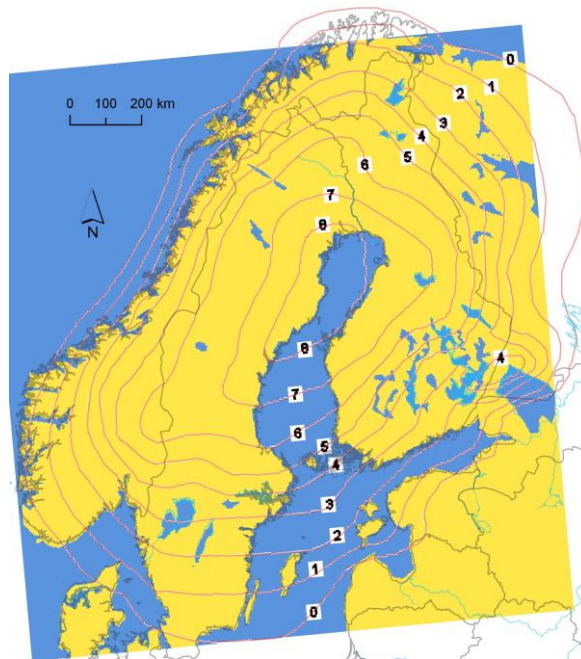


Figure 4. To get the values for absolute uplift from the centre of the Earth, 1.1 mm/yr must be added to the values shown on this map of present apparent land uplift (Hokkanen 2008, Koivisto 2004, in UTM33N).

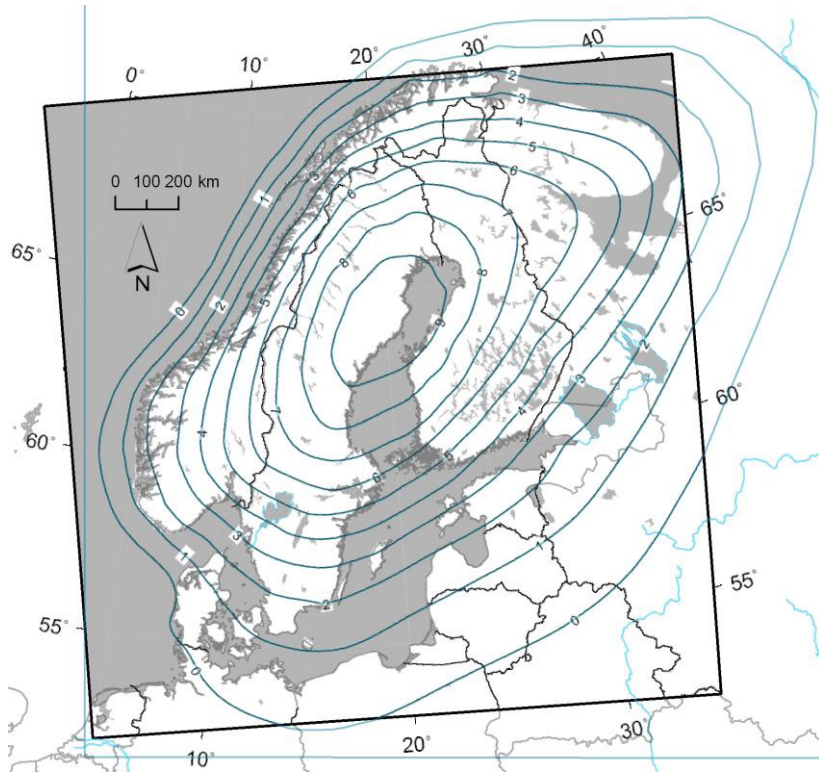


Figure 5. The map shows the absolute land uplift from the centre of the Earth, mm/year. It has been calculated using the Nordic countries' land uplift model NKG2005LU on the basis of also the absolute values given for the permanent GPS stations of Nordic countries in the thesis by Lidberg (2007). To obtain the distance from the sea surface, about 1.5 mm / year must be subtracted from the numbers on the map. The model was calculated from the original model, which was related to the sea surface but in which Lidberg's results were not included yet (Poutanen 2008 reprojected to UTM33N).

As can be seen above, various current uplift map versions exist. Poutanen ended up with the one above because NKG2005LU has also been used as a basis for the new Finnish N2000 elevation system calculations. His sole own contribution was adding the constant of 1.5 mm/year, so that the map is no longer relative, related to the sea level, but absolute. In this map, the third Finnish precision levelling results have been used. A rough estimation is that isostatic uplift values can generally be estimated with an accuracy of ± 0.5 mm/year, based on how different the values are that are produced by the various techniques (Poutanen 2008, Lidberg et al. 2008).

Figure 5 was used in the study (especially the derivative-based method), but in that figure, the value of 1.5 mm / year is not based on any particular data, and the geoid uplift was not taken into account. At the very end of the project, another slightly different version of the map was provided by FGI (Mäkinen 2009) with the values and references defined more accurately. The Figure 6 uplift map version has not been previously published either.

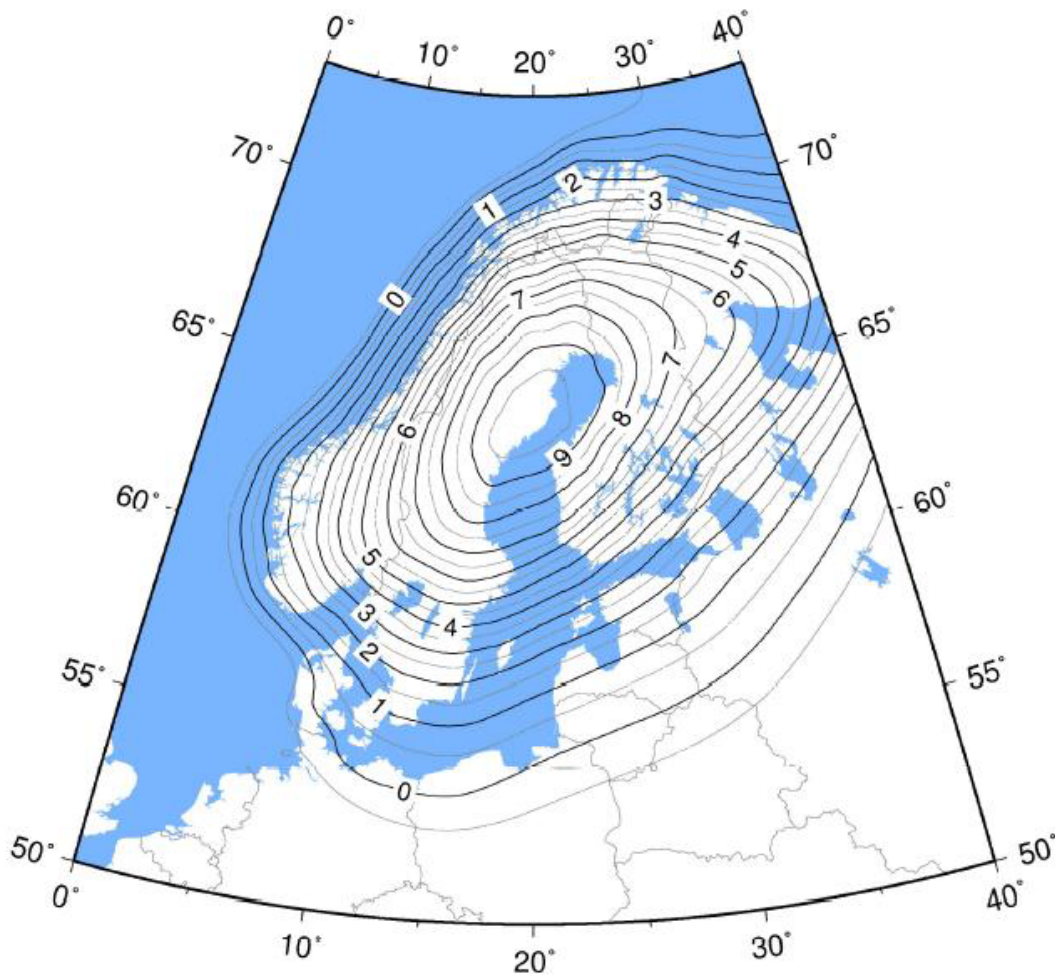


Figure 6. Land uplift model NKG2005LU (absolute) (Mäkinen 2009).

In future studies, the version in Figure 6 should be preferred. The map shows absolute uplift, i.e., uplift relative to the Earth's centre of mass in mm/yr. In the determination of the Finnish height system N2000, of the Swedish height system RH 2000, and of the European Vertical Reference Frame EVRF2007, the corresponding uplift model NKG2005LU (apparent) was used. Apparent uplift refers to the mean sea level (MSL), in the case of NKG2005LU to the MSL at (Baltic) tide gauges 1892–1991. NKG2005LU (apparent) was derived by Ågren & Svensson (2007), who merged the empirical uplift model by Vestøl (2006) with the geophysical model of postglacial rebound by Lambeck et al. (1998). In addition, we must consider uplift relative to the geoid, or levelled uplift, from NKG2005LU (levelled). Let h_{abs} , h_{lev} and h_{app} be the absolute, levelled, and apparent uplift, respectively, for NKG2005LU. Using Vestøl (2006) they are related by

$$h_{lev} = h_{app} + 1.3 \text{ mm / yr} \quad \text{Equation 1}$$

$$h_{abs} = 1.06 h_{lev} \quad \text{Equation 2}$$

The terminology (absolute, levelled, apparent uplift) is due to Ekman (1989).

3 METHODOLOGY

3.1 Shoreline displacement

Vertical shore-level displacement (S , m) in Fennoscandia is mainly due to two interactive vertical movements, i.e. glacio-isostatic uplift (U , m) of land and global or regional eustatic sea level rise (E , m). As can be seen from Figure 7, the shore-level displacement is estimated by Pässe (2001) as

$$S = U - E \text{ (m)}. \quad \text{Equation 3}$$

The difference in sign between all of Pässe's E graphs and his equations must be due to the counterintuitive definition of the term *eustatic rise* E , defined as the current absolute water level minus the level at another moment (either past or future). The $-E$ curve describes the absolute sea level measured from the centre of the Earth but uses the "current" absolute sea level as the point of reference. The negative curve $-E$ therefore describes the *rise* visually (Figure 7) but with opposite sign compared to the definition of E . About 20 000 years ago (at the Last Glacial Maximum), the global sea level was about 120 m below the present sea level. The fast eustatic rise ended about 7000 BP. U correspondingly describes the absolute isostatic uplift that has occurred from a certain moment to the present time, i.e. current absolute elevation minus any moment's absolute elevation. E , U , and S could have been originally defined as their negatives, too.

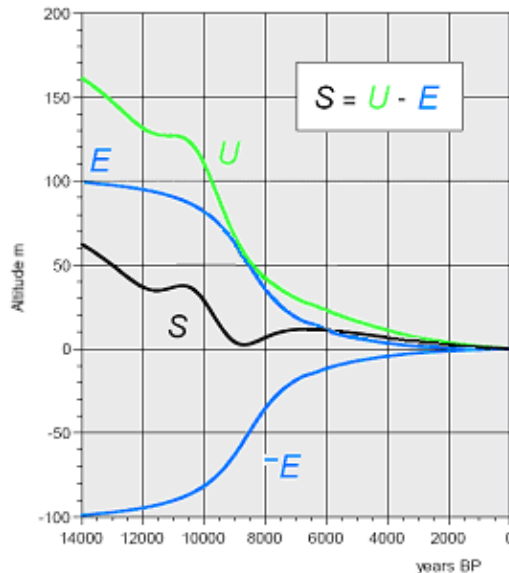


Figure 7. Eustasy (E , m) and crustal uplift (U , m) have determined shore-level displacement (S , m) in the past according to $S = U - E$. The lower curve is actually $-E$ instead of the E given by the E equations presented. The figure is modified from Pässe (2001). Note that E basically represents the global ocean level, or the level of a bay with a free connection to the ocean, and local inland water levels differ from that. It is not documented if the figure represents any particular area.

To make certain graphs more intuitive, the signs of (only) U and E as defined by Pässe (1996) were changed by Löfman (1999) and Andersson et al. (2007), and also time (t) was defined with opposite sign. Then the absolute and relative land uplift curves were plotted and compared with data by Eronen et al. (1995). In any case, the S curve and formulae originally described the relative shore level compared to the current one. For the past, S is typically positive in Fennoscandia; the shore level was higher in the past. For the future in Fennoscandia, U is negative (see Figure 42), and so is S ; the relative shore level will become lower than currently.

The shore level curves S are empirically determined for each region by using ^{14}C datings of several sites located geographically close to one another but at different altitudes. When S is known well enough from such samples, and the model for E has been decided, the most suitable absolute land uplift U parameters can be determined.

The apparent shore level displacement derivative is correspondingly

$$\frac{dS}{dt} = \frac{dU}{dt} - \frac{dE}{dt} \quad \text{or} \quad S' = U' - E' \quad (\text{m/year}). \quad \text{Equation 4}$$

Especially with derivatives, one must be careful which is the positive time axis, and one must stick with the definitions, e.g. the positive E . Originally, the U and E equations are based on a cal BP time axis. Because of the way S is defined or what it describes, the above apparent land uplift maps actually describe the change of S (i.e. S') in cal BP time but $-S'$ in chronological time (in which the maps have been drawn). E' is the almost constant but varying absolute sea level rise (with a current magnitude of considerably more than 1 mm/year, but according to the general $-E'$ models only about 0.5 mm/year on the AD axis). U' is the absolute land uplift rate related to the centre of the Earth.

Note also that S cannot be directly calculated from the rates (crustal uplift U' and sea level rise $-E'$). S is just a level in metres, relative to the current sea level. It is calculated using the contemporaneous U and E levels and is not dependent on how fast they were changing at the time.

Note that the origin of U , E , and S in the models is $t=0$ years cal BP or AD 1950, even though that date is in the past already. All the graphs have the function value 0 at the origin.

3.2 On the regional parameter estimation

The aim was to analyse and visualise the values of the isostatic uplift parameters and to find possible regional differences. The analysis was started by collecting the existing data, both maps and sea-level index points.

The less simple processes (see Figure 8) first use the threshold altitude vs. age information of the sea-level index points close to one another to estimate the shoreline displacement curve parameters (i.e. fit the curve parameters into regional subsets) for a new location. The new location is the average location of sea-level index points used,

but accuracy is not crucial. The isostatic uplift parameter value maps were interpolated from the combined set of old and new points.

The more simple processes (see Figure 9) only use some existing maps and mathematical models. By first using the maps (or models) of the crust or lithosphere depths, and the previously estimated relationships of these values with the slow component inertia factor B_s , it is possible to produce estimates for the latter. Then by selecting the maps or models of the relative land uplift S' and eustasy change E' , and defining some derivatives of such models, it is possible to produce estimates also for A_s (i.e. half of the total isostatic uplift) for the desired year. Pässe & Andersson (2005) have recently reported some alternatives for A_s and B_s maps, too.

In this study, the task was to use the more recent and more local information to improve the maps, especially within the Olkiluoto area, and to create the maps in raster formats understandable by ArcGIS and with a suitable resolution. In other words, to collect data and to produce more “land uplift curves” or to fit the equations given by Pässe (2001) to the sea-level index points of different sites and areas. Then the results were merged into the uplift parameter Table 3-1 in Pässe (1991) or his other studies, and the mentioned maps of A_s and B_s were updated.

The Pässe (2001) report structure was followed, to which was added the raster production and accuracy analysis.

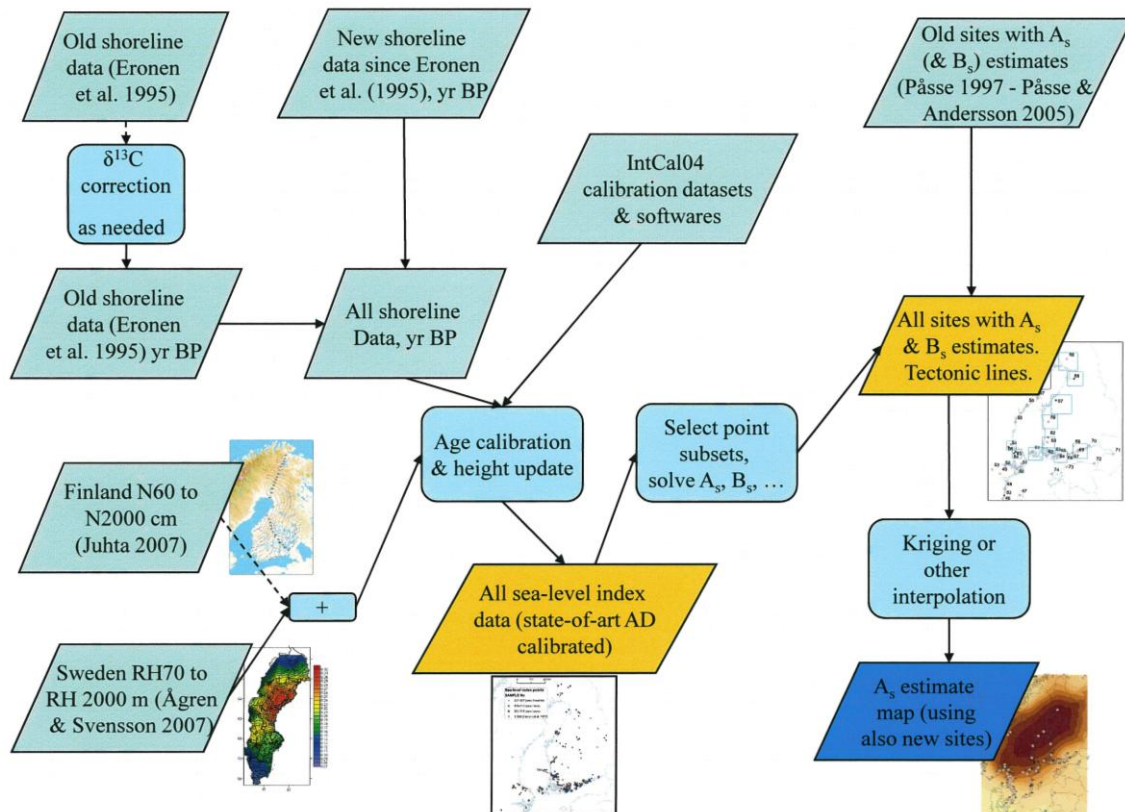


Figure 8. More comprehensive processes of the project to estimate the distribution of the isostatic uplift parameters A_s and B_s are based on shore-level displacement analyses. “All sea-level index data” does not include all the original sea-level index points available to Pässe (1997, 2001) and Pässe & Andersson (2005).

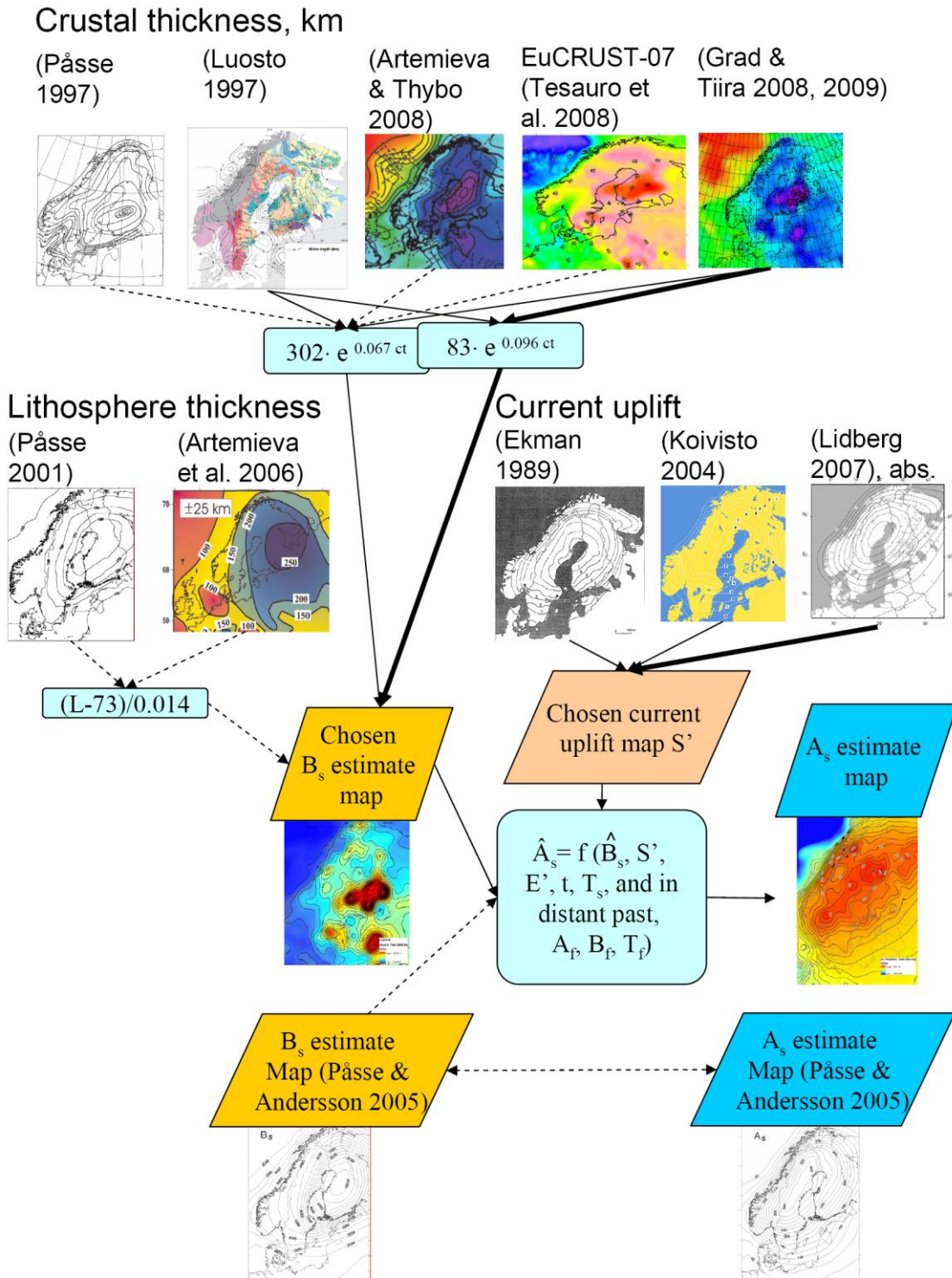


Figure 9. Simple processes to estimate the isostatic uplift parameter B_s and further A_s distribution for the desired year t . The workflows with solid lines and B_s estimate equations Pässe (1997) were tested and compared, but the final model chosen was the one with a Moho map from Grad & Tiira (2008, 2009) with its own exponential coefficients and the current uplift by Lidberg (2007, via the absolute version by Poutanen 2008), see the **bolded** arrows. Earlier reports not mentioned in the figure also include isoline map versions for estimates of parameters like A_s (Pässe 1996, 1997) and B_s (Pässe 2001).

3.3 Corrections and co-ordinate transformations

The KJ geodetic datum transformation in ERDAS IMAGINE 9.1 and older software versions is less accurate. Even though accuracy is not crucial in land uplift applications, the parameters ought to be as in version 9.2:

```
"Finnish KJ" -96.0617 -82.4278 -121.7535 -2.3276244e-5
-1.6746919e-6 6.6732664e-6 1.4964e-06
```

These values were used in the *spheroid.tab* files, e.g. for coordinate transformations with the Coordinate Calculator application of ERDAS.

The initial output coordinate system had digital (i.e. decimal) degrees geographic coordinates with the WGS 84 datum. Use of this kind of general, unprojected coordinate system enables less ambiguous transformation of the points into any map projection. UTM 33 North with the WGS 84 spheroid and datum were used for most maps. The Swedish coordinates were given in the research papers directly in degrees, minutes, and sometimes also seconds, and they were interpreted as WGS 84 datum.

In this report, the following different sets of data were used:

- The sea-level index points collected by Eronen et al. (1995). He and some others called them *sites*, but here that term is reserved for analysed results that use data from many sea-level index points.
- New lakes (after 1995)
- New mires (after 1995)
- Swedish points after 1995
- The sites reported by Pässe (These were not available as sea-level index points but as sites with already calculated isostatic uplift parameters.)

Eronen et al. (1995) have corrected the elevations according to the current uplift. The reason the corrections were necessary is that the land uplift rates vary even within relatively small areas; e.g. in southern Finland, the land uplift in the northwest part of any study area is faster than in the southeast part. A difference of one mm/year causes a 1 m effect in a thousand years. Therefore, when basin elevations are projected on the same graph, there would be reason to use corrected values. Eronen et al. (1995) used land uplift isobases of 4 and 5 mm / year (probably relative) as baselines. In areas with faster current uplift, the basin elevations were therefore corrected downwards, and correspondingly upwards in areas with smaller uplift (Miettinen 2008). The correction, $C_{baseline}$, was calculated by Eronen et al. (1995) as

$$C_{baseline} = BP \cdot (Baseline - Current) \quad \text{Equation 5}$$

It would be better to use an absolute rather than a relative baseline and to use current rates for the correction because there is no guarantee that the water level rise model is correct. It would be best to perform the correction by integrating the varying post-glacial rates, which were previously higher than currently. A correction based on fixed rates is in any case better than no correction.

The Finnish national elevation system has been typically N60, and the Swedish has been RH70. In order to combine the Swedish and the Finnish height systems, the numerical applications utilise three approaches: a rigorous approach, a bias fit, and a three-parameter fit. The differences between the values of the Swedish RH70 and the Finnish N60 systems were estimated to be -19.3 ± 6.5 , -17 ± 6 , and -15 ± 6 cm, respectively (Pan and Sjöberg 1998).

The older Finnish and Swedish elevation systems N60 and RH70 will eventually be out of date because of land uplift. Increasing international co-operation also causes pressure to choose a new vertical datum comparable to that used in neighbouring countries. It is difficult to combine the two old systems (Kallio 2008, Poutanen 1999). There is no single number or equation to transform a value from one system to another. The main differences are the following according to Poutanen (2008):

- N60's origin level is the Helsinki mean water altitude in 1960, while the Swedish RH70's is the Amsterdam null point + about 2 cm.
- N60 uses orthometric height, RH70 normal height (difference is a few cm max.).
- N60 is reduced according to annual average tide of the crust, RH70 according to zero tide, causing a N-S difference of a few cm.
- N60 land uplift has been calculated according to the year 1960, RH70 acc. to 1970

As both countries have started to use a new height system, it cannot be recommended to use the old systems. It is better to use the N2000 system in Finland and the RH2000 system in Sweden (Ågren et al. 2006), whose differences are of the order of magnitude of a millimetre. As a result, there is no need to define the differences as described above (Poutanen 2008). This report evaluated whether there is a need and whether it is possible to transform the existing old points into points in the new systems, and using which models and with what accuracy. To increase the accuracy and usability of the results even moderately, it was concluded that it would be useful to transform the old values, although some (other) original values were not always given with full accuracy or their definition was not obvious (e.g. end of isolation, but phase is unclear). Practical methods to transform the points included first digitising a height system transformation map (Juhta 2007), see Figure 10 and Figure 11.

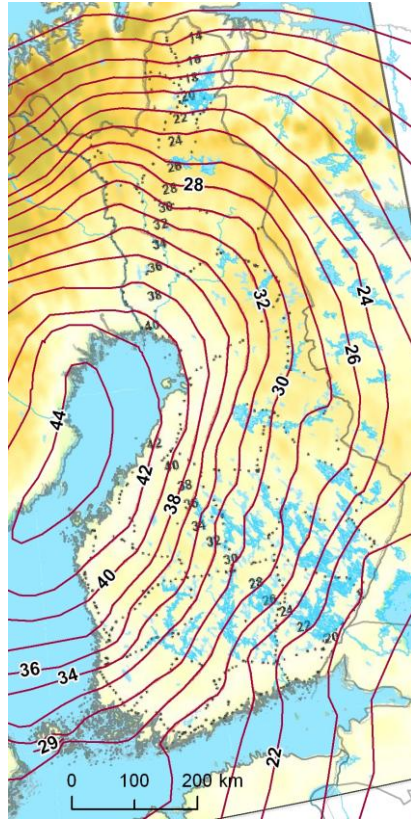


Figure 10. Differences between values in N60 and N2000 height systems in cm; amounts to be added to N60 values to get N2000 values, within Finland only. The smallest local variations cannot be seen on the map, and accuracy is better at the black precision levelling lines than between them (modified from Juhta 2007). The 44-cm curve was extrapolated in the Kvarken area (Merenkurkku) as well as the 12-cm curve in the north. Projection is UTM33N.

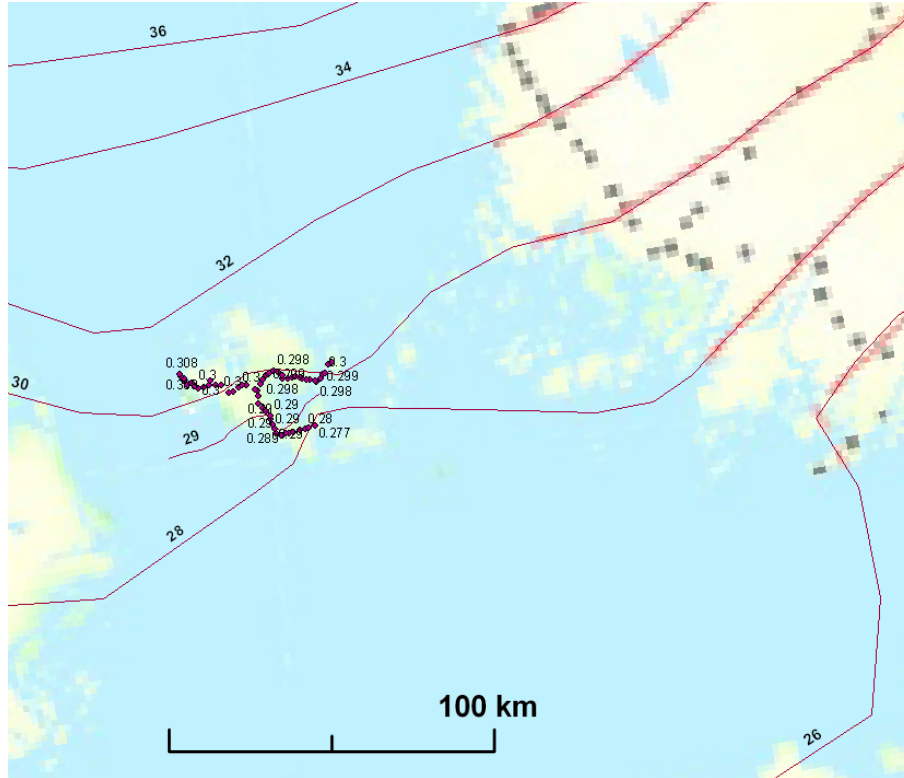


Figure 11. To get updated elevations also for Åland in this project already, the map contours were extended using the benchmark list (Lehmuskoski et al. 2008), from where the Åland points of the levelling lines P1.2, P2, and P3 were put on the map. The vector data isolines were interpolated into a “hydrologically correct” surface with the ArcGIS Topo to Raster tool, with no sink fill drainage enforcement.

The Finnish old points must have been in the N60 system because N2000 was set up recently. The Swedish points were assumed to have been in RH70, correspondingly.

The transformation ΔE between elevation systems is mostly due to the land uplift, and there the contribution of other corrections is small. If elevation system transformation is done, it thus already includes the uplift correction. Only otherwise – or for some future epoch – it is easy to calculate the uplift if the altitude reference system and the current apparent uplift rate ($-S'$) are known. A possible combined altitude correction C_{old} to be added to old observations consists of taking into consideration the elevation system update, the correction from the latest elevation system’s epoch, plus a possible differential correction.

$$C_{old} = \Delta E + (-S') \cdot (Epoch_{future} - Epoch_E) + \Delta diff \quad \text{Equation 6}$$

The correction according to the current uplift depends only on the elevation systems used, not on the publication year of the report (Lehmuskoski 2008b). The epoch difference of elevation systems is 40 years in Finland and 30 in Sweden (already taken into consideration in ΔE) but only 8 years (2008–2000) for the current epoch, so the second term was considered zero.

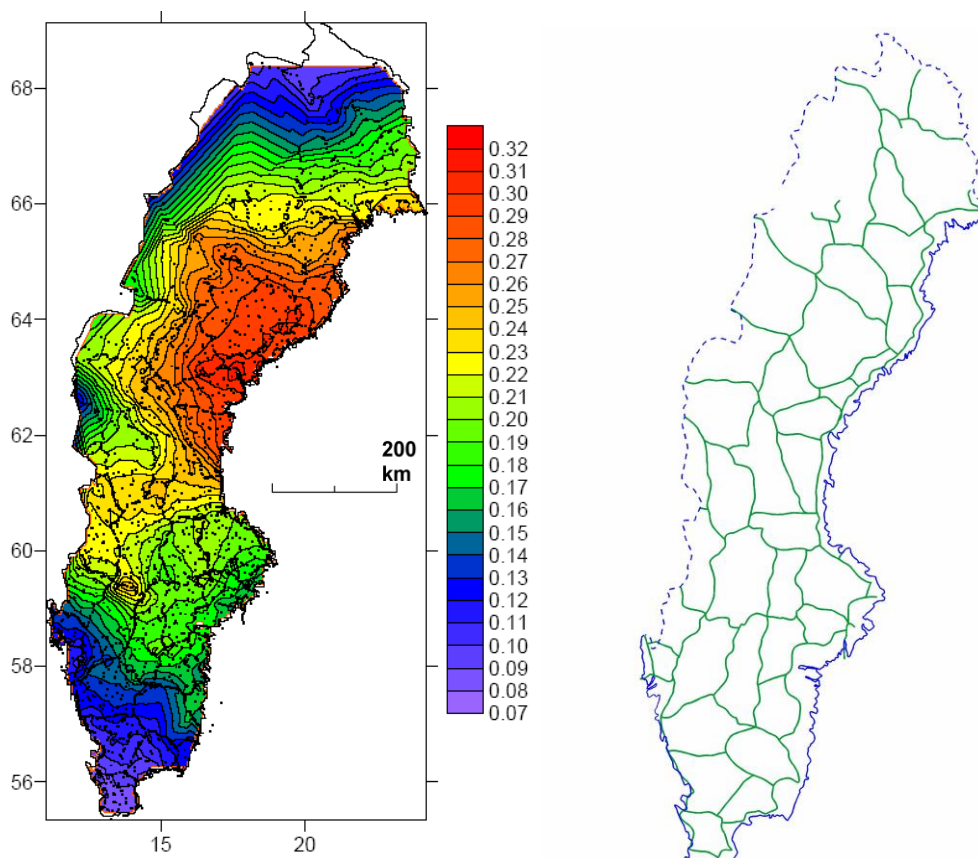


Figure 12. It was necessary to convert the points from Swedish areas separately. Differences (m) between RH70 and Swedish RH 2000 computed using the land uplift model NKG2005LU (smoothed inverse distance model with minimum of -2.00 mm/year), from Ågren & Svensson (2007).

The older Finnish threshold elevations, listed by Eronen et al. (1995) were not very old but from about 1966 onwards; therefore some land uplift had taken place, and it was debated whether it was necessary to add some height due to subsequent uplift or to transform the values from the Finnish 1960 elevation system into those of the 2000 system. A correction directly due to subsequent uplift would correspond to column 5 of Table 3 of Berglund (2005) but is rather small in a time frame of <40 years. Most often, the correction for the uplift of the last decades makes little difference for geological issues. From the 1960s until today, there was a small total uplift of, for example, >2 dm for the 6-mm/year curve in S-W Finland. The oldest Finnish points listed by Eronen et al. (1995) were simply transformed from N60 to N2000.

A rasterised version of the correction isolines was available for Sweden, see Figure 12. There also exists a map showing corrections for the different land uplift epochs and permanent tide systems (Ågren & Svensson 2007 Figure 4.7). It shows the unexplained difference between the two height systems, i.e. the differences after correcting for all known effects. But the map shown above was used alone for the transformation (Ågren 2008). The corrections defined by this map have to be added when transforming RH 70 into RH 2000. The accuracy in the sea-level index point data is not so high, and the heights could be considered to be in RH 2000 without any correction, or if desired, the maps shown could be used to get a correction. Also in the Swedish correction map the

accuracy of the RH 70 height outside the precision levelling lines is not so high. These levelling lines don't correspond to all of the dots shown but only to those that are so close together that a "line structure" can be seen in the second precision levelling (Figure 12 right image, Engberg 2008).

In this study, a raster model with 0.02 x 0.04 degree resolution was used for the Swedish height system difference, in the SWEREF 99 (ETRS 89) geographical coordinate system. It was defined as WGS 84 spheroid and ETRS 89 geodetic datum, which ought to be close. The given model fits the above map but has not been officially released by Lantmäteriet as a grid in numerical form, and it must only be used on the Swedish mainland. It is not valid on Gotland (Ågren 2008).

It was not felt to be necessary to transform height values of points in other countries such as Norway, Denmark, etc. for the present study. N2000 has been made to fit also into the Norwegian system and defined during the so-called Baltic Levelling Ring project (Saaranen et al. 2006). It is based on the Nordic countries' land uplift (LU) model (Ågren & Svensson 2007). NKG2005LU is the land uplift model for RH 2000.

The geometric corrections done are listed in Table 1. No regional differential corrections were done. The values for the vector points were taken from rasters with the ArcGIS Surface Spot tool in the UTM33N/WGS 84 coordinate system, using bilinear interpolation.

Table 1. The *geometric* corrections of the data (after which the data were used to generate the shoreline displacement curves).

Data	Geometric corrections
Eronen et al. (1995)	From C_{old} , only the ΔE term, the correction between elevation systems (see Figure 10 and Figure 11). Latitude/longitude transformation to UTM33N/WGS 84.
New Finnish points	
Swedish data	From C_{old} , only the ΔE term, the correction between elevation systems (see Figure 12). Latitude/longitude transformation to UTM33N/WGS 84.

3.4 ¹⁴C dating calibration alternatives and methods

The original ¹⁴C datings, in years BP, remain the same, but age calibration methods and curves are changing. The production of state-of-the-art age calibration for old and new sea-level index points included the important step of switching from the general functions used, e.g., by Pâsse (2001) to the IntCal04 calibration curve.

Table 2. The *dating* corrections of the data (after which the data were used to generate the shoreline displacement curves).

Data	Dating corrections
Eronen et al. (1995), Appendices 1 and 3.	$\delta^{13}\text{C}$ for the cases where it hadn't been performed already. Uncal BP age calibration in years AD with IntCal04.
New Finnish points, Appendix 4.	Uncal BP age calibration in years AD with IntCal04.
Swedish data, Appendix 4.	Uncal BP age calibration in years AD with IntCal04.

Prior to using that, $\delta^{13}\text{C}$ correction had to be done for the samples for which it had not been done already. Finding out if the $\delta^{13}\text{C}$ correction had been done already or not required some efforts for the old samples. The date corrections are listed in Table 2.

3.4.1 $\delta^{13}\text{C}$ correction

Before the necessary calibrations could be done as described later, it was useful to first perform an isotope fractionation correction. Conventional radiocarbon ages have been corrected for isotope fractionation by normalising to -25‰ PDB (Pee Dee Belemnite carbonate isotope standard) or the equivalent VPDB (Vienna PDB). CALIB software no longer supports the correction for isotope fractionation within the program for the following reason: The $\delta^{13}\text{C}$ correction depends on whether the original measurement was a $^{14}\text{C}/^{12}\text{C}$ ratio (all radiometric and some AMS) or a $^{14}\text{C}/^{13}\text{C}$ ratio (some AMS systems).

An MS Excel spreadsheet with the formulas for both types of systems is available from the CALIB website (Stuiver et al. 2006, Manual Chapter 5), for conducting the $\delta^{13}\text{C}$ correction prior to calibration. For peat material, which was also dealt with, the $\delta^{13}\text{C}$ values are not -25‰ but -27‰, and it was good to find out if the corrections had already been applied or not. A correction may make an original ^{14}C dating for example 20 years younger and add a few years to its standard deviation. It is not always known which type of ^{14}C measurement was done, and the correction is not typically mentioned in the reports. Thus, all laboratories that supplied the radiocarbon datings, giving the laboratory (analysis) number, when available, were tried to contact. Some laboratories no longer existed.

See APPENDIX 3 for the details in finding out if the $\delta^{13}\text{C}$ correction was done or not.

The Helsinki University radiocarbon laboratory calibrated the I, St, T, and TKU samples that had been $\delta^{13}\text{C}$ -corrected using CALIB software's MS Excel table at Pöyry Environment Oy.

In addition, the new samples for which the laboratory (analysis) number was not given remain unconfirmed. However, these are so recent – collected from papers from the late ‘90s or early 2000s – that it may well be assumed, or it was checked, that the values used already include the isotope fractionation correction. For example, all ^{14}C dates from the Poznan (Poz) laboratory are calculated with the correction for isotopic fractionation, using $\delta^{13}\text{C}$ values measured in the AMS spectrometer in parallel to $^{14}\text{C}/^{12}\text{C}$ ratios (Goslar 2008). All the ^{14}C datings were – after a possible $\delta^{13}\text{C}$ correction – calibrated with IntCal04.

3.4.2 ^{14}C Calibration

The reference year of radiocarbon analysis is 1950 (van der Plicht 2000):

$$\text{cal BP} = 1950 - \text{cal AD} = 1949 + \text{cal BC} \quad \text{Equation 7}$$

It was decided to use AD years in this project’s results. The BC/AD scales have no year 0, but the inaccuracy of the missing year 0 was considered negligible with negative AD values.

Modern methods for ^{14}C calibration are preferably irregular calibration curves like IntCal04 (Reimer et al. 2004) and Marine04 (Hughen et al. 2004), instead of general functions as used by Pässe (e.g. 1997, Pässe & Andersson 2005).

The ^{14}C datings with \pm error were collected from the research papers and entered into MS Excel tables. They had to be evaluated with a calibration curve (see for example Figure 13 left side) based on the most suitable calibration datasets (here IntCal04.14c) to be able to see the results and to determine the corresponding calibrated date range(s). Blaauw (2008) seems to have a similar approach in MS Excel, and his current version of the original code (Blaauw et al. 2003) does use IntCal04. Firstly, in this project a non-cumulative version of his probability distribution sheet was made. ^{14}C calibration is not so complicated, actually; for each calibrated year yr , the process just has to find the corresponding ^{14}C age $Cage_{yr}$ and the error of the calibration curve, σ_{yr} , and compare this age with the C14 age of the sample to be calibrated. The Excel code applies the error (i.e. σ):

$$\text{Error} = \sqrt{(\sigma_{\text{sample}}^2 + \sigma_{\text{yr}}^2)} \quad \text{Equation 8}$$

to the normal distribution probability density function:

$$p_x = \frac{1}{\sigma \cdot \sqrt{2\pi}} \cdot e^{-(x-\mu)^2 / 2\sigma^2} \quad \text{Equation 9}$$

giving:

$$P_{\text{sample},yr} = \frac{1}{\sqrt{\sigma_{\text{sample}}^2 + \sigma_{\text{yr}}^2} \cdot \sqrt{2\pi}} \cdot e^{-\frac{(Cage_{\text{sample}} - Cage_{yr})^2}{2(\sigma_{\text{sample}}^2 + \sigma_{\text{yr}}^2)}} \quad \text{Equation 10}$$

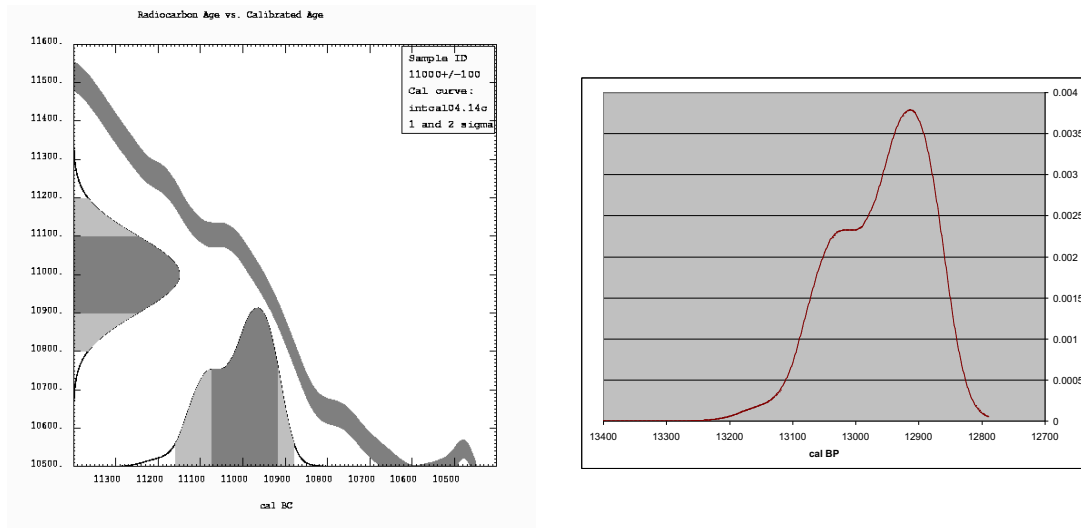


Figure 13. On the left, CALIB probability distribution of the calibrated age using a ^{14}C dating of 11000 ± 100 BP looks similar to the Excel versions tested in this project (on the right in cal BP) but a bit different from Figure 4 of Reimer et al. (2004). This is because a preliminary version of the IntCal curve was used in that original article (Reimer 2008).

Next, the resulting probability has to be plotted for every calibrated age (Blaauw 2008b). See Figure 13 for the 11000 ± 100 BP example by Reimer et al. (2004).

Instead of performing one's own calculations, one can also use published and well-tried software that performs calibration. Applications for conducting calibrations include CALIB (Stuiver et al. 2006), BCal (University of Sheffield 2008, Buck et al. 1999), OxCal (Ramsey 2008), and WinCal25. The www.radiocarbon.org site as well as Hillaire-Marcel & De Vernal (2007) and Boudin & Strydonck (2006) list such applications. In addition, the statistical software R is free, open source, and very user-friendly – once one gets the hang of it (Blaauw 2008b).

The CalPal application (University of Cologne 2008) uses not only the IntCal04 dataset, but many of its datasets may be considered subjectively modified (Hillaire-Marcel, De Vernal 2007: 205). According to Weninger et al. (2005), there are some differences even with various programs using the IntCal04 dataset but no discernible differences in the calendric output-ages (in the range of a few decades) between the test candidates (calibration programs and data sets) in the age range 0 to 11 ka ^{14}C BP. This means that for example the on-line CalPal, using the CalPal_HULU calibration curve, could suit the purposes of this study because all the data used were less than 11000 ^{14}C BP, and typically less than 8000 ^{14}C BP. However, Weninger et al.'s (2005) test was based on purely hypothetical standard errors of ± 1 . With larger standard deviations, it is not sure how large the differences would become. Secondly, only calibration using IntCal is standardised and internationally accepted.

The uncertainty of the ^{14}C date samples as well as the uncertainty of the chosen calibration curve are – and should be – taken into account during calibration. The errors of the calibration curve are usually much smaller, at least for samples that are

not too old. IntCal04's "± Error" is the uncertainty of the C14 age of the calibration curve at this time. The errors are as quoted in Reimer et al. (2004) and give the 1 standard deviation or uncertainty of 68% (Blaauw 2008b).

For example, using the 95% rule, the 2.5 and 97.5 percentiles – corresponding in effect to the minimum and maximum calibrated BP ages – could be reported. There are some traditions as to what numbers to report from calibration in this application field. On the basis of conversations with well-informed statisticians over the years, it seems best to report all 1 standard deviation or better 2 standard deviation ranges of the multimodal distribution and not only the minimum and maximum of those ranges. Better still would be to report and draw the entire calibrated distribution (Blaauw 2008b). Using the Excel approach, this would be possible even for the shoreline displacement graphs of each subset of sea-level index points. Using just one value, e.g. median or mode, is indeed very dangerous and not at all recommended – although it's often needed to do something like that e.g. for age-depth modelling (Telford et al. 2004a, b). For example Berglund (2005) reports just median values for the main ranges, and plots the lower – upper 1 and 2 sigma ranges.

Methods and applications

Age calibration or transformation from BP into AD was done with the IntCal04 dataset but two different software applications. This study first planned to use solely the CALIB Version 5.0.1 application with the intcal04.14c dataset for the northern hemisphere atmosphere, unit (1.0) laboratory error multiplier, and 0 year curve smoothing.

But the Dating Laboratory of the University of Helsinki conducted the calibrations with OxCal 4.0 and default 5-year smoothing and reported both the BP uncal and the lowest and highest limits of all the ranges of 1 σ (68.3 %) and 2 σ (95.4 %). On the other hand, each individual 1 σ and 2 σ range and the relative areas under the probability distribution are reported using CALIB, as well as the median value of the distribution function, which was used for solving the isostatic uplift parameters. CALIB's lowest and uppermost limits typically differ from the OxCal results by only some years, as it should be for the datings 0–11000 BP (Weninger et al. 2005). See APPENDIX 3 for practical CALIB issues and options finally used.

4 FORMULAE

Arctan functions have proven to be suitable tools for describing various phenomena. In certain reports (Påsse 1997, Påsse & Andersson 2005), the hyphen (-) used in some equations with multiple rows must not be interpreted as a minus sign. This may have caused some confusion in other studies.

Some of the data on which Påsse (e.g. 1997) based his isostatic uplift parameter values can be seen as shore level curve illustrations in his reports, but all the individual samples are not available as a text list. The mentioned illustrations include the markers of the data points, a theoretical curve (i.e. calculated based on the formulae and constants used) and the original curve (i.e. drawn by hand).

4.1 Eustatic rise

In Påsse (1997), the eustatic rise (E) of water level is given as:

$$E = \frac{2}{\pi} \cdot 50 \cdot \left[\arctan\left(\frac{9350}{1375}\right) - \arctan\left(\frac{9350 - t}{1375}\right) \right] \text{ (m)} \quad \text{Equation 11}$$

where the year t is in calibrated years *BP*. To get a corresponding equation with AD, the second numerator has to be transformed. By defining some new variables, E using AD gets the general form

$$E = \frac{2}{\pi} \cdot A_E \cdot \left[\arctan\left(\frac{T_E}{B_E}\right) - \arctan\left(\frac{T_E - 1950 + t_{AD}}{B_E}\right) \right] \text{ (m)}. \quad \text{Equation 12}$$

where A_E , T_E , and B_E are half of the total rise, the time of the eustatic rise's maximum rate, and the inertia factor of the rise respectively. Here, the constant 1950 isn't included in T_E but subtracted on the right side to make the equation similar to that for the model of the slow component of isostatic uplift, which is presented later. The above equation for the case in Påsse (1997) is

$$E \cong \frac{2}{\pi} \cdot 50 \cdot \left[\arctan\left(\frac{9350}{1375}\right) - \arctan\left(\frac{9350 - 1950 + t_{AD}}{1375}\right) \right] \text{ (m)}. \quad \text{Equation 13}$$

For this study, it was decided to use the Påsse (2001) model due to an agreement (Lindborg & Lind, 2006, p. 15–16) with Posiva and SKB (Swedish Nuclear Fuel and Waste Management Co) to use basically the equations and constants from that report. For (Påsse 2001), the constants had been somewhat adjusted:

$$\begin{aligned}
E &\cong \frac{2}{\pi} \cdot 56 \cdot \left[\arctan\left(\frac{9500}{1350}\right) - \arctan\left(\frac{9500 - t}{1350}\right) \right] \\
&= \frac{2}{\pi} \cdot 56 \cdot \left[\arctan\left(\frac{9500}{1350}\right) - \arctan\left(\frac{9500 - 1950 + t_{AD}}{1350}\right) \right] \quad (\text{m}) \quad \text{Equation 14}
\end{aligned}$$

The various $-E$ models are plotted in Figure 14. Pässe & Andersson (2005) further adjusted the constants and included two additional fast E components that are noticeably effective before 10 000 BP. The negative term is meant to model into E the slowing down of the melting of the glaciers, which is an effect of the cold Younger Dryas stadial. It occurred about 12840–11440 BP, which would be about AD -13205 to -11340 (15155 to 13290 cal BP). The two additional components were centred on the dates 11500 and 12500 cal BP, and their sum has a local minimum (or the sum of their negatives has a positive peak >8 m) at 12000 cal BP. The numbers in the model therefore show some delay from the Younger Dryas as calibrated with IntCal04 above. Pässe & Andersson (2005) used the polynomial time calibration, and possibly a localised version of the Younger Dryas.

$$\begin{aligned}
E_{05,t} &= \frac{2}{\pi} \cdot 61 \cdot \left[\arctan\left(\frac{9600}{1500}\right) - \arctan\left(\frac{9600 - t}{1500}\right) \right] \\
&\quad - \frac{2}{\pi} \cdot 7 \cdot \left[\arctan\left(\frac{11500}{350}\right) - \arctan\left(\frac{11500 - t}{350}\right) \right] \\
&\quad + \frac{2}{\pi} \cdot 8 \cdot \left[\arctan\left(\frac{12500}{350}\right) - \arctan\left(\frac{12500 - t}{350}\right) \right] \quad (\text{m}) \quad \text{Equation 15}
\end{aligned}$$

$$\begin{aligned}
E_{05} &= \frac{2}{\pi} \cdot 61 \cdot \left[\arctan\left(\frac{9600}{1500}\right) - \arctan\left(\frac{9600 - 1950 + t_{AD}}{1500}\right) \right] \\
&\quad - \frac{2}{\pi} \cdot 7 \cdot \left[\arctan\left(\frac{11500}{350}\right) - \arctan\left(\frac{11500 - 1950 + t_{AD}}{350}\right) \right] \\
&\quad + \frac{2}{\pi} \cdot 8 \cdot \left[\arctan\left(\frac{12500}{350}\right) - \arctan\left(\frac{12500 - 1950 + t_{AD}}{350}\right) \right] \quad (\text{m}) \quad \text{Equation 16}
\end{aligned}$$

Pässe (1997, 2001) and Pässe & Andersson (2005) explained why they used different E models from the global ones by Fairbanks (1989) and Edwards (1993). Recently, new E curves have been defined too. They differ not very much from those of Fairbanks and Edwards. Pässe has estimated also the E component from the Baltic Sea shore data, fitting also that parameter to his data, while Fairbanks and Edwards dealt with the ocean levels. This may have created the different approach; the Baltic Sea level does not accurately follow the ocean level because sea water flow is limited in the narrow straits of Denmark, and on the other hand, the role of water coming into the basin (i.e. precipitation, runoff) is much more significant. In addition, due to land uplift, the Baltic Sea basin keeps changing.

Nevertheless, in this study it was decided to include the Ancylus phases described by Pässe (2001) and Pässe & Andersson (2005) in the water level model, either by modelling them into E or by making corrections elsewhere. The eustasy E literally describes global sea level variations, so for a *lake* area, the modification should be considered as a correction only and not as a part of E . Ancylus Lake transgression and regression period is one of the Baltic Sea phases, which are described by Tikkanen & Oksanen (2002).

The range of 8300–9600 uncal BP (Pässe 2001 Fig. 5-2) corresponds to about 9350–10915 cal BP. The present study in any case used the range of about 9100–10800 cal BP according to Pässe & Andersson (2005 Fig. 15, according to which the present study defined a correction in AD values, see Figure 15). Instead of IntCal04, Pässe & Andersson still used a simpler mathematical formula to calibrate the dates. The Ancylus Lake had a maximum relative surface height of 15 m above (the past) sea level in about 10450 cal BP (i.e. AD -8500).

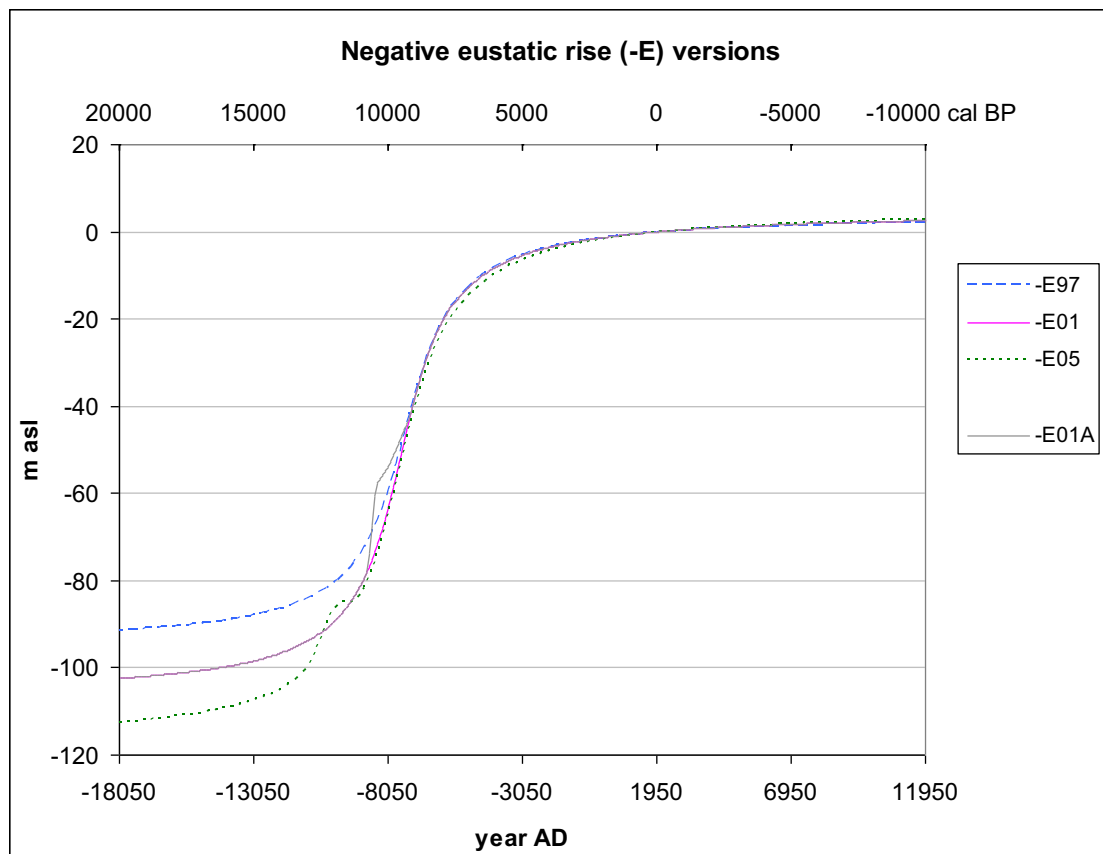


Figure 14. Versions of negative eustatic rise ($-E$) based on reports by Pässe (1997, 2001, Pässe & Andersson 2005). The curves are negatives of the values that the E equations give, and negative $-E$ here means m below the current sea level. The negative eustatic rise version $-E_{01A}$ is based on the report by Pässe (2001), to which has been added the Ancylus correction based on Degerfors and the Great Belt areas (Pässe & Andersson 2005).

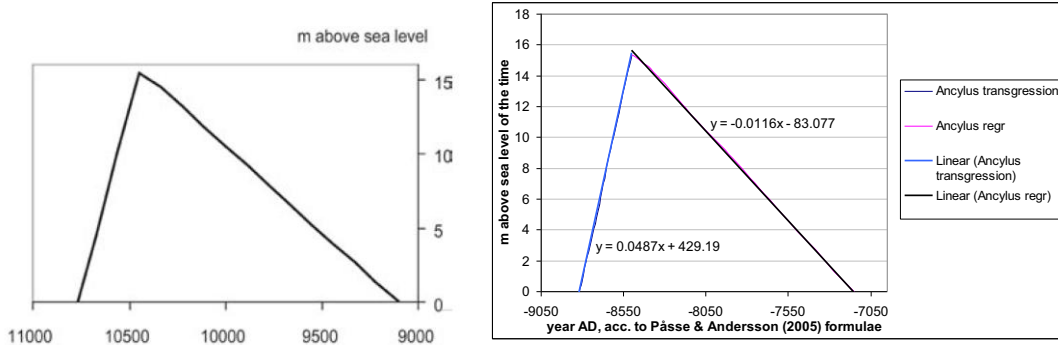


Figure 15. On the left, calculated levels for the Ancylus Lake in cal BP (Pässe & Andersson 2005). It is interpreted to describe the levels as m above the contemporaneous sea level. The Ancylus correction is based on that graph, but defined in AD (right).

The difficulty of analysing the Ancylus Lake is that even though the water surface was never tilted, the Ancylus shoreline keeps on tilting and the shoreline effects continue to vary locally. Because the isostatic uplift (U) is modelled locally and separately from the water level, the altitude (m asl) of the Ancylus Lake's shoreline is now different in different areas. The so-called fast uplift occurred during the same period. Due to the faster isostatic uplift in the north parts of the Baltic Sea, the land tilted, and especially the south parts experienced a fast increase of apparent lake shoreline elevation. In the northernmost parts, the effects of tilting were bigger, and the transgression therefore cannot be seen. For example within Finland, the effect of tilting is about 1 m in the Espoo area, and about 5 m in SE Finland. As seen in Fig. 13 B of Pässe & Andersson (2005), Bornholm was connected to north Germany before the Ancylus Lake phase, and now there is up to 60 m of water in that area. In areas which were by the ocean, like the west coast of Sweden, the Ancylus Lake should not be considered at all, but the E model (some global version) as such.

In the Bothnian Sea area, the tilting effects on the Ancylus Lake levels are clearly less than one metre. Pässe's (2001) or Pässe & Andersson's (2005) Ancylus models ought to apply if used for a correction in that area. In the studies mentioned, especially the Swedish areas of Forsmark and Oskarshamn were of interest.

The Ancylus Lake shoreline is now below the current sea level in the southern part of the Baltic Sea and above it in the northern part. In Finland, the highest altitude of the ancient shorelines is the Ancylus Lake shore in Vammavaara, Tervola, 219 m asl.

At least the first two hundred years or so of the regression could have been modelled separately, included here in the linear total regression model for simplicity. The E of Pässe (2001) with the Ancylus correction (for the Ancylus Lake areas only) is given here only using t_{AD} :

$$E_{01A} \cong \frac{2}{\pi} \cdot 56 \cdot \left[\arctan\left(\frac{9500}{1350}\right) - \arctan\left(\frac{9500 - 1950 + t_{AD}}{1350}\right) \right] \\ - 0.0487 \cdot t_{AD} - 429.19 \quad , -8817 < t_{AD} \leq -8498 \quad (m) \quad \text{Equation 17} \\ + 0.0116 \cdot t_{AD} + 83.077 \quad , -8498 < t_{AD} < -7150$$

As the reference was the sea level, the Ancylus correction does not replace the E curve (or the first row of the formulae) in the mentioned ranges, but is added to it. The sign of correction must be so that the water level has risen faster than it did in the ocean. The regression has not been as strong as the sea level rise, so the water has always been rising in the Ancylus Lake area (to which the correction is to be applied only), i.e. the E derivative is always negative. Even though the land has tilted below the lake, the crustal uplift is modelled by other components than E , which can be modelled separately and is not tilted relative to the global ocean level. It was not considered necessary to describe the Ancylus Lake area as a function of time.

Using the equations above, the anomaly due to the Ancylus correction in the 2001 E curve is on the same side as the one in the 2005 curve, although the correction describes faster water level rise, and at least the negative component of the 2005 model describes the slower phase of the rise. Either this indicates some error or possibly the tail of their E curve has not been considered as essential as the more recent part. As shown below, the early versions of the model of fast isostatic uplift also modelled especially the most recent stages correctly, whereas the period of wider ice covering was less emphasised. Pässe (1997 p. 32) talks about glacio-isostatic subsidence (of soil) and Younger Dryas transgression on the Norwegian and Swedish west coasts. But as transgression means *relative* rise of the water level, the additional terms of their 2005 E model can not model that but the *absolute* water level.

Litorina transgression was another phenomena that took place and caused transgression especially in the southern and eastern Baltic Sea area about two thousand years after the Ancylus transgression and regression phases had started.

4.2 Slow component of isostatic uplift

Previously, exponential models have been used for Fennoscandian isostatic uplift. Pässe (1996) introduced the *arctan* functions, the parameters of which are explained here. Corresponding models and parameters are also used in the E models above.

The model of Pässe (1997) indicated that there are two mechanisms involved in glacio-isostatic uplift, one slow and the other fast. The main uplift, still in process, acts slowly. *Arctan* functions have proved to be suitable tools for describing the slow glacio-isostatic uplift. The time of maximal uplift rate is isochronous, meaning that the slow uplift occurs simultaneously in all Fennoscandia in an interactive movement. For slow isostatic uplift, there is a relationship between the rate of decline and the crustal thickness. In areas with greater crustal or lithospheric thickness, the rate of decline of the glacio-isostatic recovery is lower than in areas with thinner crust (Pässe 1997).

The slow component of isostatic uplift is defined by Pässe (1997) as

$$\begin{aligned}
 U_s &= \frac{2}{\pi} \cdot A_s \cdot \left[\arctan\left(\frac{T_s}{B_s}\right) - \arctan\left(\frac{T_s - t}{B_s}\right) \right] \\
 &= \frac{2}{\pi} \cdot A_s \cdot \left[\arctan\left(\frac{T_s}{B_s}\right) - \arctan\left(\frac{T_s - 1950 + t_{AD}}{B_s}\right) \right] \quad (\text{m}), \quad \text{Equation 18}
 \end{aligned}$$

here also using AD. The constant T_s can be considered effectively fixed. Decreasing merely T_s by even 1000 years naturally produces a zero difference now (because now $t \approx 0$ or $t_{AD} \approx 1950$), but an effect of about 4 m in AD 10000. Various component parameters are listed in Table 3.

T_s is the interval from the time of the slow isostatic uplift's maximum rate to the present. In the equations, T_s and time t are in calibrated years BP, not conventional calendar years. A_s (m) is the download factor, or half of the total isostatic uplift taking place. B_s is the inertia factor (year^{-1}), which determines how steep the function is. All curves pass through the cal BP origin (i.e. AD 1950, not in fact the present year). Note that in Figure 16, only B_s varies; in reality, when B_s is smaller (or the total isostatic uplift takes place more quickly) at the edges of the depressed area, A_s also becomes smaller there. The centre of Fennoscandia has a larger B_s , meaning that the uplift will last longer in the future, and A_s is correspondingly bigger there. A_s and B_s are therefore linearly correlated (but maximums are not necessarily in the same area, see Pässe & Andersson 2005 Fig 8).

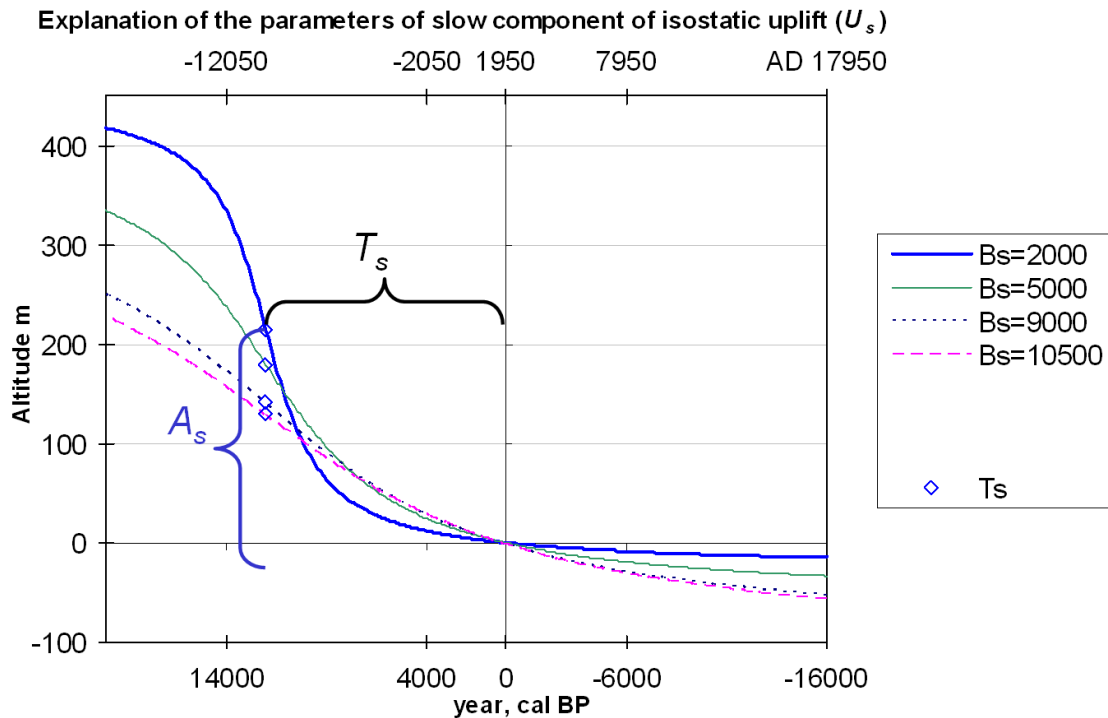


Figure 16. The definitions of the slow isostatic uplift parameters are only visualised here. T_s is here 12000 years cal BP and $A_s=240$ m for each curve (but its vertical position highlighted only for the case of $B_s=2000 \text{ year}^{-1}$). T_s is in cal BP. The tail on the right determines the total remaining slow uplift.

The total remaining slow uplift varies even if A_s and T_s remain the same and only B_s varies. This is because the origin is in different locations on the curves relative to the symmetry point of the arctan function. Note that if B_s becomes smaller, so does the remaining uplift. This may be counterintuitive; even though most of the whole uplift takes place or has practically already taken place more quickly than it would have done with a higher B_s value, the remaining total uplift is going to take place more slowly.

Ice vanished from the whole modelling area between 10300 and 9000 BP (i.e. about 12150–10200 cal BP), see Figure 17. Therefore the maximum isostatic uplift rate may have occurred at about that time, too. But as crustal uplift or depression takes place with a delay after each glacial load change, a smaller cal BP constant T_s could be justifiable. The delay is due to the slow viscous flow mechanism and flow velocity that has been concluded to govern the development of crustal changes in time. Both the ice thickness and the duration of the glacial load are very important for the crustal changes (Morén & Pässe 2001).

Table 3. Development of the parameters of the slow isostatic uplift component.

	T_s (cal BP)	<i>Olkiluoto</i>	
		A_s (m)	B_s (year ⁻¹)
Pässe (1996)	12500	245	9500
Pässe (1997)	12500	265	8600
Pässe (2001)	12000	258	7600
Pässe & Andersson (2005)	12000	240	9000

Estimates of A_s and B_s , the other two parameters of the slow component of isostatic uplift, vary regionally, unlike estimates of T_s . The reasons for differences between the estimate versions is not so obvious for the slow components, but it has to do with the iterative definition of local values according to the new research. The differences between slow uplift models for the time 10 000 years AP are less than 1 m. The various estimate versions of the slow land uplift component at the Olkiluoto site are presented in Figure 18. For the slow uplift models, the version by Pässe (2001) was the reference in this study.

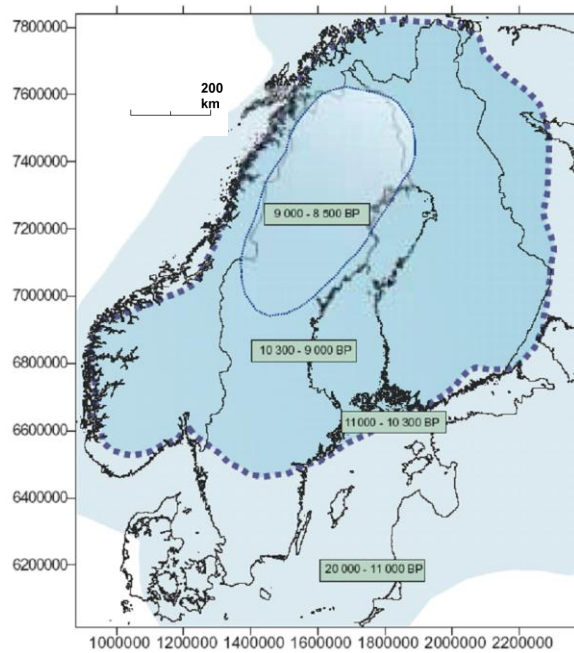


Figure 17. T_s determination can also be based on ice recession (modified Figure 1-5 of Pässe 2001). Swedish map projection.

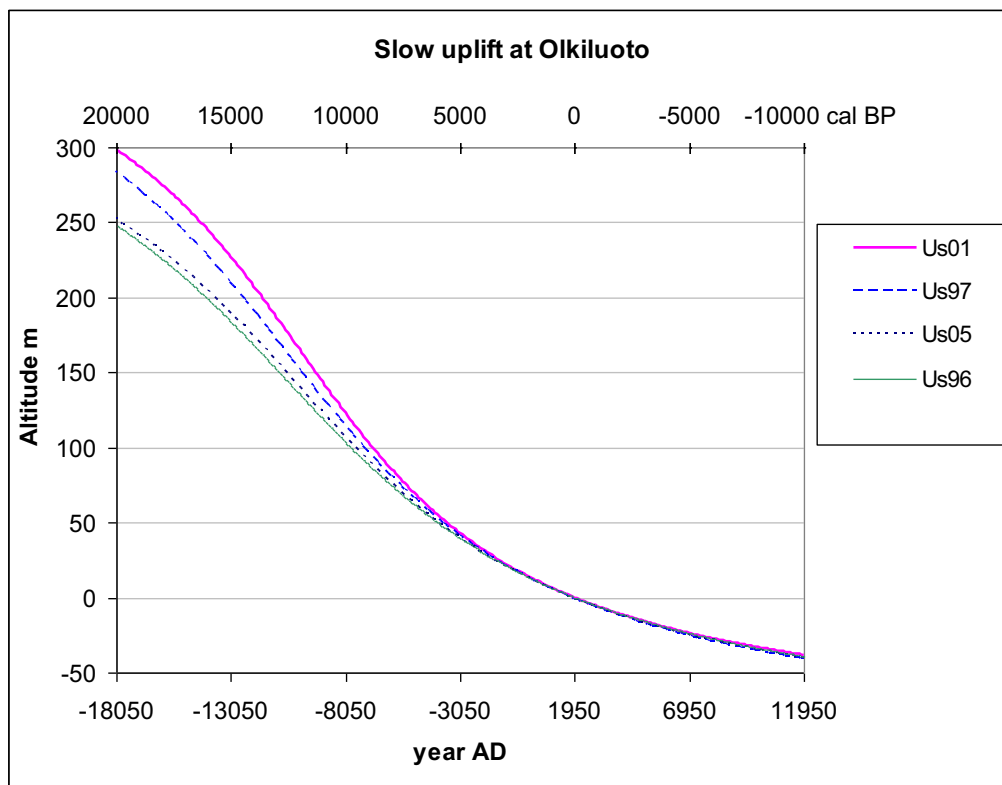


Figure 18. The slow component of isostatic uplift at the Olkiluoto site, according to various reports by Pässe (1996, 1997, 2001 and Pässe & Andersson 2005 respectively).

4.3 Fast isostatic uplift component and total uplift

In this study, there was not much interest in the very distant past. However, some differences between various models of the fast component of isostatic uplift were analysed. The fast uplift took place before about 10300 BP and probably only lasted 1000–2000 years. The older models of fast isostatic uplift were based on the normal distribution

$$U_f = A_f \cdot e^{-0.5 \left(\frac{t-T_f}{B_f} \right)^2} = A_f \cdot e^{-0.5 \left(\frac{1950-t_{AD}-T_f}{B_f} \right)^2} \quad (\text{m}) \quad \text{Equation 19}$$

and have practically no influence on estimating current or future land uplift. The time of the fast uplift's maximum rate (T_f) and the time t are in calibrated years BP (cal BP). B_f controls the duration of the fast uplift.

Later, Pässe & Andersson (2005) started using an *arctan*-based model for the fast component too. According to this kind of a model, the fast component has a strong effect *before* the deglaciation; in other words, the model proposes that the fast component is strong already before that period. This is probably correct because the glacier was getting thinner although not yet disappearing. This latest fast component version (applied as such, without recalculating with data time-calibrated with the latest methods) has only a little influence on estimates of the future land uplift; the difference between the estimate of all others and the 2005 fast uplift model for the time 10 000 AP is about 1.6 m (see Figure 19). None of the fast component models is meant for future prediction. Pässe & Andersson (2005) also introduced modelling of the fast component parameter B_f as a function of A_f instead of keeping it as an independent one. In both models, A_f controls the magnitude of the fast uplift. The fast component parameters are nevertheless used in two ways because the models are different. The parameter values in the 2005 model – at least A_f and B_f – are not perfectly comparable with those in the previous models.

$$U_{f05} = \frac{2}{\pi} \cdot A_f \cdot \left[\arctan \left(\frac{T_f}{6.6 \cdot A_f + 335} \right) - \arctan \left(\frac{T_f - t}{6.6 \cdot A_f + 335} \right) \right] \\ = \frac{2}{\pi} \cdot A_f \cdot \left[\arctan \left(\frac{T_f}{6.6 \cdot A_f + 335} \right) - \arctan \left(\frac{T_f - 1950 + t_{AD}}{6.6 \cdot A_f + 335} \right) \right] \quad (\text{m}) \quad \text{Equation 20}$$

Figure 19 presents the fast isostatic uplift component at the Olkiluoto site. Various estimate versions of the fast component parameters are listed in Table 4.

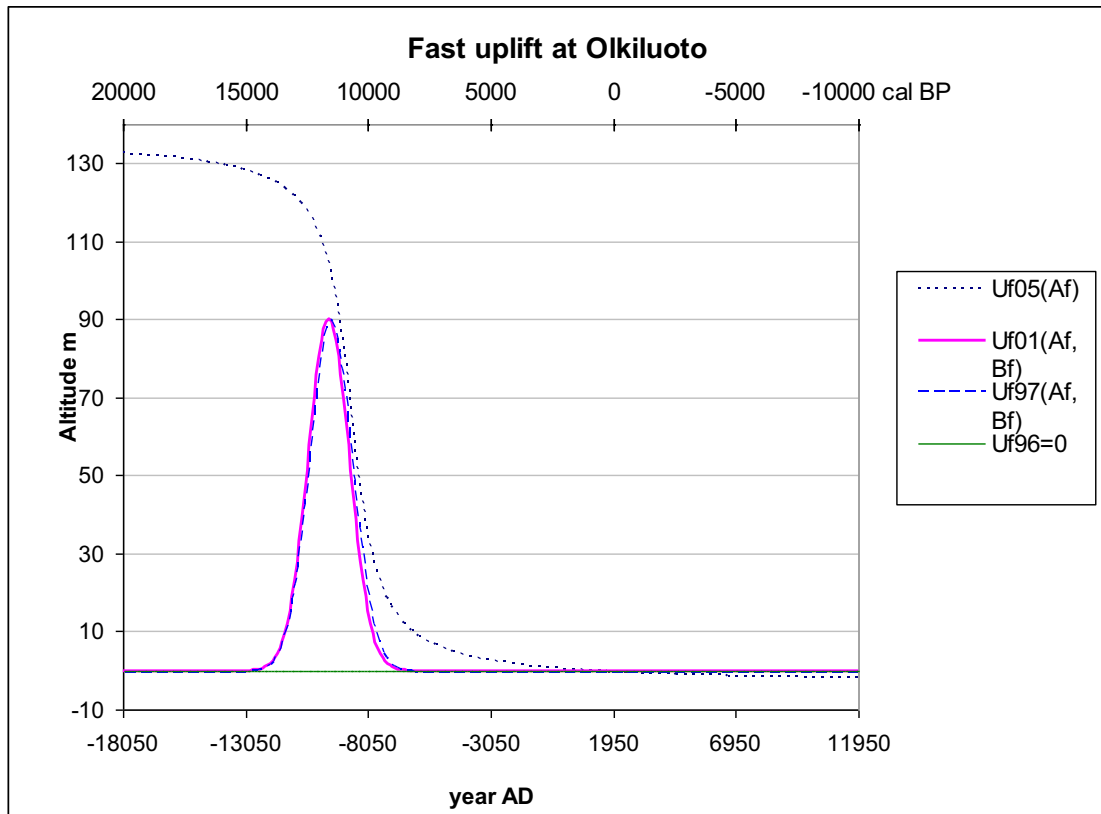


Figure 19. The fast isostatic uplift component at the Olkiluoto site, according to various reports by Pässe (1996, 1997, 2001 and Pässe & Andersson 2005 respectively). In the 1996 report, no fast component variables were determined.

Table 4. Development of the fast isostatic uplift component's parameters at Olkiluoto. Note the two ways of using the fast component parameters. The 2005 report uses an arctan-based model.

	T_f (cal BP)	A_f (m)	B_f (year ⁻¹)
Pässe (1997)	11500	90	900
Pässe (2001)	11600	90	850
Pässe & Andersson (2005)	10650	70	$6.6 \cdot A_f + 335 = 797$

The total isostatic uplift is the sum of the slow and fast components:

$$U = U_s + U_f \quad \text{Equation 21}$$

Figure 20 presents the total isostatic uplift at the Olkiluoto site.

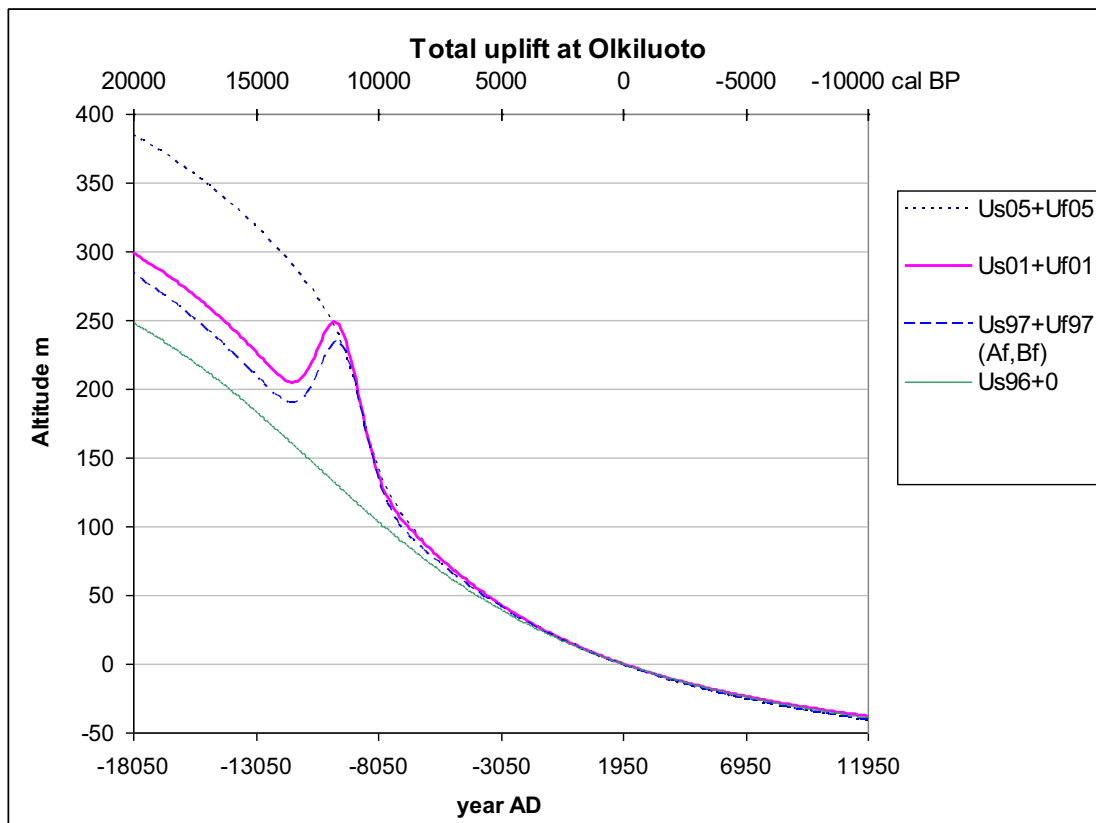


Figure 20. The total isostatic uplift at the Olkiluoto site, according to reports by Påsse (1996, 1997, 2001 and Påsse & Andersson 2005). It is the sum of the slow and fast uplift components.

5 CRUSTAL AND LITHOSPHERE THICKNESSES

5.1 Crust and definitions

The course of isostatic land uplift is nowadays mostly dependent on the declining factor B_s rather than the factor A_s , defined as half of the total uplift (Påsse 2001). The relationship between the B_s parameter of isostatic land uplift and the crustal thickness ct in km was defined by Påsse (1997) as

$$B_s = 302 \cdot e^{0.067 \cdot ct} \text{ (year}^{-1}\text{)}. \quad \text{Equation 22}$$

An alternative to using crustal thickness would be to use the lithosphere thickness. On the Earth, the **lithosphere includes not only the crust but also the uppermost mantle**, which is joined to the crust across the Mohorovičić discontinuity (Moho), see Figure 21. Seismic velocity increases clearly at the Moho boundary. Underneath the lithosphere is the weaker, hotter, and deeper asthenosphere, which is part of the upper mantle. The division of Earth's outer layers into lithosphere and asthenosphere should not be confused with the chemical subdivision of the outer Earth into mantle and crust. All of the crust is in the lithosphere, but the lithosphere generally contains more mantle than crust. The mantle is between the crust and the core.

The crust as the uppermost layer reaches depths of a few tens of km. It is thinnest (8 km) under the oceans and thickest under the continental mountain areas. Europe's crust shows an astonishing diversity: for example the crust under Finland is as deep (maximum about 60 km) as one only expects for crust under a mountain range such as the Alps. The lithosphere thickness is about 100 km. The lithosphere consists of tectonic plates, and the edges of the plates are most interesting. The Fennoscandian crust has been investigated e.g. by Wang (1998).

One of the models used to assess crustal stability uses the concept of isostasy, which describes the state of gravitational equilibrium existing between the Earth's lithosphere and asthenosphere. This is essentially the same as saying that the tectonic plates "float" at an elevation corresponding to their thickness and density and that buoyancy forces cause adjustments in the level of the terrain. These forces tend to compensate any instability between the Earth's lithosphere and asthenosphere, i.e. restore gravitational equilibrium between them. This state can experience temporal variations due to e.g. tectonic forces. Kuusisto (2007) describes how the Fennoscandian shield's state is temporally and locally affected, especially by the glaciation cycles or processes, the so-called glacio-isostatic adjustment of the crustal level. The load caused by glaciation pressed the crust downwards, and the crust has been recovering (or rising) since deglaciation.

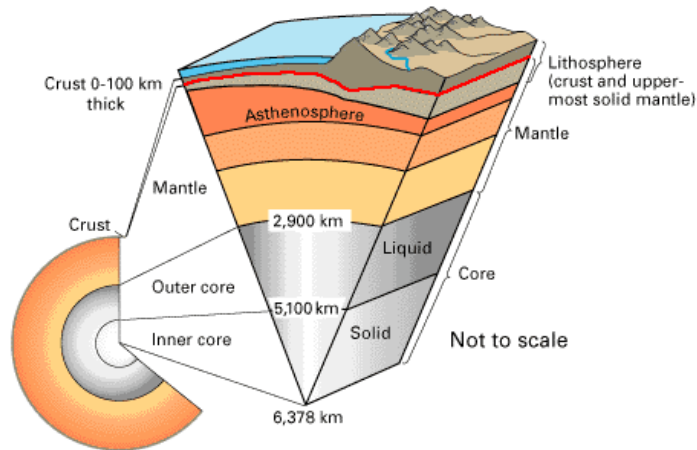


Figure 21. The thickness of the crust is also called the Moho depth (the red line). The lithosphere is thicker than the crust and also includes the uppermost mantle (USGS and Geology.com).

The structure and the properties of the lithosphere and asthenosphere are linked in a complex process of tectonic evolution. Not only thickness, but also thermal sources and flow, plate tectonic movements, rigidity (elasticity, described as density and P wave velocity), convection in the mantle, and stress fields may define the regions as being active or passive in a tectonic sense.

Precision levelling results are not available for the distant past. Recent levelling surveys have indicated that block regions of the crust are moving potentially along tectonic lines, with respect to others, in up- and downward directions. This may be generated by a stress field, e.g. the compressional forces of mid-Atlantic ridge expansion. The form of the geoid is expected to be modified due to glacial loading and rebound.

Påsse (1997) described the A_s parameter's areal distribution according to the information available at the time (Figure 22) and also showed the crustal thickness map, which has the connection to B_s described above (Figure 23).

Luosto's (1997) crustal thickness (Figure 24) is a seismic measurement result and it was considered more accurate than that calculated by Påsse (1997).

Recent European Moho depth models have been compiled by, e.g., Ziegler & Dèzes (2006), not showing Fennoscandia fully, Artemieva & Thybo (2008), Tesauro et al. (2008a, b), which is the EuCRUST-07 model, and by Grad & Tiira (2008, 2009), seen in Figure 25.

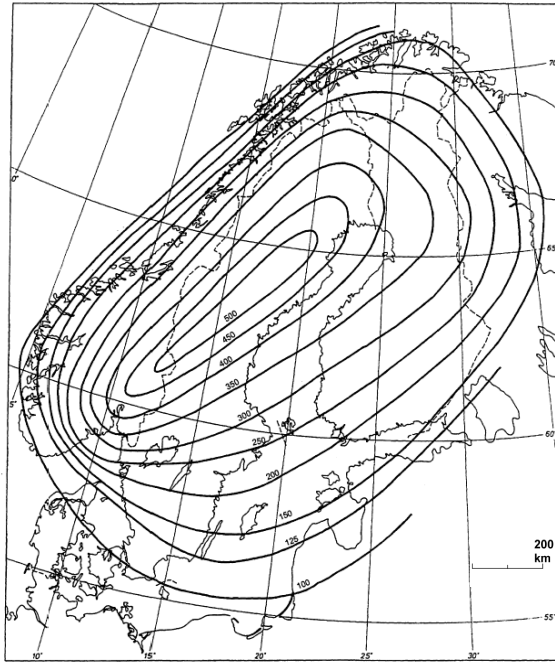


Figure 22. The A_s (m) values (Påsse 1997 Figure 3-8).

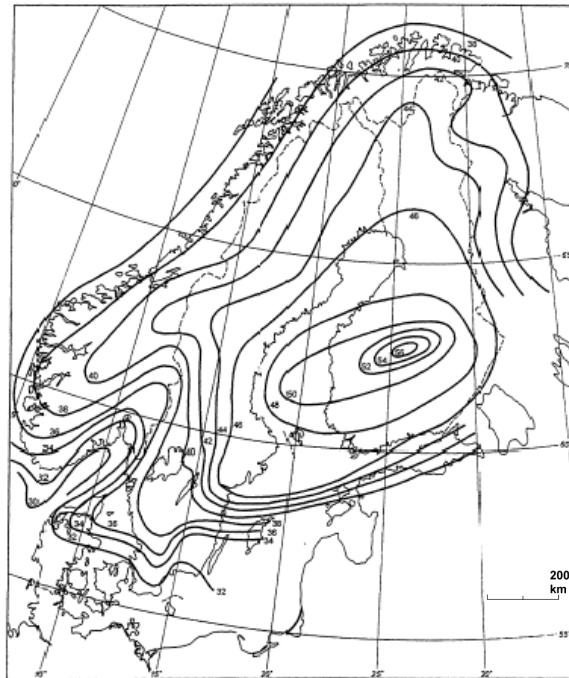


Figure 23. The crustal thickness in km (Påsse 1997 Figure 3-11). Using the above equation and constants, a B_s map could also be calculated from this very map, but it wasn't done in this study.

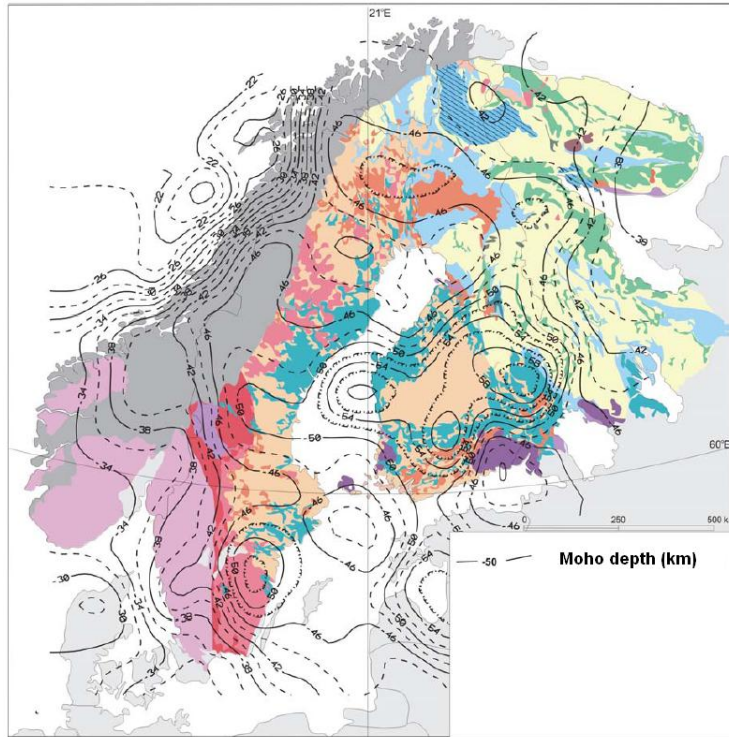


Figure 24. The crustal thickness (i.e. the Moho depth) in km (Luosto 1997, used by Lahtinen et al. 2005 and Kuusisto 2007). One B_s map version was calculated using this. Values outside the curves are naturally quite unreliable. Projection not known exactly.

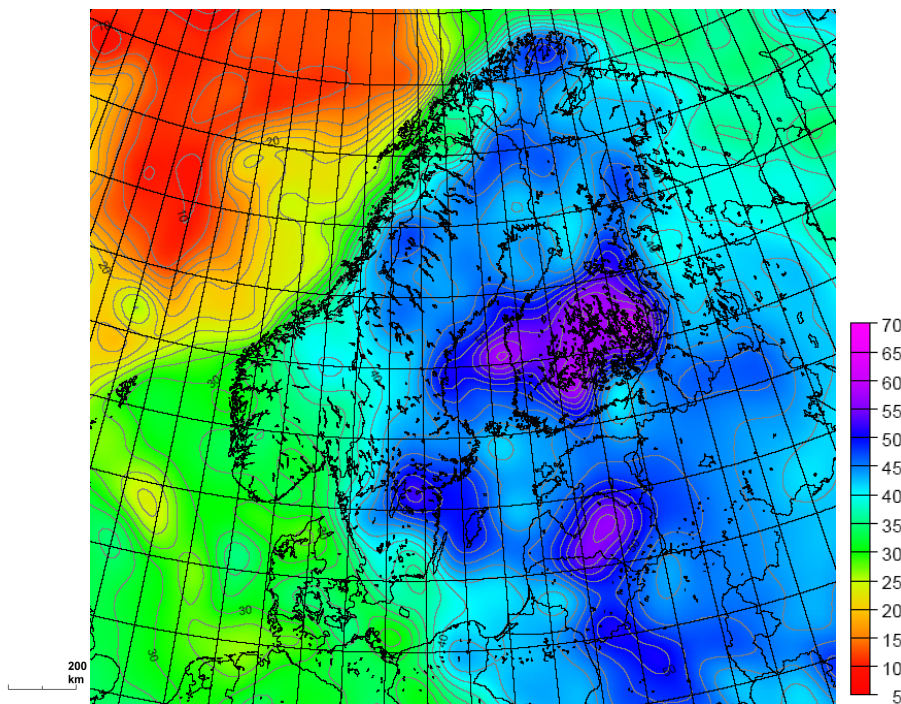


Figure 25. The crustal thickness (km) by Grad & Tiira (2008, 2009), with a $2^\circ \times 2^\circ$ grid. Projection not known.

EuCRUST-07 is also said to include some questionable data. E.g. for Russia, a large part of the constraints are based on gravity and surface tectonics. Although the authors got the data from the Russian Ministry in digital form, it does not mean that the original source is digital - the map is based on hand drawings of the teams from the GEON and VSEGEI institutes. There are big problems with any such Moho compilations, therefore the authors should at least incorporate up-to-date data and omit unconstrained regions (e.g. based on simple computer interpolations) (Artemieva 2008). The Moho map by Grad & Tiira (2008, 2009) covers all of Europe, unlike the other recent maps that are partly or wholly based on regional paper maps. For their map, Grad & Tiira (2008, 2009) always used the original models in digital form when available. This map is probably the best one for Fennoscandia at the moment, and it is more accurate than the global models.

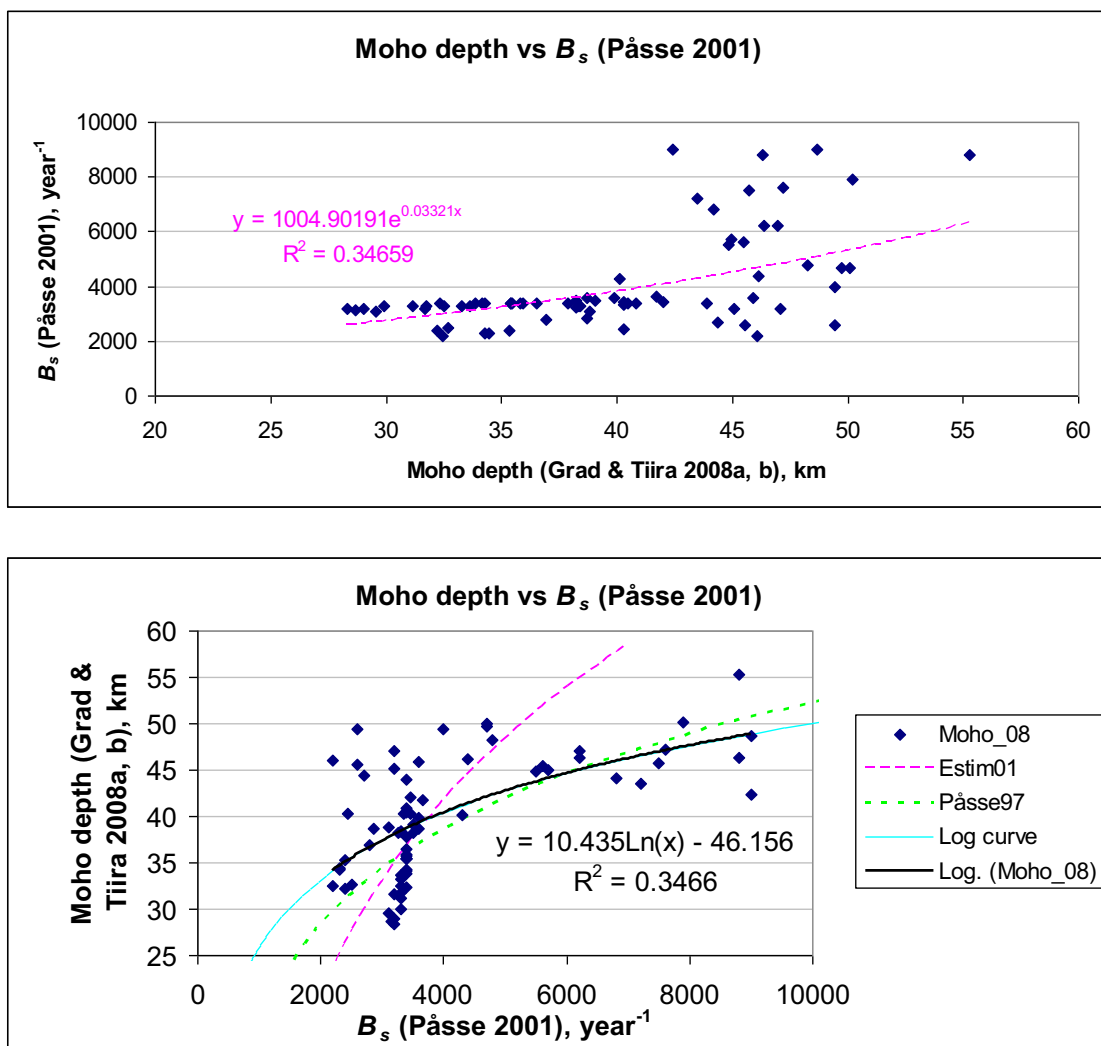


Figure 26. Direct exponential fitting of crustal thickness by Grad & Tiira (2008, 2009) vs. the B_s values by Påsse (2001) as such would re-define the coefficients of the exponential equation (top). Viewed inversely in the lower graph, that fit (the dashed magenta curve) seems to fit worse than a logarithmic curve (the black trendline and cyan logarithmic curve) or the Påsse (1997) original curve (green dashed).

As mentioned, thickness alone does not determine the behaviour of the crust. Density and strength are also properties of the crust that vary locally. These in addition depend on one another (Moisio 2005). The order of magnitude of the crustal movements could also be modelled numerically if the glacier's effects are added to the model as parameters. The parameters affecting the tectonic movements of the crust are generally the burden, strength, tension, and heat flux, and for relatively short-term burdens, the density also plays a role. When various models have been set up to describe the behaviour of the crust, the physical parameters have apparently often been neglected, and the models have concentrated on calculating the speed of changes. The paper by Kuusisto (2007) describes the interpretation of rock types with seismic methods and references. Lambeck & Purcell (2003) have modelled the glacial rebound with physical models concentrating on regional stress modelling.

To estimate B_s , an approach based on Luosto's (1997) crustal thickness (Figure 24) was first used here. The constants were still according to Pässe (1997), but the function can be updated if another crustal thickness model is used, by recalculating the exponential coefficients of B_s vs. a new crustal thickness map (Figure 26). The *Make NetCDF Raster Layer* function of ArcGIS was used to transform the data from GMT software's NetCDF format into an image. See the table in APPENDIX 5 for the Moho values.

The exponential model does not seem adequate, and the adjustments that Pässe (1997) did to the B_s values were not done here. He wrote that he either increased or decreased the values of B_s in the clusters based on information on crustal depths, if these changes fitted the shore level information. Without such adjustments or any data point exclusions, the logarithmic fit of crustal depth of Grad & Tiira (2008, 2009) and the B_s of Pässe (2001) data is, when inversed:

$$B_s = e^{+46.156/10.435} \cdot e^{(1/10.435)ct} \approx 83 \cdot e^{0.096ct} \text{ (year}^{-1}\text{)} \quad \text{Equation 23}$$

The direct exponential fit and the linear fit using logarithmic values are different, and the latter often produces more reasonable results than the direct exponential fit. That is why the logarithmic fit inversed into an exponential form may be more useful. Fitting the crustal depth to Pässe & Andersson's (2005) B_s data was not remarkably different. The coefficient of determination, R^2 , is not very strong. The new curve is also less steep, causing quite large B_s values with 50–60 km thicknesses.

5.2 B_s modelling based on lithosphere thickness

Even though the crust is the uppermost, solid layer of the Earth, properties of the layer(s) below it also have an influence on the characteristics of isostatic land uplift. Compared to the correlation between B_s and crustal thickness, the correlation between B_s and lithosphere thickness is said to provide even better estimates and a more plausible explanation of the uplift process (Pässe 2001).

The equation 4-1 in Pässe (2001) included an extra 0 compared to that study's Figure 4-2, where 100/7000 is about 0.014, not 0.0014. Therefore, the lithosphere thickness estimate L must actually be:

$$L = 0.014 \cdot B_s + 73 \text{ (km)}. \quad \text{Equation 24}$$

The used L had been interpreted according to analysis of wave data. Pässe (2001 Figure 4-3) gives a lithosphere thickness map based on that study's B_s values, which in turn are based on both shore-level curves and recent relative land uplift. Pässe & Andersson (2005) include another B_s map, which could also be transformed into L .

Conversely, if an independent lithosphere thickness L (km) map would be available,

$$\hat{B}_s = (L - 73) / 0.014 = 71.429 \cdot L - 5214 \text{ (year}^{-1}\text{)} \quad \text{Equation 25}$$

can serve as a reasonable estimate, or the coefficients could be updated first. Kukkonen (2000, 2006) mentions that new information on lithosphere thickness has been received by combining theoretical models with samples that are deep from within the crust but originating from depths of up to 230 km. For information on the lithospheric configuration of Fennoscandia, the latest sources are Artemieva et al. (2006), Figure 28, and Artemieva & Thybo (2008), Figure 27. While such models are different firstly from one another due to different techniques or data used, and secondly different from Pässe (2001), the coefficients of the above equations should be updated, if such models are to be used for B_s estimation.

The function coefficients should be updated if the lithosphere model is changed, but the selection of the lithosphere model would also make a big difference due to the different nature of the models.

Artemieva et al.'s new crustal (and lithosphere) model is in review and hopefully will come out in 2009 on www.lithosphere.info.

The vertical structure of the Earth's mantle – mainly its viscosity values – can be defined also with the GPS very roughly. For the mantle's layers, only a few different values can be estimated, from which two or three for the upper mantle. The resolution gets worse for the deeper layers (Milne et al. 2004).

The latest precision levelling campaigns including the Baltic levelling network have contributed to the latest current uplift models (Ågren et al. 2006, Ågren & Svensson 2007). The DynaQlim committee (<http://dynaqlim.fgi.fi>) aims to combine also models of upper mantle dynamics and composition, rebound mechanism and uplift.

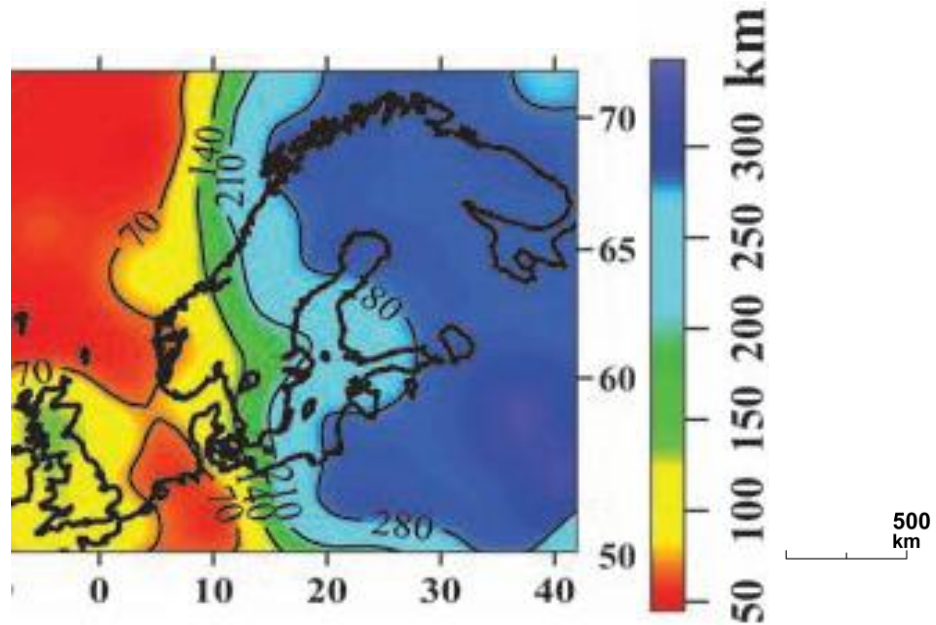


Figure 27. A lithosphere thickness map (Artemieva & Thybo 2008), based on a global body-wave seismic tomography model.

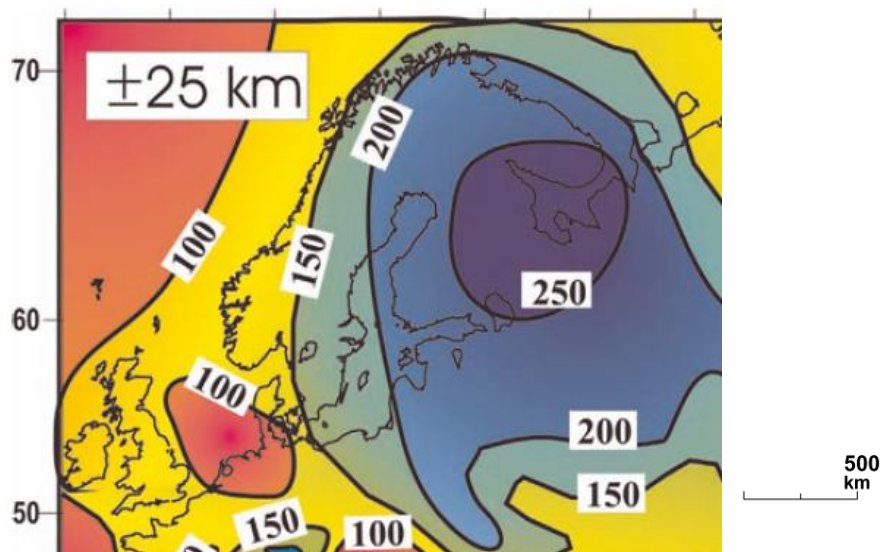


Figure 28. A lithospheric thickness map, based on seismic, thermal, MT, electromagnetic and gravity interpretations. In general, a direct comparison of lithospheric thickness values, constrained by different techniques, is not valid, as they are based on measurements of diverse physical parameters (Artemieva et al. 2006).

6 REGIONAL ESTIMATION OF ISOSTATIC LAND UPLIFT PARAMETERS

6.1 The derivative-based simple processes

The slow mechanism parameters are the most interesting in this study. Using the arctan derivative

$$\frac{d \arctan t}{dt} = \frac{1}{(1+t^2)}, \quad \text{Equation 26}$$

the chain rule and other rules of derivatives (for sum, constant multiplier and quotient derivatives), the isostatic land uplift component derivatives are, using only the slow component:

$$\begin{aligned} U' &= 0 - \frac{2}{\pi} \cdot A_s \cdot \frac{1}{1 + [(T_s - t)/B_s]^2} \cdot \frac{d(T_s - t) \cdot B_s - (T_s - t) \cdot 0}{B_s^2} \\ &= \frac{-2}{\pi} \cdot A_s \cdot \frac{B_s^2}{B_s^2 + (T_s - t)^2} \cdot \frac{-B_s}{B_s^2} = \frac{2}{\pi} \cdot A_s \cdot \frac{B_s}{B_s^2 + (T_s - t)^2} \quad (\text{m/yr}) \quad \text{Equation 27} \end{aligned}$$

The derivative according to t_{AD} can be defined correspondingly as

$$U' = \frac{-2}{\pi} \cdot A_s \cdot \frac{B_s}{B_s^2 + (T_s - 1950 + t_{AD})^2} \quad (\text{m/yr}) \quad \text{Equation 28}$$

Note that all derivatives using t are according to the cal BP axis, and such derivative values have to be later multiplied with -1 if used with a reversed, chronological time axis like AD. For the Pässe (2001) case, the slow component derivatives are

$$\begin{aligned} U' &\cong \frac{2}{\pi} \cdot A_s \cdot \frac{B_s}{B_s^2 + (12000 - t)^2} \quad (\text{m/yr}) \quad \text{Equation 29} \\ U' &\cong \frac{-2}{\pi} \cdot A_s \cdot \frac{B_s}{B_s^2 + (12000 - 1950 + t_{AD})^2} \end{aligned}$$

Similarly, for the E model shown earlier, the derivatives generally and applied to Pässe (2001) are

$$\begin{aligned} E' &= \frac{2}{\pi} \cdot A_E \cdot \frac{B_E}{B_E^2 + (T_E - t)^2} \quad (\text{m/yr}) \quad \text{Equation 30} \\ E' &= \frac{-2}{\pi} \cdot A_E \cdot \frac{B_E}{B_E^2 + (T_E - 1950 + t_{AD})^2} \end{aligned}$$

$$E' \cong \frac{2}{\pi} \cdot 56 \cdot \frac{1350}{1350^2 + (9500 - t)^2} \quad (\text{m/yr}). \quad \text{Equation 31}$$

$$E' \cong \frac{-2}{\pi} \cdot 56 \cdot \frac{1350}{1350^2 + (9500 - 1950 + t_{AD})^2}$$

The sign of E itself may cause confusion. The derivative formulae above are defined for the E itself, not for that of $-E$ plotted previously. Figure 29 shows the global E and U_s plotted for Olkiluoto, and Figure 30 shows their derivatives together with the shore-level derivative based on them.

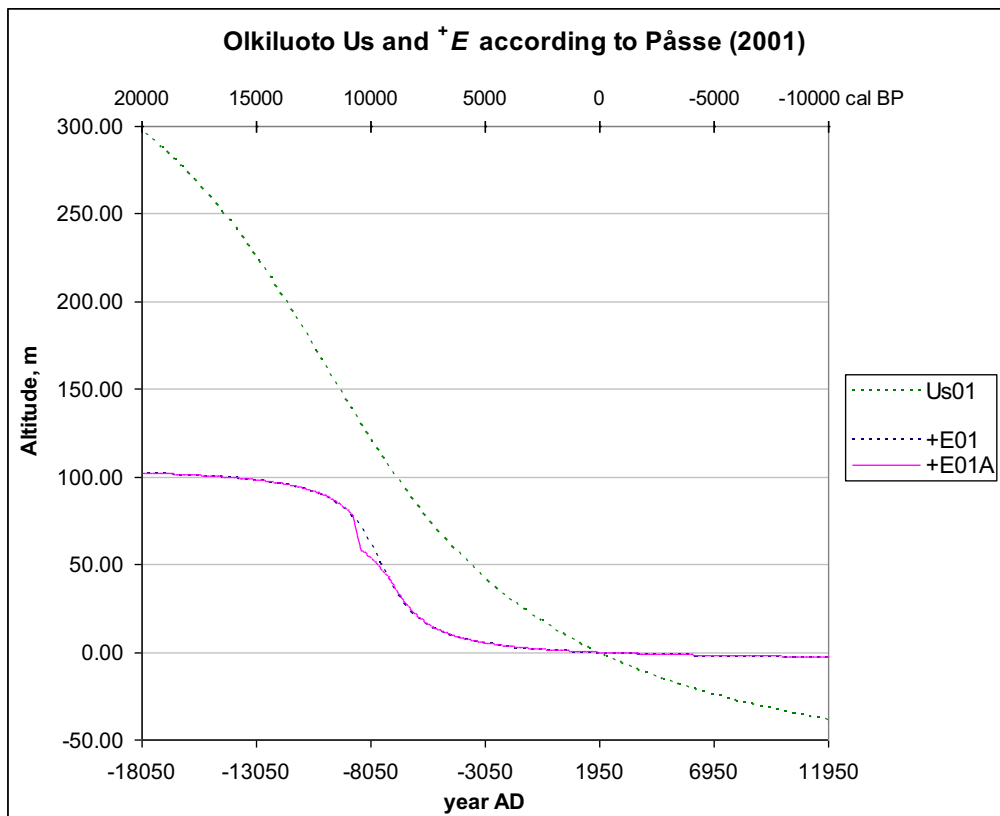


Figure 29. The slow isostatic land uplift component U_s at Olkiluoto according to Pässe (2001) and the values of the eustatic sea level rise function E as such (blue), and with the Ancylus correction (magenta).

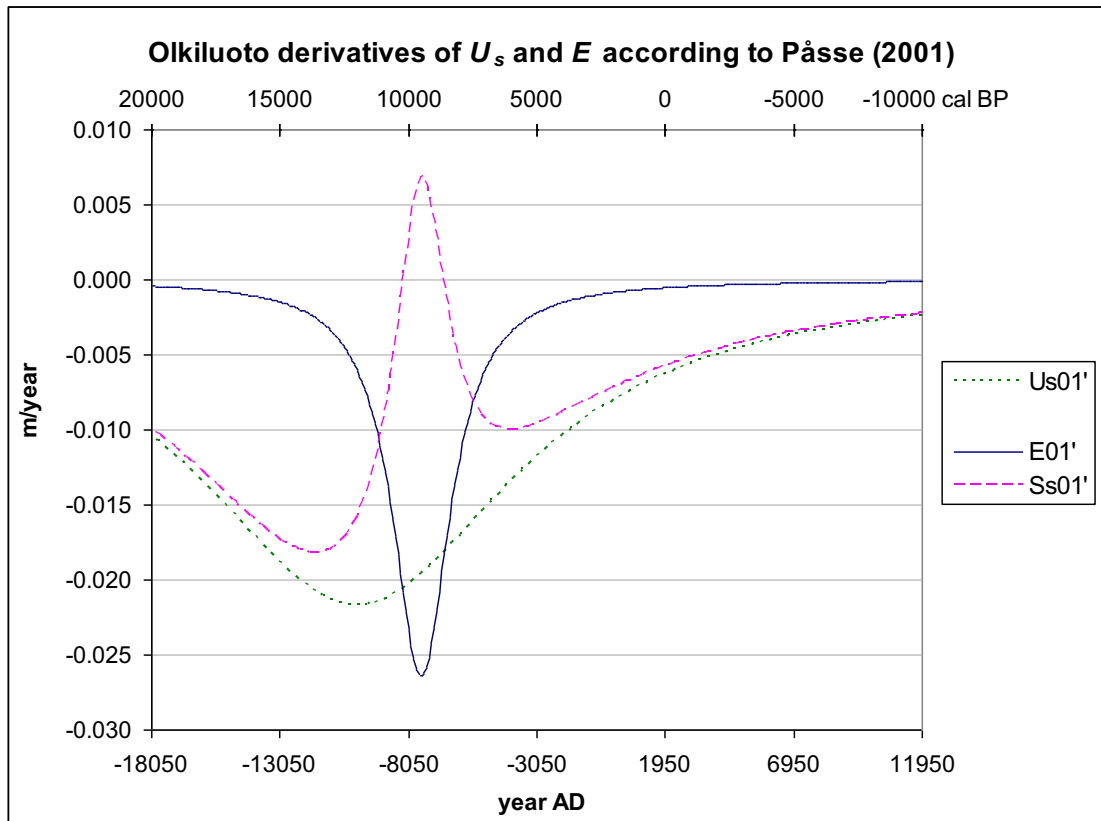


Figure 30. The t -based derivatives of the eustatic sea level rise function (E), Olkiluoto slow isostatic land uplift component U_s and $S=U_s-E$ by Pässe (2001), plotted as sign-switched on a chronological time axis. In the next 5000 years, the (slow) isostatic land uplift will slow down from the current value of about 6 mm/year to about 4 mm/year. It can be seen also how (in this area and with this E model) the magnitude of isostatic land uplift will remain bigger than that of the sea level rise. On the chronological time axis, E' is currently about -0.5 mm/year or $-E'$ about 0.5 mm/year.

E'_{01A} , meaning the derivative of Pässe's (2001) E with the Ancylus correction, is given here, only using t_{AD} :

$$E'_{01A} \cong \frac{-2}{\pi} \cdot 56 \cdot \frac{1350}{1350^2 + (9500 - 1950 + t_{AD})^2} \quad (\text{m/yr}) \quad \text{Equation 32}$$

$$-0.0487 \quad , -8817 < t_{AD} \leq -8498$$

$$+0.0116 \quad , -8498 < t_{AD} < -7150$$

As the reference is assumed to be the sea level of the time, the slopes of the Ancylus transgression and regression line derivatives have not been used to replace the E'_{01} curve, but have been added to it (Figure 31).

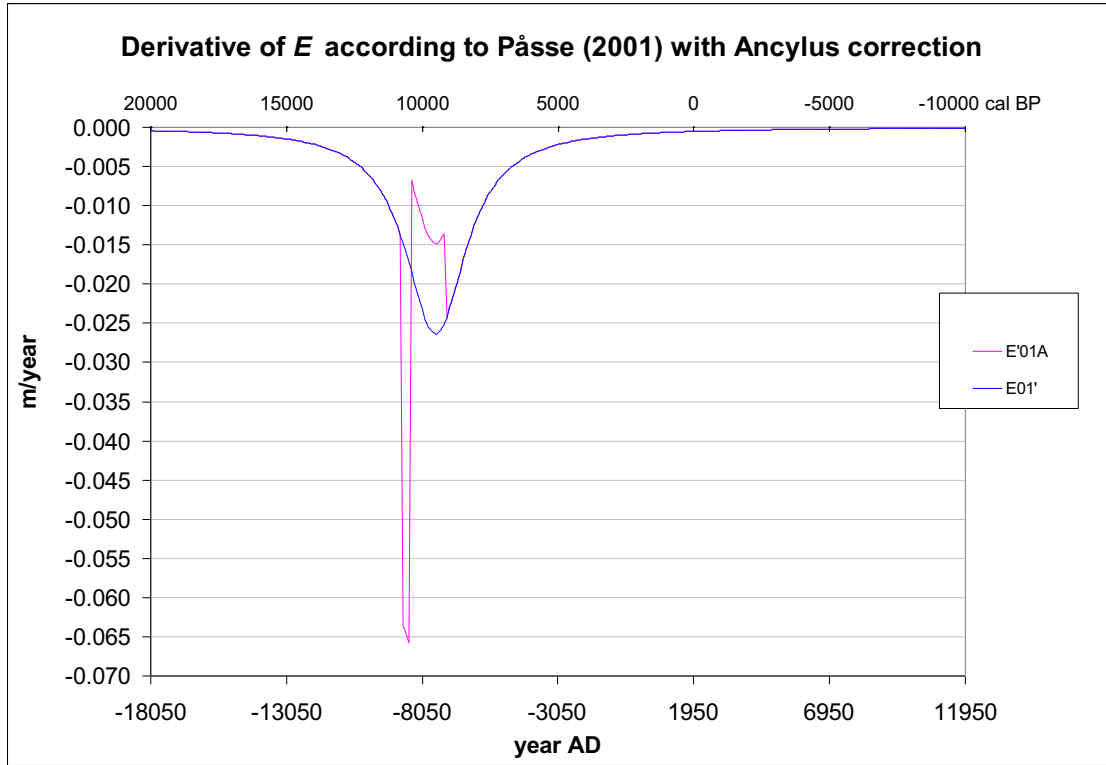


Figure 31. The derivatives of eustatic sea level rise E according to Pässe (2001), with (magenta) and without (blue) the Ancylus correction, on a chronological time axis. This matches with the statement that during transgression the water was rising 5–10 cm / year (Tikkanen & Oksanen 2002), which probably means absolute rise rather than the locally varying relative rise.

The current land uplift maps represent the map-based relative S' , per year, in cases where some eustatic sea level rise E' has been subtracted from them already (otherwise it would represent U'). But note that once the equation of E has been fixed, then:

$$U'_t = S'_{\text{map}} + E'_t \quad (\text{m/year}), \quad \text{Equation 33}$$

where S'_{map} is the value (in meters) from the apparent land uplift maps. And even though the maps describe a derivative naturally defined on a chronological time axis, its sign should not be switched when used with the two other derivatives based on t cal BP, due to the definitions explained in Chapter 3.1. For the S'_{map} variables, T_s has been fixed. Thus the first estimate for A_s can be defined on the cal BP axis from the equations above, generally and for the Pässe (2001) case, as

$$\begin{aligned} \hat{A}_s &= \left[S'_{\text{map}} + E'_t \right] \cdot \frac{\pi}{2} \cdot \frac{\hat{B}_s + (T_s - t)^2}{\hat{B}_s} \\ &\cong \left[S'_{\text{map}} + \frac{2}{\pi} \cdot 56 \cdot \frac{1350}{1350^2 + (9500 - t)^2} \right] \cdot \frac{\pi}{2} \cdot \frac{\hat{B}_s + (12000 - t)^2}{\hat{B}_s} \quad (\text{m}). \quad \text{Equation 34} \end{aligned}$$

Using t_{AD} and the AD axis,

$$U'_{t_{\text{calAD}}} = -S'_{\text{map}} + E'_{t_{\text{AD}}} \quad (\text{m/year}) \quad \text{Equation 35}$$

and

$$\begin{aligned} \hat{A}_s &= \left[-S'_{\text{map}} + E'_{t_{\text{AD}}} \right] \cdot \frac{-\pi \cdot \hat{B}_s + (T_s - 1950 + t_{\text{AD}})^2}{2 \cdot \hat{B}_s} \\ &\cong \left[-S'_{\text{map}} - \frac{2}{\pi} \cdot 56 \cdot \frac{1350}{1350^2 + (9500 - 1950 + t_{\text{AD}})^2} \right] \cdot \frac{-\pi \cdot \hat{B}_s + (12000 - 1950 + t_{\text{AD}})^2}{2 \cdot \hat{B}_s} \end{aligned} \quad \text{Equation 36}$$

(m),

which equation is given here without the Ancyclus correction within E'_{01A} . The three minus signs of the terms could be switched as well.

For Pässe & Andersson's (2005) E model, E' has slightly different constants and modifications due to the added two fast components. In this study, such E' versions were not used:

$$\begin{aligned} E'_{05,t} &\cong \frac{2}{\pi} \left(\frac{61 \cdot 1500}{1500^2 + (9600 - t)^2} - \frac{7 \cdot 350}{350^2 + (11500 - t)^2} + \frac{8 \cdot 350}{350^2 + (12500 - t)^2} \right) \\ E'_{05} &\cong \frac{-2}{\pi} \left(\frac{61 \cdot 1500}{1500^2 + (9600 - 1950 + t_{\text{AD}})^2} - \frac{7 \cdot 350}{350^2 + (11500 - 1950 + t_{\text{AD}})^2} \right. \\ &\quad \left. + \frac{8 \cdot 350}{350^2 + (12500 - 1950 + t_{\text{AD}})^2} \right) \quad (\text{m/yr}) \end{aligned} \quad \text{Equation 37}$$

The B_s estimate versions were obtained via the Moho depth maps, here the ones by Luosto (1997) and Grad & Tiira (2008, 2009), according to the equations in Chapter 5.1. Alternatively, the B_s estimate version could be taken directly from Pässe & Andersson (2005, Fig. 8) or Pässe (2001, Fig. 3-12).

Using the above A_s estimate equation, the first estimates were produced in a raster mode. The times t (cal BP) were here small negative values (i.e. <100 years – if any – after AD 1950).

The fast component U_f derivative could be defined also, in order to estimate A_s more accurately for older cases too. Full models with the fast component included may be good also if some integrals over time would be calculated. Another possible use of U_f' is that if estimates for some components were available, then for example A_f could be estimated using also the U_f' equation. The U_f derivative (Figure 32) would be:

$$U'_{f,t} = A_f \cdot \left[e^{-0.5 \left(\frac{t-T_f}{B_f} \right)^2} \cdot \ln e \right] \cdot -\frac{1}{2} \cdot \left[2 \cdot \left(\frac{t-T_f}{B_f} \right)^{2-1} \cdot d \left(\frac{t-T_f}{B_f} \right) \right]$$

$$= A_f \cdot e^{-0.5 \left(\frac{t-T_f}{B_f} \right)^2} \cdot \frac{T_f - t}{B_f} \cdot \frac{B_f - 0}{B_f^2} = A_f \cdot e^{-0.5 \left(\frac{t-T_f}{B_f} \right)^2} \cdot \frac{T_f - t}{B_f^2} \text{ (yr}^{-1}\text{)}. \text{ Equation 38}$$

or using t_{AD} ,

$$U'_f = A_f \cdot e^{-0.5 \left(\frac{1950-t_{AD}-T_f}{B_f} \right)^2} \cdot \frac{T_f + t_{AD} - 1950}{B_f^2} \text{ (yr}^{-1}\text{)}. \text{ Equation 39}$$

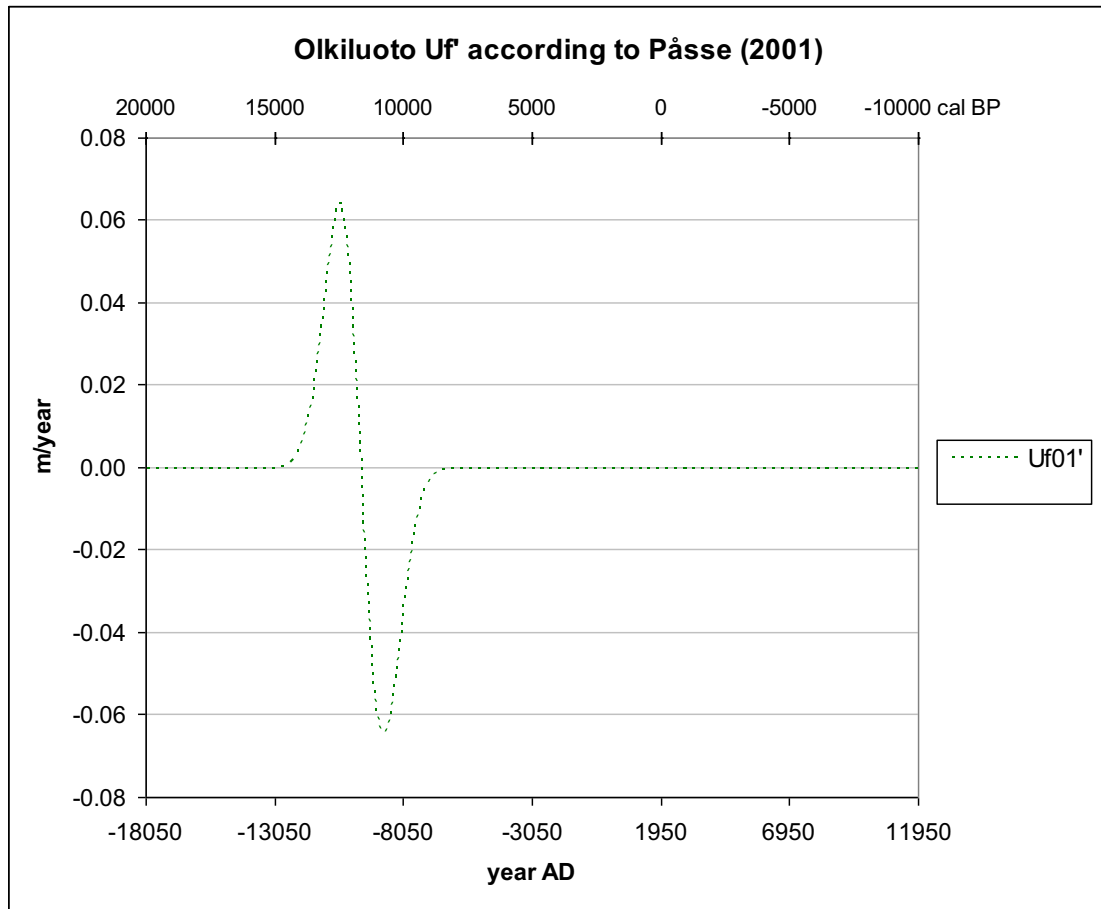


Figure 32. The derivative of the fast isostatic land uplift component U_f for the Olkiluoto site according to Pässe (2001).

For Pässe & Andersson's (2005) arctan-based U_f model, there is one variable less, and B_f would be not needed for U_{f05}' – the equation of which is not shown here.

Because actually

$$U_s' = S' + E' - U_f', \quad \text{Equation 40}$$

then an estimate for A_s , including the fast component by Pässe (2001) but without the Ancyclus correction would be:

$$\hat{A}_s = \left[S'_{\text{map}} + \frac{2}{\pi} \cdot 56 \cdot \frac{1350}{1350^2 + (9500 - t)^2} - A_f \cdot e^{-0.5 \left(\frac{t - T_f}{B_f} \right)^2} \cdot \frac{T_f - t}{B_f^2} \right] \cdot \frac{\pi}{2} \cdot \frac{\hat{B}_s^2 + (12000 - t)^2}{\hat{B}_s} \text{ (m)}. \quad \text{Equation 41}$$

Using t_{AD} ,

$$\hat{A}_s = \left[-S'_{\text{map}} - \frac{2}{\pi} \cdot 56 \cdot \frac{1350}{1350^2 + (9500 - 1950 + t_{AD})^2} - A_f \cdot e^{-0.5 \left(\frac{1950 - t_{AD} - T_f}{B_f} \right)^2} \cdot \frac{T_f + t_{AD} - 1950}{B_f^2} \right] \cdot \frac{-\pi}{2} \cdot \frac{\hat{B}_s^2 + (12000 - 1950 + t_{AD})^2}{\hat{B}_s} \text{ (m)}, \quad \text{Equation 42}$$

where the four minus signs of the terms could be switched too. Note that only for the distant past the fast component term is useful to be included, but there the current uplift maps do not represent the situation properly. The equation is given in the summary chapter with the Ancyclus correction within E'_{01A} . That version could be used when t_{AD} is within the range -8817 to -7150, but for such a range, the current S'_{map} values are not valid.

The accuracy of the A_s estimate for the B_s estimate could be evaluated, too, as dA_s/dB_s .

6.2 Estimation based on shore-level curves

Other A_s estimates were calculated by selecting groups of sea-level index points and calculating the isostatic land uplift parameters for them. This was done using the Solver Add-In for MS Excel (like Brydsten 2006) and the square sum of the differences between the observations and the model was minimised. The Solver estimates the most suitable A_s value (and B_s and fast component parameters). The models were according to Pässe (2001) with the Ancyclus correction, and for isostatic land uplift, for both the slow and fast components. The variable T_s was still fixed to 12000 cal BP despite the new dating calibration methods.

Shore-level or shoreline displacement can be investigated with two methods. One is to describe the relevant geophysical processes as accurately as possible. Another is to use statistics and mathematics to interpret empirical historic shore-level data (Pässe & Andersson 2005). The latter method is used here. Shore level curves are empirically defined for each region by using several ^{14}C datings of basin isolation from the sea due to apparent land uplift. Many sea-level index points should be geographically located close to one another but at different altitudes asl. If there are enough representative samples, the displacement curve can be defined well enough. The aim is to estimate the shoreline levels of the past, but primarily of the future (see also Brydsten 1999, 2000, 2006, Mäkiaho 2005; and for the near future, Huhta & Korsman 2005).

Depending on how many datings per site are available, the estimation accuracy of parameters of various isostatic land uplift models using least squares (LSQ) methods can vary. B_s was usually solved, sometimes fixed, e.g., when the time span was too short to cover the old enough period. If only points located near the coast (i.e. in effect often in low elevations) are used, it is possible that B_s , e.g., cannot be estimated. This corresponds to trying to calculate the inertia factor using only the tail part of the curve (see Figure 16). If a case like that is really needed, it is better to either complement the points from nearby sites or fix the B_s and solve A_s only. A problem here is that B_s estimates according to Pässe & Andersson (2005) and Pässe (2001) maps may vary more than 1000 year^{-1} . Because there are a lot of parameters to calculate and a limited amount of sea-level index points available regionally, the task is not trivial.

Generally, it is best to select the subsets from circular or longish areas perpendicular to the isolines of current land uplift to guarantee that sea-level index points from a long enough time period (from high enough locations) will be included.

The Solver was applied to find such parameter A_s (and B_s) values that minimise (for the selected subset of isolation sea-level index points) the unweighted squared sum

$$\sum_i (T_i - S_i)^2 \text{ (m}^2\text{)}, \quad \text{Equation 43}$$

where T_i is the threshold altitude (m above current sea level) of the sea-level index point (i) itself and S_i is the S value according to the $U_s + U_f - E_{01A}$ model for the calibrated time of the sea-level index point (i). The fast isostatic uplift component U_f is involved according to Pässe (2001) and taken into consideration in the curve fitting for approximately 11600 ± 425 years cal BP for the Olkiluoto area. The U_f parameters either can be solved here or must be chosen case by case, according to e.g. Pässe & Andersson (2005, Fig. 8), or for B_f , according to Pässe (2001, Figure 3-7). The Ancyclus correction was always included because Solver analysis was only done for areas that were within the Ancyclus Lake area.

The parameters were defined both based on crustal thickness and by fitting them to the data based on ^{14}C dating. In the shoreline curve fitting, the strategy is to define A_s (and B_s) by fitting the curve into data on each rather small area, e.g. Pyhäjärvi-Olkiluoto, between the tectonic lines. After this, A_s and B_s are generalised between such analysed sites by interpolation. In addition to smooth interpolation methods, it is reasonable to try to use ones that leave thresholds at the known tectonic lines.

The old sites with isostatic land uplift parameters by Pässe (2001) or Pässe & Andersson (2005) plus the new sites created in this project were combined. Before interpolation, it is reasonable to reject some older analysed points, because the new ones can replace them.

The analysed sites can be considered independent because known and unknown fractures occur between them. The results of interpolation ought to represent the (super)regional isostatic land uplift. Local variations may still occur, as can be seen from the Olkiluoto precision levelling campaigns (Lehmuskoski 2008).

Because A_s is half of the total isostatic uplift, it should not be confused with the lake basin's threshold or any other directly measurable feature. The basins may have changed a number of times after the melting of the glacier. The only means of determining A_s is therefore to fit the *arctan* function or the whole S model into the shoreline displacement data or curves, and then to generalise the results by interpolation for the areas not analysed.

Some anomalies may be noticed in the sea-level index point subsets. These may indicate movements of tectonic blocks or less representative isolation points. The analyst should evaluate the data and see if the model fits regularly into the data or should try slightly different fits for different parts of the selected region (or for different intervals).

Generally, the empirical methods by Pässe (1997, 2001) and Pässe & Andersson (2005) seem to mean that the shoreline displacement curve of a selected region is plotted in a graph (dating vs. the threshold elevation from the current sea level), and the functions or the calculated curve parameters are fit in each such case. Then the results are interpolated for the whole modelled area. The iterative nature of the method comes in when a parameter (some A , B , or E function) of this interpolation is fixed and the fit is repeated locally. The iteration can be continued, but there are limitations because the tectonic blocks cause some disturbances. Iterations are needed also if no other data than the isolation datings are used; the E model must be decided and fixed before the crustal movements themselves can be reviewed. Pässe & Andersson (2005) improved their maps' inland areas by utilising data on the present relative uplift.

For the current study, the E model by Pässe (2001) was accepted as such but updated with the *Ancylus* correction according to Pässe & Andersson (2005), and the latest crustal depth model by Grad & Tiira (2008, 2009) was ascertained. The fast component by Pässe (2001) was chosen, but its T_f is quite coarse, and it was recalculated whenever enough points were available from that oldest period. Once the whole S model was determined, it was possible to calculate at least A_s for each regional subset of sea-level index points, preferably chosen without crossing any tectonic lines.

Some separate "what if" cases were checked, too.

7 RESULTS

7.1 B_s estimates based on crustal thickness maps

Because the course of isostatic land uplift in the later phases is mainly dependent on B_s (Påsse 2001, p. 33), any new information about B_s may be useful. The new information ought to be based especially on measured data (Moho depth, lithosphere thickness, etc.) rather than purely theoretical approaches.

B_s estimate maps were calculated using a few different sources. Crustal density and strength data of the Moho map by Grad & Tiira (2008, 2009) were not used. Figure 33 is based on the Moho map by Luosto (1997) and the old exponential equation coefficients, so both sources are old.

Figure 34 is based on the new Moho map by Grad & Tiira (2008, 2009) and the updated exponential equation coefficients, so both sources are new. This is the B_s estimate map that was used in the present study.

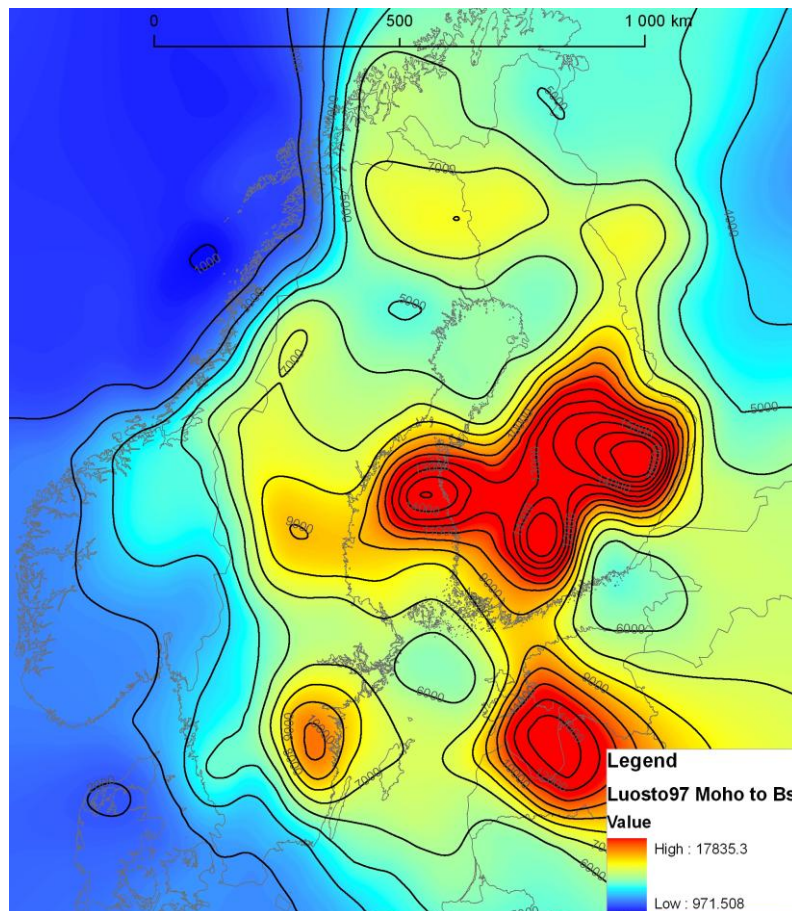


Figure 33. The B_s estimate (year^{-1}) raster, based solely on the crustal thickness by Luosto (1997) and the exponential equation by Påsse (1997).

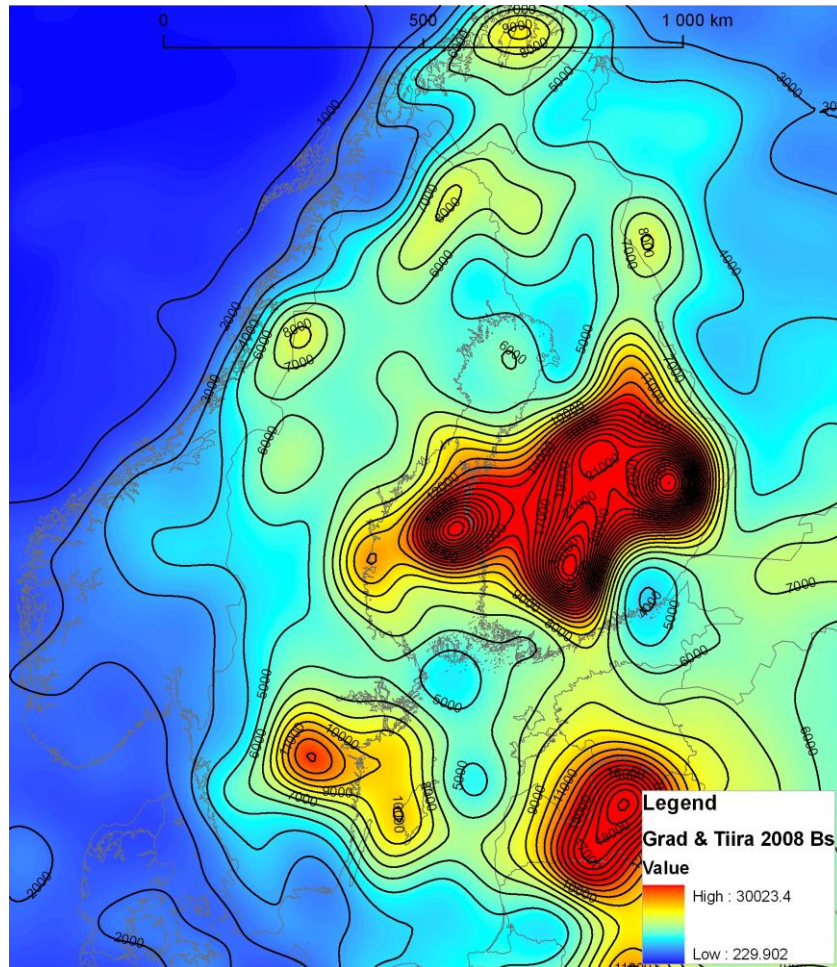


Figure 34. The B_s estimate raster, based solely on the newest crustal thickness model by Grad & Tiira (2008, 2009) and the new exponential equation. The map area is the same as in Figure 33.

These different maps enable a comparison of the old and the updated model, see Figure 35.

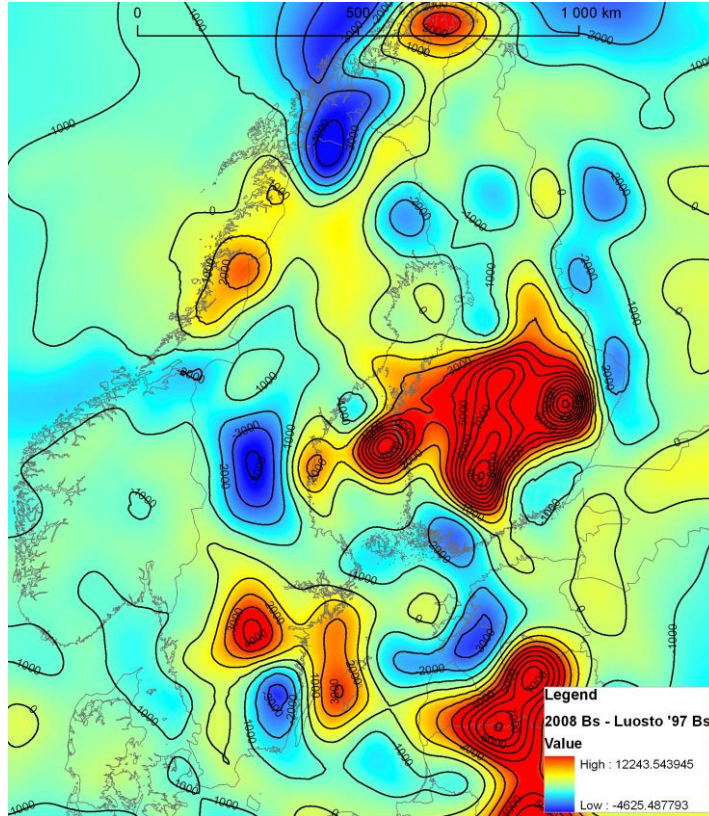


Figure 35. The map of the B_s estimate differences based on the new B_s calculated with the Moho map by Grad & Tiira (2008, 2009) and the new exponential equation minus the B_s calculated with the old Moho map by Luosto (1997) and the old equation by Pâsse (1997).

As expected, the biggest differences are in deep crustal areas.

It is also possible, e.g., to stick to the old exponential coefficients and use the two different Moho models. The comparison of the results is in Figure 36.

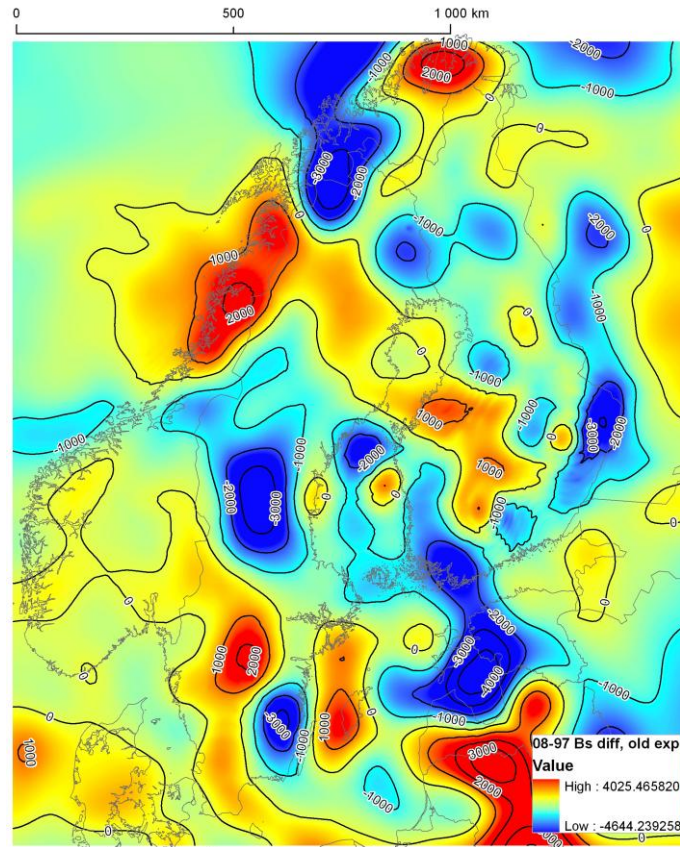


Figure 36. The B_s estimate raster difference map based on the B_s calculated according to the new Moho map by Grad & Tiira (2008, 2009) minus the B_s calculated according to the old Moho map by Luosto (1997). Both B_s maps here use the older equation by Pässe (1997).

The differences caused by using the other Moho map are smaller than those due to changing the exponential model. If the Moho map by Grad & Tiira (2008, 2009) is used with the updated equation and the old Pässe (1997) equation (no B_s map shown here), the differences would be bigger than in Figure 36 (see Figure 37).

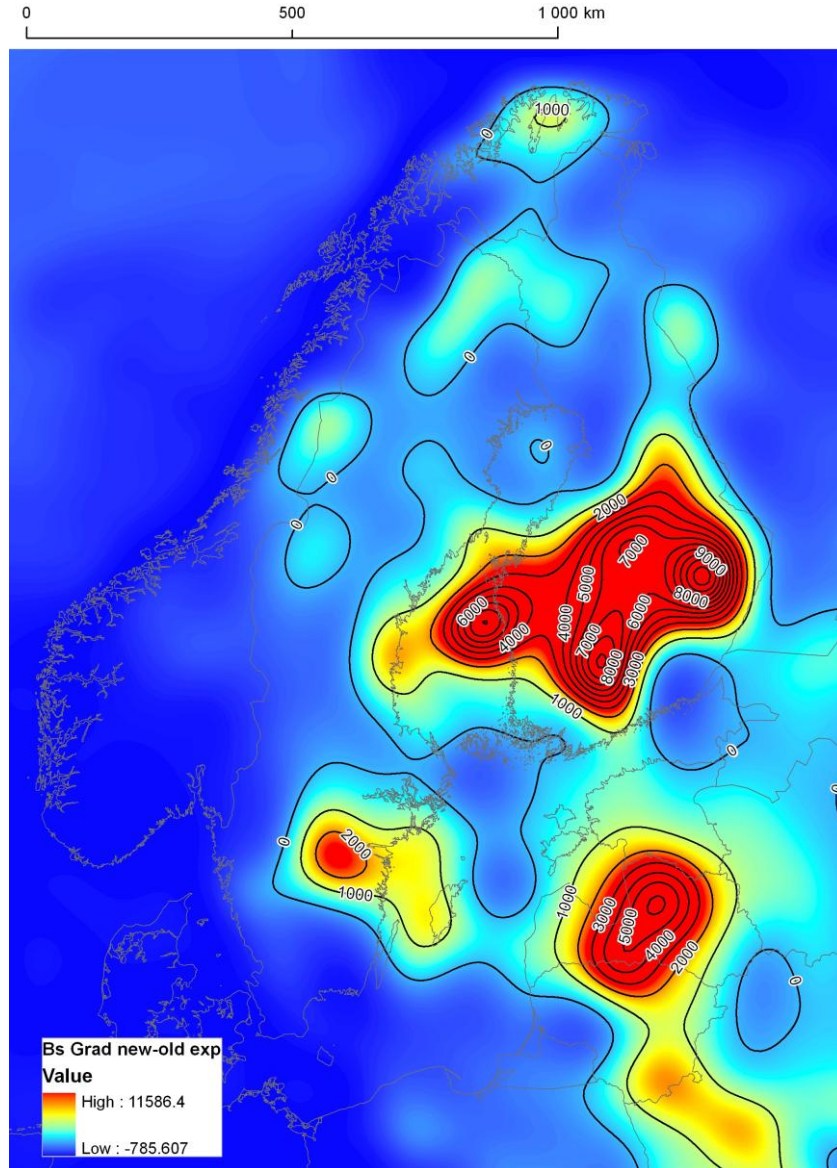


Figure 37. Comparison of B_s values based on the new exponential equation minus the values based on the old exponential equation. Both equations use the new Moho depth according to Grad & Tiira (2008, 2009).

To conclude, updated B_s maps can be produced, but the relation between Moho depth and B_s is not stable or well defined as had been hoped. It was not known how the adjustments of B_s values were done by Pässe (1997). Quite much is left to the choice of the exponential model, and also the Moho depth models are being developed constantly.

7.2 A_s estimates based on B_s maps

First, A_s parameter estimates were calculated using B_s estimates based on crustal depth according to Luosto (1997) and two different current relative uplift models. (The results are in Figure 38 and Figure 39. No fast isostatic land uplift components were included because the A_s of the current uplift was modelled.

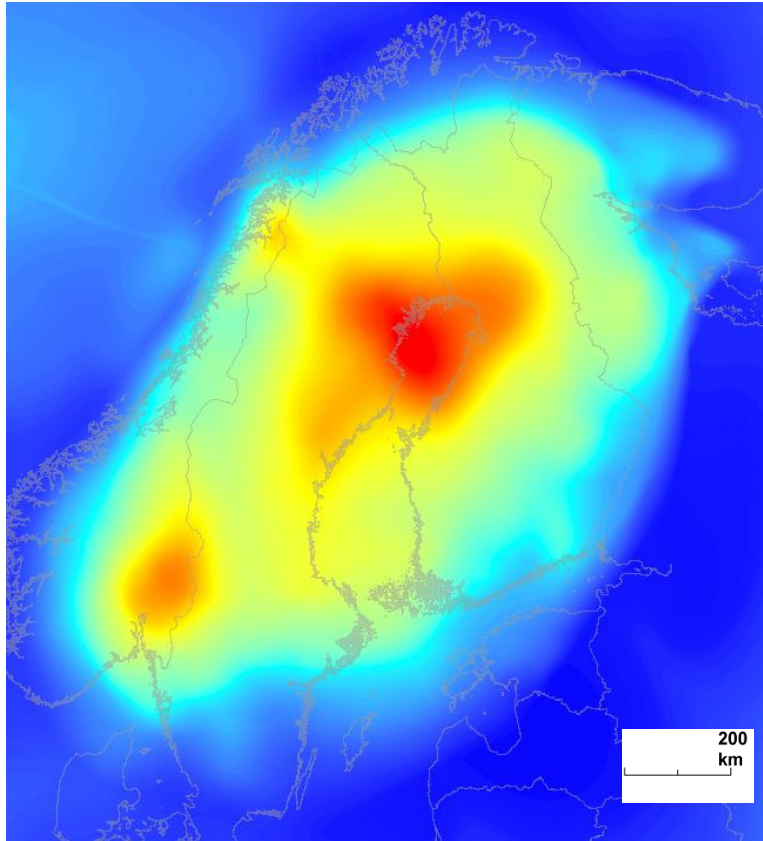


Figure 38. The A_s estimate raster based on the apparent land uplift map from Eronen et al. (1995) as such, $t=0$ (more accurate would be $t=-45$ cal BP or AD 1995), and the crustal thickness according to Luosto (1997). The maximum value is about 510 m. Based on this map, locally varying behaviour of A_s could be expected. Equations by Pässe (1997).

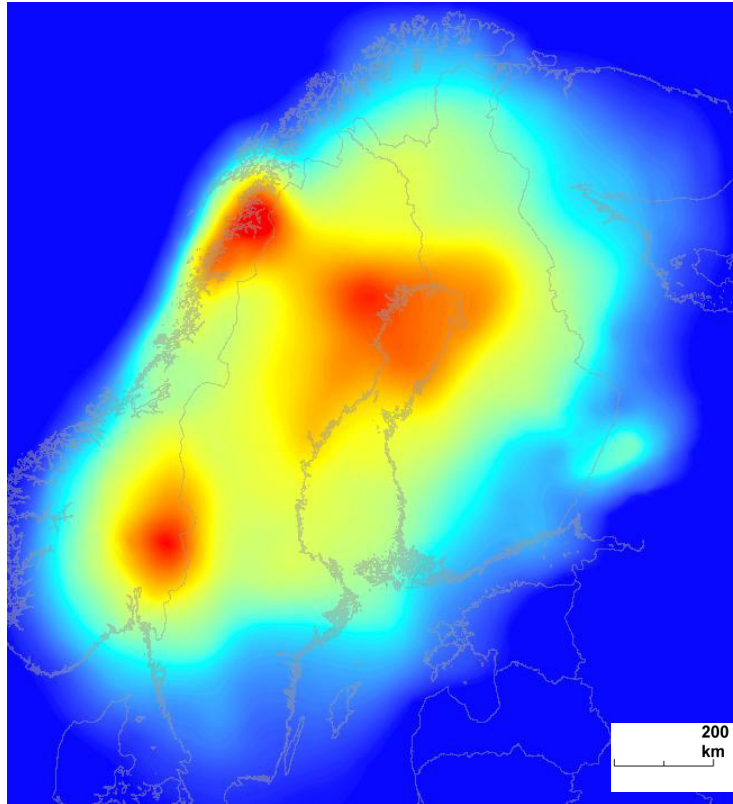


Figure 39. The A_s estimate raster based in this case on the apparent land uplift map by Hokkanen (2008) as such, $t=0$ (more accurate would be $t=-58$ cal BP or AD 2008), and the crustal thickness according to Luosto (1997). The maximum value is about 524 m. Equations by Pässe (1997).

The influence of both the crustal thickness map and the apparent land uplift maps can be seen in the results. It was decided to concentrate on using the current absolute uplift map by Poutanen (2008) or originally Lidberg (2007), diminished by 1.5 mm/year to get the apparent uplift. It was obvious to use the Moho map by Grad & Tiira (2008, 2009) but less obvious to choose the exponential function to estimate B_s . The slow component results based on the derivative-based method are given in Table 5.

Table 5. Derivative-based estimates of parameters in the maps of Figure 34 and Figure 41 for a spot in Olkiluoto. Moho depth = 48.208 km and absolute land uplift = 7.085 mm/year. $t=-45$ cal BP.

Exponential coefficients	B_s (year ⁻¹)	A_s (m)
By Pässe (1997)	7633.631	255.383
New	8489.265	245.208

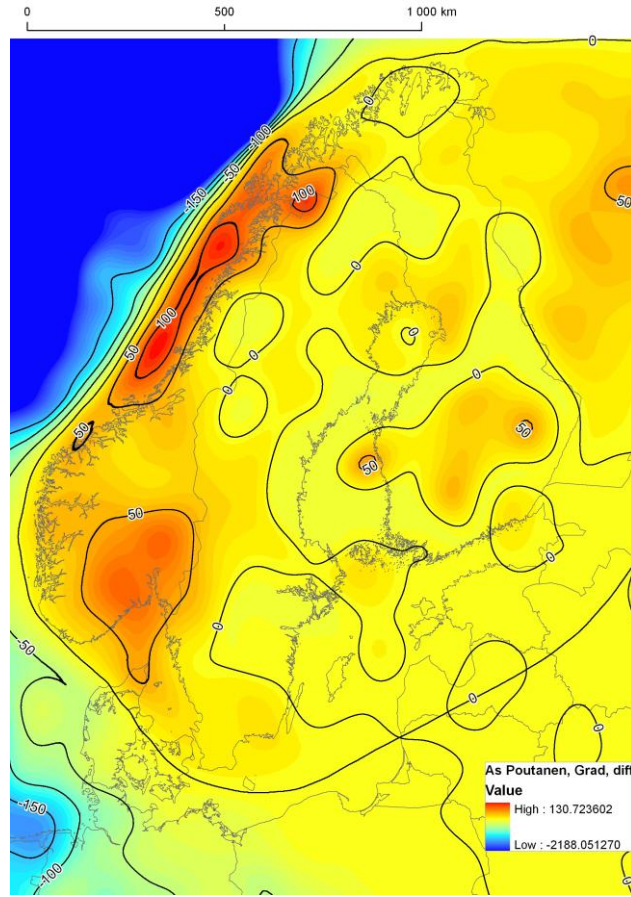


Figure 40. Comparison of A_s values with B_s values calculated using the new and the old exponential equations. The current uplift is always according to Poutanen (2008) or Lidberg (2007), and the Moho map is according to Grad & Tiira (2008, 2009). (In areas where the current apparent uplift becomes negative in the smooth model, the A_s estimate as such becomes negative too, and only the isolines down to -150 m are displayed here. The colours are scaled.)

Fortunately, A_s seems not to be very sensitive to the exponential equation used for B_s . In any case, there are tens of meters of differences between the results produced using the different exponential function versions (Figure 40).

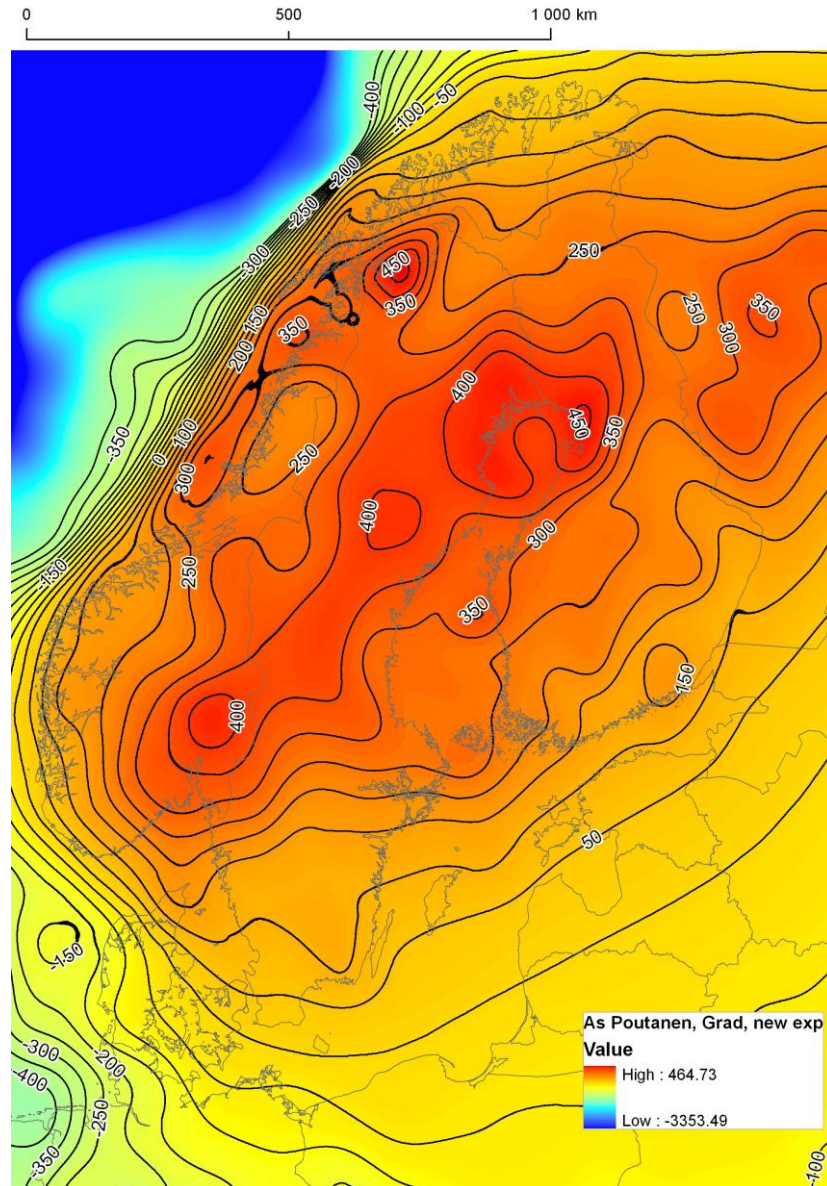


Figure 41. An A_s map based on the new exponential function (to estimate the intermediate B_s). The current uplift is according to Poutanen (2008) and the Moho map according to Grad & Tiira (2008, 2009), so all the elements are new.

The A_s estimate map based on all the latest information available is shown in Figure 41. It is one major result of the project. The negative values are to be ignored.

The uplift model at the Olkiluoto site is compared with models in previous literature. A_s and B_s from Table 5 were used to create Table 6 and Figure 42. The predicted uplift for about AD 12000 at Olkiluoto is only 0.53 m more than that predicted by Pässe (2001), or 0.28 m less than that value when the old exponential coefficients defined by Pässe (1997) are used.

Table 6. Derivative-method-based slow uplift at Olkiluoto. Comparison with the Pässe (2001) model is possible. To be precise, that model is for the Olkiluoto site (located between Olkiluoto Island and Pyhäjärvi), while the two others are for a location on Olkiluoto Island itself (pinpointed from the rasters).

	Uplift (m) AD 11950	Remaining uplift (m), AD 2M
Pässe (2001)	-38.097	-92.109
Derivative-based results, old exponentials by Pässe (1997)	-37.814	-91.497
Derivative-based results, new exponentials	-38.625	-95.455

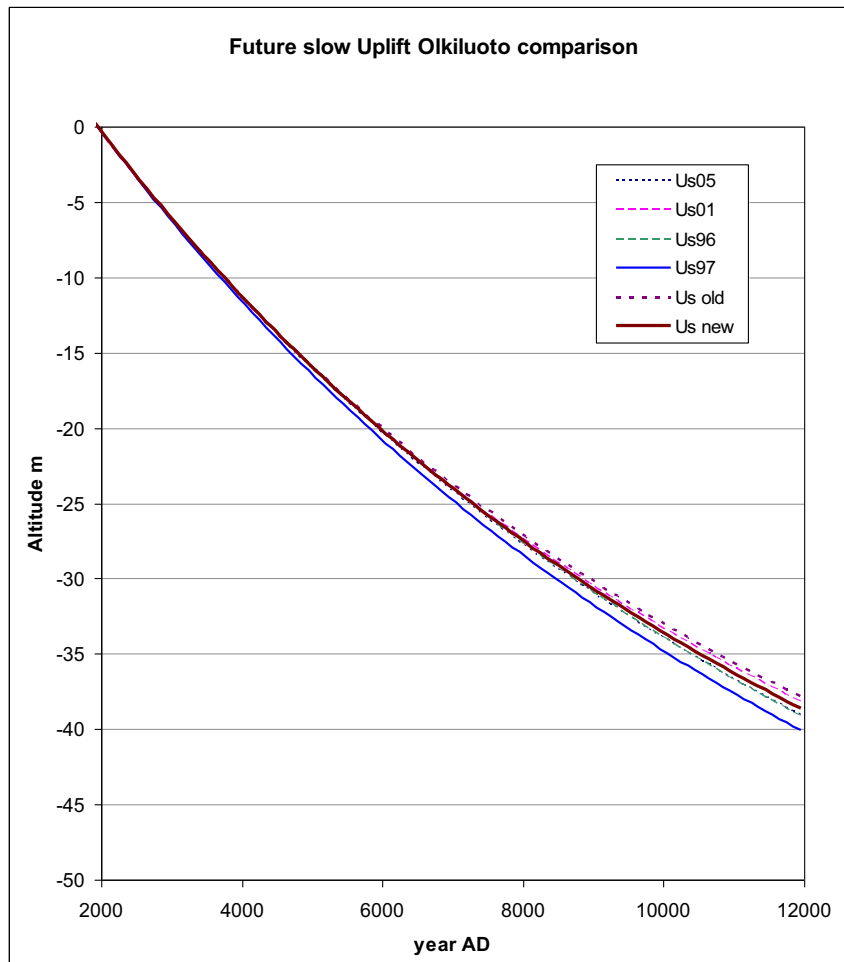


Figure 42. Comparison of slow isostatic land uplift curves for the future in Olkiluoto, based on the maps calculated as above. The shown U_s components are negative (and so is S ; the shoreline keeps getting lower relative to the land). The models using Lidberg's (2007) uplift map and Grad & Tiira's (2008, 2009) Moho map are on both sides of the model by Pässe (2001), the differences still being within about 0.5 m in about AD 12000.

Already from Figure 14 it can be seen that if the E models are valid, about 2.5 m of the approximately 38 m of predicted absolute land uplift will not take place in the relative sense. The remaining 35.5 m will be the apparent land uplift. But due to climate change, E needs to be revised. That's why it is reasonable to present U for predictions of even 100 years, rather than the apparent uplift S , in which E would already be considered.

Based on the derivative-based method and the available maps and using the old coefficients, the total remaining slow uplift in Olkiluoto is 0.6 m less than calculated by Pässe (2001). Using the new coefficients, it is 3.3 m more. These estimates are calculated for the distant future year AD 2000 000, even though all of the uplift may not take place, and the new glaciation scenarios aren't considered. 100 kyr is a more relevant time scale.

7.3 Estimates based on shore-level displacement curves

7.3.1 The shore-level displacement curve plots

At least Eronen et al. (1995, 2001) have used the box and whisker type of chart, showing in these applications probably the 1σ and 2σ lower and upper limits instead of the otherwise used 25 % and 75 % quartiles. Actual box and whisker plot tools are not directly available in MS Excel but can be created; in any case, the series are typically in columns (Peltier 2008), whereas each line or record in a GIS is a case. With >255 points, the whole table cannot be transposed in MS Excel which has a maximum of 255 columns.

The graphs here are based on the median values of AD probability functions and the lower and upper 1σ and 2σ limits rather than the individual ranges. The two error bars are formatted differently, and no actual box and whisker plots are used. A_s is always calculated. The corresponding point subset plots are shown before each graph. The active, selected points are cyan or yellow coloured, in other words do not follow the legend. Baseline-corrected shoreline graph versions were not produced even for visual purposes. The sites (Figure 43) are presented in an order downwards from the north. The Rovaniemi site (58) is situated north of the Gulf of Bothnia (Figure 44).

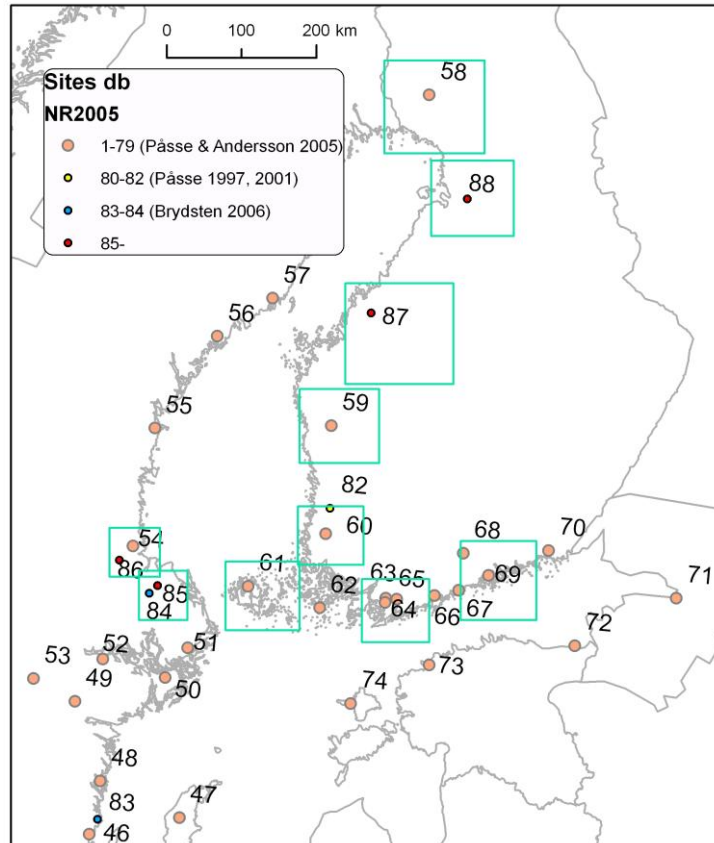


Figure 43. Locations of the newly solved sites, and approximate locations of the maps below. The Turku site (62) was tested as well, but the results were not kept. The projection is Finnish KKJ1.

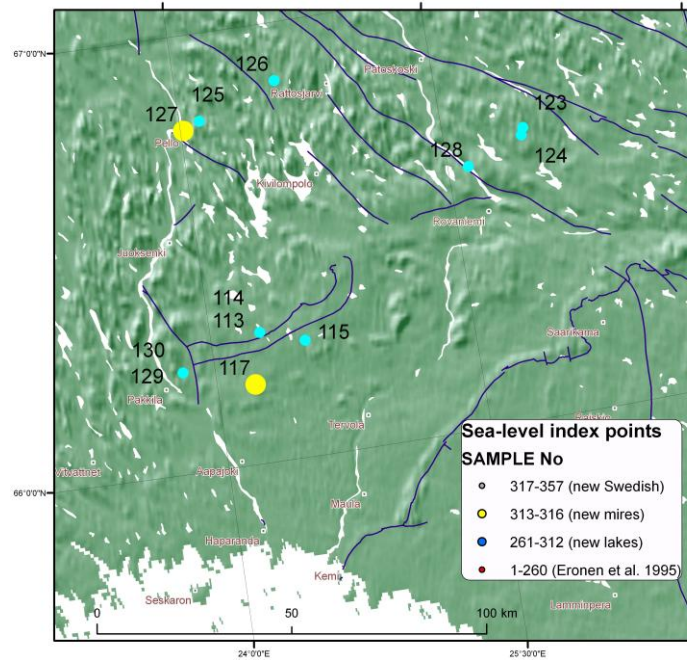


Figure 44. Plot of the Rovaniemi samples, with the cyan and yellow samples selected as a subset and the yellow points behaving differently than the others. The dark blue lines are the tectonic lines, © Geological Survey of Finland.

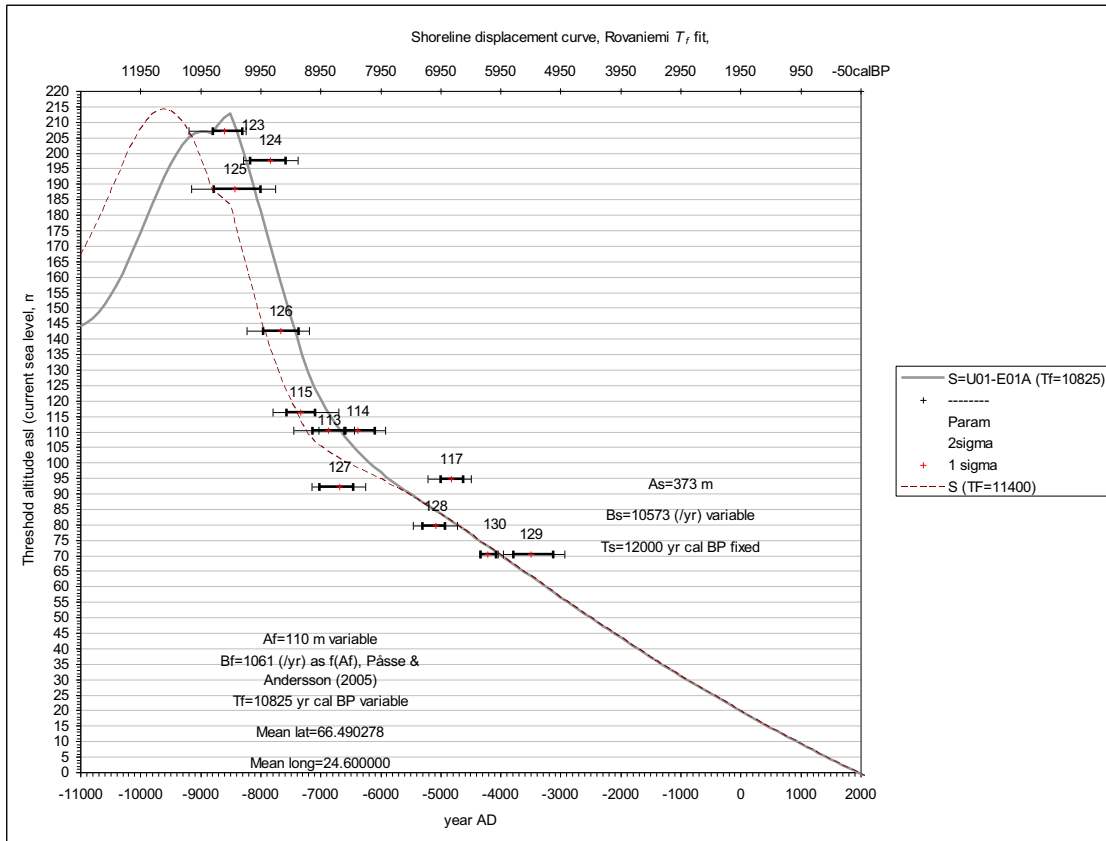


Figure 45. The graph of the Rovaniemi samples demonstrates how $T_f=11400$ years cal BP according to Pässe (2001), shown by the dashed line, would not be good. Here, T_f is matched to the data too. No sea-level index points were removed. A_f and thus B_f via the Pässe & Andersson 2005 function are also calculated.

From the results (Figure 45), it can be seen that T_f is more than 400 years less than in Pässe (2001). The other component values of Pässe (2001) for Rovaniemi were $A_s = 330$ m, $B_s = 9000 \text{ year}^{-1}$, $A_f = 145$ m, and $B_f = 1300 \text{ year}^{-1}$. There are no recent points available, so the slow component estimates may be unreliable.

Some attention was paid to why no site had been previously analysed in the Oulu region (Figure 46 and Figure 47). No new points were available for Oulu either.

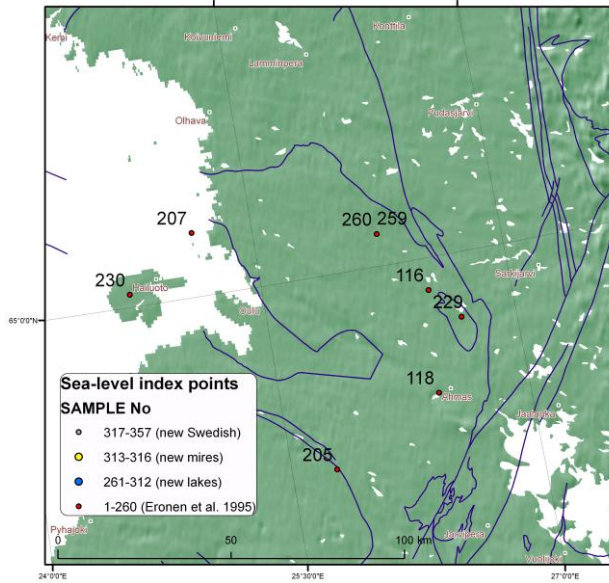


Figure 46. Plot of the Oulu region's old samples. All the points visible here were selected as a subset. The dark blue lines are the tectonic lines, © Geological Survey of Finland.

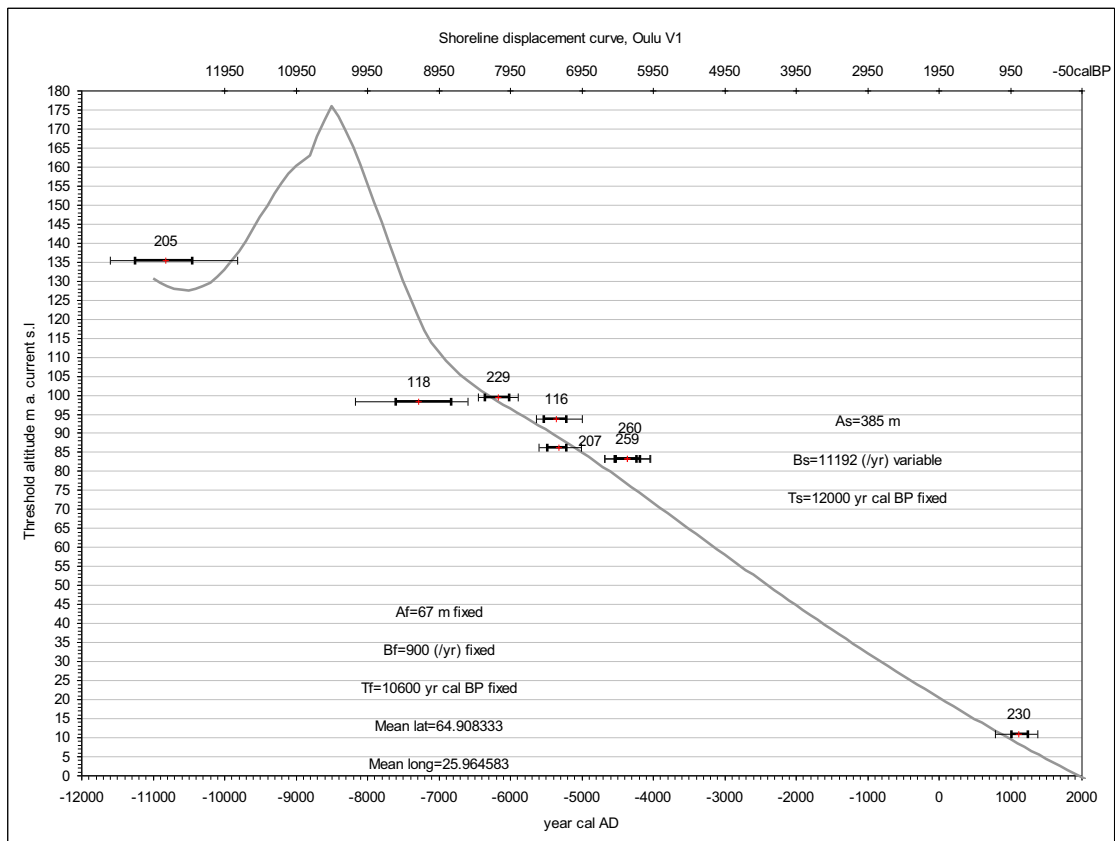


Figure 47. Graph of the Oulu case. Here, if point 118 is excluded, A_s is even 402 m and $B_s = 11464 \text{ year}^{-1}$.

The Oulu results may be questionable due to the area being under the glacier until about AD -7400 (Eronen et al. 1995 Appendix 1). In addition, if the E_{05} model were used, the point 205 would fit more poorly into the data. Points from elevations 15–75 m are missing, making the slow component estimates less reliable.

No site has been previously established in the Kronoby region, south of Kokkola, therefore this region must also have been problematic, as Oulu. In Kokkola, a group of new points were available from low elevations. There were hopes of establishing a new site by analysing the old and the new points. The results from the first chosen subset, shown in Figure 48, seem promising (Figure 49). In any case, more subset versions were tested.

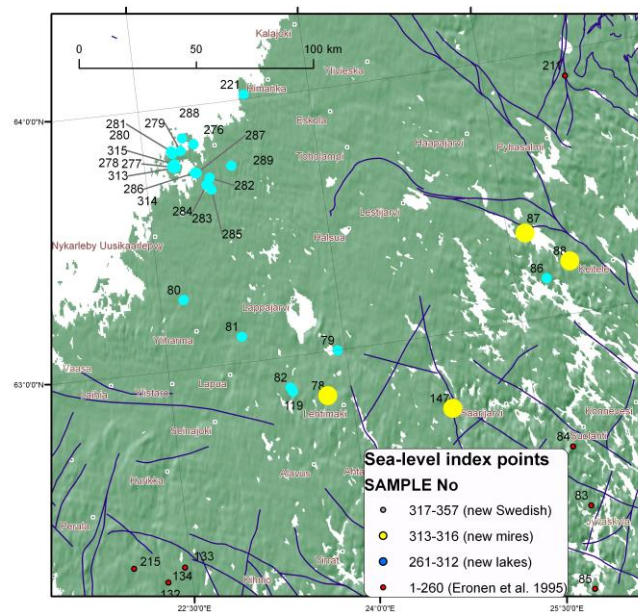


Figure 48. Plot of the Kronoby samples (Case1), with the cyan and yellow samples selected as a subset and the yellow points behaving differently than the others. The dark blue lines are the tectonic lines, © Geological Survey of Finland.

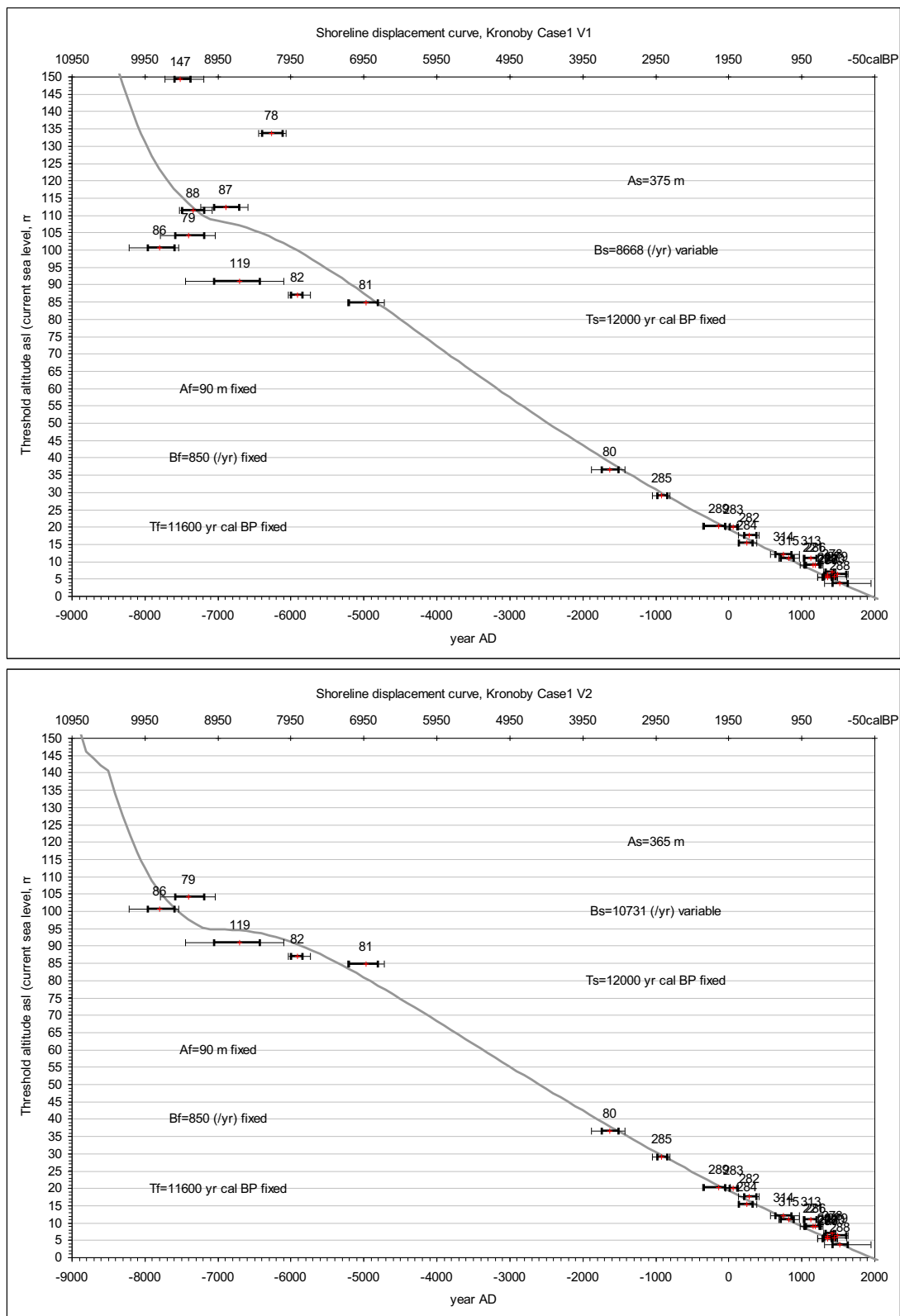


Figure 49. Graph of the Kronoby (Case1) samples. The points 147 and 78 strongly don't seem to fit in with the other points (top graph), so there is probably some undocumented tectonic line between 78 and the other points. Point 86 also behaves a bit differently from 87 and 88. The bottom graph shows the Case1 samples without the points 147, 78, 87, and 88.

For the Kronoby site, the points chosen are not that obvious, and all the Kokkola points are from low altitudes. As Case2, it was also tested if the points in the SW portion of the site could be excluded, which resulted in a value of 394 m for A_s and 10684 year^{-1} for B_s . Fast component information cannot be estimated, but if point 86 is also excluded, A_s becomes 386 m and $B_s=8981 \text{ year}^{-1}$. The new samples (with Sample No>260) fit in well with the other points but give little new information.

If points 86 and 79 would be removed too, T_s , A_s , and B_s would become too high.

Using the higher fast component values $A_f = 150$ and $B_f = 1500$ (according to Pässe 2001 maps), B_s can not be calculated but it grows to the user-defined upper limit of 12000, which is too large. The conclusion from Kronoby Case2 is that there are too few samples to solve B_s properly. It is essential to include point 80. Case2 also shows that the chosen (fixed) fast component values have an effect on the calculations of the slow component parameters, especially B_s .

As Kronoby Case4 (Case3 is from another site), it was further tested to exclude all the northern points and to use only the SW portion of the site, with 3 points added in the east (Figure 50).

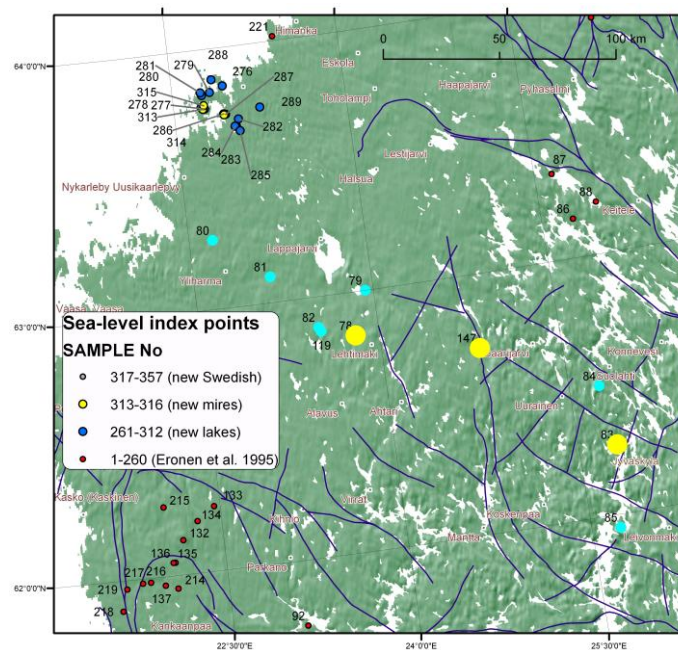


Figure 50. Plot of the Kronoby (Case4) samples, with the cyan and yellow samples selected as a subset. The yellow ones behave differently than the majority of points in the first fitting. The dark blue lines are the tectonic lines, © Geological Survey of Finland.

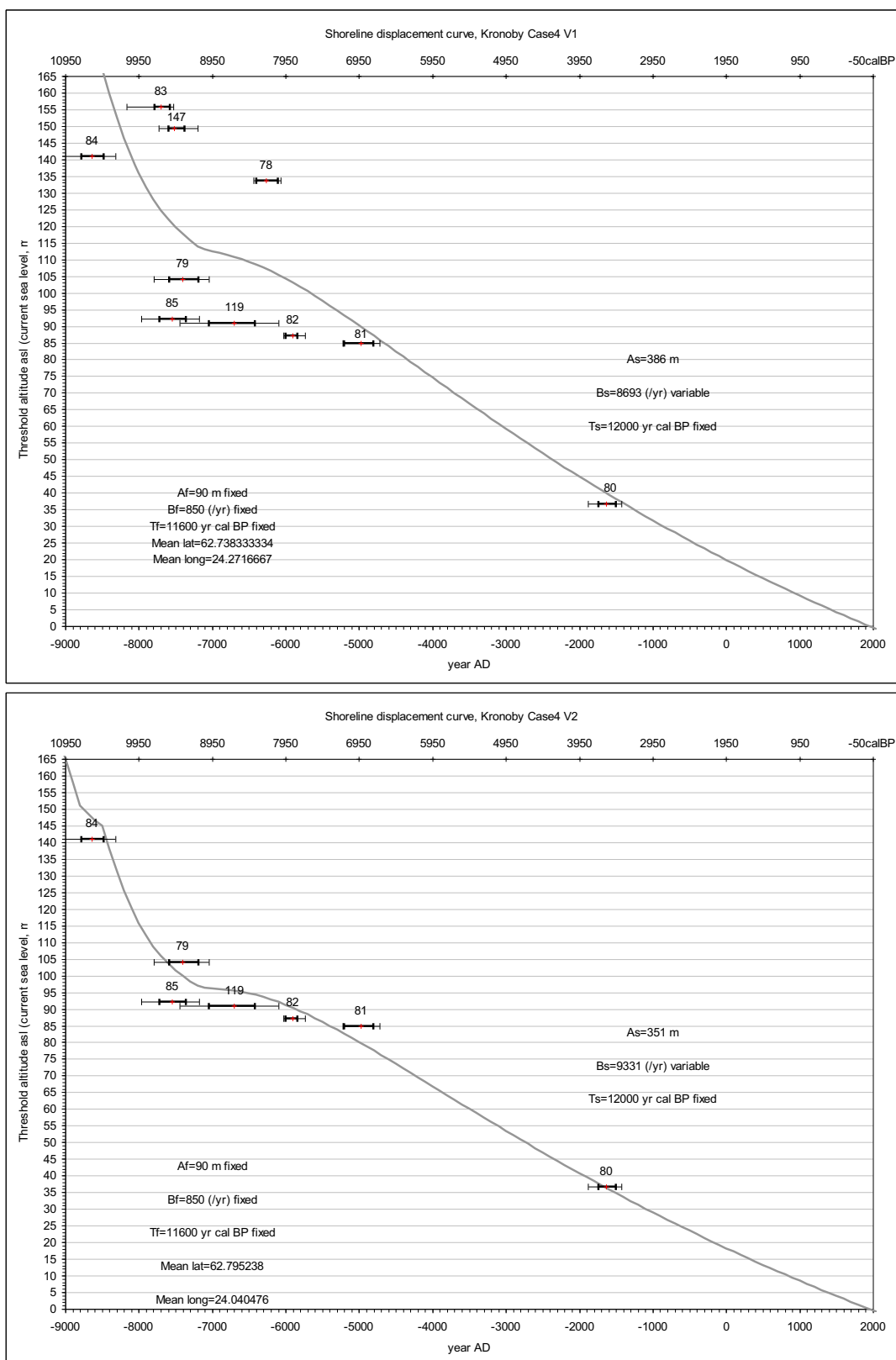


Figure 51. Graph of the Case4 samples. At least points 11, 12, 13, 14, 18, and 76 behaved differently and are highlighted yellow on the map. The effect of the Ancylus correction can be seen in the S curve in the top left part of the graph. The solution without the mentioned points is shown in the lower graph.

The Jyväskylä region (point 83) and the north side of it (point 84) seem to behave quite differently. The results in Figure 51 are possible, but the remaining two points in the east are somewhat far from the others.

It was decided to keep **the edited Case1 results** for Kronoby; there, both A_s and B_s are probably properly calculated.

Lauhanvuori (Figure 52) is a case for which there is little recent data available (from low elevations) but more data relevant for the fast component. The results (Figure 53) suggest new values for T_f and for the inertia factor B_s , whose value of 6027 year^{-1} is 2773 year^{-1} less than in Pässe (2001), and the final A_s is very close to Pässe's value. The B_s estimate in any case varies easily: if no points are removed but A_f is calculated too (as 111 m), A_s becomes 316 m and the B_s estimate would be 9331 year^{-1} . These results were kept in Appendix 5. Pässe & Andersson (2005) suggest $B_s=9500 \text{ year}^{-1}$. B_f was calculated now as 1071 year^{-1} and T_f as 10759 cal BP.

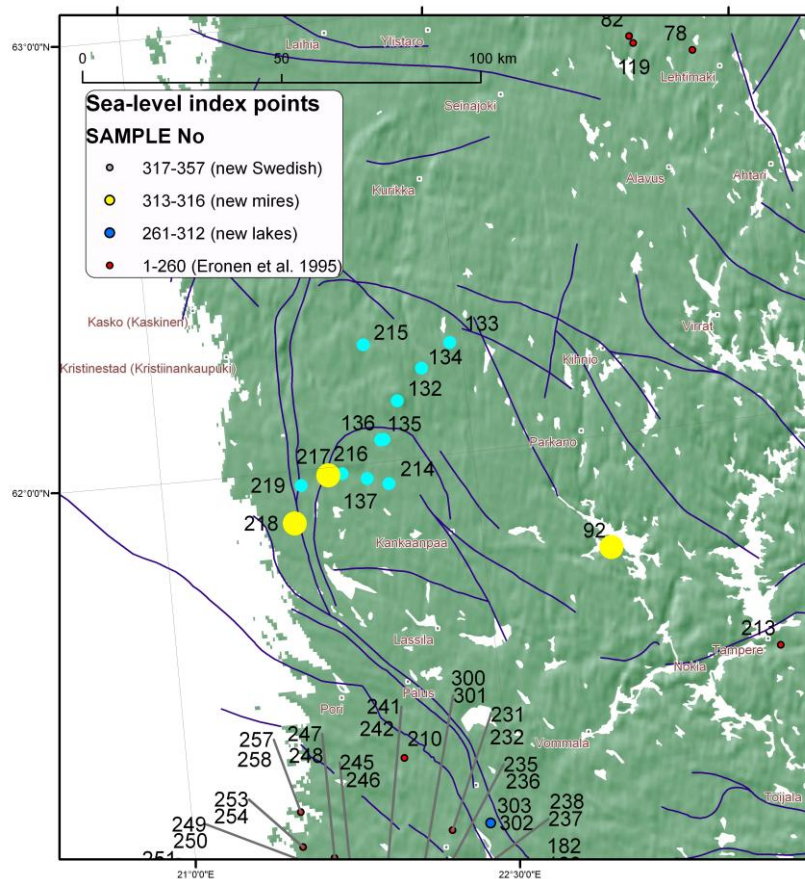


Figure 52. Plot of the Lauhanvuori samples, with the cyan and yellow samples selected as a subset, and the yellow points behaving slightly differently than the others. The dark blue lines are the tectonic lines, © Geological Survey of Finland.

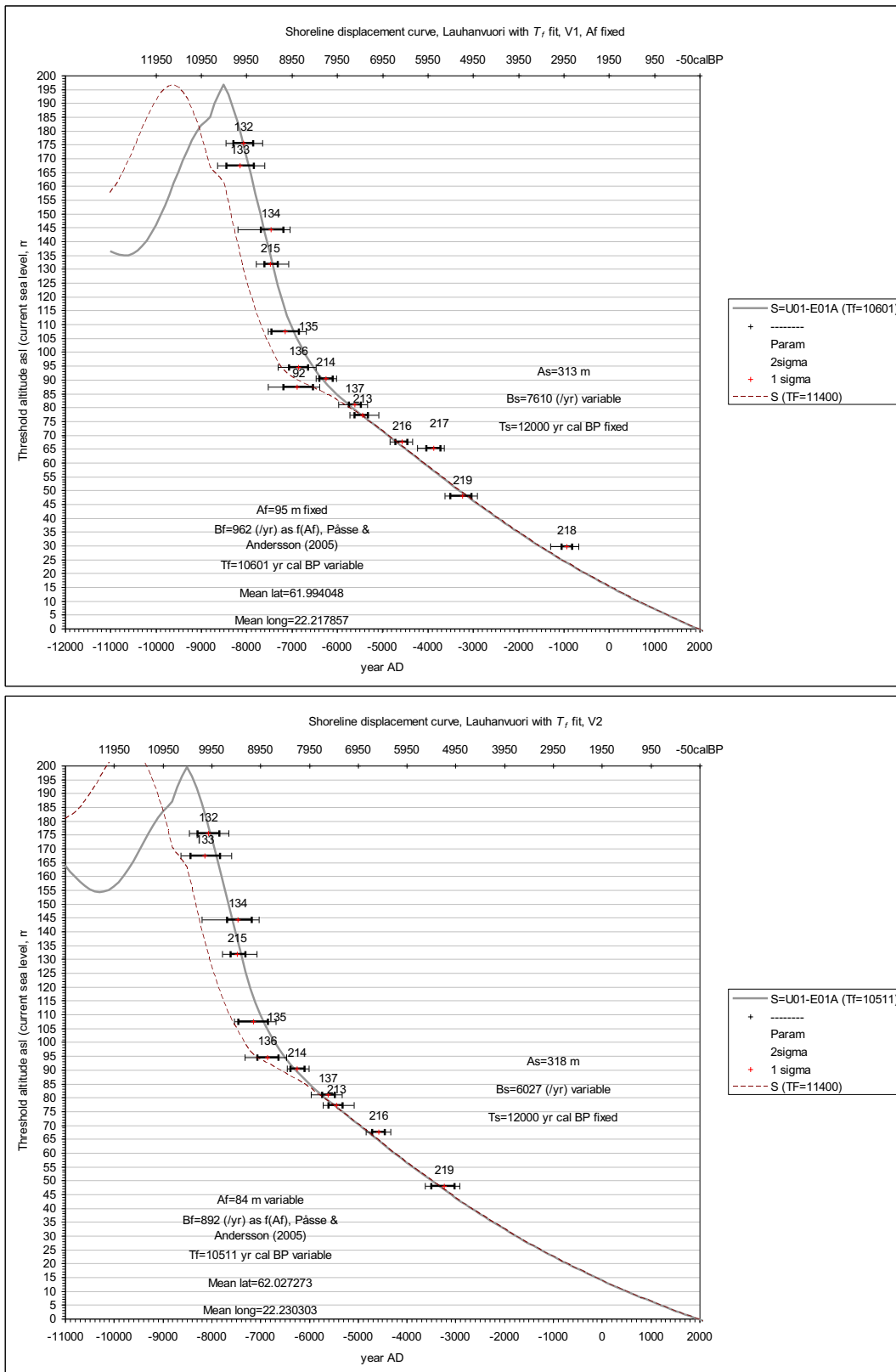


Figure 53. The graphs of the Lauhanvuori samples.

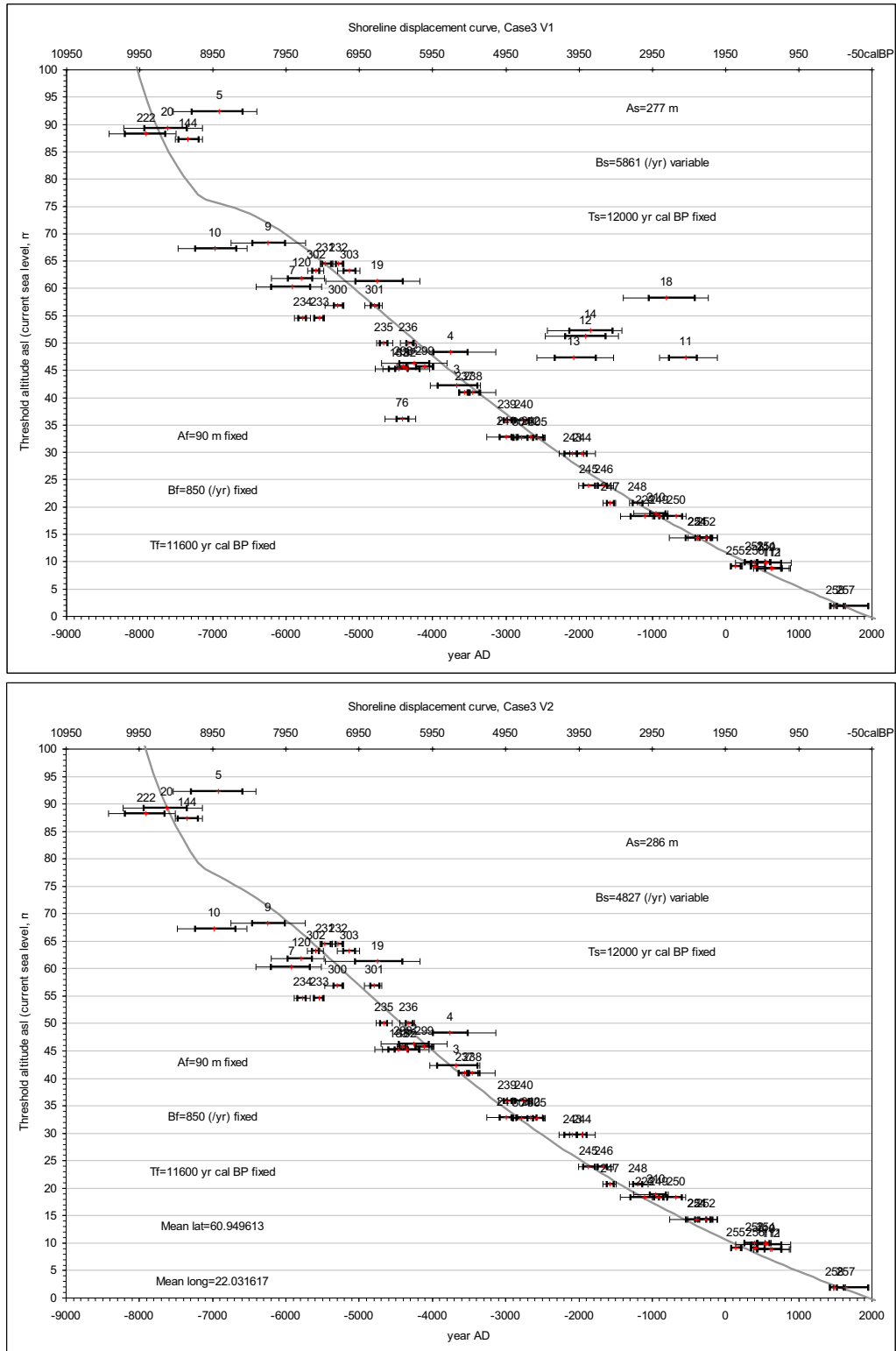


Figure 55. Graph of the Olkiluoto-Turku Case3 samples. At least points 11, 12, 13, 14, 18, and 76 behaved differently and are highlighted yellow on the map. The analysis without the mentioned points is shown in the lower graph. The results shown here were not kept but the subset was split.

It is better to exclude the mentioned points even if the Olkiluoto (Figure 56) and Turku (Figure 58) areas are analysed separately, as is done below.

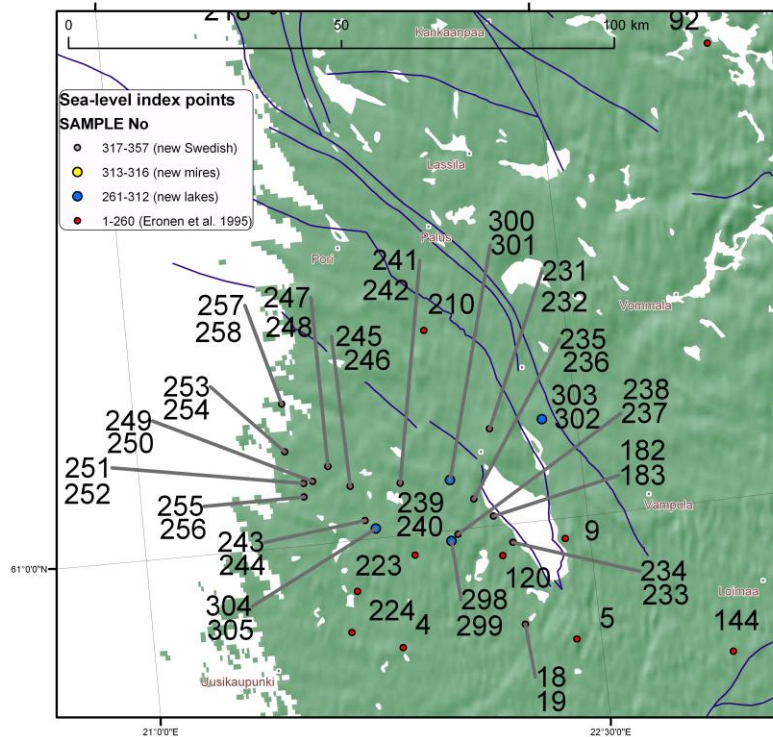


Figure 56. Plot of the 47 Olkiluoto samples. All the visible ones except number 18 were included in the site's calculations. The dark blue lines are the tectonic lines, © Geological Survey of Finland. Olkiluoto itself is located at points 257 and 258.

The Olkiluoto points (Figure 57) can be mainly used to estimate the slow component parameters, whose values should be quite reliable, except that the fast component parameters remain unreliable and that this has some effect on the slow component estimates too.

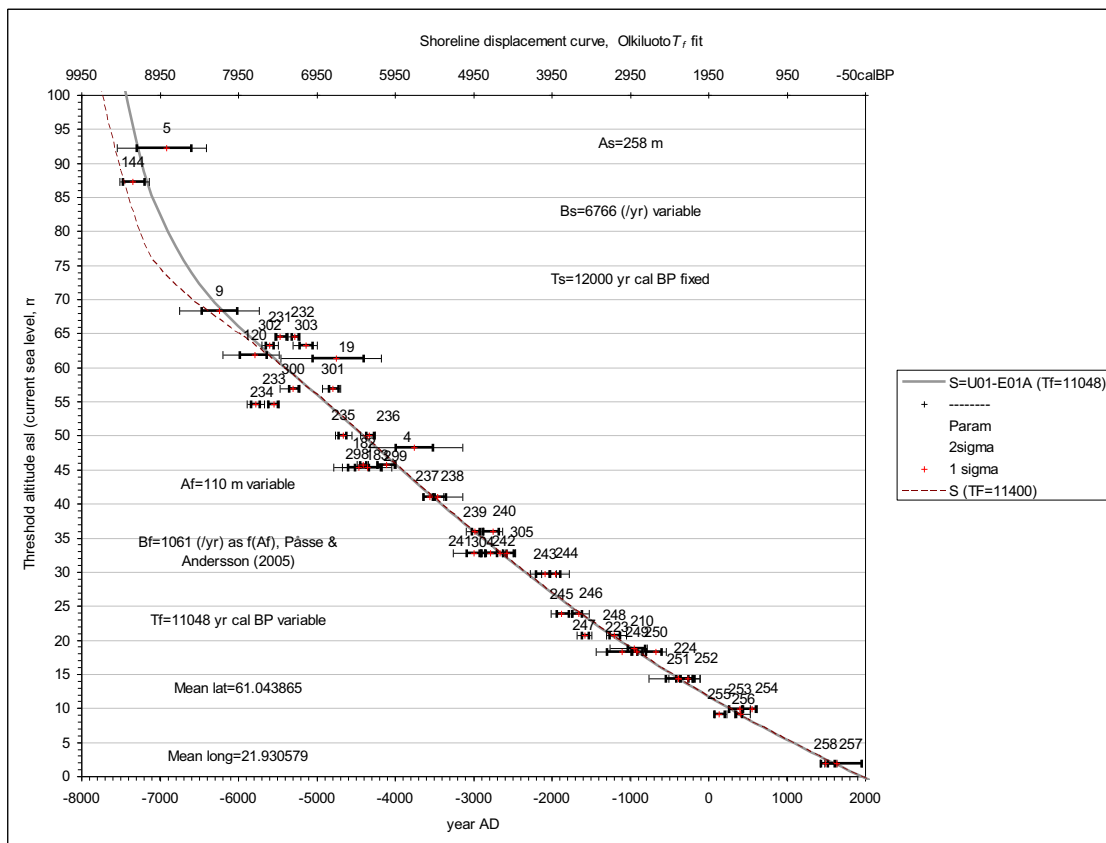


Figure 57. Graph of the Olkiluoto samples. No reliable fast component information can be estimated.

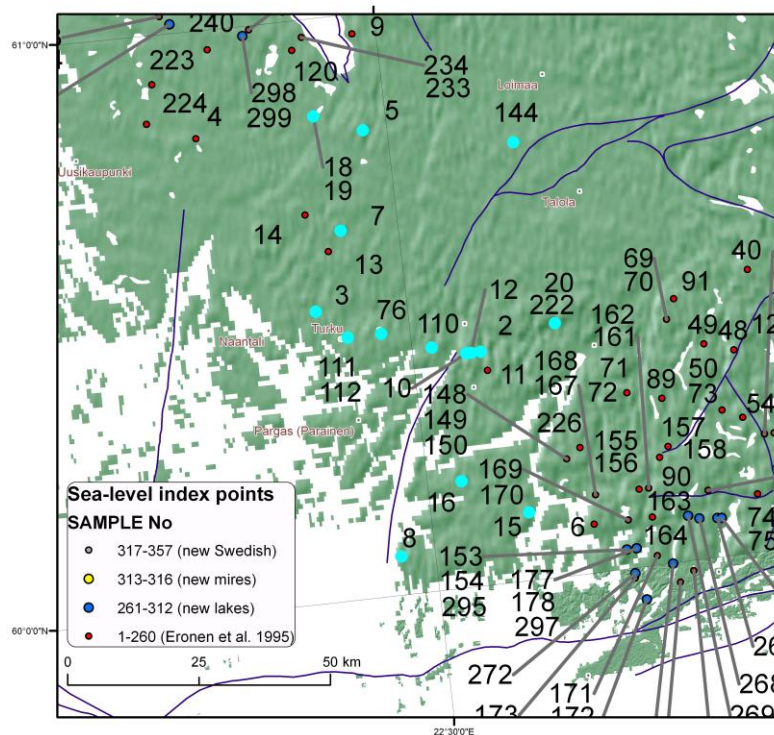


Figure 58. Plot of the Turku samples, with the cyan samples left as a subset. The dark blue lines are the tectonic lines, © Geological Survey of Finland.

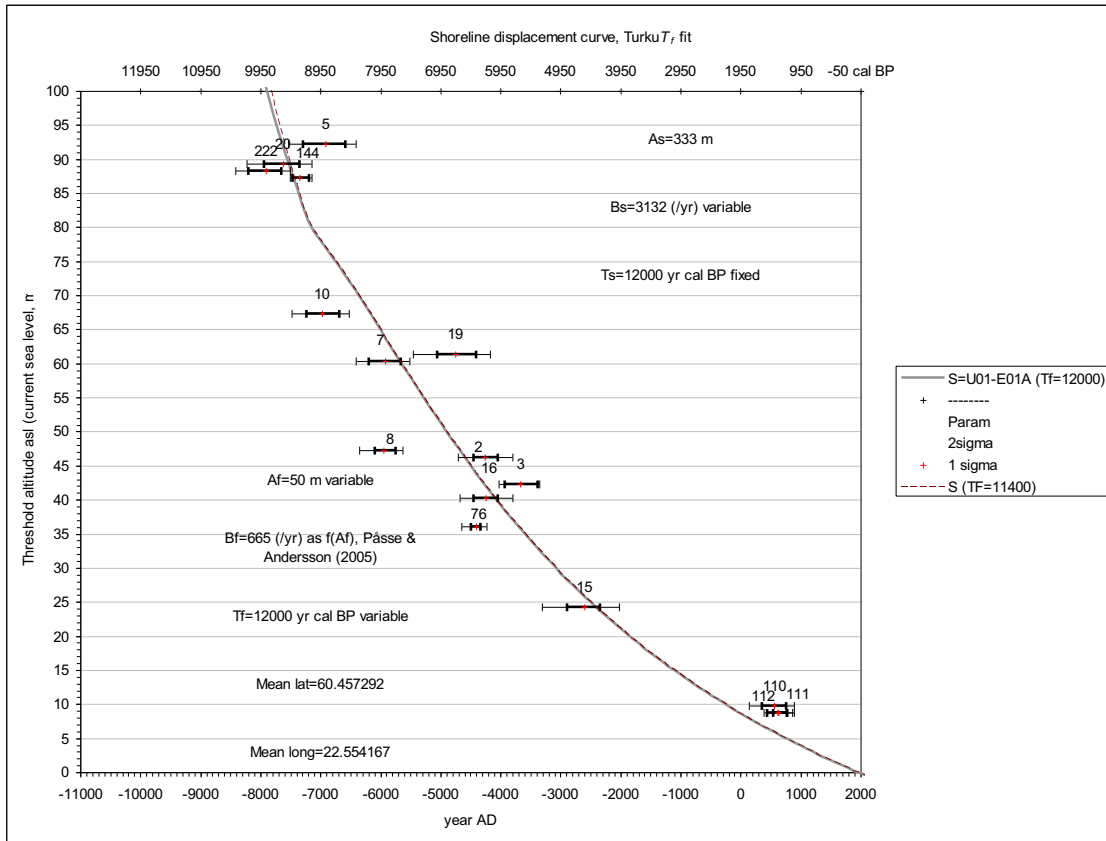


Figure 59. Graph of the Turku samples.

Using the Turku points (Figure 59), no fast component information can be estimated, and even the slow component values' reliability is not very good with such a heterogeneous subset. This time the new values were not used.

In the Tammisaari region, there were a number of new points available (Figure 60). Some points that were previously included in the Karjalohja and Lohja sites were included too, but many of them were in any case rejected in the second phase (Figure 61).

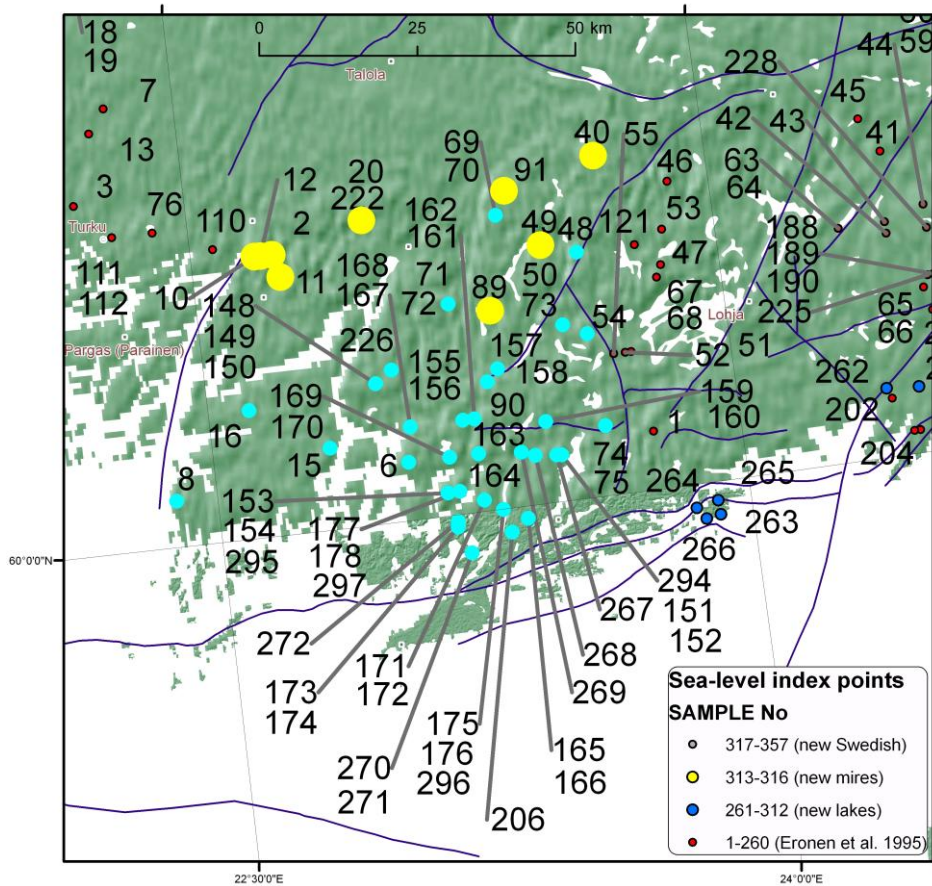


Figure 60. Plot of the Tammisaari samples, with the cyan samples left as a subset and the yellow ones behaving differently than the others. The dark blue lines are the tectonic lines, © Geological Survey of Finland.

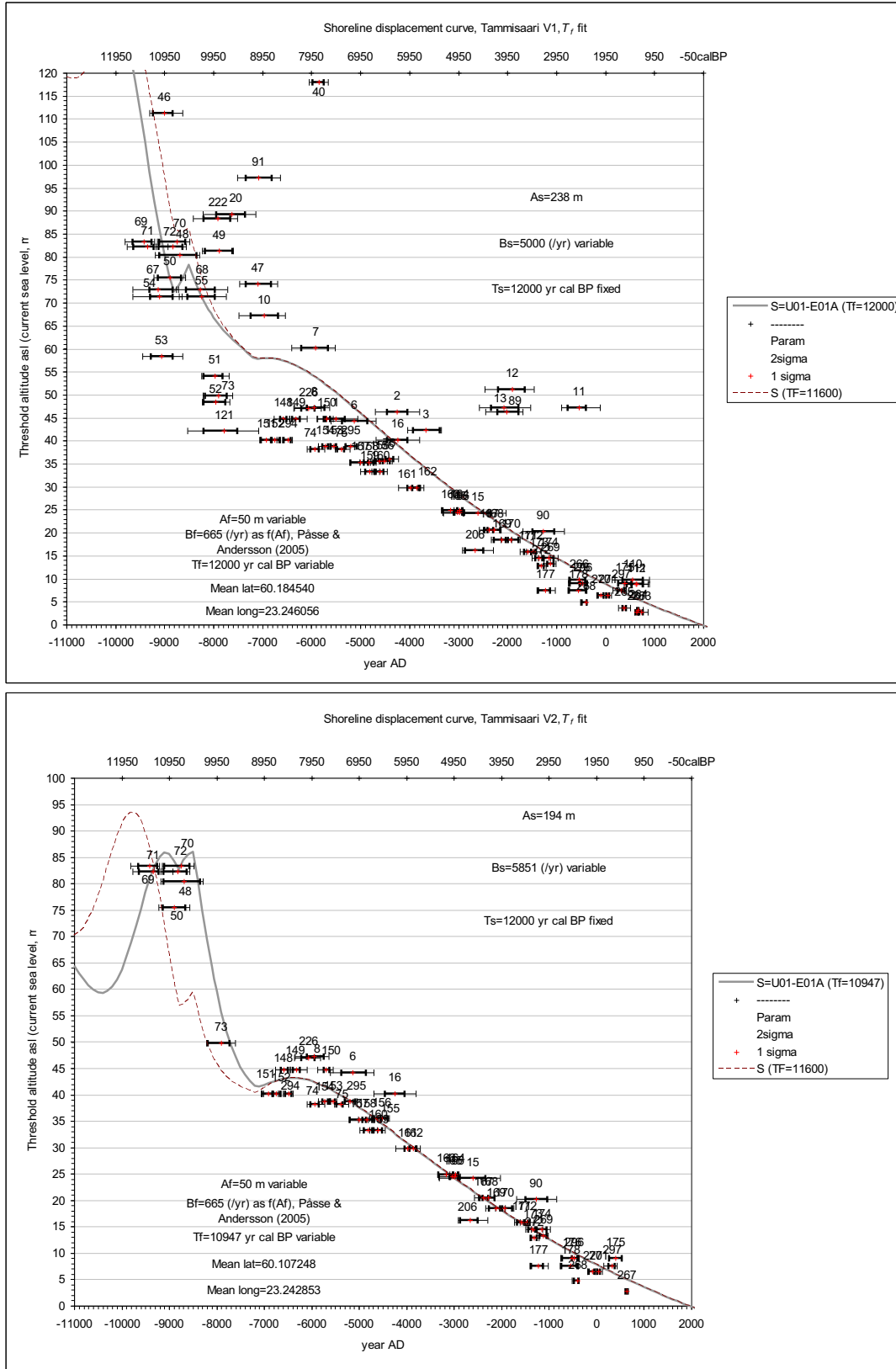


Figure 61. Graphs of the Tammisaari samples. Points 2, 10–12, 20, 40, 49, 89, 91, and 222 were not included in the lower graph calculations.

More points were also used for the Porvoo region (Figure 62) than used in the Porvoo graphs in previous literature. Points in the Helsinki region and new points from farther east were also included.

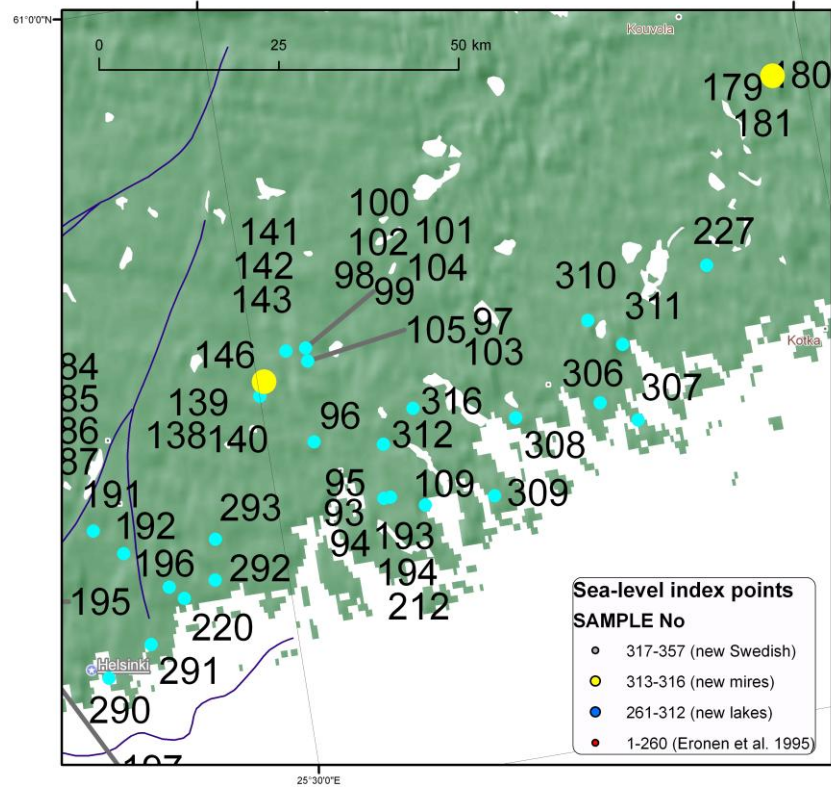


Figure 62. Plot of the Porvoo samples, with the cyan & yellow samples selected as a subset, and the yellow ones behaving differently than the others. The dark blue lines are the tectonic lines, © Geological Survey of Finland.

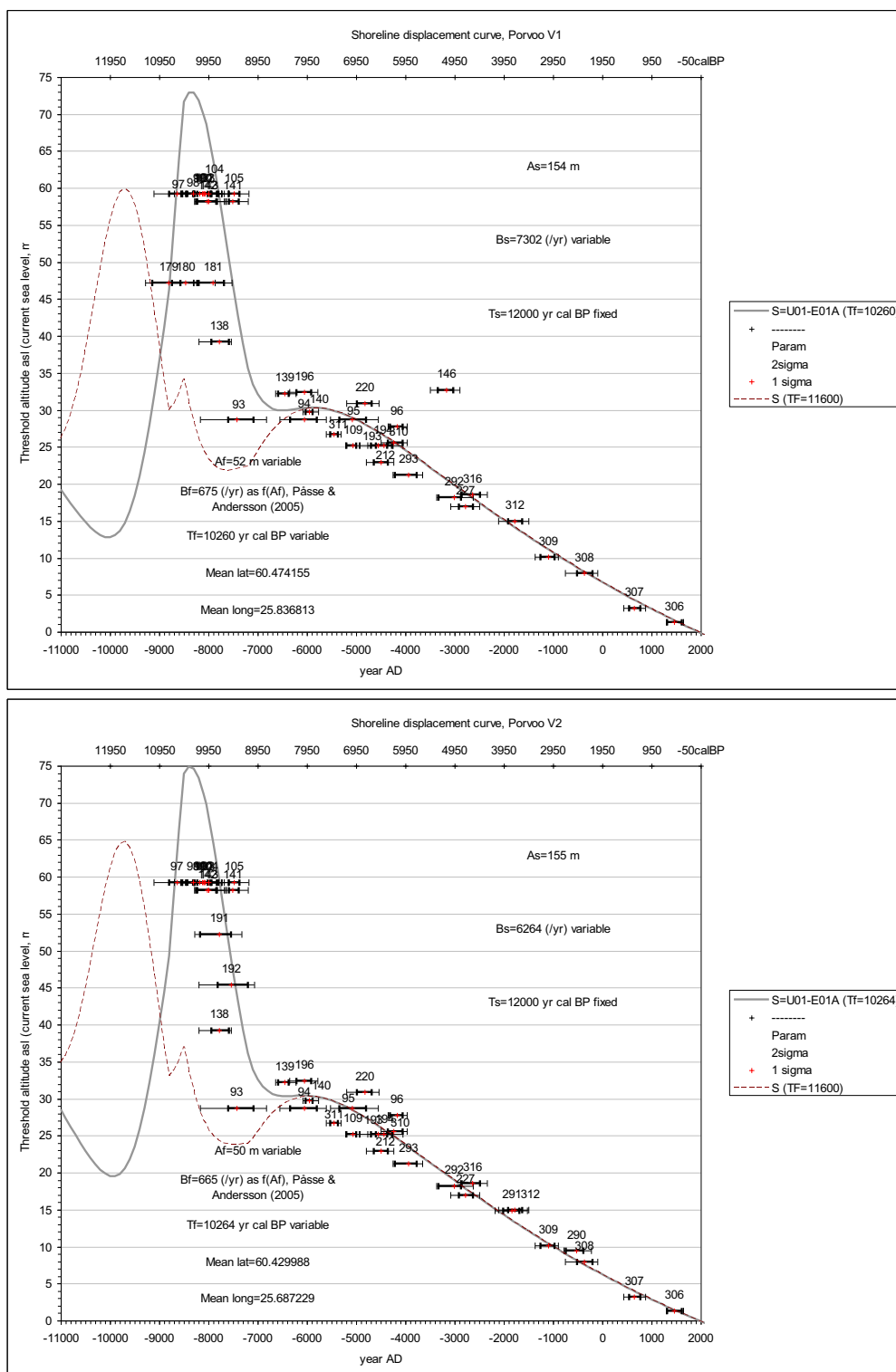


Figure 63. The graphs of the Porvoo samples show how the value $T_f=11600$ years cal BP of Pässe (2001), the dashed line, would not be optimal. Here, T_f was calculated from the data too. In the lower graph, certain sea-level index points have been removed or replaced. The used minimum constraint of A_f (50 m) was reached.

For Porvoo, the fast component parameters are again less reliable than the slow ones (Figure 63). The points at the altitudes 55–60 m result in a B_f estimate that is 869 year⁻¹ smaller than calculated without those points, but then the 110 m maximum constraint of A_f would be reached. When some or certain sea-level index points are removed, the slow component inertia factor B_s therefore seems to vary as much as 1000 year⁻¹. Earlier, for example in Pässe (1996 Figure 4-63), the effect of the Ancyclus correction was not included in the calculated curve.

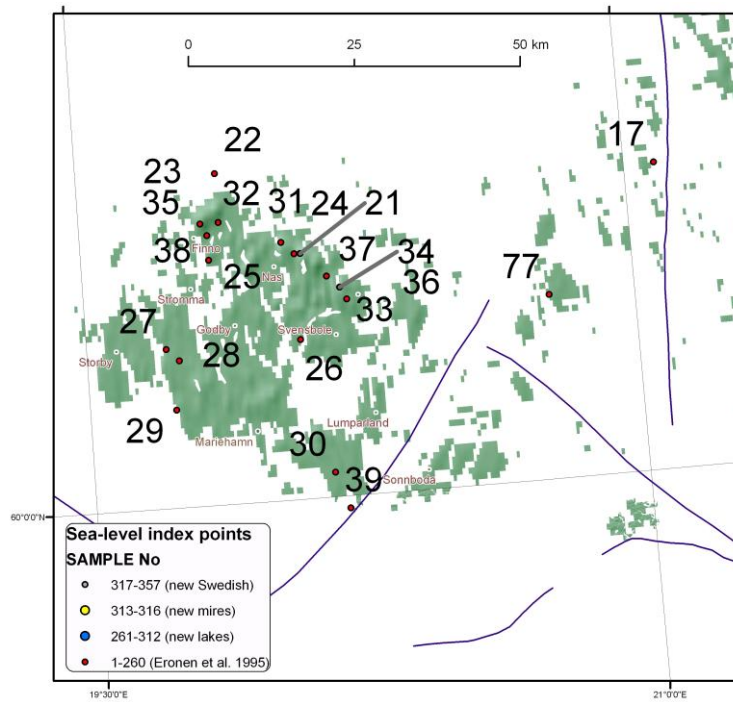


Figure 64. Plot of the Åland points. The dark blue lines are the tectonic lines, © Geological Survey of Finland.

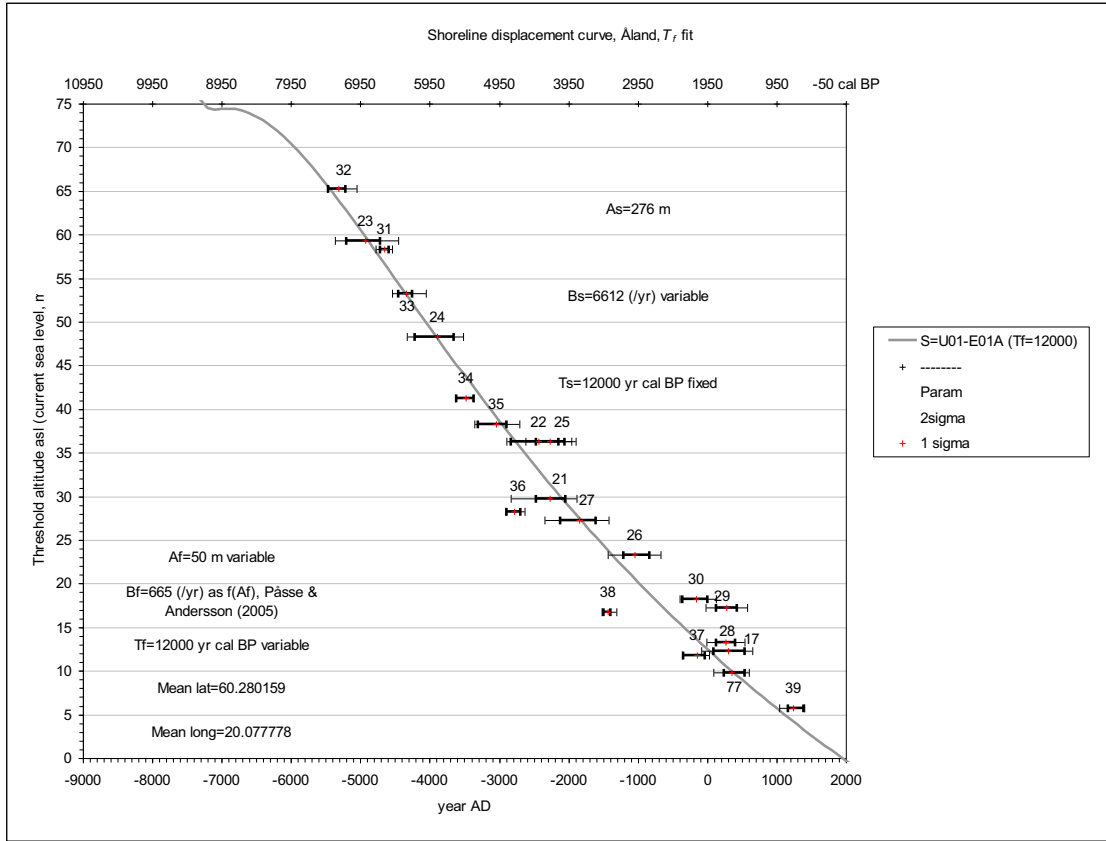


Figure 65. The graph of the Åland samples. No fast component information was estimated.

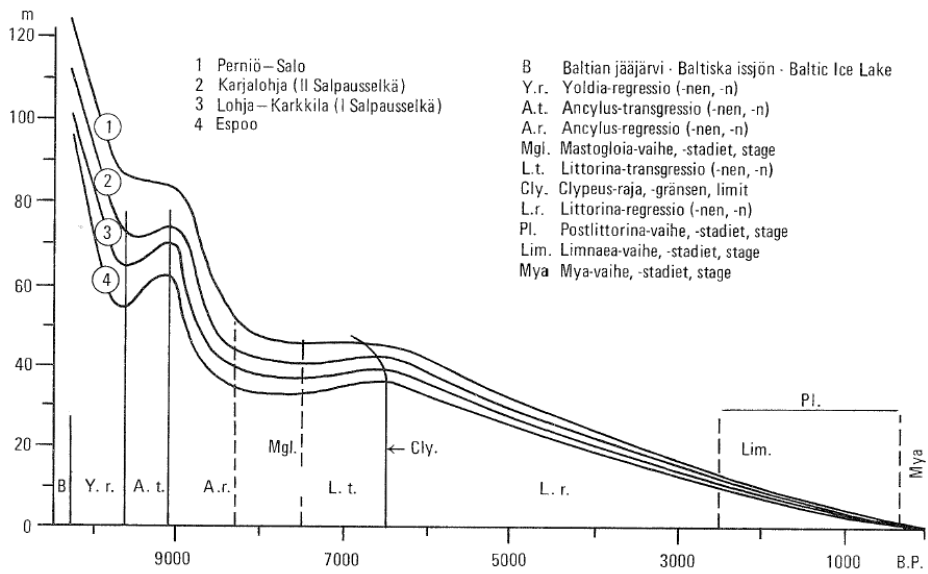


Figure 66. Stages of the Baltic Sea and displacement curves for southeastern Finland as reported by Ristaniemi & Glückert (1987) (Eronen 1990). The Finnish south coast uplift has also been studied later.

For Åland, no fast component information can be extracted. In this case the slow component values can be regarded reliable, even though the minimum constraint was met. Fixing the A_f as 80 m has no effect on them.

The Karjalohja, Lohja, Espoo, and Hangassuo sites were not recalculated even though there were some new points along the south coast. The plan was to calculate the sites on the Finnish west coast and Åland only. The differences between the Finnish south coast sites (Figure 66) could be redetermined by recalculating them. The Suursaari results (Heinsalu et al. 2000) could be included.

Two Swedish sites were calculated, even though only the new points were available. The first one is the Forsmark site (number 84), Figure 67. It is interesting for Sweden due to the same reasons that Olkiluoto is for Finland; due to the plans for a final repository for spent nuclear fuel at this site. The results (Figure 68) for the site were this time saved under the new number 85. The new points included no points from high altitudes, but they are rather evenly distributed, giving some stability for the slow component estimations.

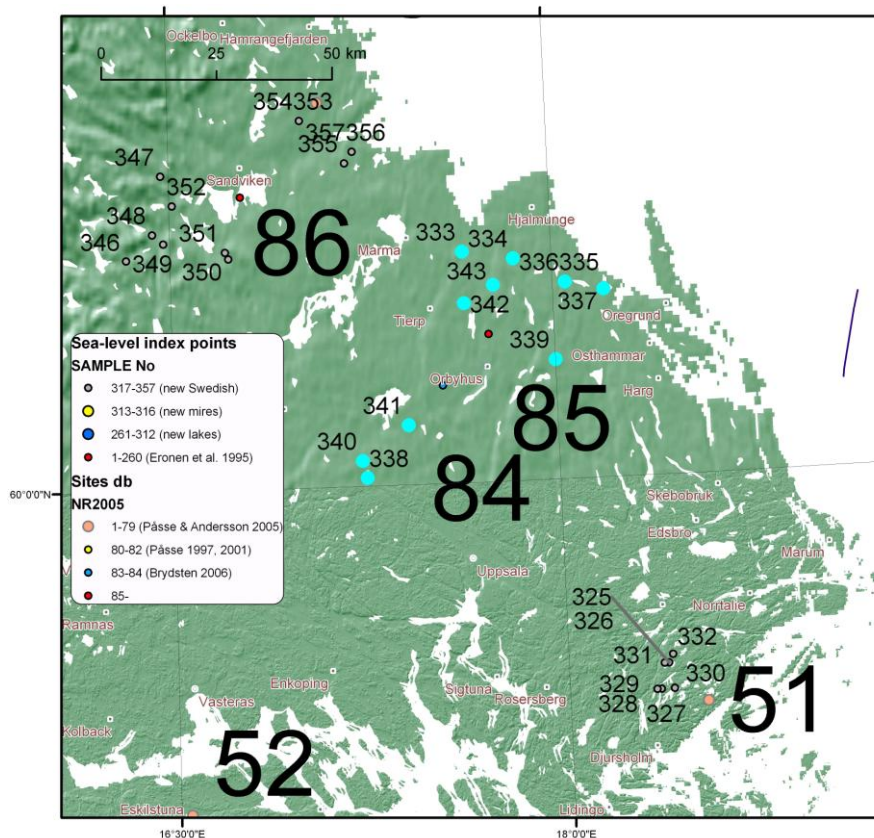


Figure 67. Plot of Forsmark's 11 samples (note: new ones only), with the cyan samples selected as a subset. The Swedish sea-level index points are all grey. The large numbers are site numbers, and the red site 85 is the average location, and the blue 84 the one provided by Brydsten (2006).

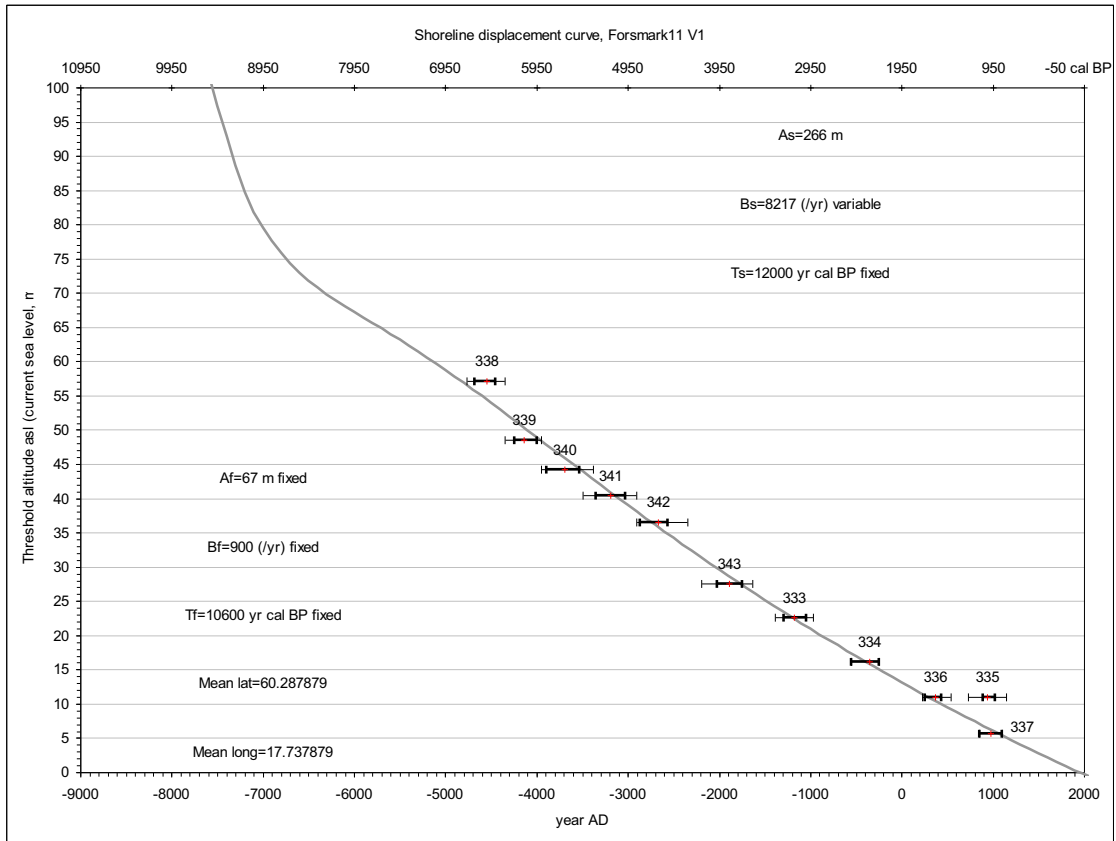


Figure 68. Graph of the Forsmark case with 11 points. Point 335, located exactly in the same location as 336, deviates from the general trend. No information on the fast component can be extracted.

The reasons for a larger B_f value for the Forsmark site than in Brydsten (2006) are that his datings may not be based on IntCal04 and that the older points not available here can make the difference.

Most of the Swedish sea-level index points are close to the Swedish repository site candidates, but this study does not take a stand on how well that data is applicable to the areas around these sites.

West of the Forsmark site is the Gästrikland site (Figure 69). In the results for Gästrikland (Figure 70), the S curve goes down before AD -8500 mostly due to the local nature of the fast component of Påsse (2001). The U_f parameters may actually be different here. Point 352 seems to be slightly different from the others.

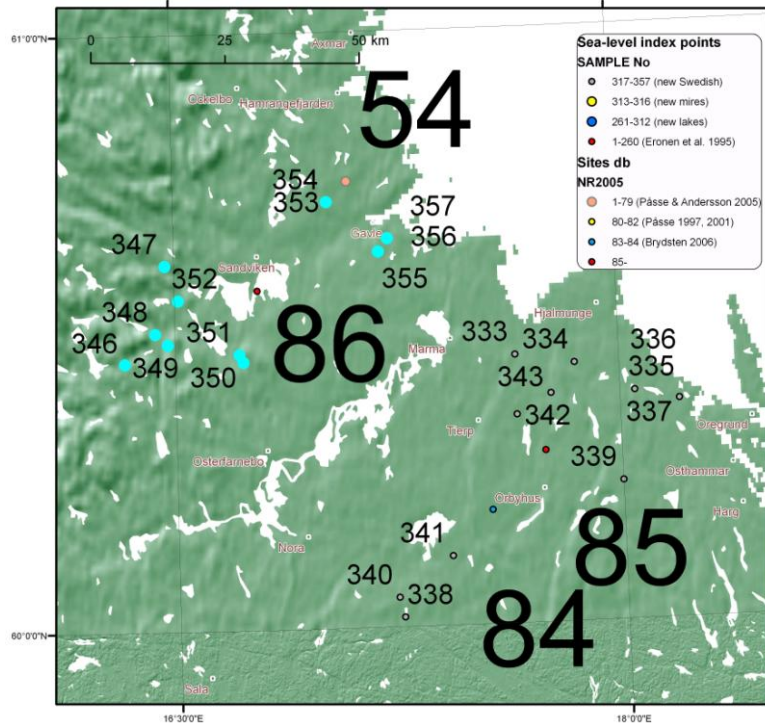


Figure 69. Plot of Gästrikland's 12 samples (note: new ones only), with the cyan samples selected as a subset. The large numbers are site numbers, and the red site 86 is the average location.

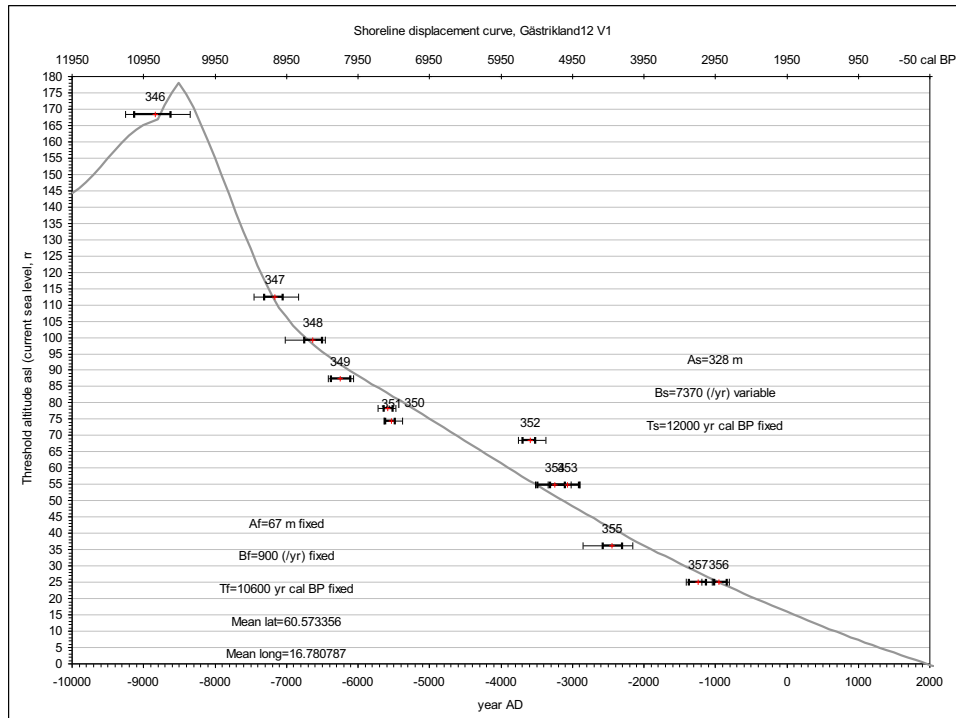


Figure 70. Graph of the Gästrikland 12 case with 12 points. Most of the Swedish sea-level index points are close to the Swedish repository site candidates, but this study does not take a stand on how well that data is applicable to the areas around these sites.

7.3.2 Combination of the old and new shore-level displacement analyses

It was possible to combine the previously analysed sites by Pässe (1997, 2001), Pässe & Andersson (2005), Brydsten (2006), and the new sites described above, including calculations of the isostatic land uplift parameters at all these sites. Not all the parameters are solved for each point, but the ones considered too unreliable were left blank. Deciding when an A_s or B_s estimate is too unreliable may be subjective.

Brydsten (2006) had already solved the A_s and B_s parameters for the site Simpevarp (average location estimated visually as 57.435833° N/ 16.665556° E), stating that there was no fast uplift component. Probably this means that it could not be determined. Brydsten had also calculated A_s , B_s , A_f , and B_f for Forsmark (avg. location 60.19166667° N/ 17.55277778° E using the six sea-level index points listed by Hedenström & Risberg (2003)).

See the table in APPENDIX 5 for all previous sites plus all the new analysed sites.

If there is enough data for before AD -6000 that is relevant for determining the fast component, better estimates can be given than by Pässe (2001). T_f is an important parameter, and its estimates probably improved much thanks to the better time calibration. But it may be best to calculate also the other fast uplift components. One must decide either to handle B_f as a function of A_f (see Table 4) or to solve B_f independently. Here, the fast component parameters were not systematically re-calculated.

If there is little recent data available (for after AD -6000), A_s and B_s estimates are not very reliable. Especially the B_s estimate varies a lot when sea-level index points are removed from a subset or when some fast component parameters are also calculated.

7.4 Parameter surface interpolation

7.4.1 By kriging

The Pässe (2001) table includes more fast component values for the sites than Pässe & Andersson (2005), but for example the T_f values are less reliable in the former. The question arose as to which dataset to use together with the new calculated sites. The dataset in the 2001 report was the default. Only points with no slow component values in Pässe (2001) got the A_s and B_s values from the 2005 report. The A_s and B_s site dataset for which the interpolation was done was therefore a combination of data in the 2001, 2005, and the present report.

It is possible to create perspective view visualisations of the data (Figure 71, Figure 72). Due to the overlapping bars, a video with rotation would provide even better visualisation. Y is the north axis, X the east.

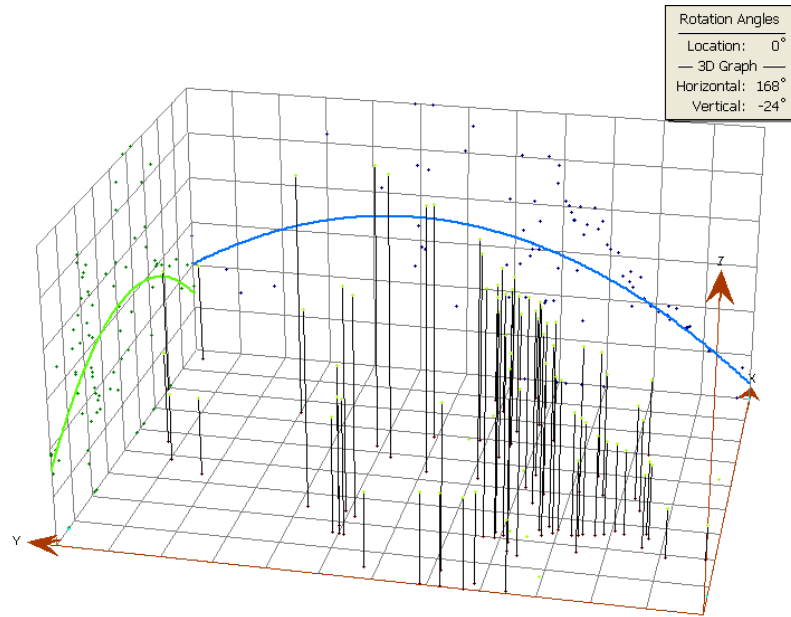


Figure 71. An example A_s trend analysis of Pässe (2001) data visualises the distribution of the parameter.

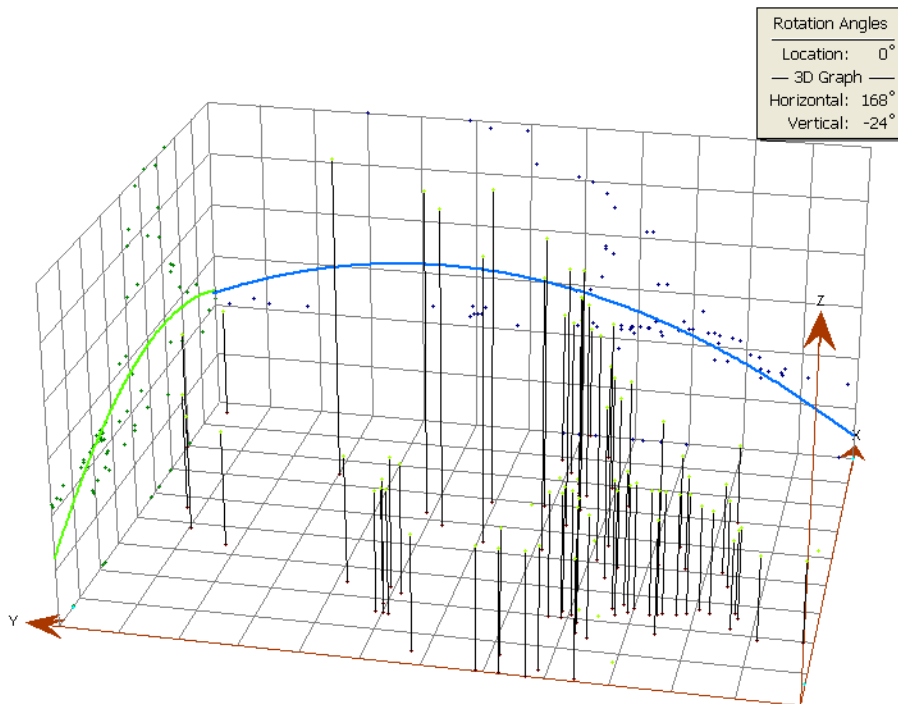


Figure 72. An example B_s trend analysis of Pässe (2001) data visualises the distribution of the parameter.

Due to the flexibility of the ArcGIS Geostatistical Wizard, many parameters that concern kriging are adjustable. Kriging allows the user to investigate graphs of spatial autocorrelation (Figure 73). Kriging uses statistical models that allow a variety of map outputs including predictions, standard error prediction (see also Figure 74), probability, etc. The flexibility of kriging can require a lot of decision-making. Not to

mention the other interpolation methods, it is therefore possible to produce quite different maps from the available sites.

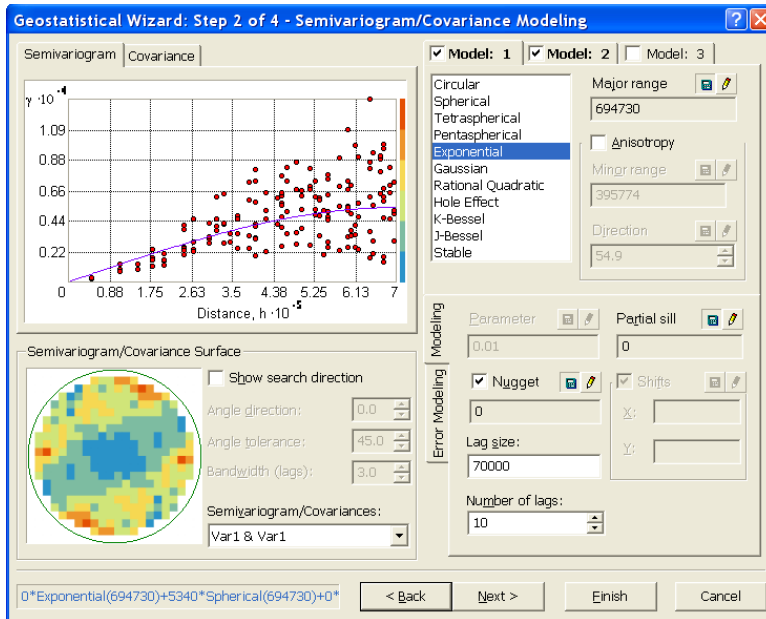


Figure 73. Selecting suitable lag size, number of lags, etc. for the ordinary kriging method of the ArcGIS Geostatistical Wizard.

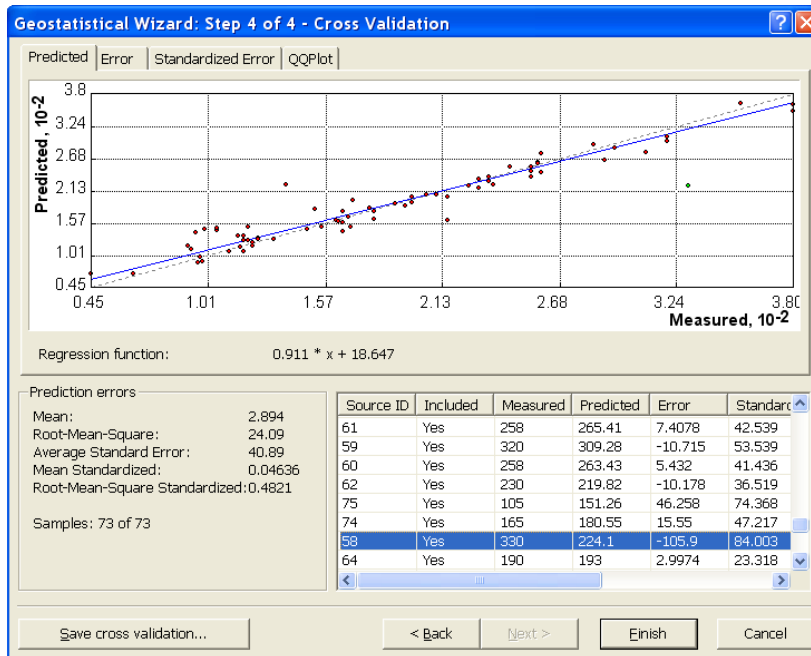


Figure 74. The kriging prediction errors, e.g. here of A_s by Pässe (2001) suggest that Dalnie Zelentsy (79) and Rovaniemi (58) have the biggest errors. Both are in the north with few other sites to support them.

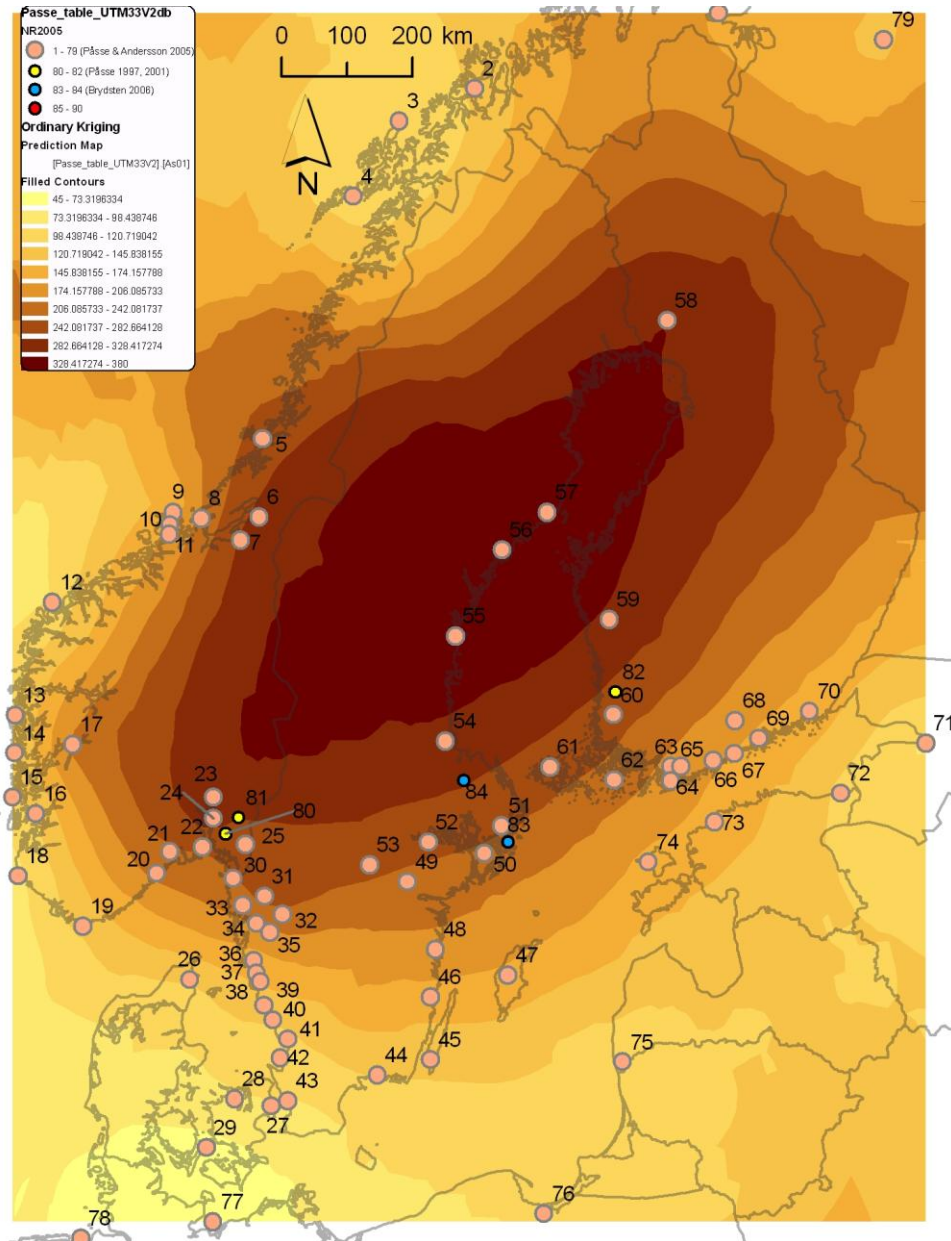


Figure 75. An example A_s estimate surface by kriging without trend removal, from the Pässe (2001) data.

Kriging revealed that at least the Eskilstuna site (52) with $A_s=50$ m does not agree with the maps of Pässe & Andersson (2005), so it must be a typo and is probably 250 m as in Pässe (1997). Pässe (2001) gave 255 m.

The kriging with pure Pässe (2001) data (Figure 75) was done in order to compare the distributions shown on the map produced here with those shown on the maps in Pässe (2001, Figure 3-9). The differences are rather small. Pässe's (2001) maps seem to present a bit smoother distribution than what was produced here, probably due to the generalisation settings.

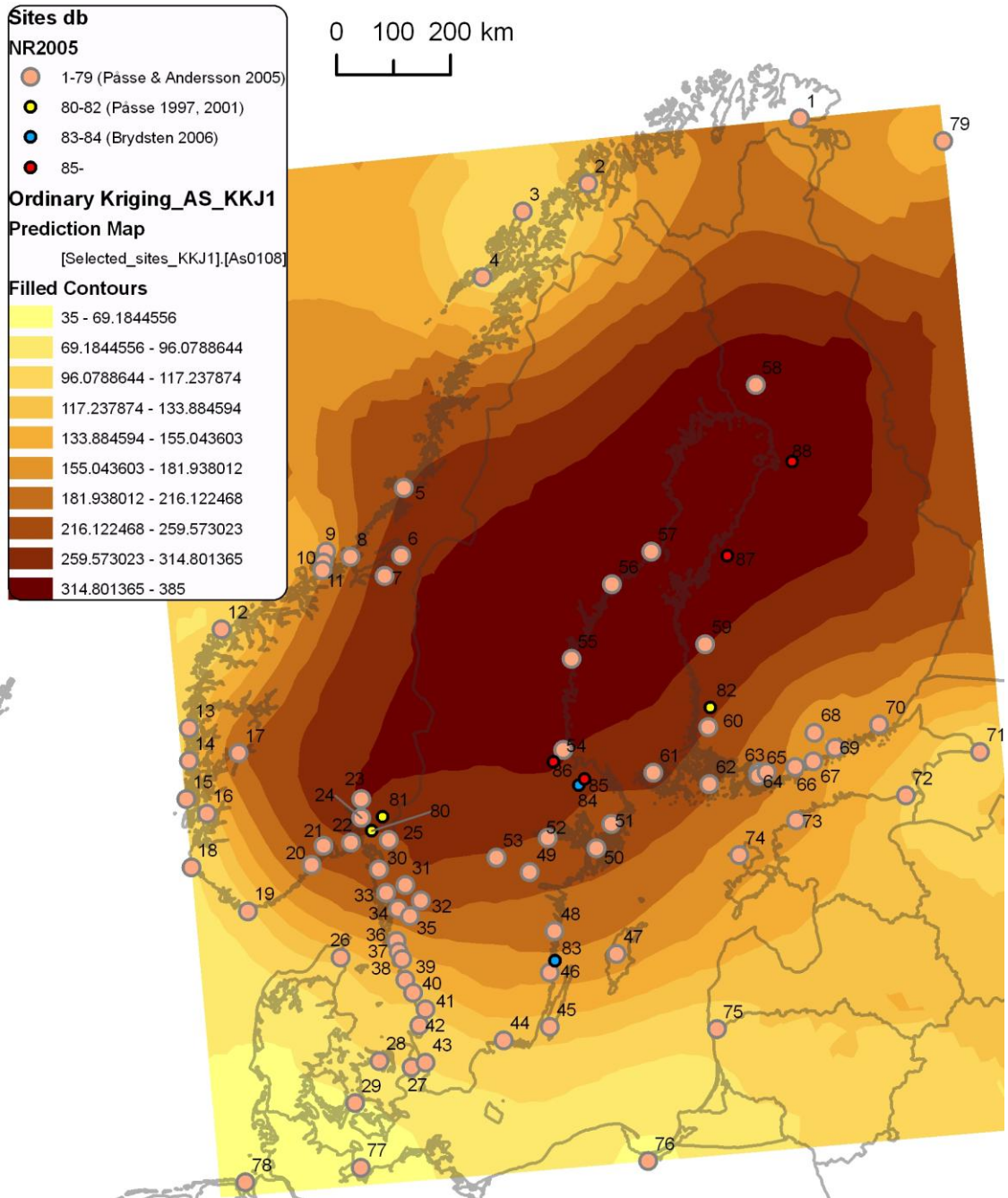


Figure 76. An A_s estimate surface by kriging without trend removal based on the data in Pässe (2001), Pässe & Andersson (2005) (for sites that did not exist in 2001), and Brydsten (2006) and on new data. The Finnish sites 62, 63, 65, and 82 and the Swedish sites 54 and 84 were excluded. The Kronoby site 87 had a relatively large prediction error. The Oulu site (88) now had the maximum value 385 m.

The A_s estimate based on all the old sites (some of which were recalculated) and the new sites (Figure 76) shows that the north part of the maximum distribution is longer and farther east than in the previous results.

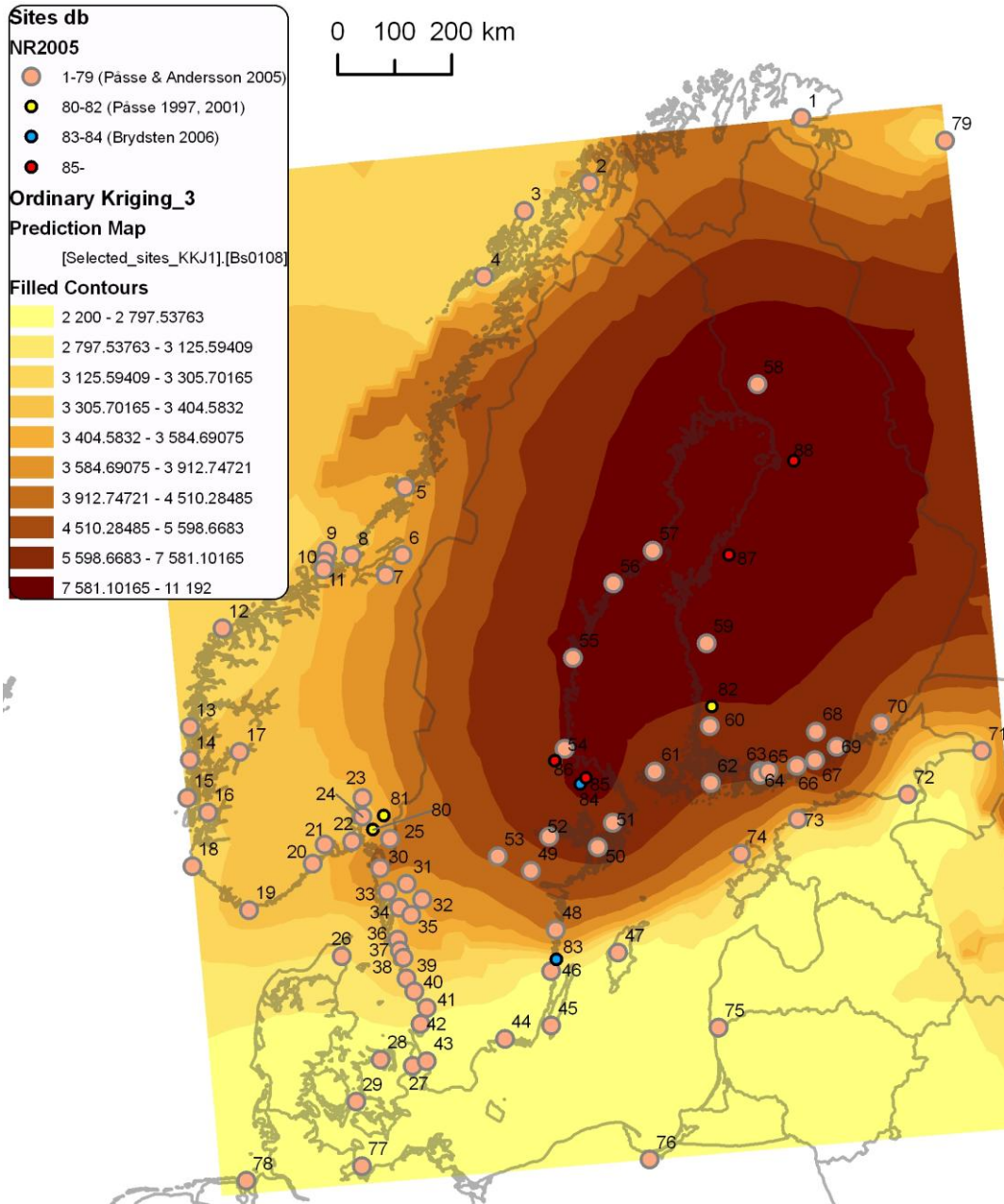


Figure 77. A B_s estimate surface by kriging without trend removal based on data in Pässe (2001), Pässe & Andersson (2005) (for sites that did not exist in 2001), and Brydsten (2006) and on new data. The sites mentioned above were excluded. The values are larger than before in the Ostrobothnian regions due to the new sites 87–88.

The sites Gästrikland (54), Turku (62), Karjalohja (63), Lohja (65), Satakunta (82), and Forsmark (84) were excluded from the interpolations because an updated site had been set up next to them with new calibration methods. Otherwise the interpolation would cause artificial curves between old and new or recalculated sites. This was noticed at least in the case of the old and new Forsmark sites (84 and 85). Some old sites like Helsinki (67) and those on the Swedish coast (55–57) were nevertheless included.

The B_s estimate based on all the old sites (some of which were recalculated) and the new sites (Figure 77) also shows larger values in west Finland than before. For Figure 77, the Lauhanvuori site (59) still had the B_s value 9165 year^{-1} , based on the constrained A_f (110 m). Making the constraint higher lead here to a merely 1.4 m higher A_f value but to a 166 year^{-1} higher B_s value (9331 year^{-1}).

7.4.2 By other means

Other methods than ordinary kriging are available. It is interesting for example to create breaklines at the tectonic lines. The problems are firstly that each site is typically calculated from points collected from more than one subregion between the tectonic lines. The region of the used points should in any case not be too large. Probably all the area from which the subset has been chosen should be given similar uplift properties. Thresholds or breaklines should be placed only outside the blocks from which the points were collected.

Secondly, the number of sites is relatively small, or there are more lines than desirable. Many regions between the blocks would remain without an estimate, or it is ambiguous where to set the breakline during the interpolation.

The crustal lines have attributes, some of which may help to decide which lines more probably separate different uplift behaviour. Certain crustal lines, on the other hand, can be considered more stable or more probable to have regions with similar land uplift properties on both sides.

Additionally, the regions with little data can be revealed by means of triangulation methods, see Pässe (2001, Figure 3-10).

In the study, the related problematics were discussed, but no alternative interpolations were produced. Placing the breaklines was too ambiguous. There are a lot of points on the south coast of Finland, and further tests may reveal the probable borders of different isostatic land uplift behaviour.

7.5 Interpretation of the results

7.5.1 Derivative-based results

For the Olkiluoto case, the derivative-based models for the future uplift agree with the previous models by Pässe (2001). But the vicinity of the thicker crust on the north side and the Moho depth to B_s modelling are factors that create uncertainty. Elsewhere, the differences between various models may be larger. The A_s estimates produced this way may be too local, for example because a limited-size thicker area in the crust does not determine the isostatic uplift alone. Including the lithospheric thickness and other properties of the crust would be reasonable, or at least a regionally varying exponential equation could be used for the Moho depth to B_s transformation. It would be useful to analyse where the poorly matching points are geographically located and to find explanations for the poor exponential fit. The sites that have a B_s value higher than

5000 year⁻¹ are located roughly in the Gulf of Bothnia area (about in the triangle Lohja – Rovaniemi – Gästrikland).

Note that Figure 41 suggests local maximums of A_s in northern Sweden and the Oulu region, and the shore-level displacement analysis of the Oulu site, although not very reliable and located a bit eastward from that maximum, seems to support that maximum.

While crust density and strength were not at all used in the study (only thickness), these maps may give more hints on possible local behaviour than the general map by Pässe (1997) shown earlier (Figure 22). But the maps created here are not necessarily as accurate as the one by Pässe & Andersson (2005), where the maps interpolated by kriging from the site values were improved with information from precision levelling and tide gauges (Figure 78). No A_s estimates from the sites listed by Pässe were used with the derivative-based method.

The reason this study's maps exhibit local behaviour is that there are local features both in the crustal thickness maps and in the external maps of the current isostatic land uplift. On the A_s map in Figure 41, created using the current uplift map in Figure 5, some more recent precision levelling information may be included at least from Finland than on the map in Figure 78. The Finnish third levelling was done mostly in 2004 but published later.

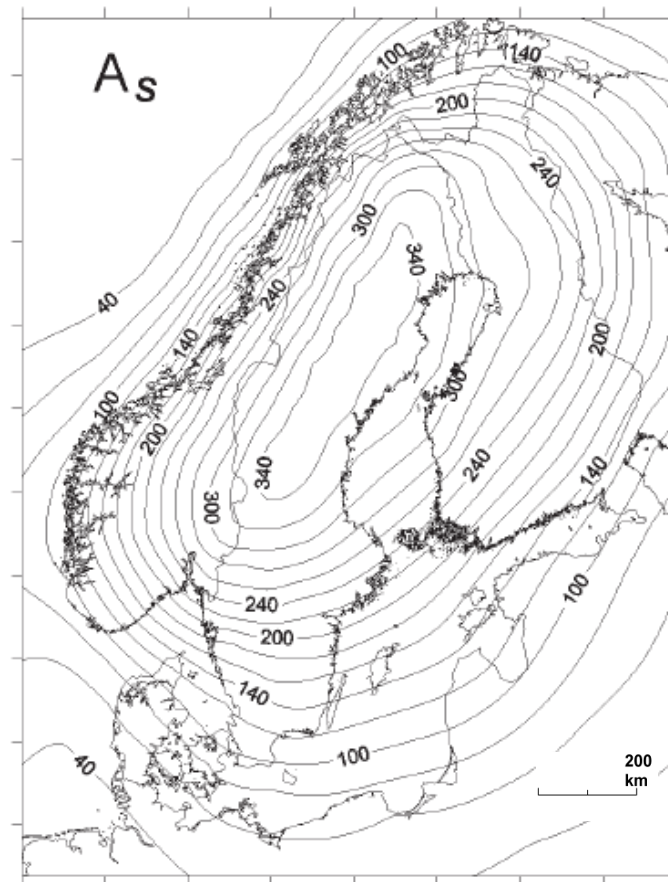


Figure 78. The A_s estimate by Pässe & Andersson (2005). It seems like the maps are in RT 90 2.5 gon V (RT90 25 gon V.prj in ArcGIS) coordinate system. RT 90 is the old Swedish national reference system and 2.5 gon V is the standard projection for this system (see Lantmäteriet 2008) (Ågren 2008).

In this study, we refer to a few latest land uplift models that include some differences. The correct version has to be yet confirmed in the future, but the models don't include local behaviour that is as local as in Lehmuskoski (2008).

7.5.2 Shore-level-based results

The A_s value of the Olkiluoto site (number 60) is 258 m, exactly as in Pässe (2001). The B_s values are on average 6% bigger than in Pässe (2001), but for Olkiluoto, the B_s value of 834 year^{-1} or 10% smaller should be considered reliable as well. The difference is probably due to the calibration improvements and a slightly different set of points. The nearby Åland site confirms the smaller B_s , and no new points are used there. Compared with Pässe & Andersson (2005), the new A_s of Olkiluoto is 18 m bigger and the B_s value of 6766 year^{-1} is even 2234 year^{-1} smaller. On average, the differences to previous results are within 10% (Figure 79).

For the Turku and Tammisaari regions, the points behaved more heterogeneously than expected, and the Turku site's values have not been updated. The Karjalohja points

could be separated from the Tammisaari site (as the subset was chosen here). The Finnish south coast sites could all be re-analysed.

The fast components were not always calculated. But T_f is clearly bigger than in the previous studies. This is due to the new time calibration IntCal04 producing larger values for the oldest points.

Two things seem to be uncertain about the previous studies:

- How Pässe (1997) complemented the point subsets by points at the nearby sites
- Manually drawn shoreline curves may have given more nodes and stability for calculating than the mere dating points. But the original sea-level index points are actual, measured information. It is not obvious how the original curves were constructed and whether strong interpolation or extrapolation were used or what additional information was at hand.

The surface interpolation used and combined the new sites or results, the results based on the models by Pässe (2001), and those based on the models of Pässe & Andersson (2005).

No model versions were produced that are based merely on Pässe (2001) and the new sites or merely on Pässe & Andersson (2005) and the new sites. In addition, B_f was typically modelled via the 2005 equation from A_f , even though the fast component function type used was normal distribution.

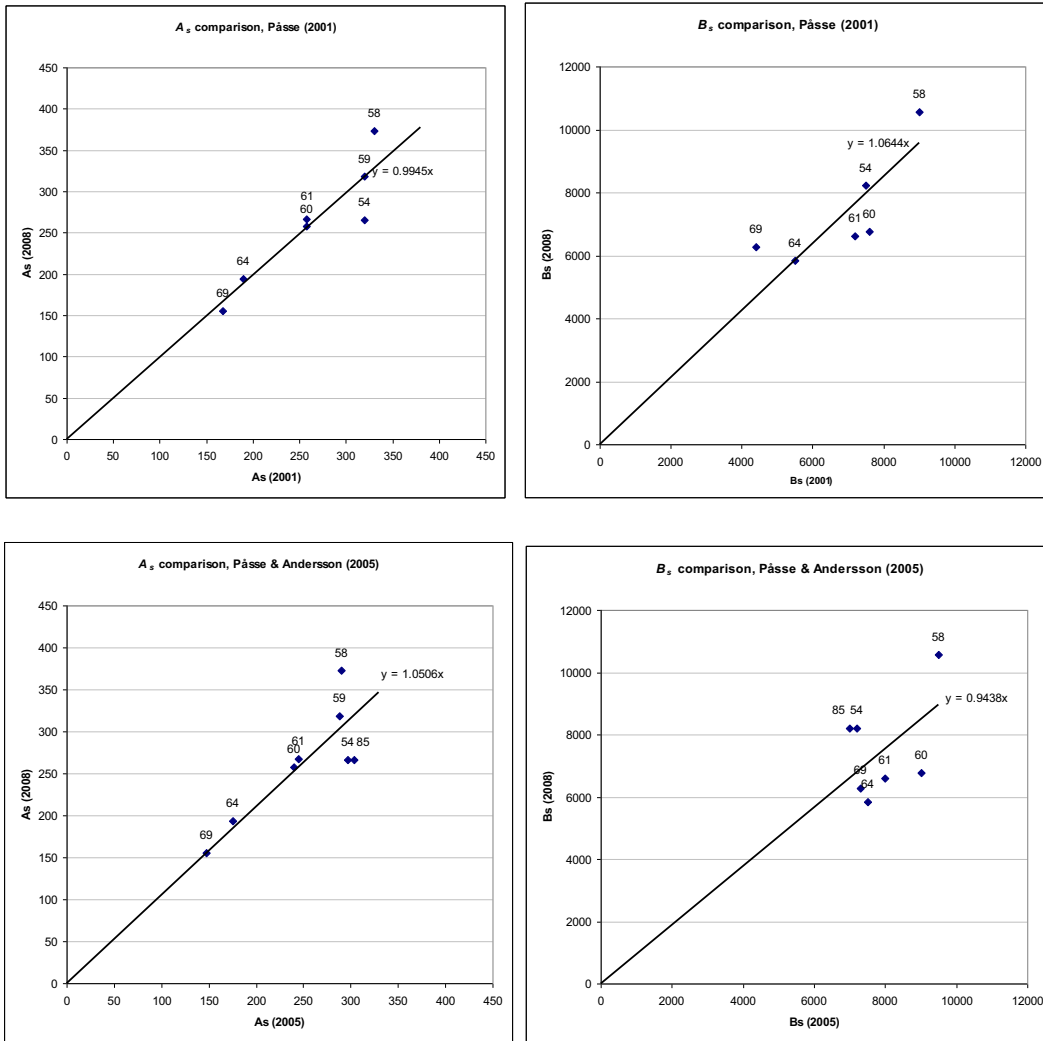


Figure 79. Comparison of the recalculated slow component parameter values and those in Pässe (2001) and Pässe & Andersson (2005). Site 85 was calculated with new data only and is compared here with Brydsten (2006). The new sites are not included. For the site numbers, see APPENDIX 5.

Table 7. Slow uplift component comparison for the Olkiluoto site based on the shore-level displacement.

	Uplift (m), AD 11950	Remaining uplift (m), AD 2M
Pässe (2001)	-38.097	-92.109
New U_s model	-35.319	-83.773

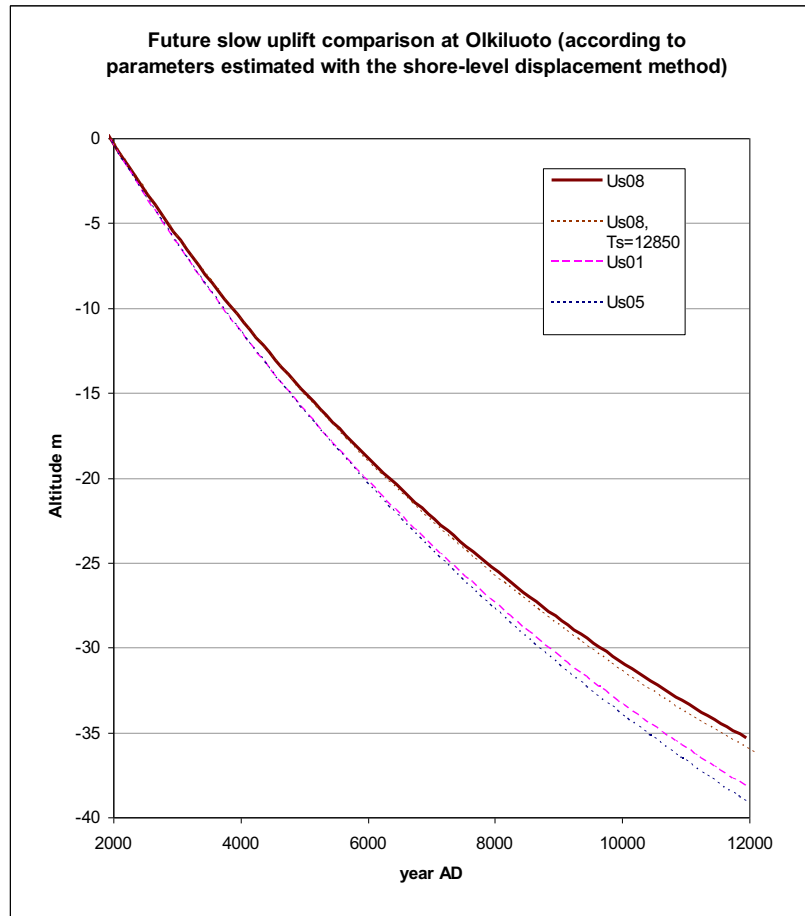


Figure 80. Comparison of the slow component isostatic land uplift curves at Olkiluoto for the future, purely based on calculating the parameters with the shore-level displacement analysis. The shown U_s differences compared to Pässe (2001) are within about 3 m in about AD 12000.

The uplift model at the Olkiluoto site is compared with that in Pässe (2001). The values of 258 m for A_s and of 6766 year^{-1} for B_s were used to create Table 7 and Figure 80. Uplift for about AD 12000 at Olkiluoto is 2.78 m less than calculated by Pässe (2001) due to the smaller B_s or the estimated shorter duration of the uplift (see Figure 16). The used upper constraint of A_f was 110 m for the Olkiluoto site, and it was reached, meaning that the fast component parameters were not properly solved. This has a (limited) effect on the slow component parameters too.

The remaining total uplift, based on the shore-level displacement and calculated for AD 2 000 000, is 8.3 m less than according to the parameters in Pässe (2001). 100 kyr could be considered a maximum relevant time scale in talking about land uplift at the final repository site since nuclear waste would be harmless by then due to its half life value (Figure 81).

The result calculated with the shore-level displacement method is considerably different from the derivative-based result. It may be considered more reliable than the derivative-based result because of the uncertainty of the B_s estimation in the latter. Recalculating the sites 55–57 in Sweden and the remaining Finnish sites would still have some effect on the Olkiluoto Island's interpolated estimates.

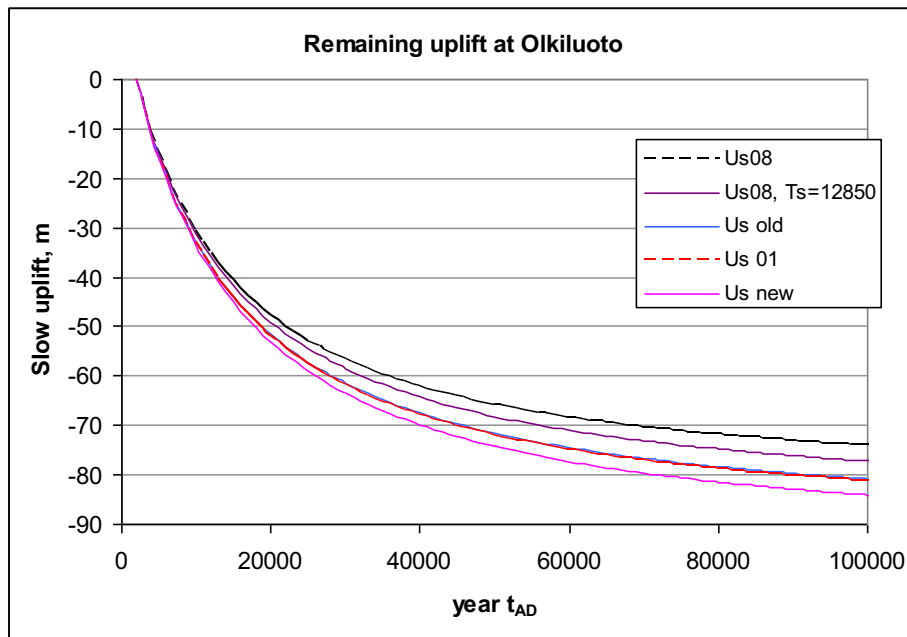


Figure 81. Comparison of the slow component isostatic land uplift curves at Olkiluoto for the distant future, based on calculating the parameters with various methods: the shore-level displacement method (U_{s08} , also the version with a different T_s , and U_{s01} by Pässe 2001), and the derivative-based method (with old and new exponential coefficients).

It would be useful to recalculate also other old sites in Fennoscandia with IntCal04 to update the fast component's time (T_f) but to revise Pässe & Andersson's (2005) models first.

B_s had a different value at the Lauhanvuori site compared to the recalculated Åland and Olkiluoto sites. Some attention could be paid to how to improve the Lauhanvuori estimates and their reliability.

The mere vertical movement is not the only uncertainty. In order to achieve a better understanding, the tilting phenomena ought to be included for the hundreds of square kilometres that are relevant to the biosphere modelling: from Olkiluoto to the future downstream area, and in addition, the Eurajoki and Lapinjoki basins. Some of this work has already been done (Ojala et al. 2006). On the other hand, tilting is of no importance unless it essentially changes the watercourses (directions of flow of the currents, or the sizes or surface levels of lake basins). This, in turn, depends on the inaccuracies of the elevation model (Pohjola 2008), and the evaluation of all phenomena ought to be done together. This is a large work and left for further studies.

8 UNCERTAINTIES AT DIFFERENT STAGES AND THEIR IMPACT

Most of the uncertainty of the analysis may be related to the following factors:

- Lack of samples; the latest field samples concentrate on certain areas (in Finland the south coast, but less on the west coast)
- The reliability or representativeness (sampling depth) of the analysed samples. The calculated curve does not always pass between the error limits of the samples or ^{14}C time calibrations. The use of only the median value of results, instead of more information. The error margin for the half-life of radiocarbon itself, 5730 ± 40 years, is an uncertainty for data on the past.
- Sometimes being forced to calculate only A_s even though B_s is more essential for the future uplift (Påsse 2001, p. 33)
- Uncertainty in the eustatic rise E models. The possible additional components in the past. For the future, the current E models are not valid due to the climate change. Is there really a need in Fennoscandia for an E model different from the common global models, or should the observed differences be explained by other factors? Modifications or corrections to the local water level due to the historic lake basins.
- The time constants of Påsse (1997, 2001) or Påsse & Andersson (2005) in cal BP must be based on ^{14}C time calibration by formulae, not the new and more irregular IntCal04. The new calibration datasets and software have been developed and give different results especially for samples older than 10 kyr BP. Especially the parameters with values >9500 BP seem to be inaccurate. For example $T_S = 12000$ cal BP corresponds according to the Påsse (2001) formula to 10852 BP, which would be 12850 cal BP according to IntCal04. As stated earlier, T_S is not as critical as some other parameters such as T_f or the additional terms of E_{05} . The time constants were not updated in the way mentioned here for this project. But to demonstrate the effect in the slow component: If $T_S = 12850$ cal BP, A_s at the Olkiluoto site is 292 m, B_s is 6605 year^{-1} , and the remaining uplift is -87.65 m (or -35.952 m in AD 11950, see Figure 80 and Figure 81).

The time calibration formulae of Påsse (2001) included the figure $1,095$, interpreted here as the decimal number 1.095 such as with the other three such constants and as in Påsse (1997) and Påsse & Andersson (2005).

Between 12000 and 14000 BP, IntCal04 and some other calibration datasets are said to be data-free extrapolation (Weninger et al. 2005).

The older the modelled times are, the more uncertainty is involved. This is true in interpreting glacial lakes, the glacier's edge position, and the fast crustal uplift component. The ^{14}C datings of Påsse (2001) and Påsse & Andersson (2005) also differ the most from IntCal04 at the oldest dates, which is why their calculations of the fast component etc. are also the most unreliable, and updating the dating method has the biggest improvement on these calculations. The improvement can be seen in Figure 82's Y axis on the left.

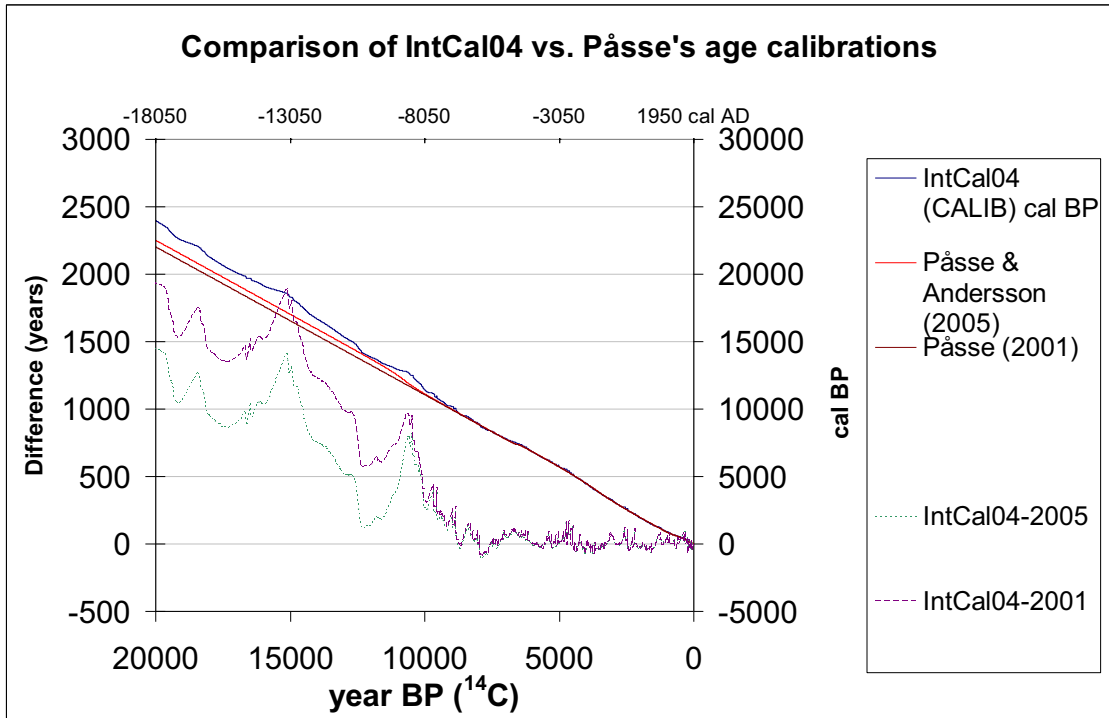


Figure 82. Differences between IntCal04 calibration and Pässe & Andersson's (2005) function-based calibration may cause their additional E components not to be dated optimally. At Pässe & Andersson's dates 11500 and 12500 cal BP, the differences are 588 and 419 years correspondingly. The 2005 calibration formula is in any case closer to the IntCal04 medians than Pässe's (2001) formula is. The T_f map by Pässe & Andersson (2008 Fig. 8) could also be updated based on new calibration.

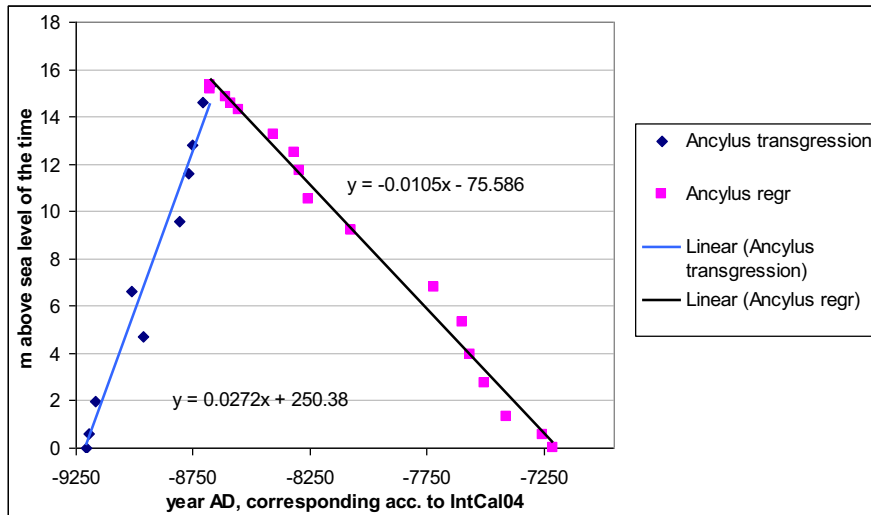


Figure 83. The AD values of the few points measured along the Ancylus correction lines (for Figure 15) can also be transformed into corresponding ones according to IntCal04 using the comparison tables used for Figure 82.

The tables for Figure 82 were created with CALIB and a 5 years \pm error (considerably smaller than a typical σ of isolation datings). Age span or smoothing of e.g. 0 or 3 years has no significance.

If the AD look-up-tables are used to transform the digitised Ancylus Lake transgression and regression lines, the Ancylus correction is about 150 years earlier than in the initial version (Equation 17).

$$E_{01A} \cong \frac{2}{\pi} \cdot 56 \cdot \left[\arctan\left(\frac{9500}{1350}\right) - \arctan\left(\frac{9500 - 1950 + t_{AD}}{1350}\right) \right]$$

$$-0.0272 \cdot t_{AD} - 250.38 \quad , -9205 < t_{AD} \leq -8646 \quad (m) \quad \text{Equation 44}$$

$$+0.0105 \cdot t_{AD} + 75.586 \quad , -8646 < t_{AD} < -7199$$

But as was seen, e.g., in Figure 53, it is not reasonable to take a variable, at least the previously only roughly estimated T_f by Pässe (2001), and transform it via the look-up-tables of Figure 82. The T_f correction would be in a different direction than what the actual fit would suggest; the T_f of Lauhanvuori changed from the estimated 11400 to 10511 cal BP due to the fit but would have become 12088 through the look-up-tables. Added complementary points may play a role here, too. For more accurately defined variables, for example the Ancylus Lake levels, the results would be better, but the look-up-tables were not applied as widely as possible. It would be good to reanalyse the uplift parameter sites based on the IntCal04 calibration results using all the sea-level index points that Pässe & Andersson (2005) had as input, along with some new isolation points.

Also a correction of the Baltic Ice Lake (about 10200 – 12000 BP) would be possible according to Figure 6-5 by Pässe (1997) for the relevant areas. But the correct dating versus the ^{14}C calibration used is essential in such corrections, and secondly, Pässe & Andersson (2005) criticise use of the term Baltic Ice Lake and suggest it be named Baltic Ice Sea.

The selection of fast component parameter values, at least for T_f , contributes to the resulting curve fitting in the distant past and also influences the future predictions at least if there is little or no recent data from low elevations. The T_f values vary a lot between Pässe (2001) and Pässe & Andersson (2005) and have a much more detailed distribution pattern in the latter. If some old sea-level index points are included, the fast component values can be calculated, and they have an effect on calculations of also the slow component parameters, especially B_s . Sometimes it is best to use only the most recent data (sea-level index points from $> \text{AD } -6000$), and to estimate A_s (and B_s) only.

The used upper constraint of A_f was 110 m for the Olkiluoto site, and it was reached, meaning that the fast component parameters were not properly solved. This has some effect on the slow component parameters too.

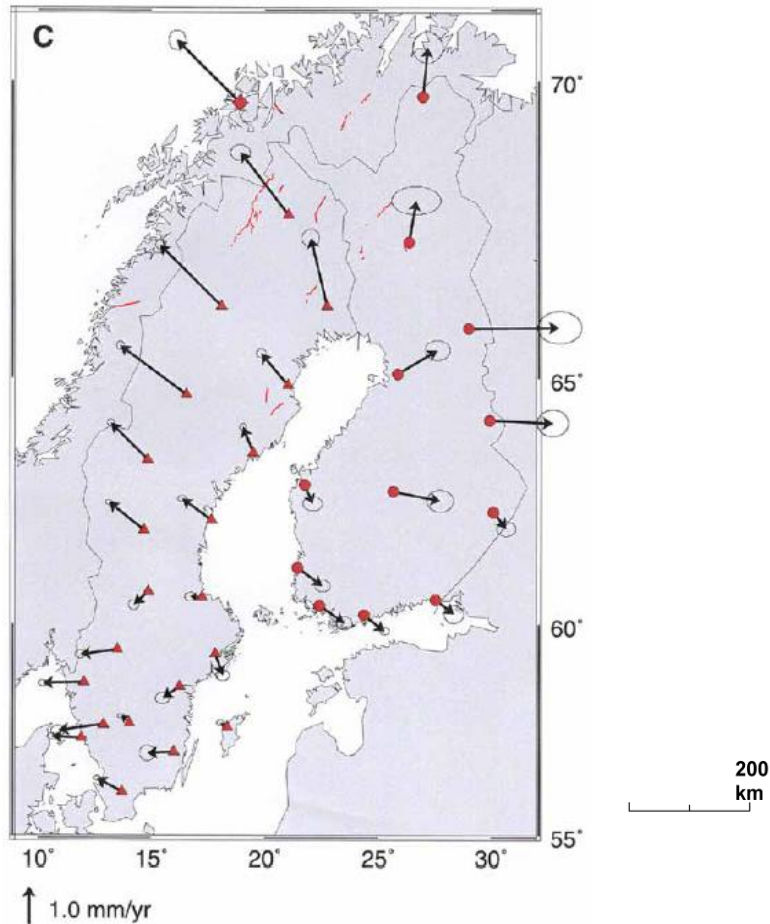


Figure 84. Estimated horizontal bedrock velocity vectors (Paulamäki & Kuivamäki 2006). The scale associated with each of these vectors, as well as with the associated 1σ error ellipses, is given at the bottom of the plot. The locations of known postglacial faults in Fennoscandia (the red lines) have been added to the map. Note that another local maximum of the A_s parameter, revealed by the derivate-based method, is located in north Sweden ($18^{\circ}24'E$ $68^{\circ}18'N$), west of one of these faults (see Figure 41).

There are also estimates for the bedrock horizontal velocity vectors (Figure 84, Paulamäki & Kuivamäki 2006), Lidberg (2008). The horizontal velocities are another uncertainty, not included in the models of this study due to lack of further information and due to the limited scope of this study.

As the target area was especially the Olkiluoto region and the Bothnian Sea, the results in Swedish (or other) areas are not necessarily accurate.

Morén & Pässe (2001) predicted the future shoreline with an extended model that pointed out a causal connection within the glacio-isostatic development, namely the strong time dependence. Crustal uplift takes place with a delay after the glacial load changes because the growth and decay of ice sheets is a fast process compared to mantle flow. During ice free periods, uplift usually ends at a level “far” from isostatic equilibrium. This may mean that all of the modelled total uplift will not take place in the future.

Alternative ways to correct the samples *locally* are not very clear. Berglund's (2005) altitudes were still in RH70 and originated from the topographical maps published by the Swedish Land Survey in the 1990s – or from altitude data in older publications, in which case Berglund has added height due to subsequent uplift (Berglund 2008). Berglund has also done some more local corrections. We do not present Berglund's table 3 and figure 8 here but just give some explanations:

- In table 3, Berglund (2005) listed the reported altitude in column 3, and the *threshold* altitude in column 4, which can be either lower or higher than the altitude. Column 4 differed from the reported altitude since Berglund thought the original authors did not always do a close examination of the actual threshold areas.
- The correction for differential uplift (Δ_{diff} in the equation above) in column 6 should be understood in order to evaluate whether it is necessary to apply it to the current study's subsets too. The lines in Berglund's (2005) figure 8 simply connect the sea-level index points to the reference line and have no other significance. The distance along the lines multiplied by the gradient (according to table 3's caption) gave the correction in column 6.
- Another comment on column 6 of Table 3 in Berglund (2005): The larger the area and the further back in time, the greater the need for a correction due to a different isostatic uplift. As is seen in table 3, the gradients are small for the "youngest" sea-level index points, but the large geographical spread produces substantial corrections. If for example the latitude of the town Gävle would be used as the reference line, the sea-level index points 9–11, would hardly need any correction (Berglund's figure 8). Thus, whether or not to perform the differential uplift correction depends on the site or the sea-level index points and also, of course, on the precision needed (Berglund 2008).
- The differential correction may have to do with the lake-tilting (Påsse 1996 p. 68–70). Berglund's selection of the reference line was along a latitude because more northerly sea-level index points have experienced greater uplift. So if one tries to apply a differential correction for a large area like the Gulf of Bothnia, more than two sea-level index points (Hälsingland & Södertörn) are necessary, and implementation would need more attention. A surface model of the gradient would be needed, but the methodology could probably still not be applied otherwise than more locally. The correction values as calculated by Berglund would otherwise be too large.

The relation between B_s and crustal thickness (Figure 26) is not very strong, and regional differences in the relation could be analysed, or possible corrections conducted first.

The $\delta^{13}\text{C}$ correction's effect was small, about 0.5 % in age for peats. The elevation corrections were <0.5 m and also considered minor, even though the altitudes of basin thresholds had been measured with an apparent accuracy of ± 0.05 –0.1 m (Eronen et al. 1995 p. 7).

Pairs like the start and end of a certain isolation (the interpretations of which are sometimes not sure) were not combined for the analysis but treated individually.

It is not obvious how Pässe (1997, 2001) has complemented or extended the curves by means of new data from nearby sea-level index points. His curves are in years BP, except in Pässe & Andersson (2005) in cal BP, in which system the calculated curves were originally defined.

The two uppermost points in Pässe's Olkiluoto curves are not radiocarbon-dated sites but the levels of the highest coastline and the *Ancylus* limit. Pässe has estimated these two levels are based on some map but he does not remember which. As this part of the curve is extremely important for the modelling, it is necessary to complement the shore level curves with this data. The lowermost data point at Lauhanvuori is obviously wrong. Pässe has never seen the original data at this site but used a curve from a compiled work. In the process, he obviously took the lowermost point from another curve. That point did not suit the modelling (Pässe 2008). The importance of the two uppermost points in the Olkiluoto curve must be taken into consideration at least for the fast components. The slow components should be rather well defined, as there are many points available from a long period and various altitudes.

The effects of possible circular argumentation were not recognised or analysed.

There were no old sea-level index points available for the two Swedish area analyses done.

9 SUMMARY OF THE FORMULAE AND RASTERS USED

One of the most remarkable differences between this and previous studies was the use of state-of-the-art ^{14}C age calibration (the IntCal04 dataset) instead of more general functions.

Vertical shore-level displacement (S , m) in Fennoscandia is calculated from glacio-isostatic uplift (U , m) of land and global or regional eustatic sea level rise (E , m) as

$$S = U - E \text{ (m)}. \quad \text{Equation 45}$$

The total isostatic land uplift is the sum of the slow and fast components:

$$U = U_s + U_f = \frac{2}{\pi} \cdot A_s \cdot \left[\arctan\left(\frac{T_s}{B_s}\right) - \arctan\left(\frac{T_s - 1950 + t_{AD}}{B_s}\right) \right] \text{ (m)} \quad \text{Equation 46}$$

$$+ A_f \cdot e^{-0.5 \left(\frac{1950 - t_{AD} - T_f}{B_f} \right)^2}$$

where T_s was 12000 cal BP in all calculations, but 12850 cal BP would be even better. For Olkiluoto, $A_s = 258$ m, $B_s = 7600$ year $^{-1}$, $T_f = 11600$ cal BP, $A_f = 90$ m and $B_f = 850$ year $^{-1}$ according to Pässe (2001). The eustatic rise E model of Pässe (2001) with the addition of the Ancylyus correction terms (for the Ancylyus Lake area only) is, using t_{AD} :

$$E_{01A} \cong \frac{2}{\pi} \cdot 56 \cdot \left[\arctan\left(\frac{9500}{1350}\right) - \arctan\left(\frac{9500 - 1950 + t_{AD}}{1350}\right) \right] \text{ (m)}. \quad \text{Equation 47}$$

$$- 0.0487 \cdot t_{AD} - 429.19, \quad -8817 < t_{AD} \leq -8498$$

$$+ 0.0116 \cdot t_{AD} + 83.077, \quad -8498 < t_{AD} < -7150$$

The logarithmic fit of crustal thickness (ct) data from Grad & Tiira (2008, 2009) and the B_s data from Pässe (2001) defined the revised exponential equation

$$\hat{B}_s = 83 \cdot e^{0.096 \cdot ct} \text{ (year}^{-1}\text{)}. \quad \text{Equation 48}$$

For estimating A_s ,

$$\hat{A}_s = \left[-S'_{map} + E'_{01A} - A_f \cdot e^{-0.5 \left(\frac{1950 - t_{AD} - T_f}{B_f} \right)^2} \cdot \frac{T_f + t_{AD} - 1950}{B_f^2} \right]$$

$$\cdot \frac{-\pi}{2} \cdot \frac{\hat{B}_s^2 + (12000 - 1950 + t_{AD})^2}{\hat{B}_s} \text{ (m)}, \quad \text{Equation 49}$$

where

$$E'_{01A} \cong \frac{-2}{\pi} \cdot 56 \cdot \frac{1350}{1350^2 + (9500 - 1950 + t_{AD})^2}$$

$$\begin{aligned} & -0.0487 \quad , -8817 < t_{AD} \leq -8498 & \text{(m/yr),} & \text{Equation 50} \\ & +0.0116 \quad , -8498 < t_{AD} < -7150 \end{aligned}$$

where the last two terms apply to the Ancylus Lake area only. The Ancylus Lake area mask was not necessary here because all the new data collected were from the area of the lake. The fast component term is also not necessary for estimating the current A_s .

GIS approaches for estimating land uplift have strengths in modelling the sea shoreline position and local slope angles – in other words the past and future landscape. Using rasters is not a must in a GIS, but in this study the digitised isoline maps were also interpolated into rasters. The rasters are referred to in Figure 9 and Figure 8 and include the following:

- The crustal thickness (Moho depth) map by Grad & Tiira (2008, 2009) and the resulting B_s estimate(s), Figure 34
- The current uplift maps, at least the one by Lidberg (2007), i.e. the absolute uplift version by Poutanen (2008) minus 1.5 mm/year
- The A_s estimate(s) resulting from calculations based on such maps and derivative models, Figure 41
- The Finnish N60 to N2000 correction, defined here also for Åland, updated with extrapolated curves at the N and W borders
- The Swedish RH70 to RH 2000 elevation correction (Ågren & Svensson 2007)
- The A_s and B_s estimates from site data interpolation, Figure 76 and Figure 77

For example in the interpolation, the results by Pässe (2001) and some results of Pässe & Andersson (2005) were combined.

For the Olkiluoto area, the new slow uplift parameter estimates based on the derivative-method and the new exponential equation were $A_s = 245$ (m) and $B_s = 8489$ (year⁻¹). This was based on the Moho depth according to Grad & Tiira (2008, 2009) and the current uplift map by Lidberg (2007).

Based on the analysis of sea-level index points (i.e. the shore-level displacement curve fit) especially for the Olkiluoto site, $A_s = 258$ m and $B_s = 6766$ year⁻¹. It can be stated that the remaining uplift is about 9% less than estimated by Pässe in 2001 (or only 5% less, if T_s is updated via the calibration look-up tables as 12850 cal BP and the parameters are re-calculated as $A_s = 292$ m and $B_s = 6605$ year⁻¹).

10 CONCLUSIONS

The study reconstructed and evaluated the isostatic land uplift and shoreline displacement models (especially Pässe 2001), i.e. the models of the past change in local sea level relative to land, in order to be aware of how they were developed, and to be able to model the future Bothnian Sea uplift behaviour. The aim has been to evaluate the modelling method and the input data used to estimate the shoreline level primarily for the future. Raster surfaces were created, and the sensitivity to some parameters was evaluated. The calculated AD times are shown in the tables, and the cal BP scale is also shown in the graphs.

A useful data set for further analysis was put together from the old and more recent literature. The older Finnish data of 260 sea-level index points (Eronen et al. 1995) was rebuilt and corrected. The more recent research reports found, which date from 1994 and later, contributed data about 52 lakes and 4 mires in Finland and 41 lakes or mires in Sweden. Most of the Swedish points are close to the Swedish repository site candidates, but this study does not take a stand on how well that data is applicable to the areas around these sites. A total of 357 sea-level index points or basins were used in this study.

Various map versions showing present apparent land uplift were found, digitised, and compared. In the Ladoga and Oulunjärvi areas, the relative uplift may differ from the general trends. A new derivative-based method was created, using maps of the crust and current uplift, to estimate B_s and half of the total uplift (A_s). The derivative-based uplift for AD 12000 at Olkiluoto is 0.5 m more than that estimated by Pässe (2001).

Isostatic land uplift parameters were estimated from sets of sea-level index points with ^{14}C datings mostly in Finland and partly in Sweden collected from existing literature. However, during the last 10-15 years or so, there has not been very much new research on lake isolation with ^{14}C datings of threshold altitudes. In addition, many new dating studies have concentrated on the south coast of Finland, mainly on the area south-east of the Salpausselkä formations, which is the area with less isostatic land uplift and is thus not so relevant to the Olkiluoto area. The Olkiluoto uplift estimated for AD 12000 is 2.78 m less than that estimated by Pässe (2001).

Both the derivative-based method and the shore-level displacement method show a local maximum of A_s (half of the total uplift) in the northeastern Gulf of Bothnia. The northern part of the A_s distribution maximum is farther east than in the previous results, and the maximum distribution of the inertia factor B_s is wider. The remaining Olkiluoto uplift is 91.5–95.5 m according to the derivative-based method and 83.8 m according to the shore-level displacement method.

A number of uncertainties in the modelling of crustal uplift were pointed out. It is not clear how Pässe (1997) complemented or extended the sea-level index point lists of the sites by using new data on points near those sites. The biggest uncertainties deal with the following decisions: which sea-level index points to include in the S curve fit and which (typically fast uplift) parameters are best to fix (and according to what criteria).

In Pässe (2001), the weakness was still the T_f parameter and its strict threshold between 11400 and 11600 cal BP near the Olkiluoto region. T_f has been improved by means of

the enhanced time calibration. A better estimation of the time of maximum slow uplift, T_s , than the commonly used 12000 cal BP would apparently be 12850.

The fast uplift is closely related to the period when crustal movements (earthquakes and formation of the large tectonic lines) were more probable. That period is more interesting for determining the stability of the bedrock at the final repository's site. These issues were not investigated in the present study; instead, the approach was to produce source data estimates for modelling the future biosphere.

In the Turku and Karjalohja-Tammisaari regions, the measurements at the sea-level-index points were somewhat heterogeneous. The isostatic land uplift mechanisms are related to the mosaic nature of Finland's bedrock. It is probable that the blocks bounded by the tectonic lines are moving in different ways. In any case, the regional level of observation of the phenomena in the study was such that the block movements could not be determined for long periods but seem to be similar on average.

Future improvement of the analysis could include the following:

- Collect the old points outside Finland and re-calibrate the data. Find out how it is best to complement the point subsets. Recalculate at least all the sites not dealt with here and located near Olkiluoto.
- Pay more attention to fast uplift models and parameters. T_f is no doubt more precise in Pässe & Andersson (2005) than in Pässe (2001), but it should be recalculated using the new calibration. It would be reasonable to investigate the fast uplift better, not only using the methods used here but also others that take into consideration the other crustal mechanics and ice sheet modelling.
- Use revised eustasy models E for the past and the future, e.g. a revised version of the Pässe & Andersson model (2005) or another recent global model, which is possibly irregular as the IntCal04 curve is too. Local differences and corrections of the estimated water level (e.g. Ancylus Lake and Baltic Ice Lake) can be added to some E model presented here or other global sea level models.
- Take into consideration the precision levelling results for inland areas
- Collect more field sample isolation datings from areas with missing information since these are needed to calculate the values at more sites and to improve reliability. The graphs in the study or a GIS with suitable data could be used to define optimal targets, e.g. lakes near Lauhanvuori (or Oulu) and below an elevation of 55 m, with a suitable size and surroundings and taking into consideration the tectonic lines.
- Integration of isostatic uplift over time to analyse past shorelines. Iterative adjustment. The workflows implemented here are not a comprehensive GIS with elevation and bathymetry models and lake outlet analysis included. See Pässe & Andersson (2005, 2006).
- Use of the individual ranges and the probabilities in shoreline parameter fittings
- The variables of the Moho or lithosphere models include average P wave velocities, topography, depth of the basement or of the upper/lower crust

discontinuity (Tesauro et al. 2008b). Use of these data instead of only the depth values could yield improved estimations of parameters like B_s .

InSAR techniques – especially long-term monitoring of super-regional areas with persistent scatterers – would also reveal local behaviour, and typically at many more points than revealed by precision levelling. So far it has been considered that InSAR techniques would not give enough added value compared to the GeoSatakunta and Olkiluoto GPS networks and precision levelling activities. In any case, the deformation models would become more like raster surfaces by using InSAR.

REFERENCES

- Aario, L. 1932. Pflanzentopografische und paläogeographische Mooruntersuchungen in N-Satakunta. Fennia. Vol 55, p. 1-179.
- Ågren, J., Svensson, R., Olsson, P-A., Eriksson, P-O. & Lilje, M. 2006. The Swedish height system RH 2000 as a national realisation of EVRS. Symposium of the IAG subcommission for Europe (EUREF), Riga, 14–17 June 2006. www.euref.eu/symposia/2006Riga/02-03.pdf
- Ågren, J. & Svensson, R. 2007. Postglacial Land Uplift Model and System Definition for the New Swedish Height System RH 2000. LMV-Rapport 2007:4 – ISSN 280-5731, Gävle. 124 p. www.lantmateriet.se/upload/filer/kartor/geodesi_gps_och_detaljmatning/Rapporter-Publikationer/LMV-rapporter/LMV-Rapport_2007_4.pdf
- Andersson, J., Ahokas, H., Hudson, J., Koskinen, L., Luukkonen, A., Löfman, J., Keto, V., Pitkänen, P., Mattila, J., Ikonen, A.T.K. & Ylä-Mella, M. 2007. Olkiluoto Site Description 2006. Posiva report 2007-03, 15.11.2007. www.posiva.fi
- Artemieva, I.M., Thybo, H. & Kaban, M.K. 2006. Deep Europe today: Geophysical synthesis of the upper mantle structure and lithospheric processes over 3.5 Ga. Geol. Soc., London, Mem. 12, 11-42. <http://www.lithosphere.info/papers/2006-ELD-DeepEurope.pdf>
- Artemieva, I.M. & Thybo, H. 2008. Deep Norden: Highlights of the lithospheric structure of Northern Europe, Iceland, and Greenland. Episodes, v. 31(1), 98-106. http://www.lithosphere.info/papers/2008-Norden3_6.pdf
- Begon, M., Townsend, C. R. & Harper, J. L. 2006. Ecology - From Individuals to Ecosystems. Fourth edition. Blackwell publishing, Oxford, UK. ISBN: 978-1-4051-1117-1.
- Berglund, M. 2005. The Holocene shore displacement of Gästrikland, eastern Sweden: a contribution to the knowledge of Scandinavian glacio-isostatic uplift. Journal of Quaternary Science. Vol. 20, pp. 519–531. ISSN 0267-8179. <http://www3.interscience.wiley.com/cgi-bin/fulltext/111089099/PDFSTART>
- Björck, S. 1995. A review of the history of the Baltic Sea, 13.0–8 0 ka BP. Quaternary International 27, 19–40.
- Blaauw, M., Heuvelink, G.B.M., Mauquoy, D., van der Plicht, J. & van Geel, B. 2003. A numerical approach to C-14 wiggle-match dating of organic deposits: best fits and confidence intervals. Quaternary Science Reviews 22: 1485-1500.
- Boudin, M. & Van Strydonck, M. 2006. Calibration of Radiocarbon dates. Royal Institute for Cultural Heritage, Brussels, Belgium. TRACE 2006 Conference. <http://trace2006.africamuseum.be/Abstracts.html>
- Brandt, A. 1948. Über die Entwicklund der Moore im Küstengebiet von Süd-Pohjanmaa am Bottnischen meerbusen. Ann. Bot. Soc. Vanamo. Vol. 23, no. 4, 134 p.

Brydsten, L. 1999. Shore line displacement in Öregrundsgrepen. Technical Report TR-99-16. www.skb.se/upload/publications/pdf/TR-99-16.pdf

Brydsten, L. 2000. Change in coastal sedimentation conditions due to positive shore displacement in Öregrundsgrepen. Technical Report TR-99-37. www.skb.se/upload/publications/pdf/TR%2099-37webb.pdf

Brydsten, L. 2006. A model for landscape development in terms of shoreline displacement, sediment dynamics, lake formation, and lake choke-up processes. Umeå University, Department of Ecology and Environmental Science. SKB TR-06-40. www.skb.se/upload/publications/pdf/TR-06-40webb.pdf

Buck C.E., Christen J.A. & James G.N. 1999. BCal: an on-line Bayesian radiocarbon calibration tool. *Internet Archaeology*, 7. <http://intarch.ac.uk/journal/issue7/buck/>

Chivas, A., Sander, A., van der Kaars, G., Couapel, M., Holt, S., Reeves, J., Wheeler, D., Switzer, A., Murray-Wallace, C., Banerjee, D., Price, D., Wang, S., Pearson, G., Edgar, N., Beaufort, L., Deckker, P., Lawson, E. & Cecil, C. 2001. Sea-level and environmental changes since the last interglacial in the Gulf of Carpentaria, Australia: an overview. *Quaternary International*, 83-85 (1), 19-46.

Donner, J. & Eronen, M. 1981. Stages of the Baltic Sea and late Quaternary shoreline displacement in Finland. Excursion Guide. INQUA, Subcommission on shorelines of northwestern Europe. Excursion in southern Finland with a symposium at Lammi Biological Station 9-14 Sept. 1981. Univ. of Helsinki, Dept. of Geology, Division of Geol. and Paleontology. Stencil No. 5. Helsinki 1981. 53 pp.

Edwards, R.L., Beck, J.W., Burr, G.S., Donahue, D.J., Chappel, J.M.A., Bloom, A.L., Druffel, E.R.M. & Taylor, F.W. 1993. A large drop in atmospheric $^{14}\text{C}/^{12}\text{C}$ and reduced melting in the Younger Dryas, documented with 230 Th ages of corals. *Science* 260, 962–967.

Ekman, M. 1989. Impacts of geodynamic phenomena on systems for height and gravity. *Bulletin Géodésique* 63, 281–296.

Ekman, M. 1996. A consistent map of the postglacial uplift of Fennoscandia. *Terra-Nove* 8/2, 158-165.

Ekman, M. & Mäkinen, J. 1996. Recent postglacial rebound, gravity change and mantle flow in Fennoscandia. *Geophysical Journal International* 126, 229–234.

Eronen, M. 1974. The history of the Litorina Sea and associated Holocene events. *Soc. Sci. Fennica, Comm. Phys.-Meth.* 44, 4, p. 79-195.

Eronen, M. 1976. A radiocarbon-dated *Ancylus* transgression site in southeastern Finland. *Boreas* 5, pp. 65-76.

Eronen, M. 1983. Late Weichselian and Holocene shore displacement in Finland. In: Smith, D.E. & Dawson, A.G. (eds.). *Shorelines and Isostasy*. Academic Press, pp. 183-207.

Eronen, M. 1990. Geologinen kehitys jääkauden lopussa ja sen jälkeen. In: Alalammi, P. (ed.). 1990. Atlas of Finland, folio 123-126: Geology. Helsinki: National Board of Survey & Geographical Society of Finland 1992. 58 p.

Eronen, M., Glückert, G., Hatakka, L., van de Plassche, O., van der Plicht, J. & Rantala P. 2001. Rates of Holocene isostatic uplift and relative sea-level lowering of the Baltic in SW Finland based on studies of isolation contacts. *Boreas* 30 (1), 17-30.

Eronen, M., Glückert, G., van de Plassche, O., van der Plicht, J. & Rantala, P. 1995. Land uplift in the Olkiluoto-Pyhäjärvi area, southwestern Finland, during the last 8000 years. Report YJT-95-17. Nuclear Waste Commission of Finnish Power Companies.

Eronen, M., Glückert, G., van de Plassche, O., van der Plicht, J., Rajala, P. & Rantala, P. 1993. The postglacial radiocarbon dated shoreline data of the Baltic in Finland for the Nordic data of land uplift and shorelines. University of Turku, Finland. Swedish Nuclear Power Inspectorate.

Eronen, M., Heikkinen O. & Tikkanen, M. 1982. Holocene development and present hydrology of Lake Pyhäjärvi in Satakunta, southwestern Finland. *Fennia* 160, 2. pp. 195-223.

Fairbanks, R.G. 1989. A 17 000-years glacio-eustatic sea level record: influence of glacial melting rates on the Younger Dryas event and deep-ocean circulation. *Nature* 342, 637-642. <http://radiocarbon.ldeo.columbia.edu/pubs/1989Fairbanks.pdf>

Fjederskaar, W. 1994. The amplitude and decay of the glacial forebulge in Fennoscandia. *Norsk Geologisk Tidsskrift* 74, 2-8.

Glückert, G. 1970. Vorzeitliche Uferentwicklung am Ersten Salpausselkä in Lohja, Südfinnland. *Ann. Univ. Turkuensis, Ser. A II*, 45, 116 pp.

Glückert, G. 1976. Post-Glacial shore-level displacement of the Baltic in SW Finland. *Ann. Acad. Sci. Fennicae, Ser. A III*, 118, 92 pp.

Glückert, G. 1978. Östersjöns postglaciala strandförsjutning och skogens historia på Åland. *Publ. Dept. Quarternary Geol., Univ. Turku*, 34, 106 pp.

Glückert, G. 1979. Shore-level displacement of the Baltic and the history of vegetation in the Salpausselkä belt, western Uusimaa, South Finland. *Publ. Dept. Quarternary Geol., Univ. Turku*, 39, 77 p.

Glückert, G. 1989. Shore-level displacement of the Baltic, and the development of forests, settlement and agriculture on the island of Kumlinge, the Åland Islands, SW Finland. *Publ. Dept. Quarternary Geol., Univ. Turku*, 61, 10 pp.

Glückert, G. & Ristaniemi, O. 1980. The Ancyclus transgression in the area of Karjalohja, 2nd Salpausselkä, South Finland. *Publ. Dept. Quarternary Geol., Univ. Turku*, 41, 22 p.

Glückert, G. & Ristaniemi, O. 1982. The Ancyclus transgression west of Helsinki, South Finland - a preliminary report. *Ann. Acad. Sci. Fennicae, Ser. A III*, 134, pp. 99-110.

Glückert, G., Illmer, K., Kankainen, T., Rantala, P. & Räsänen, M. 1992. Vegetational history in the surroundings of Lake Littoinen and its natural dystrofication. Publ. Dept. Quarternary Geol., Univ. Turku, 75, 27 pp.

Glückert, G., Peltola, H. & Rantala, P. 1998. Landhöjning och Östersjöns strandförskjutning i Kronoby-Larsmo-området, mellersta Österbotten, under de senaste 3000 åren. Turun yliopiston maaperägeologian osaston julkaisuja 81. Turku: Turun yliopisto. 15 p.

Glückert, G., Rantala, P. & Ristaniemi, O. 1993. Postglacial shore-level displacement of the Baltic in Ostrobothnia. Publ. Dept. Quarternary Geol., Univ. Turku (manuscript).

Grad, M. & Tiira, T. 2008. European plate Moho depth map. Geophysical Research Abstracts, Vol. 10, EGU2008-A-05149, 2008. Data at www.seismo.helsinki.fi/mohomap.

Grad, M., Tiira, T. and ESC Working Group 2009. The Moho depth map of the European Plate. Geophysical Journal International. Vol 176:279-292, Issue 1, January 2009. doi: 10.1111/j.1365-246X.2008.03919.x. <http://www3.interscience.wiley.com/cgi-bin/fulltext/121541727/PDFSTART>

Haapanen, R., Aro, L., Ilvesniemi, H., Kareinen, T., Kirkkala, T., Lahdenperä, A-M., Mykrä, S., Turkki, H. & Ikonen, A.T.K. 2007. Olkiluoto Biosphere Description 2006. Posiva Oy, POSIVA 2007-02.

Hedenström, A. 2001. Early Holocene shore displacement in eastern Svealand, Sweden, based on diatom stratigraphy, radiocarbon chronology and geochemical parameters. Quaternaria. Ser. A: Theses and Research Papers No. 10. Stockholm University. 48 p.

Hedenström, A. & Risberg, J. 1999. Early Holocene shore-displacement in southern central Sweden as recorded in elevated isolated basins. Boreas 28, 490-504.

Hedenström, A. & Risberg, J. 2003. Shore displacement in northern Uppland during the last 6500 calendar years. Technical Report TR-03-17. www.skb.se/upload/publications/pdf/TR-03-17webb.pdf

Heinsalu, A., Veski, S. & Vassiljev, J. 2000. Palaeoenvironment and shoreline displacement on Suursaari Island, the Gulf of Finland. Bulletin of the Geological Society of Finland 72, Parts 1-2, 21-46.. <http://www.geologinenseura.fi/bulletin/Volume72/Heinsaluetal.pdf>

Hillaire-Marcel, C. & De Vernal, A. 2007. Proxies in Late Cenozoic Paleoceanography. Elsevier.

Hughen, K.A., Baillie, M.G.L., Bard, E., Beck, J.W., Bertrand, C.J.H., Blackwell, P.G., Buck, C.E., Burr, G.S., Cutler, K.B., Damon, P.E., Edwards, R.L., Fairbanks, R.G., Friedrich, M., Guilderson, T.P., Kromer, B., McCormac, G., Manning, S., Bronk Ramsey, C., Reimer, P.J., Reimer, R.W., Remmele, S., Southon, J.R., Stuiver, M., Talamo, S., Taylor, F.W., van der Plicht, J. & Weyhenmeyer, C.E. 2004. Marine04

- Marine Radiocarbon Age Calibration, 0–26 cal kyr BP. *Radiocarbon* Vol 46, Nr 3, 2004 pp. 1059–1086. (The table is found from www.radiocarbon.org/IntCal04.htm.)
- Huhta, P. & Korsman, K. (Eds). 2005. Bedrock stress field in the Satakunta region. Report P 34.4.042. Geological Survey of Finland. (GeoPori report series)
- Huikari, O. 1956. Primäärisen soistumisen osuudesta Suomen soiden synnyssä (In Finnish: Of the proportion of primary paludification in the formation of Finland's mires). *Communicationes Instituti Forestalis Fenniae*. Vol. 46, no. 6. 79 p.
- Hyvärinen, H. 1966. Studies on the late-Quaternary history of Pielis-Karelia, eastern Finland. *Soc. Scient. Fennica. Comment Biol.* 29, 4, 72 pp.
- Hyvärinen, H. 1979. Bakunkärsträsket: a stratigraphical site relevant to the Litorina shore displacement near Helsinki. *Terra* 91, 1, pp. 15-20.
- Hyvärinen, H. 1980. Relative sea-level changes near Helsinki, southern Finland, during early Litorina times. *Bull. Geol. Soc. Finland* 52, 2, pp. 207-219.
- Hyvärinen, H. 1982. Interpretation of stratigraphical evidence of sea-level history - A Litorina site near Helsinki, southern Finland. *Ann. Acad. Sci. Fennicae, Ser. A III*, 134, pp. 139-149.
- Hyvärinen, H. 1984. The Mastogloia stage in the Baltic Sea history: Diatom evidence from southern Finland. *Bull. Geol. Soc. Finland*, 56, 1-2, pp. 99-115.
- Hyvärinen, H. 1999. Shore displacement and Stone Age dwelling sites near Helsinki, southern coast of Finland. In: *Dig it all. Papers dedicated to Ari Siiriäinen*. Helsinki, Finnish Antiquarian Society, Archaeological Society of Finland, 79-89.
- JUHTA 2007: JHS 163 Suomen korkeusjärjestelmä N2000. (In Finnish.) Julkisen hallinnon tietohallinnon neuvottelukunta. www.jhs-suositukset.fi/suomi/jhs163
- Kahma, K., Johansson, M. & Boman, H. 2001. Meriveden pinnankorkeuden jakauma Loviisan ja Olkiluodon rannikolla seuraavien 30 vuoden aikana. Meritutkimuslaitos, Helsinki, Finland, 28 p (in Finnish).
- Kakkuri, J. 1987. Character of the Fennoscandian uplift in the 20th century. Geological Survey of Finland. Special Paper 2, 15–20.
- Kakkuri, J. & Poutanen, M. 1997. Geodetic determination of the surface topography of the Baltic Sea. *Marine Geodesy*, 20, no 4.
- Koivisto, M. 2004. Jääkaudet. (In Finnish.) WSOY. 240 p.
- Kuivamäki, A. & Vuorela, P. 1994. Maankohoaminen ja kallioperän rakenne. *Turun Yliopiston Maaperägeologian Julkaisuja* 78, 15–52.
- Kujansuu, R. 1964. Nuorista siirroksista Lapissa. (Summary: Recent faults in Finnish Lapland). *Geologi* 16 (3–4), 30–35.

Kuusisto, M. 2007. Suomen maankuoren kivilajikoostumuksen tulkinta seismisistä aineistoista. Licentiate thesis. (in Finnish.) Helsinki University. <http://urn.fi/URN:NBN:fi-fe20071169>

Lagerbäck, R. 1990. Late Quaternary faulting and paleoseismicity in Northern Fennoscandia, with particular reference to the Lansjärv area, northern Sweden. *Geologiska föreningens i Stockholm Förhandlingar* 112, 333–354.

Lahtinen, R., Korja, A. & Nironen, M. 2005. Paleoproterozoic tectonic evolution. In: Lehtinen, M., Nurmi, P.A., Rämö, O.T. (Eds.), *Precambrian geology of Finland – Key to the evolution of the Fennoscandian shield*. Elsevier B.V. Amsterdam, 481–532.

Lambeck, K. & Purcell, A. Glacial rebound and crustal stress in Finland. Posiva 2003-10. www.posiva.fi/raportit/Posiva_2003-10.pdf

Lambeck, K., Smither, C. & Ekman, M. 1998. Tests of glacial rebound models for Fennoscandia based on instrumented sea- and lake-level records. *Geophys. J. Int.* 135, 375–387.

Landvik, J.Y., Bondevik, S., Elverhøi, A., Fjeldskaar, W., Mangerud, J., Siegert, M.J., Salvigsen, O., Svendsen, J.I. & Vorren, T.O. 1998. The last glacial maximum of Svalbard and the Barents Sea area: ice sheet extent and configuration. *Quaternary Science Reviews* 17, 43–75.

Lehmuskoski, P. 2008. Precise Levelling Campaigns at Olkiluoto in 2006 – 2007. Posiva Working Report 2008-19. http://www.posiva.fi/publications/WR%202008-19_web.pdf

Lehmuskoski, P., Saaranen, V., Takalo, M. & Rouhiainen, P. 2008. Suomen Kolmannen tarkkavaaituksen kiintopisteluettelo. Bench Mark List of the Third Levelling of Finland. Publications of the Finnish geodetic institute, N:o 139. 220 p.

Lidberg, M. 2007. Geodetic Reference Frames in Presence of Crustal Deformations. Göteborg: Chalmers University of Technology. Diss. (Doktorsavhandlingar vid Chalmers tekniska högskola. Ny serie) ISBN/ISSN: 978-91-7385-024-7.

Lidberg, M., Nordman, M., Johansson, J.M., Milne, G.A., Scherneck, H-G. & Davis, J.L. 2008. Geodetic Reference Frames in Presence of Crustal Deformations. *Geophysical Research Abstracts*, Vol. 10, EGU2008-A-10626, 2008. SRef-ID: 1607-7962/gra/EGU2008-A-10626. EGU General Assembly 2008. www.cosis.net/abstracts/EGU2008/10626/EGU2008-A-10626.pdf

Lidberg, M. 2008. Geodetic Reference Frames in Presence of Crustal Deformations. FIG Working Week, Stockholm, June 2008. http://www.fig.net/pub/fig2008/papers/ts02a/ts02a_04_lidberg_2890.pdf

Lindborg, T. & Lind, L. R. (editors) 2006. Long-term development of the super-regional area of Olkiluoto/Forsmark/Laxemar. Minutes from the Posiva and SKB workshop, October 12–13, 2006. December, 2006 <http://www.skb.se/upload/publications/pdf/P-06-302webb.pdf>

- Lundqvist, J. & Lagerbäck, R. 1976. The Parvie fault: a lateglacial fault in the Precambrian of Swedish Lapland. *Geologiska Foreningens i Stockholm F. orhandlingar* 98, 45–51.
- Luosto, U. 1997. Structure of the Earth's crust in Fennoscandia as revealed from refraction and wide-angle reflection studies. In: Pesonen L.J. (Ed.), *The lithosphere in Finland - a geophysical perspective*. *Geophysica*, 33(1), 3-16.
- Löfman, J. 1999. Site scale groundwater flow in Olkiluoto. Helsinki, Finland: Posiva Oy. 121 p. Posiva-99-03. ISBN 951-652-058-8.
- Miettinen, A. 2002. Relative sea level changes in the eastern part of the Gulf of Finland during the last 8000 years. *Annales Academiae Scientiarum Fennicae, Geologica-Geographica* 162, 100 pp. (Ph.D. Thesis).
- Miettinen, A. 2004. Holocene sea-level changes and glacio-isostasy in the Gulf of Finland, Baltic Sea. *Quaternary International* 120, 91-104. <http://dx.doi.org/10.1016/j.quaint.2004.01.009>
- Miettinen, A., Eronen, M. & Hyvärinen, H. 1999. Land uplift and relative sea-level changes in the Loviisa area, southeastern Finland, during the last 8000 years. Posiva Report 99-28, Posiva Oy, 26 pp.
- Miettinen, A., Jansson, H., Alenius, T. & Haggrén, G. 2007. Late Holocene sea-level changes along the southern coast of Finland, Baltic Sea. In: *Quaternary land-ocean interactions: sea-level change, sediments and tsunami*. *Marine Geology* 242 (1-3), 27-38.
- Miettinen, N. & Haapanen, R. 2002. Vegetation types on Olkiluoto Island. Posiva Oy. Working Report 2002-54, 54 p.
- Milne, G. A., Mitrovica, J. X., Scherneck, H.-G., Davis, J. L., Johansson, J. M., Koivula, H., & Vermeer, M. 2004. Continuous GPS measurements of postglacial adjustment in Fennoscandia: 2. Modeling results, *J. Geophys. Res.*, 109, B02412, doi:10.1029/2003JB002619.
- Moisio, K. 2005. Numerical lithospheric modelling: Rheology, stress and deformation in the central Fennoscandian shield. Faculty of Science, Department of Physical Sciences, Division of Geophysics, University of Oulu. <http://herkules.oulu.fi/isbn9514279514/>
- Morén, L. & Pässe, T. 2001. Climate and shoreline in Sweden during Weichsel and the next 150,000 years. Technical Report TR-01-19. www.skb.se/upload/publications/pdf/Webb_TR-01-19_sid_01-68.pdf
- Mäkiäho, J-P. 2005. Development of Shoreline and Topography in the Olkiluoto Area, Western Finland, 2000 BP – 8000 AP. Working Report 2005-70. www.posiva.fi
- Mäkilä, M. & Grundström, A. 2008. Turpeen ikä ja kerrostumisnopeus Lounais-Suomen soilla. Posiva Working Report 2008-12 (in Finnish). www.posiva.fi

Mörner, N-A. 1977. Eustacy and instability of the geoid configuration. *Geologiska Föreningens i Stockholm Förhandlingar* 99, 369-376.

Mörner, N-A. 1999. Sea-level and climate: rapid regressions at local warm phases. *Quaternary International* 60, 75-82.

Ojala, A.E.K., Virkki, H., Palmu, J-P., Hokkanen, K. & Kaija, J. 2006. Regional development of river basins in the Olkiluoto-Pyhäjärvi area, SW Finland, 2000 BP-8000 AP. Posiva Oy, Working Report 2006-113.

Pan, M. & Sjöberg, L.E. 1998. Unification of vertical datums by GPS and gravimetric geoid models with application to Fennoscandia. *Journal of Geodesy*, Volume 72, Number 2 / February, 1998.

Paulamäki, S. & Kuivamäki, A. 2006. Depositional History and Tectonic Regimes within and in the Margins of the Fennoscandian Shield During the last 1300 Million years. Posiva Working Report 2006-43. www.posiva.fi

Peltier, R.W. 1994. Ice Age Paleotopography. *Science* 265, 195–201.

Pohjola, J. 2008. Creation of a statistical high resolution digital elevation model using thin plate spline interpolation (in Finnish with an English abstract; "Korkearesoluutioisen tilastollisen korkeusmallin luominen thin plate spline -interpolointia käyttäen"). M.Sc. thesis. Tampere University of Technology, Master's degree in Information Technology.

Poutanen, M. 1999. Use of GPS in unification of vertical datums and detection of levelling network errors. In *Proceedings, Geodesy and surveying in the future. The importance of heights. March 15-17 1999, Gävle, Sweden.* (Ed. M. Lilje) LMV Rapport 1999:3, 301-312.

Pässe, T. & Andersson, L. 2005. Shore-level displacement in Fennoscandia calculated from empirical data. *GFF*, Vol. 127. (Pt. 4, December), pp. 253–268. Stockholm. ISSN 1103-5897. www.gff-online.se/site/article.asp?articleID=845

Pässe, T. 1990a. Empirical estimation of isostatic uplift using the lake-tilting method at lake Fegen and at Lake Sväven southwestern Sweden. *Mathematical geology* 22. No. 7, 803-834.

Pässe, T. 1996. A mathematical model of the shore level displacement in Fennoscandia. SKB Technical Report 96-24. www.skb.se/upload/publications/pdf/SKB96-24webb.pdf

Pässe, T. 1997. A mathematical model of past, present and future shore level displacement in Fennoscandia. SKB technical report 97-28. 2nd edition December 1997. www.skb.se/upload/publications/pdf/TR-97-28webb.pdf

Pässe, T. 1998. Lake-tilting, a method for estimation of isostatic uplift. *Boreas* 27, 69-80.

Pässe, T. 2001. An empirical model of glacio-isostatic movements and shore-level displacement in Fennoscandia. SKB technical report R-01-41. www.skb.se/upload/publications/pdf/R-01-41webb.pdf

Posiva Oy. 2008. Safety Case Plan 2008. Posiva Report 2008-05. Posiva Oy. July 2008. www.posiva.fi

Reimer, P.J., Baillie, M.G.L., Bard, E., Bayliss, A., Beck, J.W., Bertrand, C.J.H., Blackwell, P.G., Buck, C.E., Burr, G.S., Cutler, K.B., Damon, P.E., Edwards, R.L., Fairbanks, R.G., Friedrich, M., Guilderson, T.P., Hogg, A.G., Hughen, K.A., Kromer, B., McCormac, G., Manning, S., Bronk Ramsey, C., Reimer, R.W., Remmele, S., Southon, J.R., Stuiver, M., Talamo, S., Taylor, F.W., van der Plicht, J. & Weyhenmeyer, C.E. 2004. IntCal04 Terrestrial Radiocarbon Age Calibration, 0–26 cal kyr BP. *Radiocarbon* Vol 46, Nr 3, 2004 pp. 1029–1058. <http://courses.washington.edu/twsteach/ESS/302/ESS%20Readings/Reimer2004.pdf>, www.radiocarbon.org/IntCal04.htm

Risberg, J. 1999. Strandförskjutningen i nordvästra Uppland under subboreal tid. In Segerberg A. 1999. Bälunge mossar. Kustbor i Uppland under yngre stenåldern. Doctoral thesis. Uppsala Universitet, Uppsala. Aun 26, 233-241. (In Swedish with English summary).

Ristaniemi, O. 1984. Shoreline displacement of the Baltic during the Ancylus stage in the Karjalohja-Kisko area, the Salpausselkä belt, SW-Finland. *Publ. Dept. Quaternary Geol., Univ. Turku*, 53, 75 pp.

Ristaniemi, O. 1987. The highest shore and Ancylus limit of the Baltic Sea and the ancient Lake Päijänne in central Finland. *Ann. Univ. Turkuensis, Ser. C*, 59, 102 pp.

Ristaniemi, O. & Glückert, G. 1987. The Ancylus transgression in the area of Espoo - the First Salpausselkä, southern Finland. *Bull. Geol. Soc. Finland* 59, 1, pp. 45-69.

Ristaniemi, O. & Glückert, G. 1988. Ancylus- ja Litorinatransgressiot Lounais-Suomessa. In: Lappalainen, V. & Papunen, H. (eds.): *Tutkimuksia geologian alalta*. *Ann. Univ. Turkuensis, Ser. C*, 67, pp. 129-145.

Saaranen, V., Lehmuskoski, P., Rouhiainen, P., Takalo, M. & Mäkinen, J. 2006. The New Finnish Height System N2000. Symposium of the IAG Subcommission for Europe (EUREF), Riga, 14–17 June 2006. www.euref.eu/symposia/2006Riga/02-04.pdf

Seppä, H. & Tikkanen, M. 1998. The isolation of Kruunuvuorenlampi, southern Finland, and implications for Holocene shore displacement models of the Finnish south coast. *Journal of Paleolimnology* 19 (4), 385-398.

Seppä, H., Tikkanen, M. & Shemeikka, P. 2000. Late-Holocene shore displacement of the Finnish south coast: diatom, litho- and chemostratigraphic evidence from three isolation basins. *Boreas* 29 (3), 219-231.

STUK 2001. Long-term safety of disposal of spent nuclear fuel. Guide YVL 8.4. Radiation and Nuclear Safety Authority (STUK). www.stuk.fi

Svendsen, J.I., Astakhov, V.I., Bolshiyakov, D.Y., Demidov, Y., Dowdeswell, J.A., Gataullin, V., Hjort, C., Hubberten, H., Larsen, E., Mangerud, J., Melles, N., Möller, P., Saarnisto, M. & Siegert, M. 1999. Maximum extent of the Eurasian ice sheets in the Barents and Kara Sea region. *Boreas* 28, 234–242.

Telford, R.J., Heegaard, E. & Birks, H.J.B. 2004. All age–depth models are wrong: but how badly? *Rapid Communication, Quaternary Science Reviews* 23 (2004) 1–5. [www.ig.uit.no/norpast2/PDFer til homepage/Telford QSR 23 04.pdf](http://www.ig.uit.no/norpast2/PDFer%20til%20homepage/Telford%20QSR%2023%2004.pdf)

Telford, R.J., Heegaard, E. & Birks, H.J.B. 2004. The intercept is a poor estimate of a calibrated radiocarbon age. *The Holocene* 14,2 (2004) pp. 296–298. [www.ig.uit.no/norpast2/PDFer til homepage/Telford Holocene 14 04.pdf](http://www.ig.uit.no/norpast2/PDFer%20til%20homepage/Telford%20Holocene%2014%2004.pdf)

Tesauro, M., Kaban, M. K. & Cloetingh, S.A.P.L. 2008. EuCRUST-07: A new reference model for the European crust, *Geophys. Res. Lett.*, 35, L05313, doi:10.1029/2007GL032244

Tesauro, M., Kaban, M.K., Koulakov, I. & Cloetingh, S.A.P.L. 2008. EuCRUST-07: A new 3D crustal model for the WECEP area as a basis for modelling mantle structure. EUCOR URGENT – TOPO-WECEP, 8th International Symposium on Upper Rhine Graben Evolution and Neotectonics. March 2008. http://omnibus.uni-freiburg.de/~dh751/wecep_2008/mso08/talks-pdf/17_Magdala_Presentazione.pdf

Tikkanen, M. & Oksanen, J. 2002. Late Weichselian and Holocene shore displacement history of the Baltic Sea in Finland. *Fennia* 180: 1-2, pp. 9-20. Helsinki. ISSN 0015-0010. <http://www.helsinki.fi/maantiede/geofi/fennia/demo/pages/oksanen.htm>

Trautman, M.A. & Willis, E.H. 1966. Isotopes, Inc. radiocarbon measurements V. *Radiocarbon*, vol. 8, 1966, p. 161–203. http://radiocarbon.library.arizona.edu/Volume8/Number1/azu_radiocarbon_v8_161_203_v.pdf

University of Cologne. 2008. CalPal - the cologne radiocarbon calibration & palaeoclimate research package. Universität zu Köln, Institut für Ur- und Frühgeschichte, Radiocarbon Laboratory. www.calpal.de

van der Plicht, J. 2000. Introduction. The 2000 radiocarbon varve/comparison issue. *Radiocarbon*, Vol 42, Nr 3, 2000, p 313–322. <http://cio.eldoc.ub.rug.nl/FILES/root/2000/RadiocarbonvdPlicht/2000RadiocarbonvdPlicht.pdf>

Vartiainen, T. 1980: Succession of island vegetation in the land uplift area of the northernmost Gulf of Bothnia, Finland. *Acta Bot. Fennica* 115:1-105.

Vestøl, O. 2006: Determination of postglacial land uplift in Fennoscandia from leveling, tide-gauges and continuous GPS stations using least squares collocation. *J. Geodesy* 80(5), 248–258. doi 10.1007/s00190-006-0063-7.

Vieno, T. & Ikonen, A. T. K. 2005. Plan for Safety Case of spent fuel repository at Olkiluoto. Posiva Oy. POSIVA 2005-01. 70 p. <http://www.posiva.fi>

Wang, Z. 1998. Geoid and Crustal Structure in Fennoscandia. Publications of the Finnish Geodetic Institute, 126, 118 p.

Westman, P., Wastergård, S., Schoning, K., Gustafsson, B. & Omstedt, A. 1999. Salinity change in the Baltic Sea during the last 8,500 years: evidence, causes and models. Swedish Nuclear Fuel and Waste Management Co, Stockholm. Technical Report 99-38. 52 pp.

Ziegler, P. A. & Dèzes, P. 2006. Crustal evolution of Western and Central Europe. Geological Society, London, Memoirs; 2006; v. 32; p. 43-56; DOI: 10.1144/GSL.MEM.2006.032.01.03. See also http://comp1.geol.unibas.ch/downloads/Crust_evolution_europe_with_figs.pdf

INTERNET SOURCES

Blaauw, M. 2008. Excel code for C-14 wiggle-match dating. Tutorial ¹⁴C wiggle-match dating: an Excel-approach. <http://www.anst.uu.se/maab1971/wiggles/> code accessed Feb 15, 2008.

Hokkanen, J. 2008. Nykyinen maankohoaminen Satakunnassa. <http://hokkanen.wellfish.org/suurijoki/> (Accessed 10.1.2008) or www.pilvive.com/suurijoki/

Lantmäteriet 2008. Tvådimensionella system - RT 90. www.lantmateriet.se/templates/LMV_Page.aspx?id=4766(Accessed March 2008)

Kallio, H. Land Uplift & Subsidence. www.gsf.fi/slr/article.php?id=77 (Accessed April 2008)

Kukkonen, I. 2000. Suomi sijaitsee hyvin tukevalla kallioperällä, jolla on poikkeuksellisen syvät juuret. (In Finnish) Geological survey of Finland. <http://www.gtk.fi/Media/lehdistotiedotteet.html?number=281> (Accessed 20.11.2008)

Kukkonen, I.T. 2006. FIRE reflection seismics: New images of the earth's crust [online]. Espoo: Geological Survey of Finland. <http://en.gtk.fi/Research/CR/fire.html> (Accessed 18.11.2008)

Pässe, T. & Andersson, L. 2006. Visualization of shoreline displacements. http://www.sgu.se/sgu/eng/geologi/strand_intro_e.html (Accessed 10.12.2008)

Prof. C. Bronk Ramsey. OxCal. Oxford Radiocarbon Accelerator Unit. Research Lab for Archaeology. <http://c14.arch.ox.ac.uk/oxcal.html> (Accessed 22.2.2008)

Peltier, J. 2008. Horizontal Box and Whisker Plots. <http://www.peltiertech.com/Excel/Charts/BoxWhiskerH.html> (Accessed October 2008)

Stuiver, M., Reimer, P.J. & Reimer, R. CALIB Radiocarbon Calibration. <http://calib.qub.ac.uk/calib/> (2006, accessed 22.2.2008)

University of Sheffield. Department of Probability and Statistics.
<http://bcal.sheffield.ac.uk> (accessed 22.2.2008)

Weninger, B., Danzeglocke, U. & Jöris, O. 2005. Comparison of Dating Results achieved using Different Radiocarbon-Age Calibration Curves and Data. Version 19. May 2007. www.calpal.de/calpal/files/CalCurveComparisons.pdf

PERSONAL COMMUNICATIONS

Ågren, J. Lantmäteriet. Personal communication, March 2008.

Artemieva, I. Personal communication, October 2008.

Berglund, M. Mid Sweden University. Personal communication, March 2008.

Blaauw, M. Personal communication, February 2008. (Blaauw 2008b)

Engberg, L.E. Senior Adviser in Geodesy. Lantmäteriet, Sweden. Personal communication, March 2008.

Erlenkeuser, H. Dr. Christian-Albrechts-Universität zu Kiel. Leibniz-Labor für Altersbestimmung und Isotopenforschung. Personal communication, April 2008.

Gulliksen, S. NTNU Vitenskapsmuseet. Personal communication, April 2008.

Goslar, T. Poznań Radiocarbon Laboratory. Personal communication, March 2008.

Hokkanen, J. Personal communication, April 2008. www.pilvivene.com/suurijoki/

Jungner, H. (Ex. University of Helsinki Dating Laboratory director). Personal communication, March & June 2008.

Lehmuskoski, P. Finnish Geodetic Institute. Personal communication, 2008. (Lehmuskoski 2008b)

Miettinen, A. Norwegian Polar Institute, Polar Environmental Centre. Personal communication, June 2008.

Mäkeläinen, E. & Mäkilä, M. Geological Survey of Finland. Personal communication, March 2008.

Mäkinen, J. Finnish Geodetic Institute. Personal communication, February 2009.

Museum of Natural History and Archaeology, NTNU, Trondheim, Norway. National Laboratory for ¹⁴C dating. Personal communication with staff, 28th March 2008.

Oinonen, M. Helsinki University, The Finnish Museum of Natural History, Dating Laboratory. Personal communication, Feb-March 2008.

Olsson, I. Uppsala Universitet, Institutionen för fysik och materialvetenskap. Personal communication, April 2008.

- Påsse, T. The Geological Survey of Sweden. Personal communication, Dec 2008.
- Poutanen, M. Finnish Geodetic Institute. Personal communication, March 2008.
- Reimer, P.J. Personal communication, Feb 2008.
- Saarnisto, M. Personal communication, June 2008.
- Salonen, V-P. Helsinki University. Personal communication, October 2008.
- Schutz, D.F. Personal communication, April 2008.
- Skog, G. Lunds Universitet. Centrum för GeoBiosfärsvetenskap, Kvartärgeologiska avdelningen. Personal communication, March 2008.
- Skripkin, V.V. Kyiv Radiocarbon Laboratory. Personal communication, April 2008.
- Smith-Deenen, H.E. Centrum voor IsotopenOnderzoek, Groningen. Personal communication, March 2008.
- Strucke, U. Riksantikvarieämbetet (Swedish National Heritage Board). UV Mitt. Instrumentvägen 19, SE-126 53 Hägersten. Personal communication, April 2008.

APPENDICES

Appendix 1	Samples by Eronen et al. (1995) Literature references by Eronen et al. (1995)
Appendix 2	Codes used
Appendix 3	Age calibration practices for lakes and peats
Appendix 4	The new samples (Finland and Sweden) References of the new samples (Finland and Sweden)
Appendix 5	The analysis site table

APPENDIX 1. SAMPLES BY ERONEN ET AL. (1995)

Some confusion was found in the Eronen et al. (1995) data set:

Sample no.	Comment
145	Mieslahti basin number 129 was considered a typo in an ordinal number list and renumbered to 119.
133	Hel-1293 aging would be actually 8920 ± 180 BP, but it seems (from Figures 35 and 39 of Eronen et al. 1993) as if the laboratory code would be actually Hel-1294, the ^{14}C of which is 9070 ± 190 BP as Eronen et al. (1995) lists, therefore their Hel-1293 code is based on a typo and ought to be Hel-1294.
102	Hel-1972's \pm error is in Eronen's paper 140, but actually 110 according to the database of Helsinki University.

Column explanations of the table below:

- **Sample number** is the ordinal number of the sea-level index point and serves as an ID, also in the plotted shoreline displacement curve graphs.
- **Basin number** is the number shown in the original source report. One basin can have many **Samples**.
- **Point** is the lake or mire name, and **Locality** is the municipality or other place name.
- **N** and **E** are the geographic coordinates, latitude and longitude, with WGS 84 spheroid and datum assumed.
- **Threshold N60** is the original threshold altitude, and **Threshold N2000** is that corrected according to the surface in Figure 10.
- **Age ^{14}C** is the original radiocarbon age, years BP; \pm is its error value or σ ; and **Laboratory number** is its analysis number.

- **$\delta^{13}\text{C}$ corrected age** is the $\delta^{13}\text{C}$ corrected ^{14}C age (still in years BP), different from **Age ^{14}C** , which does not always include the correction; and **$\delta^{13}\text{C}$ corrected \pm** is the corresponding corrected error or σ of the **$\delta^{13}\text{C}$ corrected age**. Helsinki University made their own samples' $\delta^{13}\text{C}$ corrections based on $^{14}\text{C}/^{12}\text{C}$ ratios.
- **Median AD from CALIB** is the median value of the whole probability distribution function.
- **1 σ LL: UL AD OxCal** are the lower limit and upper limit of all one-sigma ranges, and **2 σ LL: UL AD OxCal** are the corresponding two-sigma limits. Helsinki University produced the limits of calibrations using OxCal.
- **1 σ AD ranges and probabilities, CALIB** are the individual one-sigma ranges of the probability distribution function, and **2 σ AD ranges and probabilities, CALIB** the corresponding two-sigma ranges. The minimum and maximum values of these can be compared with the two previous columns to get an idea of the differences between the values obtained using the OxCal and CALIB applications. Both used the same calibration dataset version and the same 5-year smoothing. The distribution function medians, each individual range, and their probabilities (summing 1.0) were calibrated at Pöyry Environment Oy.
- **Comments** field may point out the interpretation of the phase of isolation of the lake or mire from sea.
- **Reference** is the report referenced in the original source report Eronen et al. (1995) and at the end of this appendix here.
- **Validity** field may give some remarks on the validity of the sample.

Sample no	Basin No.	Point	Locality	N	E	Threshold N60	Threshold N2000	Age ^{14}C	\pm	Lab no.	$\delta^{13}\text{C}$ corrected age	$\delta^{13}\text{C}$ corrected \pm	Median AD from CALIB	1 σ LL: UL AD OxCal	2 σ LL: UL AD OxCal	1 σ AD ranges and probabilities, CALIB	2 σ AD ranges and probabilities, CALIB	Comments	Reference	Validity Eronen et al.
1	1	Kievarinsuo	Karjaa	60° 05'	23° 45'	44.5	44.76	6640	190	Hel-56	6570	200	-5506	-5700:-5320	-5893:-5063	-5673:-5320 1	-5886:-5195 0.957429 -5180:-5061 0.042571	isolation from Ancylus Lake (AV)?	Glückert 1970	
2	2	Nummensuo	Paimio	60° 24'	22° 44'	46	46.29	5500	180	Hel-494	5430	190	-4256	-4452:-4043	-4703:-3803	-4452:-4044 1	-4689:-3914 0.972945 -3877:-3804 0.027055	isolation from Litorina Sea (L II)	Glückert 1976	
3	3	Isosuo	Turku	60° 30'	22° 11'	42	42.30	4950	140	Hel-564	4880	150	-3671	-3930:-3384	-4035:-3350	-3928:-3877 0.108147 -3804:-3517 0.869776 -3396:-3385 0.022077	-4035:-4024 0.002886 -3992:-3348 0.997114	isol L II	Glückert 1976	
4	4	Sammal-	Laitila	60°	21° 54'	48	48.32	5030	200	Hel-	4960	210	-3758	-3987:-	-4324:-	-3986:-3519 1	-4321:-4292 0.006107	isol L II	Glückert 1976	

Appendix 1

33	33	Holmmosaberget	Sund	60° 16'	20° 13'	53	53.30	5500	100	Su-709	5500	100	-4346	-4455:-4251	-4543:-4052	-4456:-4253 1	-4542:-4219 0.871133 -4213:-4149 0.06255 -4135:-4054 0.066317	isol L II	Glückert 1978a	
34	34	Stormyrån	Sund	60° 17'	20° 14'	41	41.30	4700	50	Su-711	4700	50	-3476	-3623:-3374	-3631:-3368	-3624:-3601 0.151513 -3524:-3495 0.212093 -3463:-3376 0.636394	-3632:-3559 0.247892 -3537:-3369 0.752108	isol L II / III	Glückert 1978a	
35	35	Timmermossen	Geta	60° 23'	19° 50'	38	38.31	4370	100	Su-713	4370	100	-3039	-3311:-2889	-3358:-2711	-3313:-3294 0.046994 -3287:-3274 0.030417 -3265:-3238 0.075643 -3167:-3166 0.002234 -3107:-2890 0.844712	-3358:-2862 0.971418 -2807:-2758 0.024424 -2718:-2708 0.004158	isol L III	Glückert 1978a	
36	36	Holmmosen	Sund	60° 16'	20° 13'	28	28.30	4200	50	Su-710	4200	50	-2776	-2891:-2695	-2903:-2629	-2892:-2852 0.285065 -2812:-2744 0.523043 -2726:-2696 0.191892	-2903:-2831 0.28101 -2821:-2630 0.71899	isol L IV	Glückert 1978a	
37	37	Tjäman	Saltvik	60° 18'	20° 10'	11.5	11.80	2110	70	Su-714	2110	70	-143	-345:-41	-360:23	-346:-320 0.098919 -206:-42 0.901081	-361:-270 0.173743 -264:23 0.826257	isol L VII	Glückert 1978a	
38	38	Lillträsk	Geta	60° 22'	19° 51'	16.5	16.81	3160	50	Su-712	3160	50	-1438	-1494:-1400	-1527:-1310	-1495:-1403 1	-1527:-1312 1	isol L VI	Glückert 1978a	
39	39	Storträsket	Lemland	59° 59'	20° 10'	5.5	5.78	760	100	Su-716	760	100	1241	1160:1386	1041:1399	1160:1306 0.907197 1363:1385 0.092803	1042:1107 0.100607 1117:1399 0.899393	isol L VIII	Glückert 1978a	
40	40	Saarijärvi	Somerniemi	60° 29'	23° 41'	117.7	117.97	6970	110	Su-672	6970	110	-5854	-5976:-5745	-6046:-5661	-5977:-5948 0.13881 -5921:-5746 0.86119	-6046:-6041 0.003898 -6032:-5661 0.996102	isol Y III	Glückert 1978b	
41	41	Kuorlampi	Vihti	60° 26'	24° 30'	82.7	82.96	9860	110	Su-821	9860	110	-9368	-9649:-9224	-9814:-8921	-9650:-9604 0.08889 -9527:-9487 0.074081 -9460:-9224 0.837028	-9813:-9123 0.974967 -9000:-8921 0.025033	isol late Yoldia	Glückert 1979	
42	42	Kaillampi I	Vihti	60° 19'	24° 29'	94	94.26	9850	120	Su-786	9850	120	-9357	-9651:-9211	-9850:-8843	-9652:-9598 0.093334 -9588:-9584 0.007585 -9545:-9482 0.10486 -9461:-9207 0.794221	-9815:-9117 0.933858 -9076:-9055 0.004862 -9014:-8912 0.044262 -8905:-8843 0.017019	isol early Yoldia	Glückert 1979	
43	43	Kaillampi II	Vihti	60° 20'	24° 29'	73.4	73.66	9840	120	Su-823	9840	120	-9339	-9650:-9180	-9810:-8841	-9651:-9603 0.07728 -9542:-9536 0.008584 -9529:-9485 0.067638 -9460:-9178 0.846499	-9807:-9116 0.916652 -9077:-9054 0.007039 -9016:-8842 0.07631	isol late Yoldia	Glückert 1979	
44	44	Iso Lehmlampi	Vihti	60° 21'	24° 36'	92	92.26	9740	150	Su-788	9740	150	-9163	-9356:-8836	-9747:-8711	-9336:-9111 0.557405 -9085:-9040 0.073535 -9029:-8837 0.369059	-9740:-9729 0.002492 -9671:-8709 0.995676 -8666:-8659 0.001831	isol early Yoldia	Glückert 1979	
45	45	Ahvenlammen-suo	Vihti	60° 29'	24° 27'	104.1	104.36	9860	100	Su-791	9860	100	-9360	-9645:-9227	-9800:-8950	-9645:-9613 0.060595 -9518:-9507 0.020409 -9456:-9227 0.918997	-9798:-9788 0.002716 -9769:-9138 0.989047 -8972:-8943 0.008238	isol early Yoldia	Glückert 1979	
46	46	Kakarlampi	Nummi-Pusula	60° 26'	23° 53'	111	111.27	9640	130	Su-792	9640	130	-9012	-9240:-8835	-9311:-8638	-9240:-9111 0.363341 -9086:-9041 0.110515 -9029:-8837 0.526143	-9306:-8696 0.981471 -8683:-8639 0.018529	isol middle Yoldia	Glückert 1979	
47	47	Innonlampi	Sammatti	60° 19'	23° 50'	73.9	74.16	8120	140	Su-964	8120	140	-7103	-7334:-6829	-7475:-6691	-7333:-7001 0.789837 -6989:-6985 0.006553 -6971:-6912 0.105579	-7473:-6691 1	isol Ancyclus I hiatus	Ristaniemi 1984	

Appendix 1

				20° 9'						1074					-7572	-7522	-7754:-7573 0.98869		transgress ?	Glückert 1987	
61	57	Kaliton	Espoo	60° 18'	24° 4'	60.2	60.45	9410	100	Su-1076	9410	100	-8706	-9108:-8492	-9136:-8349	-9108:-9088 0.03341 -8835:-8545 0.947872 -8503:-8493 0.018718	-9136:-8972 0.138493 -8938:-8423 0.844361 -8405:-8391 0.005001 -8378:-8349 0.012145	beginning of Ancyclus transgr	Ristaniemi & Glückert 1987		
62	57	Kaliton	Espoo	60° 18'	24° 4'	60.2	60.45	9310	170	Su-1077	9310	170	-8587	-8757:-8307	-9155:-8241	-8755:-8309 1	-9172:-9169 0.000771 -9157:-8235 0.999229	end of Ancyclus transgress	Ristaniemi & Glückert 1987		
63	58	Lakiassuo	Vihti	60° 20'	24° 2' 1'	69	69.26	9080	90	Su-1003	9080	90	-8299	-8448:-8223	-8554:-7974	-8447:-8363 0.276253 -8355:-8224 0.723747	-8553:-8168 0.892548 -8118:-7973 0.107452	beginning of Ancyclus transgr	Ristaniemi & Glückert 1987		
64	58	Lakiassuo	Vihti	60° 20'	24° 2' 1'	69	69.26	8780	110	Su-1004	8780	110	-7883	-8168:-7650	-8208:-7601	-8169:-8117 0.117995 -7978:-7650 0.882005	-8208:-7602 1	end of Ancyclus transgress	Ristaniemi & Glückert 1987		
65	59	Kakarlampi	Espoo	60° 14'	24° 3' 4'	57	57.25	9450	100	Su-1100	9450	100	-8774	-9117:-8608	-9175:-8479	-9118:-9071 0.105885 -9059:-9009 0.107744 -8914:-8902 0.021295 -8846:-8608 0.763266 -8576:-8576 0.001811	-9176:-9163 0.004717 -9160:-8532 0.975557 -8517:-8477 0.019726	beginning of Ancyclus transgr	Ristaniemi & Glückert 1987		
66	59	Kakarlampi	Espoo	60° 14'	24° 3' 4'	57	57.25	9430	180	Su-1102	9430	180	-8761	-9128:-8484	-9227:-8311	-9128:-8994 0.222369 -8926:-8537 0.738013 -8511:-8484 0.039618	-9225:-8311 1	end of Ancyclus transgress	Ristaniemi & Glückert 1987		
67	60	Keihilampi	Sammatti	60° 18'	23° 4' 9'	72.6	72.86	9720	140	Su-1001	9720	140	-9128	-9302:-8839	-9652:-8713	-9302:-9113 0.533684 -9082:-9049 0.061967 -9022:-8839 0.404349	-9652:-9598 0.014114 -9588:-9584 0.0011 -9545:-9482 0.01558 -9461:-8707 0.966844 -8668:-8657 0.002363	beginning of Ancyclus transgr	Glückert & Ristaniemi 1982		
68	60	Keihilampi	Sammatti	60° 18'	23° 4' 9'	72.6	72.86	9080	180	Su-1002	9080	180	-8279	-8554:-7975	-8760:-7718	-8553:-8168 0.776413 -8118:-7975 0.223587	-8749:-7719 1	end of Ancyclus transgress	Glückert & Ristaniemi 1982		
69	61	Hossus	Pertteli	60° 25'	23° 2' 3'	83.1	83.37	9900	100	Su-1537	9900	100	-9423	-9650:-9257	-9815:-9206	-9651:-9603 0.117709 -9542:-9538 0.008797 -9528:-9485 0.101137 -9460:-9258 0.772358	-9813:-9207 1	isol Yoldia	Ristaniemi & Glückert 1988		
70	61	Hossus	Pertteli	60° 25'	23° 2' 3'	83.1	83.37	9440	90	Su-1538	9440	90	-8750	-9112:-8571	-9145:-8482	-9113:-9082 0.068352 -9049:-9023 0.054579 -8839:-8603 0.856878 -8584:-8573 0.02019	-9142:-8536 0.98397 -8512:-8482 0.01603	end of Ancyclus transgression	Ristaniemi & Glückert 1988		
71	62	Muurasuo	Perniö	60° 18'	23° 1' 3'	82	82.27	9850	100	Su-1411	9850	100	-9345	-9644:-9220	-9765:-8930	-9643:-9615 0.047886 -9515:-9510 0.00842 -9455:-9220 0.943694	-9762:-9130 0.981017 -8991:-8991 0.000244 -8984:-8928 0.018739	isol Yoldia	Ristaniemi & Glückert 1988		
72	62	Muurasuo	Perniö	60° 18'	23° 1' 3'	82	82.27	9480	90	Su-1412	9480	90	-8827	-9117:-8636	-9172:-8565	-9118:-9068 0.14317 -9060:-9007 0.14359 -8915:-8901 0.032057 -8849:-8637 0.681183	-9173:-9168 0.002601 -9158:-8565 0.997399	beginning of Ancyclus transgr	Ristaniemi & Glückert 1988		
73	63	Haukialampi	Kisko	60° 15'	23° 3' 2'	49.5	49.76	8800	100	Su-1335	8800	100	-7906	-8180:-7724	-8213:-7610	-8182:-8112 0.16562 -8090:-8076 0.032283 -8061:-8042 0.041425	-8212:-7631 0.984209 -7625:-7611 0.015791	isol middle Ancyclus	Ristaniemi & Glückert 1988		

Appendix 1

		Il		27° 5'					378					-6815	-6640			Yoldia		
92	81	Sarkkilanjärvi	Ikaalinen	61° 45'	23° 06'	87	87.34	7980	250	T-529	7947	255	-6886	-7176: -6529	-7524: -6388	-7175:-6566 0.980741 -6545:-6530 0.019259	-7519:-6378 1	isol late Ancyclus	Alhonen 1968	
93	82	Bastuber g	Porvoo	60° 21'	25° 46'	28.5	28.74	8480	190	Hel-394	8410	200	-7423	-7606: -7089	-8168: -6829	-7605:-7141 0.997349 -7092:-7091 0.002651	-8163:-8147 0.002772 -7968:-6906 0.985338 -6887:-6827 0.01189	isol Ancyclus	Eronen 1974	
94	82	Bastuber g	Porvoo	60° 21'	25° 46'	28.5	28.74	7250	240	Hel-392	7180	250	-6060	-6346: -5807	-6562: -5620	-6343:-6313 0.045155 -6258:-5803 0.954845	-6505:-5616 0.99774 -5583:-5572 0.00226	beginning of Litorina transgr	Eronen 1974	
95	82	Bastuber g	Porvoo	60° 21'	25° 46'	28.5	28.74	6230	220	Hel-391	6160	230	-5080	-5340: -4806	-5535: -4552	-5339:-5333 0.007041 -5330:-4828 0.978613 -4814:-4804 0.014346	-5529:-4549 1	isol Litorina	Eronen 1974	
96	83	Stormossen	Porvoo	60° 26'	25° 37'	27.5	27.74	5350	100	Su-1026	5350	100	-4176	-4321: -4052	-4356: -3969	-4322:-4292 0.125501 -4265:-4147 0.518347 -4135:-4053 0.356153	-4356:-3970 1	isol Litorina	Donner & Eronen 1981	
97	84	Huiskaisuo	Askola	60° 32'	25° 38'	59	59.25	9370	110	Su-1024	9370	110	-8647	-8796: -8461	-9120: -8308	-8794:-8463 1	-9121:-9003 0.07552 -8918:-8894 0.012505 -8878:-8306 0.911976	isol late Yoldia	Donner & Eronen 1981	
98	84	Huiskaisuo IV C	Askola	60° 33'	25° 38'	59	59.25	9160	120	Hel-2011	9090	130	-8309	-8546: -8015	-8694: -7840	-8546:-8502 0.087955 -8494:-8204 0.875775 -8036:-8015 0.03627	-8636:-7937 0.980665 -7926:-7917 0.002753 -7898:-7839 0.016582	end of Ancyclus transgression	Haila 1987	
99	84	Huiskaisuo II C	Askola	60° 33'	25° 38'	59	59.25	9090	130	Hel-1978	9020	140	-8184	-8422: -7958	-8568: -7741	-8423:-8405 0.030549 -8391:-8378 0.021846 -8349:-7958 0.947605	-8565:-7741 1	end of Ancyclus transgression	Haila 1987	
100	84	Huiskaisuo III C	Askola	60° 33'	25° 38'	59	59.25	9060	120	Hel-1876	8990	130	-8125	-8317: -7944	-8537: -7738	-8316:-7944 1	-8537:-8511 0.010243 -8485:-7735 0.989757	end of Ancyclus transgression	Haila 1987	
101	84	Huiskaisuo I C	Askola	60° 33'	25° 38'	59	59.25	9040	120	Hel-1963	8970	130	-8098	-8299: -7938	-8527: -7685	-8300:-7939 0.998456 -7922:-7920 0.001544	-8466:-7709 0.995925 -7695:-7683 0.004075	end of Ancyclus transgression	Haila 1987	
102	84	Huiskaisuo VI C	Askola	60° 33'	25° 38'	59	59.25	9040	110	Hel-1972	8970	120	-8100	-8289: -7958	-8455: -7735	-8290:-7960 1	-8453:-8361 0.037853 -8358:-7732 0.962147	end of Ancyclus transgression	Haila 1987	± err. corr.
103	84	Huiskaisuo C	Askola	60° 32'	25° 38'	59	59.25	9020	170	Hel-1771	8950	180	-8073	-8296: -7794	-8542: -7602	-8297:-7813 0.987871 -7804:-7795 0.012129	-8540:-8509 0.013432 -8487:-7601 0.986568	end of Ancyclus transgression	Haila 1987	
104	84	Huiskaisuo V C	Askola	60° 33'	25° 38'	59	59.25	8950	130	Hel-2009	8880	140	-8002	-8232: -7825	-8291: -7606	-8233:-7826 1	-8288:-7610 1	end of Ancyclus transgression	Haila 1987	
105	84	Huiskaisuo	Askola	60° 32'	25° 38'	59	59.25	8430	90	Su-1025	8430	90	-7483	-7581: -7370	-7600: -7191	-7582:-7451 0.844243 -7406:-7371 0.155757	-7601:-7289 0.971066 -7272:-7256 0.007688 -7227:-7192 0.021246	Ancyclus transgression	Donner & Eronen 1981	
106	85	Vesilampi	Juuka	63° 04'	29° 46'	220	220.25	9150	350	I-1178	9117	353	-8344	-8770: -7760	-9314: -7509	-8759:-7787 0.995424 -7766:-7761 0.004576	-9285:-7513 1	isol local ice-lake ?	Hyvärinen 1966	isol local ice-lake ?
107	86	Alasenjärvi II	Valtimo	63° 37'	28° 51'	160.2	160.48	8930	220	I-1519	8897	225	-8025	-8286: -7724	-8609: -7546	-8286:-7726 1	-8604:-8583 0.004737 -8573:-7540 0.995263	isol Yoldia	Hyvärinen 1966	
108	87	Alasenjärvi I	Valtimo	63° 37'	28° 50'	159	159.28	7670	330	I-1520	7637	334	-6549	-7027: -6123	-7447: -5895	-7026:-6964 0.060451 -6949:-6934 0.015648	-7351:-5872 0.997039 -5863:-5846 0.002961	isol Yoldia too young age	Hyvärinen 1966	too young

Appendix 1

149	122	Kirakanjärvi	Perniö	60° 12'	22° 5' 9"	44.5	44.77	7450	80	GrN-19634	7450	80	-6318	-6395:-6243	-6458:-6100	-6396:-6244 1	-6457:-6205 0.947242 -6190:-6184 0.004809 -6171:-6157 0.009561 -6144:-6102 0.038388	Litorina transgression begins	Eronen et al 1993	
150	122	Kirakanjärvi	Perniö	60° 12'	22° 5' 9"	44.5	44.77	6800	80	GrN-19633	6800	80	-5697	-5750:-5625	-5876:-5558	-5750:-5626 1	-5875:-5858 0.011192 -5848:-5604 0.942951 -5596:-5559 0.04513	Litorina transgression ends	Eronen et al 1993	
151	123	Stortjärnen	Pohja	60° 04'	23° 2' 9"	39.9	40.16	7990	40	GrN-19637	7990	40	-6918	-7041:-6828	-7055:-6710	-7042:-6983 0.316735 -6973:-6911 0.357642 -6885:-6829 0.325623	-7056:-6767 0.983056 -6763:-6754 0.008403 -6718:-6711 0.008541	beginning of isolation	Eronen et al 1993	
152	123	Stortjärnen	Pohja	60° 04'	23° 2' 9"	39.9	40.16	7895	35	GrN-19636	7895	35	-6748	-6810:-6657	-7022:-6644	-6806:-6786 0.109162 -6778:-6677 0.804816 -6673:-6659 0.086021	-7023:-6967 0.064752 -6947:-6935 0.010698 -6915:-6881 0.055326 -6839:-6645 0.869224	end of isolation Litorina I	Eronen et al 1993	
153	124	Kvarnträsket	Tenhola	60° 02'	23° 0' 9"	38.5	38.76	6605	40	GrN-19940	6605	40	-5549	-5611:-5510	-5616:-5484	-5612:-5589 0.287709 -5565:-5511 0.702974 -5496:-5496 0.009318	-5617:-5486 1	beginning of isolation ?	Eronen et al 1993	
154	124	Kvarnträsket	Tenhola	60° 02'	23° 0' 9"	38.5	38.76	6840	60	GrN-19939	6840	60	-5725	-5778:-5660	-5868:-5627	-5776:-5662 1	-5866:-5866 0.000908 -5845:-5628 0.999092	end of isolation L I / II ?	Eronen et al 1993	
155	125	Torrträsk	Tenhola	60° 08'	23° 1' 3"	35.3	35.56	5770	70	GrN-19652	5770	70	-4620	-4704:-4543	-4778:-4461	-4704:-4544 1	-4778:-4462 1	beginning of isolation	Eronen et al 1993	
156	125	Torrträsk	Tenhola	60° 08'	23° 1' 3"	35.3	35.56	5670	70	GrN-19651	5670	70	-4509	-4600:-4400	-4684:-4360	-4600:-4447 0.927194 -4418:-4402 0.069114 -4377:-4376 0.003692	-4684:-4631 0.090447 -4624:-4362 0.909553	end of isolation L II	Eronen et al 1993	
157	126	Kollarinjärvi	Perniö	60° 12'	23° 2' 0"	35.0	35.26	6080	70	GrN-19639	6080	70	-5000	-5201:-4850	-5211:-4808	-5202:-5176 0.095446 -5070:-4897 0.85463 -4866:-4851 0.049925	-5212:-4832 0.996409 -4812:-4808 0.003591	beginning of isolation	Eronen et al 1993	
158	126	Kollarinjärvi	Perniö	60° 12'	23° 2' 0"	35.0	35.26	5950	70	GrN-19638	5950	70	-4835	-4931:-4727	-5023:-4685	-4931:-4922 0.042077 -4910:-4767 0.85229 -4755:-4741 0.067514 -4736:-4728 0.038119	-5021:-4686 1	end of isolation Litorina II / III	Eronen et al 1993	
159	127	Lassilansuo	Pohja	60° 07'	23° 2' 7"	33.0	33.26	5930	70	GrN-19641	5930	70	-4811	-4897:-4720	-4996:-4617	-4899:-4865 0.169236 -4853:-4721 0.830764	-4997:-4669 0.983753 -4659:-4655 0.002857 -4638:-4618 0.01339	beginning of isolation	Eronen et al 1993	
160	127	Lassilansuo	Pohja	60° 07'	23° 2' 7"	33.0	33.26	5750	70	GrN-19640	5750	70	-4600	-4688:-4523	-4776:-4452	-4689:-4526 1	-4777:-4774 0.001386 -4770:-4752 0.015775 -4746:-4453 0.982839	end of isolation Litorina III	Eronen et al 1993	
161	128	Notträsk	Tenhola	60° 08'	23° 1' 5"	29.5	29.76	5170	70	GrN-19643	5170	70	-3979	-4048:-3808	-4227:-3793	-4049:-3936 0.756481 -3872:-3810 0.243519	-4228:-4200 0.035869 -4170:-4127 0.058489 -4122:-4091 0.027862 -4081:-3794 0.87778	beginning of isolation	Eronen et al 1993	
162	128	Notträsk	Tenhola	60° 08'	23° 1' 5"	29.5	29.76	5045	45	GrN-19642	5045	45	-3859	-3941:-3787	-3956:-3712	-3942:-3855 0.682018 -3845:-3834 0.063644 -3822:-3788 0.254339	-3957:-3758 0.940974 -3743:-3713 0.059026	end of isolation Litorina III	Eronen et al 1993	

Appendix 1

163	129	Lillträsk	Tenhola	60° 05'	23°1 5'	24.7	24.96	4460	50	GrN-19942	4460	50	-3169	-3328:-3025	-3346:-2935	-3329:-3216 0.53452 -3181:-3158 0.097669 -3124:-3083 0.18814 -3067:-3027 0.179671	-3347:-3009 0.948553 -2981:-2936 0.051447	beginning of isolation	Eronen et al 1993	
164	129	Lillträsk	Tenhola	60° 05'	23°1 5'	24.7	24.96	4370	35	GrN-19941	4370	35	-2981	-3015:-2920	-3089:-2905	-3016:-2922 1	-3090:-3044 0.139971 -3035:-2906 0.860029	end of isolation L IV	Eronen et al 1993	
165	130	Gulltjärnen	Tammisaari	59° 59'	23°2 2'	24.2	24.46	4390	60	GrN-19646	4390	60	-3028	-3092:-2916	-3329:-2895	-3092:-2918 1	-3330:-3216 0.163185 -3183:-3157 0.027474 -3125:-2896 0.809341	beginning of isolation	Eronen et al 1993	
166	130	Gulltjärnen	Tammisaari	59° 59'	23°2 2'	24.2	24.46	4350	60	GrN-19645	4350	60	-2986	-3080:-2900	-3320:-2877	-3079:-3070 0.051056 -3025:-2902 0.948944	-3321:-3272 0.026854 -3266:-3236 0.028004 -3171:-3162 0.003998 -3115:-2878 0.941145	end of isolation L IV	Eronen et al 1993	
167	131	Hästönlampi	Perniö	60° 08'	23°0 4'	20.3	20.57	3900	70	GrN-19944	3900	70	-2376	-2473:-2285	-2571:-2149	-2475:-2286 0.993445 -2246:-2245 0.006555	-2571:-2513 0.073356 -2503:-2198 0.915645 -2166:-2150 0.010998	beginning of isolation	Eronen et al 1993	
168	131	Hästönlampi	Perniö	60° 08'	23°0 4'	20.3	20.57	3825	50	GrN-19943	3825	50	-2280	-2399:-2151	-2460:-2140	-2400:-2382 0.072416 -2347:-2199 0.895483 -2161:-2153 0.032101	-2461:-2189 0.91017 -2181:-2141 0.08983	end of isolation L V	Eronen et al 1993	
169	132	Puontpyölinjärvi	Tenhola	60° 05'	23°1 0'	18.2	18.46	3720	70	GrN-17287	3720	70	-2120	-2270:-1983	-2340:-1919	-2270:-2259 0.032529 -2206:-2023 0.941671 -1991:-1984 0.0258	-2340:-2313 0.014489 -2310:-1920 0.985511	beginning of isolation	Eronen et al 1993	
170	132	Puontpyölinjärvi	Tenhola	60° 05'	23°1 0'	18.2	18.46	3580	70	GrN-17286	3580	70	-1932	-2030:-1779	-2134:-1745	-2031:-1876 0.85289 -1842:-1820 0.084186 -1797:-1781 0.062924	-2135:-2077 0.079204 -2073:-2069 0.003107 -2064:-1746 0.917688	end of isolation L V	Eronen et al 1993	
171	133	Rombyträsket	Tenhola	60° 01'	23°1 5'	15.6	15.86	3310	60	GrN-19650	3310	60	-1590	-1665:-1515	-1738:-1452	-1664:-1649 0.090322 -1643:-1518 0.909678	-1739:-1706 0.050869 -1698:-1487 0.90745 -1484:-1454 0.041682	beginning of isolation	Eronen et al 1993	Eronen et al. 2001 OxCal v3.10 3460:3620 cal BP
172	133	Rombyträsket	Tenhola	60° 01'	23°1 5'	15.6	15.86	3190	60	GrN-19649	3190	60	-1467	-1520:-1409	-1616:-1315	-1520:-1411 1	-1615:-1372 0.968042 -1344:-1317 0.031958	end of isolation L VI	Eronen et al 1993	Eronen et al. 2001 v3.10 3350:3470 cal BP
173	134	Gundbyträsket	Tenhola	59° 59'	23°1 0'	14.3	14.56	3090	60	GrN-19648	3090	60	-1353	-1429:-1292	-1495:-1134	-1429:-1294 1	-1496:-1208 0.992659 -1202:-1195 0.004311 -1139:-1135 0.003029	beginning of isolation	Eronen et al 1993	
174	134	Gundbyträsket	Tenhola	59° 59'	23°1 0'	14.3	14.56	2940	60	GrN-19647	2940	60	-1156	-1258:-1051	-1372:-977	-1258:-1232 0.13028 -1218:-1053 0.86972	-1373:-1342 0.024924 -1318:-978 0.975076	end of isolation L VI	Eronen et al 1993	

Appendix 1

175	135	Dotterböl eträsket	Tammi- saari	60° 00'	23°1 8'	8.8	9.06	1650	60	GrN- 19644	1650	60	400	264: 531	256: 541	264:276 0.0548 332:438 0.736086 487:531 0.209113	254:541 1	beginning of isolation ?	Eronen et al 1993	
176	135	Dotterböl eträsket	Tammi- saari	60° 00'	23°1 8'	8.8	9.06	2400	60	GrN- 19826	2400	60	-512	-727: -397	-755: -388	-728:-693 0.152669 -658:-654 0.016151 -542:-398 0.831179	-756:-684 0.179955 -669:-606 0.106298 -604:-389 0.713747	end of isolation L VII ?	Eronen et al 1993	
177	136	Skogsböl eträsket	Tenhola	60° 02'	23°1 1'	7.3	7.56	2990	70	GrN- 17288	2990	70	-1225	-1369: -1125	-1406: -1025	-1370:-1346 0.089935 -1316:-1126 0.910065	-1407:-1024 1	beginning of isolation	Eronen et al 1993	
178	136	Skogsböl eträsket	Tenhola	60° 02'	23°1 1'	7.3	7.56	2420	80	GrN- 17289	2420	80	-551	-746: -400	-774: -387	-747:-688 0.232231 -665:-645 0.075123 -588:-581 0.023276 -554:-401 0.66937	-775:-388 1	end of isolation L VII / VIII	Eronen et al 1993	
179	137	Hangas- suo	Anjalan- koski	60° 47'	26°5 5'	47	47.22	9510	200	Hel- 663	9470	200	-8818	-9142: -8568	-9279: -8299	-9143:-8966 0.30271 -8961:-8567 0.69729	-9273:-8301 1	isolation late Yoldia	Eronen 1976	
180	137	Hangas- suo	Anjalan- koski	60° 47'	26°5 5'	47	47.22	9280	190	Hel- 661	9210	200	-8465	-8749: -8234	-9151: -7871	-8750:-8233 1	-9138:-8970 0.054265 -8945:-7936 0.930201 -7927:-7916 0.002302 -7899:-7836 0.013232	beginning of Ancyclus transgression	Eronen 1976	
181	137	Hangas- suo	Anjalan- koski	60° 47'	26°5 5'	47	47.22	8870	170	Hel- 660	8800	180	-7921	-8201: -7680	-8313: -7529	-8202:-8107 0.196434 -8094:-8038 0.113535 -8011:-7705 0.658928 -7698:-7681 0.031103	-8305:-7529 1	end of Ancyclus transgression	Eronen 1976	
182	138	Mannilan- lahti	Eura	61° 01'	22°1 1'	45	45.32	5580	120	Hel- 1393	5510	130	-4353	-4513: -4178	-4678: -4041	-4503:-4231 0.969505 -4192:-4178 0.030495	-4676:-4676 0.000401 -4668:-4660 0.00371 -4654:-4638 0.006566 -4618:-4041 0.98851 -4008:-4005 0.000812	beginning of isolation Litorina	Eronen et al 1982	
183	138	Mannilan- lahti	Eura	61° 01'	22°1 1'	45	45.32	5680	120	Hel- 1392	5610	130	-4462	-4599: -4334	-4783: -4172	-4600:-4335 1	-4781:-4229 0.988635 -4198:-4171 0.009854 -4088:-4083 0.001511	beginning of isolation Litorina	Eronen et al 1982	
184	139	Musta- lampi	Espoo	60° 17'	24°3 9'	61.4	61.65	1013 0	190	Hel- 1226	10060	200	-9721	-10019: -9324	-	-10019:-9915 0.142605 -9889:-9325 0.857395	-10616:-10552 0.008969 -10447:-9155 0.991031	isol late Yoldia too old age	Eronen & Haila 1982	too old age
185	139	Musta- lampi	Espoo	60° 17'	24°3 9'	61.4	61.65	9780	200	Hel- 1225	9710	210	-9127	-9392: -8755	-	-9384:-8753 1	-9872:-8540 0.996632 -8508:-8488 0.003368	beginning of Ancyclus transgression	Eronen & Haila 1982	
186	139	Musta- lampi	Espoo	60° 17'	24°3 9'	61.4	61.65	9490	180	Hel- 1224	9420	190	-8748	-9125: -8470	-9236: -8297	-9125:-8998 0.202355 -8923:-8528 0.72515 -8520:-8471 0.072494	-9234:-8297 1	Ancyclus transgression	Eronen & Haila 1982	
187	139	Musta- lampi	Espoo	60° 17'	24°3 9'	61.4	61.65	9410	170	Hel- 1223	9340	180	-8633	-8810: -8305	-9194: -8257	-8809:-8306 1	-9194:-8251 1	end of Ancyclus transgression	Eronen & Haila 1982	
188	140	Laiha- lampi	Espoo	60° 15'	24°3 6'	56.8	57.05	1010 0	210	Hel- 1285	10030	220	-9685	-10022: -9295	-	-10022:-9911 0.13734 -9893:-9295 0.86266	-10622:-10541 0.01184 -10449:-9119	isol late Yoldia too old age	Eronen & Haila 1982	too old age

Appendix 1

218	167	Tuorilampi	Merikarvia	61°53'	21°37'	29.3	29.69	2830	100	Hel-1945	2760	110	-942	-1043:-805	-1291:-668	-1041:-807 1	-4081:-3646 0.931332 -1289:-1282 0.001429 -1269:-754 0.990467 -685:-668 0.005389 -609:-598 0.002715	isol Litorina	Salomaa & Matiskainen 1983
219	168	Kalliojärvi	Merikarvia	61°58'	21°40'	47.7	48.09	4610	110	Hel-1947	4540	120	-3235	-3494:-3027	-3625:-2916	-3494:-3466 0.065754 -3375:-3085 0.860011 -3063:-3029 0.074235	-3626:-3599 0.017285 -3525:-2917 0.982715	isol Litorina	Salomaa & Matiskainen 1983
220	169	Hälltingträsk	Sipoo	60°16'	25°14'	30.7	30.95	6010	110	Hel-1831	5940	120	-4829	-4987:-4689	-5206:-4540	-4988:-4690 1	-5207:-5158 0.026828 -5154:-5149 0.001624 -5137:-5129 0.003309 -5120:-5095 0.010588 -5080:-4537 0.957651	isol late Ancyclus ?	Sarmaja-Korjonen 1992
221	170	Junki	Lohtaja	64°01'	23°26'	8.5	8.93	910	100	Hel-1851	870	100	1150	1045:1253	979:1295	1044:1098 0.289467 1119:1142 0.11727 1147:1252 0.593263	982:1294 1	isol late Litorina	Alestalo 1983 unpublished?
222	171	Kankareenjärvi	Halikko	60°26'	23°00'	88	88.28	8860	180	Hel-1940	8790	190	-7913	-8198:-7650	-8418:-7510	-8199:-8110 0.175534 -8093:-8072 0.040268 -8065:-8040 0.050033 -8003:-7651 0.734165	-8332:-7495 1	isol early Ancyclus	Tolonen 1987
223	172	Väiskänso	Laitila	60°55'	21°42'	18	18.32	2960	140	Hel-581	2890	150	-1102	-1289:-905	-1438:-797	-1288:-1283 0.012494 -1269:-906 0.987506	-1438:-797 1	isol late Litorina	Tolonen et al 1976
224	173	Pärkönsuo	Laitila	60°51'	21°40'	14	14.32	2310	110	Su-437	2310	110	-390	-536:-201	-765:-111	-537:-528 0.018918 -524:-202 0.981082	-764:-679 0.092458 -674:-150 0.891165 -140:-112 0.016377	isol late Litorina	Tolonen et al 1976
225	174	Kotasuo	Espoo	60°15'	24°35'	38.7	38.95	7960	160	Hel-2260	7890	170	-6805	-7035:-6606	-7294:-6435	-7035:-6627 0.964526 -6625:-6608 0.035474	-7294:-7269 0.007081 -7258:-7225 0.009226 -7191:-6432 0.983693	isol late Ancyclus	Korhola 1990
226	175	Punassuo	Perniö	60°13'	23°02'	46.8	47.07	7190	120	Hel-2760	7190	120	-6067	-6214:-5929	-6361:-5813	-6215:-5983 0.974424 -5939:-5931 0.025576	-6358:-6291 0.035239 -6269:-5833 0.956267 -5829:-5809 0.008494	isol late Ancyclus	Korhola 1992
227	176	Munasuo	Pyhtää	60°34'	26°40'	16.8	17.02	4360	90	Hel-2808	4220	100	-2786	-2915:-2631	-3089:-2493	-2915:-2832 0.322829 -2820:-2658 0.619867 -2653:-2633 0.057304	-3089:-3049 0.019597 -3032:-2563 0.957956 -2534:-2493 0.022447	isol Litorina	Korhola 1992
228	177	Pieni Majaslampi	Espoo	60°19'	24°36'	97.3	97.56	9630	130	Hel-2705	9630	130	-9004	-9229:-8835	-9300:-8637	-9230:-9109 0.33253 -9088:-9037 0.129518 -9033:-8836 0.537952	-9299:-8696 0.978863 -8683:-8639 0.021137	isol Yoldia	Korhola & Tikkanen 1991
229	178	Järvenpäänsuo	Utajärvi	64°50'	26°40'	99	99.36	7330	150	Hel-679	7290	150	-6165	-6350:-6015	-6444:-5889	-6352:-6309 0.113699 -6264:-6014 0.886301	-6444:-5887 1	isol Litorina	Holappa 1976
230	179	Kiimisuo	Hailuoto	65°02'	24°42'	10.6	11.02	950	130	Hel-1595	910	130	1113	1019:1252	784:1384	1019:1228 0.959054 1232:1241 0.027301 1247:1251 0.013645	785:786 0.000325 828:838 0.003421 866:1306 0.986889 1363:1385 0.009366	isol Litorina	Rönkä 1983
231	180	Vähäjärvi N	Eura	61°09'	22°12'	64.2	64.53	6500	40	GrN-20902	6500	40	-5469	-5512:-5381	-5534:-5368	-5512:-5466 0.630874 -5440:-5423 0.133555	-5534:-5370 1	beginning of isolation	Eronen et al 1995a

Appendix 1

				05'	2'					21024				-1615	-1530	-1694:-1617 0.821116	-1593:-1531 0.12651	Litorina	1995a		
247	188	Tuitinjärvi	Rauma	61° 07'	21° 38'	20.4	20.74	3300	35	GrN- 20908	3300	35	-1575	-1615: -1526	-1676: -1498	-1615:-1528 1	-1678:-1675 0.004775 -1669:-1499 0.995225	beginning of isolation	Eronen et al 1995a		
248	188	Tuitinjärvi	Rauma	61° 07'	21° 38'	20.4	20.74	2970	30	GrN- 20907	2970	30	-1202	-1260: -1129	-1309: -1056	-1261:-1189 0.67176 -1180:-1157 0.196458 -1145:-1130 0.131782	-1310:-1111 0.975114 -1101:-1081 0.018581 -1065:-1057 0.006306	end of isolation Litorina	Eronen et al 1995a		
249	189	Tarvolan- järvi	Rauma	61° 06'	21° 35'	18	18.34	2770	30	GrN- 21027	2770	30	-914	-972: -846	-996: -837	-973:-958 0.158459 -938:-893 0.588864 -875:-848 0.252677	-997:-839 1	beginning of isolation	Eronen et al 1995a		
250	189	Tarvolan- järvi	Rauma	61° 06'	21° 35'	18	18.34	2540	30	GrN- 21026	2540	30	-677	-792: -593	-797: -544	-793:-751 0.511327 -686:-667 0.229435 -637:-621 0.101498 -614:-594 0.157739	-797:-735 0.412299 -690:-662 0.185593 -649:-546 0.402107	end of isolation Litorina	Eronen et al 1995a		
251	190	Monnan- järvi	Rauma	61° 06'	21° 33'	14	14.34	2320	40	GrN- 21023	2320	40	-390	-410: -259	-513: -210	-411:-360 0.928496 -273:-261 0.071504	-511:-353 0.827063 -293:-229 0.167735 -219:-213 0.005202	beginning of isolation	Eronen et al 1995a		
252	190	Monnan- järvi	Rauma	61° 06'	21° 33'	14	14.34	2180	40	GrN- 21022	2180	40	-267	-355: -176	-378: -113	-356:-286 0.581356 -252:-250 0.010777 -234:-177 0.407866	-378:-154 0.966974 -136:-114 0.033026	end of isolation Litorina	Eronen et al 1995a		
253	191	Pyytjärvi	Rauma	61° 09'	21° 30'	9.6	9.94	1655	40	GrN- 20910	1655	40	394	267: 433	259: 534	267:271 0.019215 335:432 0.980785	259:296 0.083887 321:466 0.793667 481:533 0.122445	beginning of isolation	Eronen et al 1995a		
254	191	Pyytjärvi	Rauma	61° 09'	21° 30'	9.6	9.94	1515	40	GrN- 20909	1515	40	552	443: 606	432: 624	443:449 0.036741 462:483 0.134465 533:605 0.828794	432:623 1	end of isolation Litorina	Eronen et al 1995a		
255	192	Koijärvi	Rauma	61° 04'	21° 33'	8.8	9.14	1870	30	GrN- 21021	1870	30	137	83: 211	74: 227	82:140 0.667865 150:170 0.183505 194:210 0.14863	73:226 1	beginning of isolation	Eronen et al 1995a		
256	192	Koijärvi	Rauma	61° 04'	21° 33'	8.8	9.14	1645	25	GrN- 21020	1645	25	406	356: 431	336: 533	358:362 0.032441 382:429 0.967559	335:441 0.902504 455:460 0.005685 485:531 0.091811	end of isolation Litorina	Eronen et al 1995a		
257	193	Olkiluo- donjärvi	Eurajoki	61° 14'	21° 30'	1.5	1.85	260	50	GrN- 20912	260	50	1638	1522: 1952	1482: 1955	1521:1576 0.367972 1582:1591 0.041115 1622:1669 0.428652 1780:1798 0.132196 1945:1950 0.030065	1483:1683 0.769221 1735:1805 0.184086 1930:1951 0.046692	beginning of isolation	Eronen et al 1995a		
258	193	Olkiluodo njärvi	Eurajoki	61° 14'	21° 30'	1.5	1.85	410	50	GrN- 20911	410	50	1491	1436: 1618	1421: 1635	1436:1515 0.838008 1599:1617 0.161992	1421:1529 0.685364 1544:1548 0.004634 1550:1634 0.310002	end of isolation Litorina	Eronen et al 1995a		
259	194	Pasko- lampi	Ylikiimin ki	65° 05'	26° 15'	82.8	83.18	5520	140	Hel- 3626	5520	140	-4364	-4537: -4180	-4684: -4043	-4535:-4232 0.984527 -4188:-4181 0.015473	-4685:-4628 0.031339 -4625:-4043 0.968661	isol Litorina	Hellsten 1995 unpublished		
260	194	Pasko- lampi	Ylikiimin ki	65° 05'	26° 15'	82.8	83.18	5520	130	Hel- 3627	5520	130	-4365	-4518: -4234	-4680: -4045	-4518:-4235 1	-4678:-4673 0.002812 -4670:-4658 0.005281 -4655:-4637 0.008611 -4619:-4045 0.983297	isol Litorina	Hellsten 1995 unpublished		

Literature references by Eronen et al. (1995)

References in Eronen et al. (1995 Appendix 5 Literature values). The question marks and other remarks are in the report itself, except for Eronen et al. 1995a, which may be a re-publication.

References (to the radiocarbon-dated shore-level data base of the Baltic in Finland 1966–1995).

- Alestalo 1983 Alestalo, J. 1983. Not published (?), see Jungner & Sonninen 1989.
- Alhonen 1969 Alhonen, P. 1967. Palaeolimnological investigations of three inland lakes in south-western Finland. *Acta Botanica Fennica* 76, edit Societas pro Fauna et Flora Fennica, 59 pp.
- Alhonen 1972 Alhonen, P. 1972. Gallträsket: The geological development and palaeolimnology of a small polluted lake in southern Finland. *Soc. Sci. Fennica, Comm. Biol.* 57, 34 pp.
- Alhonen 1981 Alhonen, P. 1981. Stratigraphical studies on Lake Iidesjärvi sediments. Part I: Environmental changes and palaeolimnological development. *Bull. Geol. Soc. Finland* 53, 2, pp. 97-107.
- Alhonen et al.
1978 Alhonen, P., Eronen, M., Nunez, M., Salomaa, R. & Uusinoka, R. 1978. A contribution to Holocene shore displacement and environmental development in Vantaa, South Finland: the stratigraphy of Lake Lammaslampi. *Bull. Geol. Soc. Finland*, 50, pp. 69-79.
- Donner &
Eronen 1981 Donner, J. & Eronen, M. 1981. Stages of the Baltic Sea and late Quaternary shoreline displacement in Finland. Excursion Guide. INQUA, Subcommission on shorelines of northwestern Europe. Excursion in southern Finland with a symposium at Lammi Biological Station 9-14 Sept. 1981. Univ. of Helsinki, Dept. of Geology, Division of Geol. and Paleontology. Stencil No. 5. Helsinki 1981. 53 pp.
- Ekman 1989 Ekman, M. 1989. Impacts of geodynamic phenomena on systems for height and gravity. *Bulletin Géodésique* 63, pp. 281-296.
- Ekman 1993 Ekman, M. 1993. Postglacial rebound and sea level phenomena, with special reference to Fennoscandia and the Baltic Sea. *Publications of the Finnish Geodetic Institute* 115, pp. 7-70.
- Eronen 1974 Eronen, M. 1974. The history of the Litorina Sea and associated Holocene events. *Soc. Sci. Fennica, Comm. Phys.-Meth.* 44,

- 4, p. 79-195.
- Eronen 1976 Eronen, M. 1976. A radiocarbon-dated Ancylus transgression site in southeastern Finland. *Boreas* 5, pp. 65-76.
- Eronen 1983 Eronen, M. 1983. Late Weichselian and Holocene shore displacement in Finland. In: Smith, D.E. & Dawson, A.G. (eds.). *Shorelines and Isostasy*. Academic Press, pp. 183-207.
- Eronen & Haila 1982 Eronen, M. & Haila, H. 1982. Shoreline displacement near Helsinki, southern Finland, during the Ancylus Lake stage. *Ann. Acad. Sci. Fennicae, Ser. A III*, 134, pp. 111-129.
- Eronen et al. 1982 Eronen, M., Heikkinen O. & Tikkanen, M. 1982. Holocene development and present hydrology of Lake Pyhäjärvi in Satakunta, southwestern Finland. *Fennia* 160, 2. pp. 195-223.
- Eronen & Ristaniemi 1992 Eronen, M. & Ristaniemi, O. 1992. Late Quarternary crustal deformation and coastal changes in Finland. *Quarternary International* 15/16, pp. 175-184.
- Eronen et al. 1995a Eronen, M., Glückert, G., van der Plassche, O., van der Plicht, J., Rajala, P. & Rantala, P. 1995. The postglacial radiocarbon dated shoreline data of the Baltic in Finland for the Nordic data of land uplift and shorelines. A NKS/KAN 3 project report, Stockholm (in press). (*Probably same as the study published in 1993 already.*)
- Glückert 1970 Glückert, G. 1970. Vorzeitliche Uferentwicklung am Ersten Salpausselkä in Lohja, Südfinnland. *Ann. Univ. Turkuensis, Ser. A II*, 45, 116 pp.
- Glückert 1976 Glückert, G. 1976. Post-Glacial shore-level displacement of the Baltic in SW Finland. *Ann. Acad. Sci. Fennicae, Ser. A III*, 118, 92 pp.
- Glückert 1978a Glückert, G. 1978a. Östersjöns postglaciala strandförskjutning och skogens historia på Åland. *Publ. Dept. Quarternary Geol., Univ. Turku*, 34, 106 pp.
- Glückert 1978b Glückert, G. 1978b. Das Deltakomplex von Kiikalannummi am 3. Salpausselkä in Südwestfinnland. *Publ. Dept. Quarternary Geol., Univ. Turku*, 35, 26 pp.
- Glückert 1979 Glückert, G. 1979. Shore-level displacement of the Baltic and the history of vegetation in the Salpausselkä belt, western

- Uusimaa, South Finland. Publ. Dept. Quarternary Geol., Univ. Turku, 39, 77 p.
- Glückert & Ristaniemi 1980 Glückert, G. & Ristaniemi, O. 1980. The Ancyclus transgression in the area of Karjalohja, 2nd Salpausselkä, South Finland. Publ. Dept. Quarternary Geol., Univ. Turku, 41, 22 p.
- Glückert & Ristaniemi 1982 Glückert, G. & Ristaniemi, O. 1982. The Ancyclus transgression west of Helsinki, South Finland - a preliminary report. Ann. Acad. Sci. Fennicae, Ser. A III, 134, pp. 99-110.
- Glückert 1989 Glückert, G. 1989. Shore-level displacement of the Baltic, and the development of forests, settlement and agriculture on the island of Kumlinge, the Åland Islands, SW Finland. Publ. Dept. Quarternary Geol., Univ. Turku, 61, 10 pp.
- Glückert 1991 Glückert, G. 1991. The Ancyclus and Litorina transgressions of the Baltic in southwest Finland. Quarternary International, Vol 9, pp. 27-32.
- Glückert et al 1992 Glückert, G., Illmer, K., Kankainen, T., Rantala, P. & Räsänen, M. 1992. Vegetational history in the surroundings of Lake Littoinen and its natural dystrofication. Publ. Dept. Quarternary Geol., Univ. Turku, 75, 27 pp.
- Glückert et al. 1993 Glückert, G., Rantala, P. & Ristaniemi, O. 1993. Postglacial shore-level displacement of the Baltic in Ostrobothnia. Publ. Dept. Quarternary Geol., Univ. Turku (manuscript).
- Haila 1987 Haila, H. 1987. Ancyclus-transgression ikä Etelä-Suomessa; mallialtaan tutkimustuloksia ja rannansiirtymisen erityiskysymyksiä. Unpubl. Lis. Phil. thesis. Dept. of Geology, Univ. Helsinki.
- Haila et al. 1991 Haila, H., Sarmaja-Korjonen, K. & Uutela, A. 1991. Development of a Litorina bay at Epoo, near Porvoo, southern Finland. Bull. Geol. Soc. Finland 63, 2, pp. 105-119.
- Hjelmroos 1979 Hjelmroos, M. 1979. Den äldsta bosättningen i Tornedalen. En paleoekologisk undersökning. Lundqua Report. Dept. Quarternary Geol., Univ. Lund, 60 pp.
- Holappa 1976 Holappa, K. 1976. Utajärven Järvenpäänsuon kehityksestä ja stratigrafiasta. Unpublished M.Sc. thesis. Univ. Oulu, Dept. of Geology.
- Hyvärinen 1966 Hyvärinen, H. 1966. Studies on the late-Quarternary history of Pielis-Karelia, eastern Finland. Soc. Scient. Fennica. Comment

Biol. 29, 4, 72 pp.

- Hyvärinen 1979 Hyvärinen, H. 1979. Bakunkäärsträsket: a stratigraphical site relevant to the Litorina shore displacement near Helsinki. *Terra* 91, 1, pp. 15-20.
- Hyvärinen 1980 Hyvärinen, H. 1980. Relative sea-level changes near Helsinki, southern Finland, during early Litorina times. *Bull. Geol. Soc. Finland* 52, 2, pp. 207-219.
- Hyvärinen 1982 Hyvärinen, H. 1982. Interpretation of stratigraphical evidence of sea-level history - A Litorina site near Helsinki, southern Finland. *Ann. Acad. Sci. Fennicae, Ser. A III*, 134, pp. 139-149.
- Hyvärinen 1984 Hyvärinen, H. 1984. The Mastogloia stage in the Baltic Sea history: Diatom evidence from southern Finland. *Bull. Geol. Soc. Finland*, 56, 1-2, pp. 99-115.
- Hyypä 1968 Hyypä, E. 1968 (not published?)
- Häikiö 1975 Häikiö, J. 1975 (not published?)
- Ikonen 1993 Ikonen, L. 1993. Holocene development and peat growth of the raised bog Pesänsuo in southwestern Finland. *Geol. Survey of Finland*, 370, 58 pp.
- Jungner 1979 Jungner, H. 1979. Radiocarbon dates I. Radiocarbon dating laboratory, University of Helsinki. Report no. 1, 1-131.
- Jungner & Sonninen 1983 Jungner, H. & Sonninen, E. 1983. Radiocarbon dates II. Radiocarbon dating laboratory, University of Helsinki. Report no. 2, 1-121.
- Jungner & Sonninen 1989 Jungner, H. & Sonninen, E. 1989. Radiocarbon dates III. Radiocarbon dating laboratory, University of Helsinki. Report no. 3, 1-79.
- Kakkuri 1987 Kakkuri, J. 1987. Character of the Fennoscandian land uplift in the 20th century. In: Perttunen, M. (ed.): Fennoscandian land uplift. Geological Survey of Finland, Special Paper 2, 1-61.
- Korhola 1990 Korhola, A. 1980. Palaeolimnology and hydrseral development of the Kotasuo bog, Southern Finland, with special reference

- to the Cladocera. *Ann. Acad. Sci. Fennica*, A III, 155, pp. 1-40.
- Korhola 1992 Korhola, A. 1992. Mire induction, ecosystem dynamics and lateral extension on raised bogs in the southern coastal area of Finland. *Fennia* 170, 2, pp. 25-94.
- Korhola & Tikkanen 1991 Korhola, A. & Tikkanen, M. 1991. Holocene development and early extreme acidification in a small hilltop lake in southern Finland. *Boreas* 20, pp. 333-356.
- Kääriäinen 1953 Kääriäinen, E. 1953. On the recent uplift of the Earth's crust in Finland. *Fennia* 77, 2, pp. 1-106.
- Kääriäinen 1966 Kääriäinen, E. 1966. Land uplift in Finland as computed with the aid of precise levellings. *Proc. of the Second International Symposium on Recent Crustal Movements*. Aulanko, Finland, August 3-7, 1965. *Ann. Acad. Sci. Fennicae*, A III, 90, pp. 187-190.
- Kääriäinen 1975 Kääriäinen, E. 1975. Land uplift in Finland on the basis of sea level recordings. *Report 75*, 5. *Finn. Geod. Inst.*, pp. 1-14.
- Leino 1973 Leino, J. 1973. Eräiden umpeenkasvusoiden turveolosuhteista Salon ympäristössä. Unpublished M.Sc. thesis, Dept. Quarternary Geol., Univ. Turku, 65 pp.
- Matiskainen 1989a Matiskainen, H. 1989a. The chronology of the Finnish mesolithic. In: Clive Bonsall (ed.): *The mesolithic in Europe*, III Int. Mesol. Symp. Edinburgh 1988, pp. 379-390.
- Matiskainen 1989b Matiskainen, H. 1989b. The palaeoenvironment in Askola, southern Finland. Mesolithic settlement and subsistence 10000-6000 BP. *Iskos* 8, 97 pp.
- Pearson & Stuiver 1993 Pearson, G.W. & Stuiver, M. 1993. High-precision bidecadal calibration of the radiocarbon time scale, 500-2500 BC. *Radiocarbon*, Vol. 35, No. 1, 25-34.
- Reynaud & Hjelmroos 1980 Reynaud, C. & Hjelmroos, M. 1980. ?. *Candollea* 35, pp. 257-304.
- Ristaniemi 1984 Ristaniemi, O. 1984. Shoreline displacement of the Baltic during the Ancylus stage in the Karjalohja-Kisko area, the Salpausselkä belt, SW-Finland. *Publ. Dept. Quarternary Geol., Univ. Turku*, 53, 75 pp.

- Ristaniemi 1987 Ristaniemi, O. 1987. The highest shore and Ancyclus limit of the Baltic Sea and the ancient Lake Päijänne in central Finland. *Ann. Univ. Turkuensis, Ser. C*, 59, 102 pp.
- Ristaniemi & Glückert 1987 Ristaniemi, O. & Glückert, G. 1987. The Ancyclus transgression in the area of Espoo - the First Salpausselkä, southern Finland. *Bull. Geol. Soc. Finland* 59, 1, pp. 45-69.
- Ristaniemi & Glückert 1988 Ristaniemi, O. & Glückert, G. 1988. Ancyclus- ja Litorinatransgressiot Lounais-Suomessa. In: Lappalainen, V. & Papunen, H. (eds.): *Tutkimuksia geologian alalta*. *Ann. Univ. Turkuensis, Ser. C*, 67, pp. 129-145.
- Rönkä 1983 Rönkä, A. 1983. Hailuodon Kiimisuon paleoekologiasta. Unpubl. M.Sc. thesis, University of Oulu, Dept. of Botany.
- Saarnisto 1970 Saarnisto, M. 1970. The late Weichselian and Flandrian history of the Saimaa lake complex. *Soc. Sci. Fennica. Comment, Phys.-Math.* 37, 107 pp.
- Saarnisto 1979 Saarnisto, M. 1979. Deglaciation north of the Gulf of Bothnia. Abstract: Deglaciation yngre än 10000 BP, Uppsalasymposiet 1979, 1 p.
- Saarnisto 1981 Saarnisto, M. 1981. Holocene emergence history and stratigraphy in the area north of the Gulf of Bothnia. *Ann. Acad. Sci. Fennicae, Ser. A III*, 130, 42 pp.
- Salomaa 1982 Salomaa, R. 1982. Post-glacial shoreline displacement in the Lauhanvuori area, western Finland. *Ann. Acad. Sci. Fennicae, Ser. I, III*, 134, pp. 81-97.
- Salomaa & Matiskainen 1983 Salomaa, R., & Matiskainen, H. 1983. Rannansiirtyminen ja arkeologinen kronologia Etelä-Pohjanmaalla. *Arkeologian päivät 7-8.4.1983 Lammin biolog. tutkimusasemalla*. *Karhunhammas*, 7, pp. 21-36.
- Salonen et al. 1981 Salonen, V.-P., Ikäheimo, M. & Luoto, J. 1981. The activity of man in the Kuoppajärvi area of Piikkiö, SW Finland, in the light of palaeontology and archaeology. *Publ. Depth. Quarternary Geol., Univ. Turku*, 44, 23 pp.
- Salonen et al. 1984 Salonen, V.-P., Räsänen, M. & Terho, A. 1984. Palaeolimnology of ancient Lake Mätäjärvi. Third Nordic conference on the application of scientific methods in archaeology. Mariehamn, Åland, Finland, 8-11 October 1984. *Iskos* 5, pp. 233-288.

Appendix 1

- Sarmaja-Korjonen 1992 Sarmaja-Korjonen, K. 1992. Fine-interval pollen and charcoal analyses as tracers of early clearance periods in S Finland. *Acta Botanica Fennica*, 146, 75 pp.
- Stuiver & Pearson 1993 Stuiver, M. & Pearson, G.W. 1993. High-precision bidecadal calibration of the radiocarbon time scale, AD 1950 - 500 BC and 2500-6000 BC. *Radiocarbon*, Vol. 35, No. 1, 1-24.
- Suutarinen 1983 Suutarinen, O. 1983. Recomputation of land uplift values in Finland. *Reports of the Finnish Geodetic Institute*, 83:1, 17 pp.
- Tikkanen 1978 Tikkanen, M. 1978. (not published?)
- Tikkanen 1981 Tikkanen, M. 1981. Georelief, its origin and development in the coastal area between Pori and Uusikaupunki, south-western Finland. *Fennia* 159, 2, pp. 252-333.
- Tolonen et al. 1976 Tolonen, K., Siiriäinen, A. & Hirviluoto, A.-L. 1976. Iron Age cultivation in SW Finland. *Finskt Museum*, 66 pp.
- Tolonen & Tolonen 1988 Tolonen, K. & Tolonen, M. 1988. Synchronous pollen changes and traditional land use in south Finland, studied from three adjacent sites. A lake, a bog and a forest soil. In: Lang, G. & Schlüchter, C. (eds.): *Lake and River Environments During the last 15000 years*, pp. 83-97, Balkema, Rotterdam.
- Tolonen 1987 Tolonen, M. 1987. Vegetational history in coastal SW Finland studied on a lake and a peat bog by pollen charcoal analyses. *Annales Botanici Fennici*, 24, pp. 353-370.
- Tynni & Kukkonen 1969 Tynni, R. & Kukkonen, E. 1969. (not published?)
- Vesajoki 1980 Vesajoki, H. 1980. The development phases of Lake Höytiäinen in eastern Finland, and their contributions to the morphology and stratigraphy of the lake shores. *Publ. Univ. Joensuu, Ser. B II*, 14, 56 pp.
- Vermeer et al. 1988 Vermeer, M., Kakkuri, J., Mälkki, P., Kahma, K.K. & Leppäranta, M. 1988. Land uplift and sea level variability spectrum using fully measured monthly means of tide gauge readings. *Finnish Marine Research No. 256*, 75 p.

APPENDIX 2. CODES USED

ArcGIS Desktop 9.2 and 9.3 with Topo to Raster (Spatial Analyst and 3D Analyst tool), Surface Spot (3D Analyst tool), Make NetCDF Raster Layer (Multidimension Tools), Geostatistical Wizard (Geostatistical Analyst Toolbar).

MS Excel 2002, with Solver Add-In and XY Chart Labeler.

CALIB Version 5.0.1 for the PC with intcal04.14c dataset for Northern Hemisphere Atmosphere, and the related MS Excel table for $\delta^{13}\text{C}$ isotope fractionation correction.

OxCal 4.0 with intcal04 (version 14c) dataset for Northern Hemisphere Atmosphere

Blaauw's (2008) MS Excel ^{14}C calibration application version, modified from the original code (Blaauw et al. 2003). Uses IntCal04.

ERDAS IMAGINE 9.2 and 9.3 for raster processing and Coordinate Calculator

APPENDIX 3. AGE CALIBRATION PRACTICES FOR LAKES AND PEATS

Table 8. Finding out for which old data the $\delta^{13}\text{C}$ corrections had been done.

Lab code / Eronen et al. (1995)	Date $\delta^{13}\text{C}$ corrections
Hel-	For most of the Eronen et al. (1995) dating with code Hel-, the year BP and \pm Error had not been $\delta^{13}\text{C}$ corrected, so the study asked for the corrected values from the Dating Laboratory of the University of Helsinki. The laboratory was not able to measure the $\delta^{13}\text{C}$ values before 1987. The corrections are typically only about 0.5 % for peats, but larger than the difference between values due to various calibration applications (Oinonen 2008). Small corrections like 0.5 % are due to peat's -27‰ being almost the -25‰ used for normalisation. For example Hel-717 gives a bit different results than CALIB because it has been registered as "mud" instead of "peat", and the average $\delta^{13}\text{C}$ of all "mud" samples in the laboratory is -28.9 \pm 6‰ and of "peat" samples is -27.2 \pm 1.6‰, which corresponds to the CALIB correction value -27 \pm 3‰. Generally, the Helsinki laboratory made the $\delta^{13}\text{C}$ corrections of all its own samples based on these categories and mean values. OxCal calibrations were done not only for the Hel laboratory samples but also the I, St, T, and TKU samples, but based on the CALIB $\delta^{13}\text{C}$ corrections made at Pöyry Environment Oy. Otherwise in this project, CALIB's $\delta^{13}\text{C}$ correction table was used, based on $^{14}\text{C}/^{12}\text{C}$ ratios and estimated -27 ‰ $\delta^{13}\text{C}$ with 3 ‰ uncertainty.
TKU	Turku University / Department of Chemistry laboratory did not do many datings, and they most likely had no device to measure the isotopes (Jungner 2008), so their values were corrected now, even though the corrections are fairly small.
T-529	The Trondheim sample was previously calibrated to BC 7260–6480 with the Stuiver & Pearson diagram (NTNU 2008). For T-529, the ^{13}C was not measured, and the age 7980 \pm 250 BP was consequently not yet corrected for $\delta^{13}\text{C}$ (Gulliksen 2008) and had to be done in this study.
Su-	All the Geological Survey of Finland's (Su) values include the isotope fractionation correction (Mäkeläinen & Mäkilä 2008).
Lu-	Every dating from Lund (Lu) includes $\delta^{13}\text{C}$ correction as agreed by the international C-14 community (Skog 2008).
GrN- and GrA-	The activity for all the GrN- and GrA- samples, which Eronen (1995) already listed, had been corrected for $\delta^{13}\text{C}$. GrN indicates that the samples were measured conventionally (gas counters), while GrA samples by AMS (accelerator mass spectrometry). The Gr- samples in the list were actually GrN- (Smith-Deenen 2008), and all Grn- were GrN-.

KI-	<p>The Ki- samples that Eronen et al. (1995) listed were actually dated in Kile (KI). Back when the Kiev laboratory had only 1800-1900 indices, its index was not yet Ki but Ки. In any case, at that time they made corrections by stable isotopes only based on tables (average for each type of material) (Skripkin 2008). The samples' KI-1839, KI-1840.02 and KI-1841.02 (as well as samples' KI-1840.01 and KI-1841.01) radiocarbon dates listed by Eronen et al (1995) are so-called conventional radiocarbon ages, i.e. they were corrected for isotope fractionation and have already been normalized to $\delta^{13}\text{C}=-25\text{‰}$ PDB. The $\delta^{13}\text{C}$-values are -28.94, -29.54, and -27.78 ‰ PDB for KI-1839, KI-1840.02, and KI-1841.02, respectively. The samples were sediments with a high mineral fraction. The chemical preparation involved acid treatment only. Applying hydroxide leaching might have made the organic fraction dissolve and disappear completely. Accordingly, the organic fraction might contain differently aged organic components, such as infinitely aged graphite in the minerals up to modern carbon from the time the sediments formed. One must be conscious of these problems and have a critical understanding of the significance of these total sedimentary organic carbon ^{14}C dates (Erlenkeuser 2008).</p>
St-2947	<p>Saarnisto (2008), for whose thesis this Stockholm dating was done, says the information was used as-is, and he does not expect the correction to have been done, but other factors cause more unreliability in datings than $\delta^{13}\text{C}$ correction. Olsson (2008) said that people in the St laboratory were less anxious than she to measure ^{13}C and normalise the activity results accordingly. She thus cannot give any answer to the question and cannot even guess. The St laboratory did not publish all the results. Strucke (2008) first thought the St-2947 values were not ^{13}C-corrected; then he just guessed that the correction was done with the standard -25 ‰ $\delta^{13}\text{C}$. He later found out there is no information about ^{13}C in the laboratory sheet. According to Jungner (2008), this clearly means the correction was not done, even though the means to do so were available early at the St laboratory. Therefore the correction was conducted now.</p>
Teledyne Isotopes (I)	<p>Unfortunately, there is no record that would enable accessing the data by the Teledyne Isotopes Lab Code Number. In general, they applied the correction based on the $^{12}\text{C}/^{13}\text{C}$ ratio when it came into general use, but they can't tell with certainty that it was applied to Eronen et al's (1995) samples (Schutz 2008). For many years they reported all age measurements in the Radiocarbon Journal, which is accessible at their web site. I-1178 is reported by Trautman & Willis (1966) as 1955 ± 350. There, the ratio of ^{12}C to ^{13}C is said to be measured periodically by mass spectrometry section, but not routinely on samples unless requested by clients. In vol 23, No. 3, Teledyne Isotope methods, equipment, and techniques are said to have been reported previously (Radiocarbon 1968, v 10, p 246; Radiocarbon 1970, v 12, Nr 1 p. 87 which is not on-line yet but where the measurements VIII incl. I-1519 and I-1520 are reported). According to Jungner (2008), who checked the publications, the ^{13}C value is not mentioned there with any of these I samples, nor is it mentioned that the correction would have been done. Therefore the three I samples were corrected as well.</p>

In the CALIB software's XLS → CSV input files were used

Lab Error or added variance $f^{*}2= 1$

Age Span = 5 years

d13C = 0 per mil

d13C SD = 0 years

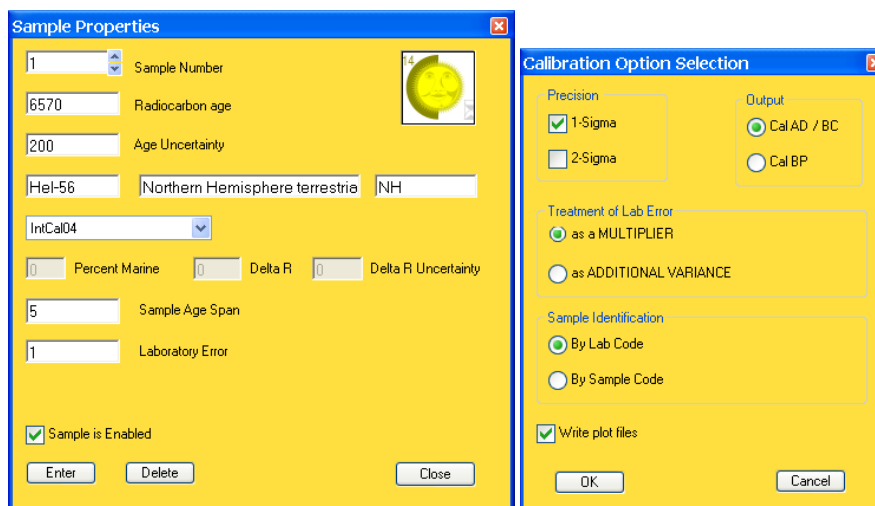
delta R = 0 years

delta R SD = 0 years

Marine Carbon percentage = 0

CalCurve Number = 2 (meaning IntCal04.14C Northern Hemisphere terrestrial calibration dataset)

It was understood that the two d13C fields are nowadays not even used by the software. It seems also to be possible to have a mixture of the marine and terrestrial models, but the IntCal04 terrestrial was used alone here.



In the regional settings of MS Windows, the dot was set as the decimal marker in order to get a decimal dot instead of a comma in the CALIB software's output files *calout.csv*. (The list separator, on the other hand, is a comma.) The files were further processed in MS Excel by collection of the ranges. The "median probability" in the last column is the distribution function's median, used when plotting the 1- and 2-sigma ranges, and as a single value when solving the A_s and B_s parameter values. In this report, calibrated years AD were used. CALIB directly reports the older AD value first, unlike with cal BP values.

The Marine04 curve should be used for marine samples such as shells, corals, fish, etc. In this case, Marine04 was not used since the samples were assumed to be non-marine, even though they describe the isolation between the sea and a lake. Marine04 is more suitable for saltier ocean conditions and does not apply fully to marine carbon samples from the Baltic Sea. No calibration curve has been defined specifically for the Baltic Sea. However, it might be useful and interesting to test how big the differences are that Marine04 usage would yield compared to IntCal04 usage (Oinonen 2008). Especially in bays like the Gulf of Bothnia or the Gulf of Finland, the less salty brackish water is much more like seawater than ocean water, so the Marine04 dataset is not needed. This

has become obvious when dating the Baltic Sea sediments dating from before isolation and directly after isolation; the relationship of the datings has been very reasonable (Miettinen 2008).

APPENDIX 4. THE NEW SAMPLES (FINLAND AND SWEDEN)

These are the new samples since Eronen et al (1995), collected through literature research. The order is the Finnish lake points, the four Finnish mires (the greyed ones), and the Swedish points.

Column explanations of the table below:

- **Sample number** is the ordinal number of the sea-level index points, continued from APPENDIX 1's table and serving as an ID, also in the plotted shoreline displacement curve graphs.
- **Point** is the lake or mire name, and **Locality** is the municipality or other place name.
- **N** and **E** are the geographic coordinates, latitude and longitude, with WGS 84 spheroid and datum assumed.
- **Threshold N60** is the original threshold altitude, and **Threshold N2000** is corrected according to the surface in Figure 10 or (Sweden) Figure 12.
- **Age ¹⁴C** is the original radiocarbon age, years BP; ± is its error value or σ (when not available or "ca.", 100 was used in CALIB), and **Laboratory number** is its analysis number.
- **$\delta^{13}\text{C}$ corrected age** is the $\delta^{13}\text{C}$ corrected ¹⁴C age (still in years BP), here typically same as **Age ¹⁴C** because the correction was already included. But **$\delta^{13}\text{C}$ corrected ±** is the used error or σ of the **$\delta^{13}\text{C}$ corrected age**, different only when error or σ of **Age ¹⁴C** was not available.
- **Median AD from CALIB** is the median value of the whole probability distribution function, AD. If no radiocarbon age was available, the estimated cal BP age range was just turned into an AD average age.
- **1 σ LL: UL AD OxCal** are the lower limit and upper limit of all one-sigma ranges, and **2 σ LL: UL AD OxCal** are the corresponding two-sigma limits. Helsinki University produced the limits of calibrations using OxCal. If no radiocarbon age was available, the estimated cal BP range was just turned into an AD range. If no **$\delta^{13}\text{C}$ corrected ±** is available, no range was given by OxCal.
- **1 σ AD ranges and probabilities, CALIB** are the individual one-sigma ranges of the probability distribution function, and **2 σ AD ranges and probabilities, CALIB** the corresponding two-sigma ranges. The minimum and maximum values of these can be compared with the two

previous columns to get an idea of the differences between the values obtained using the OxCal and CALIB applications. Both used the same calibration dataset version and the same 5-year smoothing. The distribution function medians, each individual range, and their probabilities (summing 1.0) were calibrated at Pöyry Environment Oy. If no radiocarbon age was available, the estimated cal BP range was just turned into AD ranges.

- **Comments** field may point out the interpretation of the phase of isolation of the lake or mire from sea.
- **Reference** is the report referenced, see the end of this appendix.
- **Validity** field may give some remarks on the validity of the sample. The previously estimated cal BP ages are possibly given here.

Sample No.	Point	Locality	N	E	Threshold	Threshhold N2000	Age ¹⁴ C	±	Lab no.	δ ¹³ C corrected age	δ ¹³ C corrected ±	Median AD from CALIB	1σ LL: UL AD OxCal	2σ LL: UL AD OxCal	1σ AD ranges and probabilities, CALIB	2σ AD ranges and probabilities, CALIB	Comments	Reference	Validity
261	Storträsk	Kirkkonummi	60° 06'	24° 31'	1.8	2.05	890	30	Poz-8268	890	30	1142	1052:1209	1041:1218	1051:1081 0.327351 1127:1135 0.073263 1152:1208 0.599385	1042:1107 0.363348 1117:1216 0.636652	Isol. contact	Miettinen et al. 2007	
262	Djupström	Kirkkonummi	60° 06'	24° 25'	2.5	2.75	1225	35	Poz-8275	1225	35	796	721:869	689:887	720:741 0.18262 769:831 0.5554 836:869 0.26198	688:754 0.283599 759:887 0.716401	Isol. contact	Miettinen et al. 2007	
263	Hälftes-träsket	Orslandet, Inkoo	59° 57'	23° 54'	2.5	2.75	1265	30	Poz-3546	1265	30	734	690:773	667:860	689:753 0.843226 760:773 0.156774	667:783 0.915617 788:820 0.062694 842:859 0.021688	Isol. contact	Miettinen et al. 2007	
264	Kvarnviks-träsket	Orslandet	59° 58'	23° 51'	3.0	3.25	1350	30	Poz-12510	1350	30	666	650:681	637:769	650:679 1	637:713 0.923579 745:767 0.076421	Isol. contact	Miettinen et al. 2007	
265	Rövass-träsket	Orslandet	59° 58'	23° 54'	3.4	3.65	1665	30	Poz-3551	1665	30	383	346:420	258:505	346:371 0.317989 377:418 0.682011	258:298 0.083342 319:434 0.907658 494:504 0.009	Isol. contact	Miettinen et al. 2007	
266	Petarträsk	Orslandet	59° 57'	23° 52'	9.5	9.75	2440	40	Poz-3550	2440	40	-543	-732:-411	-752:-405	-733:-691 0.228207 -661:-650 0.059212 -545:-412 0.712581	-754:-685 0.224854 -668:-610 0.132161 -598:-406 0.642985	Isol. contact	Miettinen et al. 2007	
267	Hemträsket	Tenhola, Pohja	60° 04'	23° 28'	2.5	2.76	1400	30	Poz-14722	1400	30	640	621:659	598:670	622:659 1	599:668 1	Isol. contact	Miettinen et al. 2007	
268	Sidsbacka-träsket	Tenhola, Pohja	60° 04'	23° 24'	4.6	4.86	2345	30	Poz-14676	2345	30	-402	-478:-382	-511:-376	-477:-474 0.021512 -414:-384 0.978488	-511:-378 1	Isol. contact	Miettinen et al. 2007	
269	Tjämen	Tenhola,	60° 23'		13	13.26	2925	30	Poz-	2925	30	-1128	-1191:	-1256:	-1193:-1172 0.161357	-1257:-1235 0.05245	Isol. contact	Miettinen et al.	Two close

Appendix 4

		(Tammi- saari?)	05' 22'					12513				-1053	-1017	-1168:-1142 0.210344 -1133:-1055 0.628299	-1215:-1019 0.94755		2007	one another.	
270	Tronsböle- träsket	Präst- kulla, Tammi- saari	59° 57' 12"	23° 12'	6.2	6.46	2070	35	Poz- 8279	2070	35	-90	-159: -42	-184: 4	-159:-134 0.225634 -116:-44 0.774366	-184:3 1	Isol. begins	Miettinen et al. 2007	
271	Tronsböle- träsket	Präst- kulla, Tammi- saari	59° 57' 12"	23° 12'	6.2	6.46	1950	30	Poz- 12511	1950	30	50	18: 82	-35: 126	10:10 0.008643 17:81 0.991357	-36:-30 0.014789 -21:-11 0.025261 -2:125 0.95995	Isol. ends	Miettinen et al. 2007	
272	Gundby- träsket	Präst- kulla, Tammi- saari	59° 59' 10"	23° 10'	12.6	12.86	3040	30	Poz- 12512	3040	30	-1315	-1376: -1264	-1405: -1211	-1376:-1338 0.420491 -1320:-1266 0.579509	-1405:-1252 0.933418 -1241:-1213 0.066582	Isol. contact	Miettinen et al. 2007	
273	Virojärvi	Virolahti	60° 32' 35"	27° 35'	19	19.21	7420	110	Hel- 4189	7420	110	-6288	-6424: -6124	-6460: -6065	-6425:-6212 0.982086 -6131:-6126 0.017914	-6460:-6066 1	Transgression/isol. contact (Litorina)	Miettinen 2002	
274	Saarasjärvi	Virolahti	60° 36' 37"	27° 37'	19.5	19.71	8015	135	Hela- 60	8050	140	-6981	-7176: -6710	-7450: -6635	-7176:-6754 0.986992 -6718:-6711 0.013008	-7449:-7409 0.015254 -7365:-6632 0.982719 -6619:-6612 0.002027	Transgression/isol. contact (Litorina)	Miettinen 2002	
275	Saarasjärvi	Virolahti	60° 36' 37"	27° 37'	19.5	19.71	7630	110	Hel- 3907	7630	110	-6487	-6596: -6396	-6684: -6240	-6596:-6398 1	-6679:-6243 1	Transgression/isol. contact (Litorina)	Miettinen 2002	
276	Mostro- träsket	Mostro- träsket, Öja, Karleby	63° 51' 57"	22° 57'	5.0	5.43	600	100	-	600	100	1354	1294: 1413	1216: 1486	1293:1412 1	1217:1485 0.999599 1605:1605 0.000401	Isolation	Glückert et al. 1998	
277	Molnviken	Larsmo	63° 46' 46"	22° 46'	5.3	5.74	580	50	-	580	50	1353	1311: 1412	1295: 1426	1309:1360 0.672213 1386:1412 0.327787	1294:1426 1	Isolation	Glückert et al. 1998	
278	Rörträsket	Larsmo	63° 47' 44"	22° 44'	6.7	7.14	510	50	GrN- 22703; GrN- 22702; GrN- 22914; GrN- 22915	510	50	1415	1330: 1445	1306: 1464	1330:1338 0.074576 1397:1444 0.925424	1305:1363 0.243524 1385:1463 0.756476	Isolation	Glückert et al. 1998	
279	Bäcks- träsket	Bosund, Larsmo	63° 50' 50"	22° 50'	5.9	6.34	410	50	GrN- 22697; GrN- 22913	410	50	1491	1436: 1618	1421: 1635	1436:1515 0.838008 1599:1617 0.161992	1421:1529 0.685364 1544:1548 0.004634 1550:1634 0.310002	Isolation	Glückert et al. 1998	
280	Kvånos- träsket	Norra ön, Larsmo	63° 50' 45"	22° 45'	5.2	5.64	450	40	GrN- 22699; GrN- 22917	450	40	1445	1421: 1466	1406: 1618	1422:1463 1	1407:1513 0.964197 1601:1616 0.035803	Isolation	Glückert et al. 1998	

Appendix 4

281	Långnäs-träsket	Norra ön, Larsmo	63° 50' 22"	22° 45' 5.8"	6.24	570	40	GrN-22700; GrN-22920	570	40	1353	1316:1415	1299:1430	1316:1354 0.599895 1389:1414 0.400105	1299:1370 0.599741 1380:1429 0.400259	Isolation	Glückert et al. 1998	
282	Skalaträsket	Kronoby	63° 43' 23"	23° 03' 17.3"	17.73	1760	60	-	1760	60	276	215:382	129:410	184:185 0.00412 214:358 0.918644 364:381 0.077236	129:409 1	Isolation	Glückert et al. 1998	
283	Mjöträsket	Kronoby	63° 41' 23"	23° 01' 19.6"	20.03	1940	40	GrN-22701; GrN-22916	1940	40	60	20:124	-43:136	20:89 0.821024 102:122 0.178976	-44:135 1	Isolation	Glückert et al. 1998	
284	Truträsket	Kronoby	63° 42' 23"	23° 01' 15.0"	15.43	1780	40	GrN-22705; GrN-22706; GrN-22918	1780	40	247	142:331	131:379	144:147 0.015545 171:193 0.118176 210:263 0.461079 277:330 0.4052	130:349 0.989119 369:378 0.010881	Isolation	Glückert et al. 1998	
285	Jämträsket	Kronoby	63° 40' 23"	23° 03' 28.7"	29.13	2770	55	-	2770	55	-920	-975:-840	-1047:-809	-976:-952 0.181775 -947:-842 0.818225	-1047:-811 1	Isolation	Glückert et al. 1998	
286	Stenträsket	Hästölandet, Kronoby	63° 45' 22"	22° 56' 8.5"	8.93	850	50	GrN-22704; GrN-22919	850	50	1185	1060:1259	1043:1270	1059:1063 0.017179 1155:1258 0.982821	1043:1104 0.181849 1118:1269 0.818151	Isolation	Glückert et al. 1998	
287	Verkträsket	Hästölandet, Kronoby	63° 45' 22"	22° 57' 5.0"	5.43	600	100	-	600	100	1354	1294:1413	1216:1486	1293:1412 1	1217:1485 0.999599 1605:1605 0.000401	Isolation	Glückert et al. 1998	
288	Kätö	Kätölandet Karleby	63° 53' 22"	22° 51' 3.2"	3.64	400	100	-	400	100	1523	1432:1634	1307:1952	1432:1527 0.573458 1554:1633 0.426542	1309:1361 0.037545 1386:1674 0.942066 1778:1799 0.01589 1942:1951 0.004498	Isolation	Glückert et al. 1998	
289	Stoppe-träsket	Såka, Kronoby	63° 45' 23"	23° 15' 19.8"	20.23	2110	60	-	2110	60	-140	-335:-45	-357:18	-203:-46 1	-358:-279 0.147206 -258:-242 0.013774 -236:8 0.83343 10:17 0.00559	Isolation	Glückert et al. 1998	
290	Kruunuvuorenlampi	Helsinki	60° 11' 25"	25° 01' 9.2"	9.45	2400	100	Hel-3902	2400	100	-531	-748:-392	-792:-230	-749:-687 0.207691 -666:-642 0.079611 -592:-577 0.043447 -569:-393 0.669251	-793:-354 0.955623 -292:-231 0.043269 -217:-215 0.001107	Isol. Litorina	Seppä & Tikkanen 1998	
291	Kangaslampi	Helsinki	60° 13' 25"	25° 08' 14.6"	14.85	3510	120	-	3510	120	-1843	-2015:-1687	-2190:-1529	-2015:-1997 0.041238 -1979:-1688 0.958762	-2189:-2182 0.003489 -2141:-1528 0.996511	Isolation	Seppä et al. 2000	
292	Ormträsket	Sipoo	60° 17' 25"	25° 19' 18.0"	18.25	4350	130	-	4350	130	-3016	-3328:-2875	-3365:-2625	-3329:-3216 0.226829 -3180:-3158 0.041 -3123:-2876 0.732171	-3365:-2829 0.855593 -2823:-2626 0.144407	Isolation	Seppä et al. 2000	

Appendix 4

293	Lillträsk	Sipoo	60° 20' 25"	21.0	21.25	5140	130	-	5140	130	-3945	-4221: -3770	-4252: -3659	-4222:-4210 0.024688 -4153:-4133 0.042004 -4058:-3770 0.933308	-4244:-3659 1	Isolation	Seppä et al. 2000	
294	Stortjärnen	Pohja	60° 04' 23"	39.9	40.16	7630	60	GrA- 2542	7630	60	-6482	-6561: -6429	-6597: -6395	-6562:-6548 0.090576 -6527:-6519 0.056225 -6510:-6430 0.853199	-6597:-6396 1	Isolation Litorina	Eronen et al. 2001	
295	Kvarn- träsket	Tenhola	60° 02' 23"	38.5	38.76	6230	50	GrA- 3015	6230	50	-5196	-5297: -5078	-5310: -5052	-5298:-5237 0.401795 -5235:-5206 0.206501 -5162:-5135 0.163097 -5130:-5119 0.069962 -5106:-5079 0.158646	-5310:-5054 1	Isolation Litorina	Eronen et al. 2001	
296	Dotterböle- träsket	Tammi- saari	60° 00' 23"	8.8	9.06	2370	50	GrA- 2543	2370	50	-472	-519: -388	-749: -365	-518:-391 1	-750:-686 0.113844 -667:-640 0.032516 -594:-365 0.85364	Isolation, Limnaea	Eronen et al. 2001	
297	Skogsböle- träsket	Tenhola	60° 02' 23"	7.3	7.56	1720	50	GrA- 2541	1720	50	320	256: 386	143: 428	255:304 0.415307 314:385 0.584693	144:147 0.001844 171:193 0.015228 211:427 0.982928	Isolation, Limnaea	Eronen et al. 2001	
298	Kaurajärvi	Eura	60° 59' 22"	45.4	45.72	5570	40	GrN- 21976	5570	40	-4406	-4447: -4361	-4486: -4340	-4448:-4416 0.441106 -4405:-4362 0.558894	-4487:-4477 0.01726 -4464:-4342 0.98274	Isolation Litorina	Eronen et al. 2001	
299	Kaurajärvi	Eura	60° 59' 22"	45.4	45.72	5270	40	GrN- 21975	5270	40	-4108	-4225: -3996	-4231: -3985	-4227:-4203 0.177223 -4167:-4128 0.292538 -4116:-4098 0.111416 -4076:-4038 0.278124 -4018:-3997 0.140699	-4232:-4190 0.173305 -4180:-3985 0.826695	Isolation Litorina	Eronen et al. 2001	
300	Lavajärvi	Lappi T.L.	61° 05' 22"	56.6	56.93	6320	50	GrN- 21978	6320	50	-5301	-5343: -5223	-5465: -5210	-5344:-5284 0.57241 -5274:-5224 0.42759	-5466:-5433 0.042717 -5428:-5404 0.026757 -5384:-5211 0.930525	Isolation Litorina	Eronen et al. 2001	
301	Lavajärvi	Lappi T.L.	61° 05' 22"	56.6	56.93	5920	50	GrN- 21977	5920	50	-4795	-4839: -4724	-4932: -4694	-4839:-4726 1	-4933:-4695 1	Isolation Litorina	Eronen et al. 2001	
302	Ruotana	Köyliö	61° 10' 22"	62.9	63.23	6680	60	GrN- 21980	6680	60	-5597	-5643: -5543	-5706: -5490	-5644:-5545 1	-5707:-5682 0.044504 -5678:-5509 0.939024 -5500:-5491 0.016472	Isolation Litorina	Eronen et al. 2001	
303	Ruotana	Köyliö	61° 10' 22"	62.9	63.23	6190	60	GrN- 21979	6190	60	-5138	-5217: -5052	-5300: -4998	-5218:-5054 1	-5302:-4998 1	Isolation Litorina	Eronen et al. 2001	
304	Valkkisjärvi	Laitila	61° 01' 21"	32.4	32.73	4210	50	GrN- 21982	4210	50	-2783	-2895: -2696	-2908: -2630	-2896:-2856 0.321705 -2811:-2747 0.503291 -2724:-2698 0.175004	-2908:-2832 0.313802 -2820:-2657 0.655348 -2654:-2633 0.03085	Isolation Litorina	Eronen et al. 2001	
305	Valkkisjärvi	Laitila	61° 01' 21"	32.4	32.73	4040	50	GrN- 21981	4040	50	-2572	-2622: -2480	-2856: -2465	-2623:-2481 1	-2857:-2811 0.083061 -2748:-2724 0.023719 -2698:-2467 0.893221	Isolation Litorina	Eronen et al. 2001	
306	Sundträsket	Ruotsin- pyhtää	60° 24' 26"	1.1	1.32	470	90	Hel- 4180	470	90	1450	1322: 1618	1301: 1638	1322:1348 0.110187 1392:1516 0.798463 1597:1617 0.09135	1301:1367 0.15609 1382:1638 0.84391	Isolation	Miettinen et al. 1999	

Appendix 4

307	Lappom-träsket	Ruotsin-pyhtää	60° 25' 25"	26° 21' 21"	3	3.23	1400	100	Hel-4182	1400	100	636	544:768	426:867	544:712 0.921133 746:767 0.078867	427:828 0.980442 839:865 0.019558	Isolation	Miettinen et al. 1999
308	Lillträsket	Pernaja	60° 25' 08"	26° 07' 08"	7.7	7.93	2300	110	Hel-4207	2300	110	-374	-520: -197	-760: -105	-520:-198 1	-759:-683 0.077732 -670:-103 0.922268	Isolation	Miettinen et al. 1999
309	Labby-träsket	Pernaja	60° 20' 20"	26° 02' 02"	9.9	10.14	2900	80	Hel-4167	2900	80	-1101	-1252: -979	-1370: -900	-1253:-1240 0.041866 -1213:-995 0.933058 -987:-980 0.025075	-1372:-1344 0.017289 -1317:-899 0.982711	Isolation	Miettinen et al. 1999
310	Kakar-träsket	Lapinjärvi	60° 32' 32"	26° 21' 21"	25.4	25.63	5410	130	Hel-4193	5410	130	-4236	-4355: -4052	-4497: -3965	-4355:-4218 0.533913 -4214:-4148 0.211838 -4135:-4054 0.254249	-4494:-3966 1	Isolation	Miettinen et al. 1999
311	Ryttarjärvi	Ruotsin-pyhtää	60° 29' 29"	26° 25' 25"	26.5	26.72	6500	90	Hel-4254	6500	90	-5458	-5535: -5368	-5618: -5314	-5536:-5369 1	-5618:-5315 1	Isolation	Miettinen et al. 1999
312	Storbacka	Porvoo	60° 25' 25"	25° 47' 47"	14.7	14.94	3460	110	Hel-4251	3460	110	-1782	-1913: -1634	-2115: -1502	-1911:-1635 1	-2114:-2100 0.005672 -2037:-1502 0.994328	Isolation	Miettinen et al. 1999
313	Hjortermossen	Larsmo	63° 46' 46"	22° 45' 45"	10.5	10.94	900	50	GrN-22921	900	50	1127	1046: 1207	1025: 1223	1045:1097 0.429813 1119:1142 0.174634 1147:1188 0.333198 1198:1206 0.062354	1024:1223 1	Isolation	Glückert et al. 1998
314	Lövmossen	Hästölandet, Kronoby	63° 44' 44"	22° 56' 56"	11.6	12.03	1300	100	-	1300	100	743	647: 863	566: 970	647:784 0.774627 787:824 0.149814 841:861 0.075559	569:903 0.949404 914:969 0.050596	Isolation	Glückert et al. 1998
315	Långa Hjortermossen	Larsmo	63° 47' 47"	22° 46' 46"	10.6	11.04	1200	60	-	1200	60	824	716: 895	681: 971	716:744 0.135809 768:894 0.864191	682:905 0.872772 912:970 0.127228	Isolation	Glückert et al. 1998
316	Degermossen	Pernaja	60° 27' 27"	25° 53' 53"	18.3	18.54	4070	100	Hel-4226	4070	100	-2637	-2857: -2485	-2891: -2346	-2858:-2810 0.159911 -2750:-2723 0.087254 -2700:-2487 0.752836	-2891:-2399 0.97778 -2383:-2347 0.02222	Isolation	Miettinen et al. 1999
317	Tornberget mire		59° 08' 20"	18° 00' 44"	87	87.16	8855	75	Ua-10701	8855	75	-8002	-8205: -7839	-8241: -7735	-8206:-8034 0.564974 -8018:-7937 0.263107 -7926:-7917 0.02819 -7899:-7866 0.090973 -7860:-7841 0.052755	-8242:-7735 1	After isolation from the Yoldia	Hedenström 2001: Hedenström & Risberg 1999
318	Gladö S mire		59° 10' 31"	18° 00' 47"	80.9	81.06	8625	70	Ua-10697	8625	70	-7654	-7715: -7582	-7935: -7532	-7715:-7691 0.147185 -7686:-7583 0.852815	-7935:-7928 0.003342 -7912:-7901 0.005727 -7833:-7532 0.990931	Isolation from the Yoldia	Hedenström 2001: Hedenström & Risberg 1999
319	Gladö T mire		59° 10' 22"	18° 00' 25"	78.6	78.76	8365	65	Ua-10700	8365	65	-7428	-7518: -7354	-7573: -7192	-7519:-7443 0.519428 -7440:-7422 0.100807 -7415:-7355 0.379764	-7573:-7291 0.963234 -7269:-7258 0.007474 -7226:-7193 0.029292	Ancylus regression	Hedenström 2001: Hedenström & Risberg 1999
320	Gladö T		59° 18' 18"	18° 00' 25"	78.6	78.76	8430	70	Ua-	8430	70	-7499	-7576: -7589:	-7577: -7457 0.989684	-7589:-7342 1	Ancylus ingression	Hedenström	

Appendix 4

	mire		10° 22'	00' 25"				10698				-7456	-7340	-7387:-7385 0.010316			2001: Hedenström & Risberg 1999	
321	Gladö K mire		59° 10' 46"	18° 00' 22"	74.3	74.46	8440	105	Ua- 13410	8440	105	-7483	-7587: -7359	-7650: -7180	-7588:-7448 0.79723 -7411:-7359 0.20277	-7649:-7619 0.011961 -7615:-7180 0.988039	Isolation from the Ancyclus Lake	Hedenström 2001: Hedenström & Risberg 1999
322	Slåboda- mossen mire		59° 08' 40"	18° 00' 20"	57.2	57.36	8150	90	ST- 14227	8150	90	-7161	-7305: -7054	-7455: -6827	-7306:-7213 0.326313 -7204:-7054 0.673687	-7455:-7391 0.04277 -7383:-6908 0.919882 -6886:-6828 0.037348	After isolation from the Mastogloia Sea	Hedenström 2001: Hedenström & Risberg 1999
323	Lake Vibysjön		59° 03' 15"	14° 52' 30"	62.5	62.69	8020	85	Ua- 3208	8020	85	-6925	-7066: -6777	-7175: -6661	-7067:-6811 0.975171 -6807:-6806 0.002723 -6786:-6779 0.022106	-7175:-6679 0.996535 -6667:-6661 0.003465	After isolation from the Ancyclus Lake	Hedenström 2001: Hedenström & Risberg 1999
324	Markatorp mire		59° 02' 15"	14° 54' 15"	61.5	61.69	7535	80	Ua- 4316	7535	80	-6393	-6463: -6263	-6562: -6228	-6464:-6353 0.80457 -6308:-6300 0.041333 -6295:-6265 0.154098	-6563:-6548 0.011174 -6528:-6518 0.00611 -6511:-6229 0.982716	After isolation from the Mastogloia Sea	Hedenström 2001: Hedenström & Risberg 1999
325	Lake Skären		59° 38'	18° 23'	49.5	49.66	6170	100	Ua- 16295	6170	100	-5114	-5289: -4991	-5326: -4842	-5289:-5270 0.056424 -5226:-4992 0.943576	-5325:-4843 1	Isolation from the Litorina Sea	Hedenström 2001: Westman & Hedenström (in press 2001)(Calibrati on acc. Stuver et al. 1998)
326	Lake Skären		59° 38'	18° 23'	49.5	49.66	6145	80	Ua- 15482	6145	80	-5092	-5210: -4998	-5300: -4851	-5211:-4999 1	-5300:-4898 0.988583 -4865:-4853 0.011417	Isolation from the Litorina Sea	Hedenström 2001: Westman & Hedenström (in press 2001)(Calibrati on acc. Stuver et al. 1998)
327	Lake Svulten		59° 35'	18° 21'	57.3	57.46	7010	70	Ua- 12045	7010	70	-5892	-5984: -5814	-6008: -5742	-5985:-5837 0.990347 -5818:-5816 0.009653	-6008:-5744 1	Isolation (from Litorina)	Hedenström 2001
328	Lake Lilla Harsjön		59° 35'	18° 20'	54	54.16	5620	80	Ua- 16943	5620	80	-4459	-4521: -4361	-4680: -4333	-4520:-4363 1	-4679:-4637 0.031808 -4619:-4334 0.968192	Isolation (from Litorina)	Hedenström 2001
329	Lake Lilla Harsjön		59° 35'	18° 20'	54	54.16	6360	105	Ua- 16959	6360	105	-5335	-5468: -5226	-5519: -5057	-5469:-5292 0.841446 -5266:-5228 0.158554	-5516:-5191 0.891056 -5183:-5057 0.108944	Isolation (from Litorina)	Hedenström 2001
330	Lake Fasterby-		59° 35'	18° 24'	37	37.16	5035	75	Ua- 17521	5035	75	-3835	-3944: -3765	-3969: -3660	-3945:-3767 0.995275 -3721:-3720 0.004725	-3969:-3692 0.973785 -3684:-3662 0.026215	Isolation (from Litorina)	Hedenström 2001

Appendix 4

	sjön																		
331	Lake Hoven	59° 38'	18° 22'	56	56.16	6700	150	-	6700	150	-5623	-5727: -5485	-5965: -5365	-5727:-5486 1	-5965:-5958 0.002716 -5901:-5361 0.997284	Isolation from the Litorina Sea	Hedenström 2001		
332	Stormossen mire	59° 39'	18° 24'	62	62.16	7400	400	-	7400	400	-6301	-6686: -5838	-7305: -5563	-6678:-6670 0.006055 -6660:-5837 0.990174 -5820:-5815 0.003771	-7284:-7276 0.000901 -7250:-7230 0.002588 -7187:-5523 0.996512	Isolation from Mastogloia Sea	Hedenström 2001		
333	Lake Barsjö	60° 27'	17° 39'	22.5	22.69	2955	75	Ua- 16061	2955	75	-1176	-1290: -1050	-1391: -975	-1291:-1280 0.037814 -1270:-1052 0.962186	-1392:-976 0.996389 -952:-947 0.003611	Isolation (from Post-Litorina)	Hedenström & Risberg 2003		
334	Lake Landhols-sjön	60° 26'	17° 51'	16	16.19	-	-	-	-	-	-350	-550: -250	-550: -250	-550:-250 1	-550:-250 1	Precise isolation event not dated	Hedenström & Risberg 2003	("2500-2200 cal BP")	
335	Lake Södra Åsjön	60° 23'	18° 03'	10.8	10.99	1090	70	Ua- 18965	1090	70	939	886: 1021	731: 1150	885:1020 1	772:1048 0.969205 1087:1122 0.0239 1138:1150 0.006895	Isolation from Post-Litorina	Hedenström & Risberg 2003		
336	Lake Södra Åsjön	60° 23'	18° 03'	10.8	10.99	1675	65	Ua- 18964	1675	65	368	257: 431	228: 542	256:302 0.236362 316:430 0.763638	229:541 1	Isolation from Post-Litorina	Hedenström & Risberg 2003		
337	Lake Eckarfjärden	60° 22'	18° 12'	5.5	5.68	-	-	-	-	-	975	850: 1100	850: 1100	850:1100 1	850:1100 1	Precise isolation event not dated	Hedenström & Risberg 2003	("1100-850 cal BP")	
338	Lake Bången	60° 01'	17° 15'	57	57.19	5700	ca.	-	5700	100	-4550	-	-	-4684:-4631 0.202549 -4624:-4453 0.797451	-4769:-4753 0.010904 -4744:-4734 0.00754 -4730:-4349 0.981556	Isolation	Hedenström & Risberg 2003: Risberg 1999	"6300 ± 200 cal BP"	
339	Krapelås-mossen bog	60° 14'	18° 00'	48.4	48.59	5300	ca.	-	5300	100	-4136	-	-	-4243:-4038 0.914175 -4020:-3996 0.085825	-4346:-3949 1	Isolation	Hedenström & Risberg 2003: Robertsson and Persson 1989	"6000 ± 250 cal BP"	
340	Sävastebo-mossen bog	60° 03'	17° 14'	44	44.19	4900	ca.	-	4900	100	-3697	-	-	-3892:-3884 0.018782 -3798:-3630 0.84352 -3579:-3534 0.137698	-3950:-3515 0.977509 -3423:-3404 0.011477 -3399:-3384 0.011014	Isolation	Hedenström & Risberg 2003: Risberg 1999	"5600 ± 300 cal BP"	
341	Lake Järngården	60° 07'	17° 25'	40.3	40.49	4500	ca.	-	4500	100	-3193	-	-	-3356:-3089 0.925303 -3057:-3031 0.074697	-3499:-3433 0.053332 -3379:-2911 0.946668	Isolation	Hedenström & Risberg 2003: Risberg 1999	"5100 ± 300 cal BP"	
342	Ralbo-mossen bog	60° 21'	17° 39'	36.3	36.49	4100	ca.	-	4100	100	-2674	-	-	-2866:-2804 0.222385 -2774:-2770 0.009023 -2762:-2568 0.710715 -2517:-2499 0.057878	-2906:-2456 0.986663 -2419:-2407 0.004612 -2376:-2351 0.008724	Isolation	Hedenström & Risberg 2003: Robertsson and Persson 1989	"4600 ± 300 cal BP"	
343	Visso-mossen bog	60° 23'	17° 46'	27.4	27.59	3550	ca.	-	3550	100	-1893	-	-	-2022:-1992 0.101619 -1983:-1751 0.898381	-2193:-2178 0.008266 -2143:-1632 0.991734	Isolation	Hedenström & Risberg 2003: Bergström 2001	"3800 ± 150 cal BP"	
344	Lake Axen	62° 16'	16° 17'	179.9	180.17	9460	95	Ua-	9460	95	-8789	-9117:	-9175:	-9118:-9071 0.115351	-9175:-9164 0.00451	Both close to	Berglund 2005		

Appendix 4

			26' 31"	23' 54"				17921				-8620	-8492	-9059:-9009 0.117303 -8914:-8902 0.023186 -8846:-8621 0.744161	-9160:-8544 0.989751 -8504:-8491 0.005739	isolation	(Article shows multiple datings: best (= closest value for isolation) selected)		
345	Lake Axen		62° 26' 31"	16° 23' 54"	179.9	180.17	9565	95	Ua-16744	9565	95	-8966	-9139:-8795	-9237:-8654	-9140:-8968 0.529746 -8951:-8796 0.470254	-9237:-8704 0.988575 -8671:-8654 0.011425	Both close to isolation	Berglund 2005	
346	Tintjärn bog		60° 27' 03"	16° 19' 40"	168.1	168.30	9480	145	Ua-16745	9480	145	-8836	-9130:-8623	-9249:-8354	-9131:-8980 0.317192 -8930:-8623 0.682808	-9249:-8444 0.996357 -8364:-8354 0.003643	Isolation (two datings)	Berglund 2005	
347	Skränksmyran		60° 36' 50"	16° 28' 08"	112.3	112.50	8150	90	Ua-16746	8150	90	-7161	-7305:-7054	-7455:-6827	-7306:-7213 0.326313 -7204:-7054 0.673687	-7455:-7391 0.04277 -7383:-6908 0.919882 -6886:-6828 0.037348	Isolation	Berglund 2005	
348	Lake Astjärnen		60° 30' 01"	16° 25' 56"	99	99.21	7795	85	Ua-16747	7795	85	-6636	-6746:-6496	-7023:-6458	-6746:-6725 0.055457 -6699:-6498 0.944543	-7024:-6967 0.035012 -6947:-6935 0.006855 -6915:-6881 0.025581 -6839:-6459 0.932553	Isolation	Berglund 2005	
349	Åsmunds- hyttan		60° 28' 55"	16° 28' 28"	87.1	87.31	7375	90	Ua-16748	7375	90	-6247	-6373:-6105	-6420:-6066	-6374:-6206 0.805831 -6188:-6185 0.015063 -6169:-6160 0.034485 -6142:-6106 0.144621	-6419:-6067 1	Isolation	Berglund 2005	
350	Österbo		60° 27' 00"	16° 43' 47"	78	78.20	6655	85	Ua-17922	6655	85	-5582	-5640:-5510	-5716:-5475	-5640:-5512 1	-5716:-5476 1	Isolation (three datings)	Berglund 2005	
351	Lake Lövpusstjärn		60° 27' 47"	16° 43' 02"	74.2	74.40	6575	75	Ua-17138	6575	75	-5531	-5611:-5477	-5636:-5375	-5612:-5589 0.186911 -5565:-5478 0.813089	-5636:-5462 0.903716 -5450:-5376 0.096284	Isolation (two datings)	Berglund 2005	
352	Toretorp		60° 33' 20"	16° 30' 45"	68.2	68.40	4825	65	Ua-17139	4825	65	-3591	-3692:-3523	-3760:-3377	-3693:-3681 0.062048 -3664:-3624 0.328274 -3602:-3524 0.609678	-3760:-3741 0.013962 -3733:-3725 0.005126 -3714:-3499 0.906186 -3434:-3378 0.074726	Isolation (two datings)	Berglund 2005	
353	St. Ångstjärn		60° 42' 55"	17° 01' 29"	54.6	54.80	4395	90	Ua-16750	4395	90	-3066	-3312:-2905	-3342:-2889	-3313:-3294 0.055362 -3288:-3274 0.038563 -3265:-3238 0.088225 -3167:-3165 0.002636 -3107:-2906 0.815214	-3344:-2890 1	Isolation (two of three close to)	Berglund 2005	
354	St. Ångstjärn		60° 42' 55"	17° 01' 29"	54.6	54.80	4555	75	Ua-18541	4555	75	-3243	-3484:-3103	-3516:-3022	-3484:-3475 0.030009 -3371:-3308 0.275569 -3302:-3265 0.123693 -3240:-3104 0.570729	-3517:-3396 0.144298 -3385:-3023 0.855702	Isolation (two of three close to)	Berglund 2005	
355	Järvsta bog		60° 17'	36	36.19	3950	85	Ua-	3950	85	-2445	-2571:-2848	-2571:-2512 0.237445	-2848:-2813 0.019325	Isolation	Berglund 2005			

Appendix 4

			37' 49"	11' 52"					16751				-2299	-2151	-2504:-2335 0.695882 -2324:-2306 0.057547 -2303:-2301 0.009127	-2739:-2731 0.002864 -2693:-2688 0.001456 -2679:-2198 0.971137 -2165:-2151 0.005219			
356	Lake Björsjön		60° 39' 07"	17° 13' 47"	24.9	25.10	2790	75	Ua-16752	2790	75	-955	-1017:-837	-1188:-803	-1016:-839 1	-1189:-1180 0.005329 -1156:-1145 0.007322 -1130:-804 0.987349	Both close to isolation	Berglund 2005	
357	Lake Björsjön		60° 39' 07"	17° 13' 47"	24.9	25.10	3000	65	Ua-17926	3000	65	-1240	-1371:-1129	-1409:-1048	-1372:-1343 0.124697 -1317:-1188 0.6843 -1181:-1155 0.117169 -1145:-1130 0.073834	-1410:-1049 1	Both close to isolation	Berglund 2005	

References of the new samples (Finland and Sweden)

- Berglund, M. 2005. The Holocene shore displacement of Gästrikland, eastern Sweden: a contribution to the knowledge of Scandinavian glacio-isostatic uplift. *Journal of Quaternary Science* 20 (6), 519-531.
- Bergström, E. 2001. Late Holocene distribution of lake sediment and peat in NE Uppland, Sweden. Swedish Nuclear Fuel and Waste Management Co, SKB, report R-01-12, Stockholm, Sweden. 50 pp.
- Eronen, M., Glückert, G., Hatakka, L., Plassche, O. van de, Plicht, J. van der & Rantala P. 2001. Rates of Holocene isostatic uplift and relative sea-level lowering of the Baltic in SW Finland based on studies of isolation contacts. *Boreas* 30 (1), 17-30.
- Glückert, G., Peltola, H. & Rantala, P. 1998. Landhöjning och Östersjöns strandförskjutning i Kronoby-Larsmo-området, mellersta Österbotten, under de senaste 3000 åren. *Turun yliopiston maaperägeologian osaston julkaisuja* 81. Turku: Turun yliopisto. 15 p.
- Hedenström, A. 2001. Early Holocene shore displacement in eastern Svealand, Sweden, based on diatom stratigraphy, radiocarbon chronology and geochemical parameters. *Quaternaria. Ser. A: Theses and Research Papers* No. 10. Stockholm University. 48 p.
- Hedenström, A. & Risberg, J. 1999. Early Holocene shore-displacement in southern central Sweden as recorded in elevated isolated basins. *Boreas* 28, 490-504.
- Hedenström, A. & Risberg, J. 2003. Shore displacement in northern Uppland during the last 6500 calendar years. SKB technical report ; TR-03-17. 48 p.
- Miettinen, A. 2002. Relative sea level changes in the eastern part of the Gulf of Finland during the last 8000 years. *Annales Academiae Scientiarum Fennicae. Geologica - Geographica* 162. Helsinki: Suomalainen Tiedeakatemia. 100 p.
- Miettinen, A., Eronen, M & Hyvärinen, H. 1999. Land uplift and relative sea-level changes in the Loviisa area, southeastern Finland, during the last 8000 years. Tiivistelmä: Maankohoaminen ja merenpinnan suhteellinen korkeusvaihtelu viimeisen 8000 vuoden aikana Loviisan alueella Kaakkois-Suomessa. Posiva-report 99-28. Helsinki: Posiva. 26 p.
- Miettinen, A., Jansson, H., Alenius, T. & Haggrén, G. 2007. Late Holocene sea-level changes along the southern coast of Finland, Baltic Sea. In: *Quaternary land-ocean interactions : sea-level change, sediments and tsunami. Marine Geology* 242 (1-3), 27-38.

Risberg, J. 1999. Strandförskjutningen i nordvästra Uppland under subboreal tid. In Segerberg A. 1999. Bälunge mossar. Kustbor i Uppland under yngre stenåldern. Doctoral thesis. Uppsala Universitet, Uppsala. Aun 26, 233-241. (In Swedish with English summary).

Robertsson, A.-M. & Persson C. 1989. Biostratigraphical studies of three mires in northern Uppland, Sweden. Sveriges Geologiska Undersökning, Avhandlingar och uppsatser C 821, 5-19. Uppsala.

Seppä, H. & Tikkanen, M. 1998. The isolation of Kruunuvuorenlampi, southern Finland, and implications for Holocene shore displacement models of the Finnish south coast. *Journal of Paleolimnology* 19 (4), 385-398.

Seppä, H., Tikkanen, M. & SHEMEIKKA, P. 2000. Late-Holocene shore displacement of the Finnish south coast : diatom, litho- and chemostratigraphic evidence from three isolation basins. *Boreas* 29 (3), 219-231.

Westman, P. & Hedenström, A. 2002. Environmental changes during isolation processes from the Litorina Sea as reflected by diatoms and geochemical parameters – A case study. *The Holocene* 12, 531-540.

APPENDIX 5. THE ANALYSIS SITE TABLE

Zero (0) means not defined or not applicable for the parameter.

In the study, the 79 first sites are numbered acc. to Pässe & Andersson (2005), and the references below are from there too. The grey points 80–82 come from Pässe's older publications (1997, 2001) and are not found in Pässe & Andersson (2005). Points 83– are new ones. The coordinates of the sites represent the possibly updated locations (average digital degrees location of points of the subset).

Numbering			Point	Fast component 2005				Coordinates (dd)		Reference	Slow component 1997	Fast component 1997				Slow component 2001	Moho 2008 (km)	New results		
1997	2001	2005	Point	AS05	BS05	AF05	TF05	E	N	Ref	As97	Bs97	Af97	Tf97	Bf97	As01	Bs01	Moho08	As	Bs
1	1	1	Varanger	150	5000	10	10200	29.117340	70.171989	Donner 1980	160	5000	55	1150	1100	170	3400	43.91		
3	3	2	Tromsö	120	4300	10	10000	19.072199	69.649723	Hald & Vorren 1983	130	3800	20	1150	800	125	3300	38.42		
2	2	3	Andöja	90	4000	8	10000	16.098332	69.253206	Vorren et al. 1988	88	3600	20	1150	1200	91	3200	28.33		
4	4	4	Lofoten	103	4000	9	9975	14.348494	68.216786	Möller 1984; Vorren & Moe 1986	110	3600	20	1150	1000	105	3200	29.02		
5	5	5	Näröy	205	4500	30	9900	11.506539	64.861461	Ramfjord 1982	255	3800	60	1150	1000	260	3500	38.22		
6	6	6	Verdals-öra	250	4700	39	9800	11.544485	63.788131	Sveian & Olsen 1984	305	4400	67	1150	800	295	3600	39.87		
7	7	7	Frosta	248	4600	37	9800	11.004455	63.458960	Kjemperud 1986	290	4400	56	1150	1000	290	3600	38.72		
8	8	8	Bjugn	178	4300	31	9975	9.753974	63.720500	Kjemperud 1986	223	3800	40	1150	800	210	3400	35.79		
11	11	9	Fröja	139	4100	11	10000	8.872744	63.767656	Kjemperud 1986	163	3800	22	1100	650	152	3300	32.51		
9	9	10	Hitra	157	4200	21	10000	8.815488	63.594559	Kjemperud 1986	195	3800	30	1130	600	180	3400	34.14		
10	10	11	Tjeldbergodden	157	4200	21	10000	8.813728	63.465072	Solem & Solem 1997	188	3800	35	1150	900	178	3400	35.41		
12	12	12	Leinöy	101	3700	4	10200	5.588652	62.350569	Svendsen & Mangerud 1990	100	3500	17	1150	800	99	3150	28.67		
13	13	13	Fonnes	114	3800	16	10200	5.011650	60.741151	Kaland 1984	125	3700	30	1150	1000	118	3300	29.94		
14	14	14	Sotra	115	3800	15	10200	5.165700	60.231949	Krzywinski & Stabell 1984; Kaland et al. 1984	120	3800	37	1150	900	120	3300	31.18		

Appendix 5

15	15	15	Bömlö	114	3800	15	10200	5.277147	59.632971	Kaland 1984	120	3800	30	1150	1000	118	3300	33.29		
16	16	16	Yrkje	115	3800	16	10200	5.961466	59.456096	Anundsen 1985	124	4000	36	1150	800	118	3300	33.66		
17	17	17	Hardanger	165	3900	43	10150	6.708172	60.459962	Helle et al. 1997	200	4000	75	1150	900	215	3400	33.84		
18	18	18	Jären	99	3300	10	10300	5.719056	58.579605	Thomsen 1981; Bird & Klemsdal 1986	95	3400	36	1150	800	93	3200	31.68		
0	0	19	Mandal	110	3400	15	10300	7.554555	58.007469	Midtbö et al. 2000	0	0	0	0	0	0	0	31.24		
19	19	20	Kragerö	185	3700	42	10300	9.324481	58.829130	Stabell 1980	295	2400	40	1150	900	215	3300	31.73		
20	20	21	Porsgrunn	200	4000	45	10300	9.639269	59.144856	Stabell 1980	325	2400	50	1150	800	235	3400	32.30		
21	21	22	Vestfold	235	4100	45	10500	10.479813	59.231801	Henningsmoen 1979	360	2400	15	1150	700	245	3400	34.29		
22	22	23	Oslo	270	4400	70	10300	10.703598	59.923070	Hafsten 1983	435	2700	60	1150	700	320	3400	35.41		
24	25	24	Ski	253	4400	65	10300	10.741362	59.633517	Sörensen 1979	425	2650	45	1150	700	310	3400	35.44		
0	0	25	Halden	250	4200	38	10600	11.632621	59.303549	Sörensen 1999	0	0	0	0	0	0	0	36.88		
25	26	26	Vendsyssel/Jylland	123	3400	0	0	10.402974	57.409667	Rickardt 1996	117	3400	15	1150	600	120	3100	29.56		
26	27	27	Vedbäck	106	2500	0	0	12.578815	55.737095	Christensen 1993	107	2500	0	0	0	98	2500	32.71		
27	28	28	Söborg	105	2400	0	0	11.676650	55.818495	Mörner 1976	98	2500	0	0	0	96	2400	32.19		
28	29	29	Store Bält Great Be	77	2300	0	0	11.056117	55.132764	Christensen 1993; Bennike & Jensen 1995; Jensen et al. 1999	62	2500	0	0	0	65	2300	34.43		
0	0	30	Strömstad	238	4200	34	10700	11.368650	58.833166	Pässe 2003	0	0	0	0	0	0	0	36.31		
29	30	31	Kroppefjäll	222	4300	23	10700	12.199813	58.606605	Björck & Digerfeldt 1991	282	3700	19	1135	250	255	3500	39.04		
30	31	32	Hunneberg	208	4200	17	11000	12.691627	58.371507	Björck & Digerfeldt 1982	242	4300	29	1190	600	237	3650	41.72		
31	32	33	Central Bohuslän	208	4100	15	10900	11.638077	58.473701	Miller & Robertsson 1988	245	3500	20	1150	400	225	3400	37.87		
32	33	34	Ljungskile	195	4100	13	11000	12.017517	58.228218	G. Persson 1973	217	3900	10	1150	350	205	3450	40.28		
33	34	35	Risveden	183	4000	13	11200	12.379844	58.119098	Svedhage 1985	205	3650	25	1190	600	198	3450	42.02		

Appendix 5

34	35	36	Göteborg	160	3650	4	11400	12.000846	57.721324	Pässe 1983	170	3700	10	1150	350	162	3400	40.84		
35	36	37	Sandsjö-backa	156	3600	0	0	12.083068	57.553200	Pässe 1987	161	3650	9	1150	350	155	3400	40.49		
36	37	38	Fjärås	152	3500	0	0	12.197891	57.435894	Pässe 1986	155	3700	8	1150	350	148	3350	40.28		
37	38	39	Varberg	135	3400	0	0	12.306127	57.111322	Pässe 1990b; M. Berglund 1995	137	3700	7	1150	350	132	3300	38.37		
38	39	40	Falkenberg	125	3300	0	0	12.543782	56.914935	Pässe 1988	125	3700	6	1150	350	122	3250	38.25		
39	40	41	Halmstad	123	3150	0	0	12.919983	56.661572	Caldenius & Linman 1949; Caldenius et al. 1966; Berglund 1995	118	3300	6	1150	350	116	2850	38.72		
40	41	42	Bjäre Peninsula	120	2850	0	0	12.765151	56.407662	Mörner 1980	108	3300	0	0	0	111	2800	36.95		
41	42	43	Barsebäck	103	2500	0	0	12.975250	55.822744	Digerfeldt 1975; G. Persson 1962; Ringberg 1989	95	2500	0	0	0	97	2300	34.28		
42	43	44	Blekinge	127	2600	0	0	15.156657	56.191278	Björck 1979; Björck & Möller 1987; Liljegren	125	2500	0	0	0	122	2400	35.32		
0	44	45	Öland	128	2700	0	0	16.472586	56.388440	Gembert 1987	0	0	0	0	0	125	2450	40.28		
43	45	46	Oskarshamn	155	3300	11	11400	16.500891	57.248630	Svensson 1989	177	3200	0	0	0	163	2600	45.56		
44	46	47	Gotland	152	3400	13	11400	18.483775	57.505810	Svensson 1989	170	3200	0	0	0	169	2600	49.43		
0	47	48	NE Småland	190	4200	23	11300	16.668480	57.900244	Robertsson 1997	0	0	0	0	0	195	4000	49.46		
45	48	49	Rejmyra	227	4800	37	11100	15.964284	58.835501	C. Persson 1979	220	6500	75	1150	800	230	4700	50.06		
46	49	50	Stockholm area	225	6500	45	10900	18.031468	59.185727	Åse 1970; Miller & Robertsson 1982; Brunnberg et al. 1985; Risberg 1991; Hedenström & Risberg 1999	233	7200	82	1150	1050	235	6200	46.99		
0	0	51	Tärnan	237	7000	50	10750	18.528063	59.556309	Hedenström 2001; Hedenström & Risberg 2003	0	0	0	0	0	0	0	44.14		

Appendix 5

47	50	52	Eskil- tuna	250	5900	48	10700	16.53936 0	59.369472	Robertsson 1991	250	7000	90	1150	900	255	6200	46.37		
0	51	53	Närke	245	4800	45	10800	14.95842 9	59.069929	Hedenström & Risberg 1999	0	0	0	0	0	255	4700	49.71		
48	52	54	Gästrik- land	297	7200	78	10400	17.09564 7	60.749410	Asklund 1935	333	7200	95	1150	1000	320	7500	45.75	266	8217
49	53	55	Hälsing- land	325	7800	105	9800	17.47446 9	62.184415	G. Lundqvist 1962	395	7000	120	1150	1400	355	7900	50.22		
50	54	56	Ånger- manland	330	8800	132	9600	19.00332 5	63.323477	Cato 1992	430	6500	130	1150	1900	380	8800	46.31		
51	55	57	S. Väster- botten	328	9200	132	9600	20.47476 2	63.793839	Renberg & Segerström 1981	430	6700	135	1150	1900	380	9000	48.67		
52	56	58	Rova- niemi	290	9500	100	9700	25.08301 4	66.193719	Saarnisto 1981	378	6500	115	1150	1100	330	9000	42.42	373	10573
53	57	59	Lauhan- vuori	288	9500	95	10000	22.01484 8	62.255246	Salomaa 1982; Salomaa & Matskainen 1983	330	9200	140	1150	1300	320	8800	55.27	316	9331
55	58	60	Olkiluoto	240	9000	70	10650	21.83394 0	60.951693	Eronen et al. 1995	265	8600	90	1150	900	258	7600	47.18	258	6766
56	59	61	Åland	245	8000	63	10700	19.93991 3	60.318143	Glückert 1978	285	7000	85	1150	750	258	7200	43.48	276	6612
57	60	62	Turku	212	7700	61	10800	21.66799 8	60.059098	Glückert 1976; Salonen et al. 1984	235	7500	80	1150	950	230	6800	44.19		
58	61	63	Karja- lohja	183	7600	61	10900	23.26341 0	60.157663	Glückert & Ristaniemi 1982	215	7500	70	1150	850	198	5700	44.94		
59	62	64	Tammi- saari	175	7500	58	10850	23.24143 3	60.108329	Eronen et al. 1995	195	7200	58	1150	1000	190	5500	44.81	194	5851
60	63	65	Lohja	178	7500	59	10900	23.52382 0	60.142961	Glückert & Ristaniemi 1982	190	7200	65	1150	900	190	5600	45.48		
61	64	66	Espo	163	7300	58	10900	24.43470 6	60.167060	Glückert & Ristaniemi 1982; Eronen & Haila 1982	180	7200	60	1150	900	180	4800	48.25		
0	0	67	Helsinki	163	7300	58	10900	25.02538 3	60.210662	Hyvärinen 1980 1984; Korhola 1995	0	0	0	0	0	0	0	48.69		
0	0	68	Sippo	152	7300	58	10900	25.19746 1	60.653454	Seppä et al. 2000	0	0	0	0	0	0	0	52.23		
62	65	69	Porvoo	147	7300	57	10900	25.76927 2	60.365661	Eronen 1983	163	6500	57	1150	1000	168	4400	46.13	155	6264
63	66	70	Hangas-	138	7000	57	10900	27.27641	60.603839	Eronen 1976	160	6500	60	1150	900	165	4300	40.14		

